UNIVERSITÀ DI PISA

RWTH AACHEN UNIVERSITY

International Doctorate in
Civil and Environmental Engineering

XXXII CYCLE

Passing-through Tubular Column Joints for Steel and Composite Constructions made by Laser Cutting Technology

Academic Discipline (SSD) ICAR/09

Doctoral Candidate
Dr. Andrea Piscini

Supervisor
Prof. Walter Salvatore

Supervisor
Prof. Benno Hoffmeister

Supervisor
Dr. Francesco Morelli

Coordinator
Prof. Claudio Borri

Years 2016/2019

Contents

1 Introduction

In steel moment-resisting frames, tubular columns have many structural and architectural advantages over open-section columns. Circular Hollow Sections (CHS) are in fact particularly recommended for structural elements subjected to compression and bending forces in all directions, thanks to their higher radius of gyration and the axial-symmetric distribution of their mechanical properties. Therefore, the use of CHS profiles for the realization of columns can lead to a reduction of the total costs and furthermore to simplifications in the realization process of steel-concrete composite structures. However, the difficulties in realizing tubular column joints adopting open I-section beams, the most commonly used all around the world, severely reduce the use of CHS columns.

Nowadays, I-beam-to-CHS-column steel and composite joints are commonly realized in two main ways: i) the connection is made by directly welding the beams or the beam stub to the wall of the steel tube; ii) supplemental plates are used to connect the beams to the circular column. The direct connection is the most convenient solution in terms of rapidity and easiness of fabrication but the performance of the joint is strongly limited by significant local distortions of the tube wall near the girder flanges. Therefore, the joint performance results very far from the ideal mechanical behavior of a rigid full-strength beam-to-column connection.

The local buckle of the tube wall, which can lead to brittle failures, often suggests the use of supplemental plates for the realization of the tubular column joints. Additional elements can indeed assure a more effective transfer of the stresses from the beam flanges to the column wall or from the flanges of one beam directly to the beam placed on the opposite side. In general, two types of additional elements are currently used for I-beam-to-CHS-column moment joints: interior diaphragm joints, which imply the discontinuity of the column, and exterior diaphragm joints, which guaranty the total continuity of the column. Although internal diaphragms are very effective in distributing the internal forces and improving the collaboration between the steel elements and the concrete core in the case of composite columns, their use

implies a discontinuity in the column and requires extensive welding to reconnect the column pieces. On the contrary, exterior diaphragms guarantee the steel tube continuity through the connection; nevertheless, several welding should be performed also in this case. Moreover, in the case of filled column, the composite behavior is not improved by the presence of steel elements, and the presence of big external stiffeners spoils down the aesthetic of the whole building.

To overcome the main issues inherent the direct connections and the use of diaphragms, innovative solutions with continuous passing-through elements inside the column were studied, highlighting several advantages from a mechanical point of view. Indeed, the continuous elements can pass by slots of limited size made on the column wall, without requiring the complete discontinuity of the column itself and the joint requires less cutting and welding operations, resulting in lower overall cost and better mechanical behavior. The use of passing-through elements can lead to obtain the same mechanical benefits highlighted by internal diaphragms joints, without requiring the complete discontinuity of the column wall in the joint. However, despite all these advantages, many problems arise from the fabrication and constructional points of view, limiting the effective performance of the joints. Indeed, the difficulties in implementing high precision cutting processes spoiled the development of this construction technique, favoring more practice solutions.

One of these difficulties lies in the production tolerances that affect the effective geometry of the beams. These tolerances shall be considered in the definition of the dimensions of the slots in which the beams need to pass through: dimensions of the slot very close to the nominal ones of the beam can lead to difficulties in the assembly process, whereas big gaps can result in ineffective welding. One of the solutions to overcome the difficulties in the fabrication and constructional processes of this joint typology lies in the application of the modern Laser Cutting Technology (LCT) to steel and composite structures. Laser cutting machines, commonly used in the industrial field, allow performing high precision and completely automated cutting processes on steel tubes and open sections profiles with the typical structural dimensions. To limit the influence of the beam dimensions tolerances, the laser cutting machines have the intrinsic advantage of directly providing measuring instruments that can be used to measure the elements to be passed. Therefore, the whole fabrication process can start with the simultaneous cutting and measuring process of the I-beams and plates. Subsequently, slots can be realized on the tube-wall considering the previously taken and recorded measurements and applying a defined strict tolerance margin. In this way the correct passage of the beam portions or plates through the column is guaranteed without requiring excessive gaps, and the welding processes is

performed in the best conditions. Furthermore, thanks to the possibility of cutting with different inclinations with the tube-face, the penetration welding may be realized without performing any additional preparation processes on the worked-pieces. The LCT is also a very competitive solution in terms of time of fabrication and cost, thanks to the high automatization of the process reached by the modern technologies.

However, even though the LCT provides the perspective of realizing the I-beam-to-CHS-column connection type that exhibited the best mechanical behavior in the past researches, several issues still need to be faced in order to define an appropriate fabrication process and to better characterize the behavior of the I-beam-to-CHS-column connection. For these purposes, in the presently exposed research, preliminary practical, numerical and theoretical studies are conducted to confirm the mechanical and technological advantages previously reported, and to understand the global and local behavior of the passing-through tubular column connections in case of both vertical and horizontal loadings acting on the structure.

Considering the analyzed aspects inherent the practical realization and the mechanical behavior of the I-beam-to-CHS-column with passing elements, new joint solutions are proposed for both steel and composite structures. Afterwards, the proposed joint typologies are experimentally tested in order to have information on their mechanical behavior. On the basis of the behavior exhibited in the tests, mechanical models for steel and composite joints are developed with the aim of drafting practical methods for the definition of design forces acting on the singular components, and global elastic stiffness and strength of the joints.

The introduced aspects of the present research program are developed in the following chapters of the thesis.

Chapter 2 reports briefly the state of art about I-beam-to-CHS-column steel and composite connections, showing the advantages and disadvantages correlated with the different adopted typologies.

Chapter 3 reports the open problems, fixes the objectives and highlights the methodology followed in the development of the present research program**.**

Chapter 4 shows the characteristics of the LCT processes on steel parts, considering the advantages and disadvantages over the traditional cutting techniques from different points of view, such as the obtainable precision and the characteristics of the worked-pieces, and the cost and environment impacts.

Chapter 5 focuses on the proposal of possible solutions for the fabrication, assembly and erection processes for tubular column joints with passing-through elements, considering preliminary practical, theoretical and numerical studies.

Chapter 6 reports the configurations adopted, the specimens tested and the results obtained in the preliminary experimental campaign on several two-way and four-way steel joints, highlighting the most relevant evidences.

Chapter 7 defines the whole experimental campaign required to assess the global behavior of different composite I-beam-to-CHS-column joints with passing-through elements, including the design of case study composite structures, and the definition, design and realization of the sub-structure specimens.

Chapter 8 and **chapter 9** report the experimental assessment of composite two-way and four-way substructures under vertical and horizontal loads, including information on the testing setups, the adopted instrumentations and the test results.

Chapter 10 deals with the analytical interpretation of the test results and the definition of appropriate tools for the mechanical characterization of the proposed joints, through the study of the singular components, and the development of preliminary mechanical models for the simulation of the behavior of steel and composite passing-through tubular column joints.

2 State of art of tubular column connections in steel and composite structures

In steel moment-resisting frames, open I-section beams are the most used due to their efficiency in resisting bending about their major axis, whereas columns can have either open or tubular sections. Tubular columns have many structural and architectural advantages over open-section columns.

Indeed, thanks to the intrinsic high resistance/weight ratio of steel, use of thin walled elements usually characterizes steel constructions and instability represents one of the main issues, often conditioning the design of the whole structure. The axial-symmetric distribution of the mechanical properties and the higher radius of gyration of tubular sections make the use of Circular Hollow Section (CHS) particularly indicated for structural elements subjected to compression and bending forces in all directions, as columns. Their use leads to a saving of raw material, followed by a reduction of total costs. Moreover, use of tubular sections simplified the realization of steel-concrete composite structures by directly filling the columns, reducing the influences on the carpentry operations cost.

Even though the use of CHS columns should lead to economic benefits, their use in building construction market is presently limited due to the complexity of the beam-to-column connections. In fact, in steel constructions, fabrication costs usually account for 30-40% of the overall project budget, as reported in (Barrett-Byrd-Associates 2016), where the portion related to realization of joints is the largest one. Therefore, the advantages arising from the use of CHS-columns are sometimes underexploited due to the difficult realization and design of the beam-to-column joints, considering besides the lack of design guidance on moment joints between open-section beams and tubular columns.

Nowadays, I-beam-to-CHS-column steel and composite joints are realized in two main ways. In the first type, the connection is made by directly welding the beams or the beam stub to the face of the steel tube. The second type is instead represented by the joints that use additional elements to connect beams to the circular column.

Although the direct connection is the most convenient solutions, in terms of rapidity and facility of fabrication, the joint cannot probably develop the ideal mechanical behavior of a rigid full-strength beam-to-column connection. Indeed, joints made by welding open-section beam stubs or beams directly to the outer skin of tubular columns, without the use of any stiffeners, can exhibit significant local distortions of the tube wall near the girder flanges, which prevented plastic hinging of the beam and, in some case, led to the brittle failures of the welds and column wall.

The local tube wall distortions, as well as the brittle failures of welds and tube wall, may be prevented by using additional components designed to allow the correct transfer of the axial forces from the beam flanges to the column wall. These elements can avoid the concentration of stresses in singular points and simultaneously reinforce the column in the connection regions, reducing the possibility of distortions. In general, two types of additional elements are currently use for I-beam-to-CHS-column moment joint: interior diaphragm joints, which involve the discontinuity of the column, and exterior diaphragm joints, which guaranty the total continuity of the column.

From the mechanical point of view, although internal diaphragms attempted to correctly distribute loads to the steel tube and the concrete core, these diaphragm plates completely discontinued the steel tube and required extensive welding to reconnect together the column pieces with the diaphragms. Furthermore, the fabrication processes of interior diaphragm joints require labor intensive works and spoil down the construction speed, involving an increasing of the overall building cost.

Exterior diaphragms provide an economical alternative and guarantee the steel tube continuity through the connection, avoiding the realization of a great quantity of welds to reconnect the column pieces. In fact, the beam-to-column connection is made without cutting the column and by welding around the whole column external collar plates. Although economical and mechanical benefits may arise from the adoption of exterior diaphragms, comparing to the joints with the interior ones, several welding processes should be performed anyhow. Furthermore, in case of filled column, the composite behavior is not improved by the presence of steel elements embedded in the concrete core. In addition, the presence of big external stiffeners spoils down the aesthetic of the whole building.

To overcome the main mechanical problems previously exposed with the direct connections and the diaphragms connections, innovative solutions with continuous elements inside the column were studied. The continuous elements can pass by limited slots made on the column wall, without requiring the complete discontinuity. The passing-through elements can lead to the advantages that arise from the adoption of interior diaphragms, such as the improvement of the composite behavior, in case of filled column, the improvement in the stiffeners of the column wall, the well redistribution of forces from beams to column. Moreover, the column results to be continuous through the connection and the joint require less cutting and welding operations, resulting in lower overall cost and more ductile mechanical nonlinear behavior. Although this I-beam-to-CHS-column connection type can be very advantageous from a mechanical point of view, many problems arising from a fabrication and constructional point of view. Indeed, the correct realization of welds requires precise cutting operations, to have the right welds mechanical behavior. The difficulties in implementing high precision cutting processes did not allow the development of this construction technique, favoring more practice solution.

In literature fewer studies on moment open section beam joints to circular hollow section columns were published, in comparison to their square and rectangular counterparts. This could be due to the higher difficulties in designing joints to the curved surface of CHS columns than that to the flat faces of Square or Rectangular Hollow Section (SHS or RHS) columns. Most of these studies have focused on joints to Concrete Filled Tubes (CFT) rather than joints to unfilled hollow section columns. This could be due to the advantages of the CFT columns, which combine the ductility of the steel and the stiffener of the concrete. Indeed, the concrete restrains local buckling of the steel tube, whereas the steel tube eliminates the need of construction framework, acts as longitudinal reinforcement to the concrete and provides its lateral confinement. Despite the studies on connections to composite column are largely diffused in literature, only few researches were conducted on connections between composite beams and steel or composite tubular columns.

Commonly, I-beam-to-CHS-column steel and composite joints may be grouped in two broad categories: connections with beams or stub directly welded to the face of the steel tube and joints that use additional elements to connect beams to the circular column. In both cases, the connection may be realized using beam connection stubs to be constructed and connected in the shop, under sufficient quality control, to address some of the problems noted after the 1994 Northridge earthquake with the fully welded connections realized in building site. The girders are then bolted or

welded to the beam stubs at much less critical regions compared to the beam-to-column connection region.

2.1 Directly welded connections

The most convenient solutions studied in the past, in terms of rapidity and facility of fabrication, are certainly the ones where the beams are directly connected to the column wall. Indeed, in these cases, the realization of joints requires the least amount of fabrication and construction effort, because does not require further working processes, such as cutting of the tube into pieces, and consequent excessive welding. Moreover, the aesthetic of buildings is not influenced by the presence of additional exterior elements.

Numerical and experimental assessment of directly welded I-beams-to-CHS-filled-column joints was conducted in past researches (Wardenier 1995; Alostaz and Schneider 1996a; de Winkel 1998; Schneider and Alostaz 1998) highlighting some problems of the connection mechanical behavior. In fact, joints made by welding open-section beam stubs (Figure 2.1a) or beams (Figure 2.2a) directly to the outer skin of tubular columns, without the use of any stiffeners, exhibited significant local distortions of the tube wall near the girder flanges (Figure 2.2a-b), which prevented plastic hinging of the beam and, in some case, led to the brittle failures of the welds and column wall (Figure 2.1b).

Investigations highlighted that the initial stiffness of this type of connection is very minor compared with the ideal rigid condition and, in the same way, connections did not exhibit linear behavior up to plastic bending capacity of the girder, due to severe local distortion of the tube wall in the beam flanges region. Moreover, the high diagonal tensile stresses formed in the steel pipe between the tension flanges on either side of the column, in case of interior joints, contributed to reduce the strength of the connection. However, although the panel shear was higher, there was no evidence of crushing the concrete around the girder flanges or anywhere else in the panel zone.

Despite the lack of studies about pure-steel directly welded connections, it is obvious to think that the problems on the column wall distortions condition in any case the mechanical behavior of the joint, which cannot probably develop the ideal mechanical behavior of a rigid full-strength beam-to-column connection.

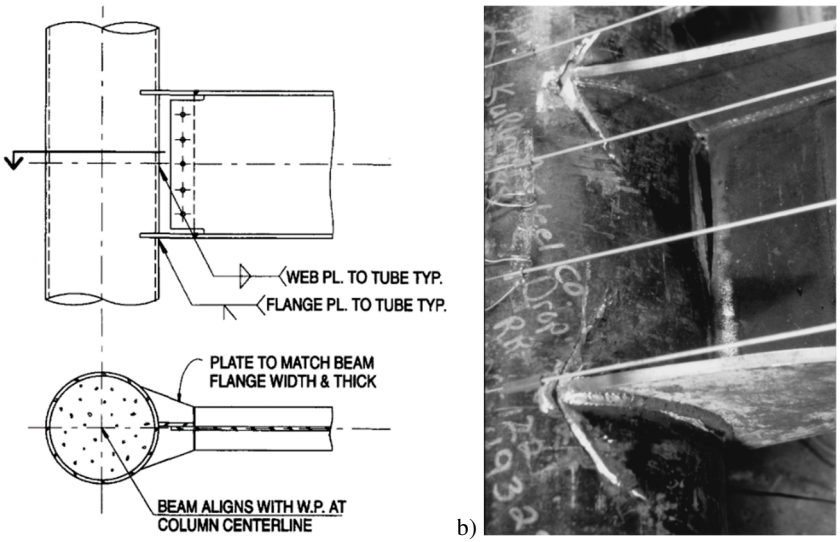

Figure 2.1 Connection with a beam stub directly welded to the outer skin of the tubular column, the mixed welded and bolted connection between the beam stub and the girder is far from the node region: a) schematic representation of the joint (Alostaz and Schneider 1996a), and b) failure mode exhibited in the cyclic tests (Schneider and Alostaz 1998)

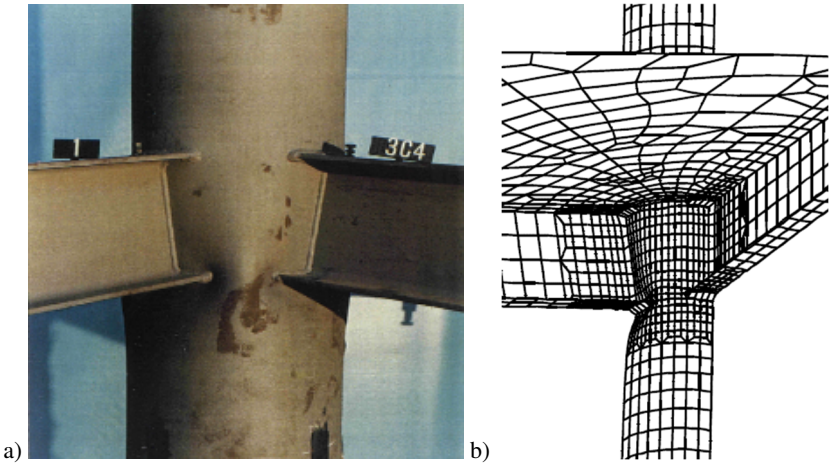

Figure 2.2 I-beam-to-CHS-column joint made by directly welding the beam to the column wall: a) failure mode observed in the monotonic test under vertical loads, and b) results of numerical simulation of the joint with a concrete slab (de Winkel 1998)

2.2 Welded connections with additional components

The local tube wall distortions, as well as the brittle failures of welds and tube wall, may be prevented by using additional components. Indeed, problems of the direct welded connections are due to the high concentration of stresses in the region where flanges are connected to the tube wall.

Consequently, additional components may be designed to allow the correct transfer of the axial forces from the beam flanges to the column wall, avoiding the concentration of stresses in singular points and simultaneously reinforcing the column at the levels of the beam flanges, reducing the possibility of distortions.

In literature, many studies on the behavior of various type of I-beam-to-CHS-column joints made through additional connection elements are published. In general, three types of additional elements are recommended for I-beam-to-CHS-column moment joint: interior diaphragm joints, which involve the discontinuity of the column, exterior diaphragm joints, which guaranty the total continuity of the column, and joints with passing-through elements, which do not require the total discontinuity of the column.

2.2.1 Interior diaphragm joints

The correct transmission of forces between beams and column and the stiffening of the column tubular wall can be jointly achieved thanks to the adoption of internal diaphragms. Furthermore, internal diaphragms have the advantage of redistributing the load, as well as to the steel tube, to the concrete core. Moreover, concrete strength in the panel zone can be enhanced by the confinement of the tube wall and of the diaphragms.

Joints with interior diaphragms are fabricated by first cutting the steel tube into three pieces and then welding them together with two horizonal plates (Figure 2.3). The horizontal through plates, together with additional exterior vertical web plates, compose the beam stubs that are themselves welded or bolted to the external girders.

Although internal diaphragms attempted to distribute load to steel tube and concrete core, the fabrication was quite labor intensive and the diaphragm plates discontinued the steel tube and required extensive welding. Therefore, the realization process of this joint typology involves an increase of the overall time and cost required to assembly the connections and erect buildings, since it requires complicated and costly processing, such as several cutting and welding operations. In spite of these weaknesses, the use of welding robots and other suitable production resources have made popular the adoption of I-beam-to-CHS-column made with through diaphragms. Nevertheless, the large amount of welding required to reconnect together the column

pieces with the internal diaphragms, results in an increased possibility of welds defects.

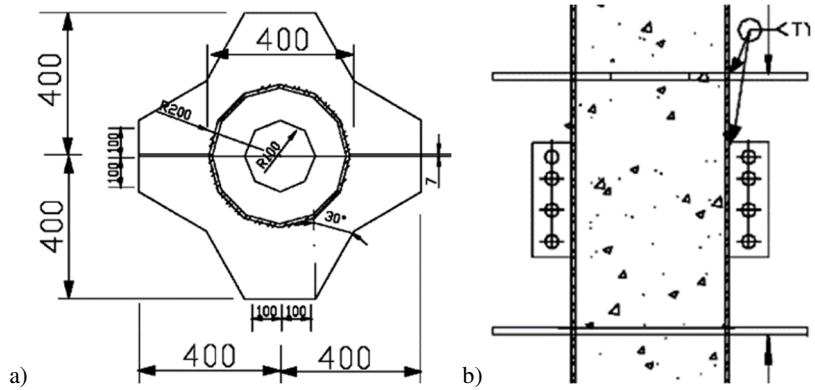

a) b)

Figure 2.3 I-beam-to-CHS-filled-column realized by interior diaphragms and web plate: a) shape of the diaphragm, and b) joint fabrication details (Cheng and Chung 2003)

Experimental and numerical analyses were performed to assess the mechanical behavior of this joint typology (Cheng and Chung 2003; Nishiyama et al. 2004). Unlike the evidence reported for the connection made by directly welding the beam to the tubular face, without any stiffeners, the observed elastic stiffness of the beam-to-column connection with interior diaphragms showed good agreement with the ideal rigid full-strength joint. However, experimental tests highlight that specimens failed due to the column welding fracture during nonlinear behavior (Figure 2.4). The fracture started in the tension region and propagate in the welds and in the steel connected member. The authors report that the welds fracture is due to the residual stress, which remarkably reduced the deformation capacity of welds. Therefore, the failure mode exhibits a brittle behavior due to the fast propagation of the weld cracks.

In conclusion, the fabrication processes of interior diaphragms joints require labor intensive works and spoil down the construction speed, involving an increasing of the overall building cost. From the mechanical point of view, although internal diaphragms attempted to distribute load to the steel tube and concrete core, these diaphragm plates discontinued the steel tube and required extensive welding to reconnect together the column pieces with the diaphragms, resulting in a brittle nonlinear behavior, caused by the weld failure in the tension region.

Figure 2.4 Welding fracture at column welds (Cheng and Chung 2003)

2.2.2 Exterior diaphragm joints

Exterior diaphragms provide an economical alternative and guarantee the steel tube continuity through the connection. The beam-to-column connection is made by welding around the whole column, in the beam flanges region, two external collar plates, each one composed by two parts welded to the column and themselves. In addition, vertical web plates are used to compose the beam stubs to be connected to the external girder (Figure 2.5a). Although several welding processes should be performed, the whole making process does not require cutting operations on the tube wall, resulting in economic benefits, comparing to the joints with interior additional components. Furthermore, fillet welding from both sides of the diaphragms, which is preferred by construction companies, may be adopted as a replacement of complete penetration welds, which is the one to be preferred in case of interior diaphragms, considering the impossibility to welds inside the tubular column.

From a mechanical point of view, the continuity of the column through the connection, avoids the brittle failure mechanisms highlighted in the interior diaphragm connections. However, the composite behavior is not improved by the presence of steel elements embedded in the concrete core, and the concrete strength in the panel zone cannot be enhanced by the confinement due to the presence of diaphragms. Many researches were conducted to investigate the mechanical behavior of I-beam-to-CHS-filled-column connections with both numerical and experimental analyses (Alostaz and Schneider 1996a; Schneider and Alostaz 1998; Li et al. 2010; Zhang et al. 2012; Khador 2015). Two main structural deficiencies in the connection region were reported in these researches using external diaphragm connections: a) distortion in the web panel (Figure 2.6a), and b) strain concentration and out-of-plane

failure deformation in the diaphragm plates, which led to fracture of these plates, welds and columns, as shown in Figure 2.5b.

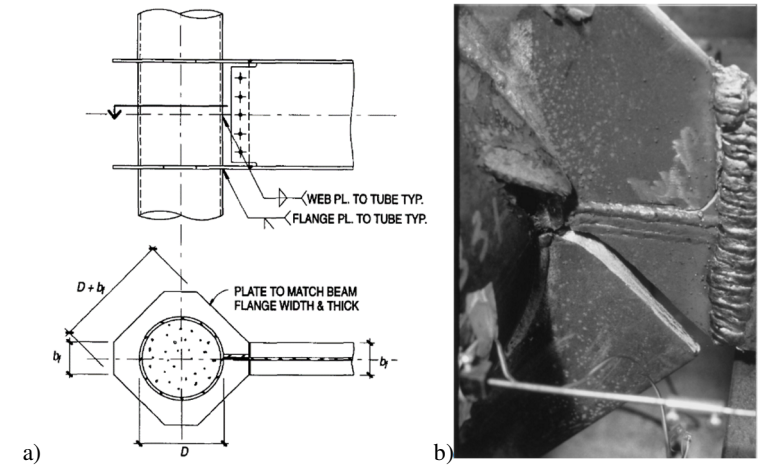

Figure 2.5 Connection with two external flange diaphragms around the whole column and one external vertical web plate: schematic representation of the joint (Alostaz and Schneider 1996a), and b) failure mode exhibited in the cyclic tests (Schneider and Alostaz 1998)

Moreover, failure modes external to the connection region are highlighted in the experimental studies conducted in the past researches: a) the local buckling of the beam (external to the joint zone), and b) local buckling of the tube-wall near the external diaphragm, as shown in (Figure 2.6b). These latter results confirm that the continuity of the column through the connection region avoids problem and allows the development of the strength in the connected members.

Further researches confirm the behavior of the exterior diaphragm joints in case of filled tubular column and composite steel-concrete beams. Indeed all the observed failure modes do not include the node region (Han and Li 2010; Li and Han 2011, 2012; Li et al. 2017). In these tests, performed on specimens with concrete slab, different failure modes were observed, e.g. the buckling of the compressed beam flanges, including weld fractures, the crushing of the concrete slab in the contact zone, the local buckling of the steel tube and the plasticization of the composite columns (Figure 2.7).

a)  b) 

Figure 2.6 Failure modes exhibited in the experimental tests: a) failure of the panel zone with diagonal concrete cracks in the interior joints (Zhang et al. 2012), and b) local buckling of the column near the external diaphragms (Li et al. 2010)

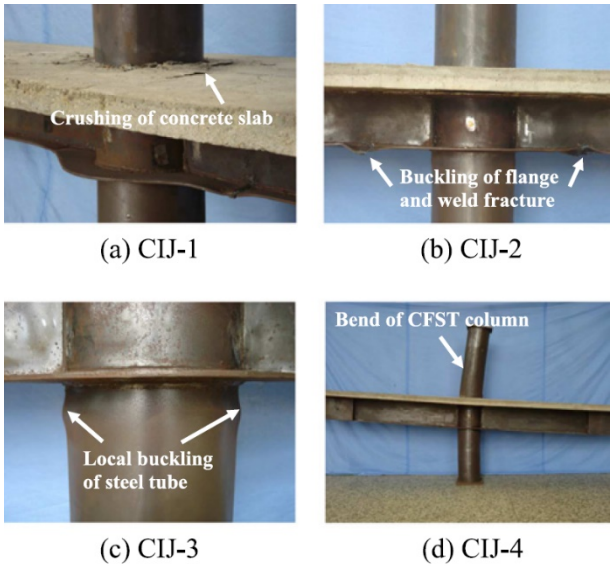

Figure 2.7 Failure modes observed in an experimental investigation (Han and Li 2010)

In case of pure-steel connection, the web panel zone is not stiffened by the concrete core inside the column. Therefore, the main failure mode that may be occur is the shear deformation of the web panel zone and the presence of the external stiffeners in the flange zones cannot improve the relative strength. An experimental campaign exposed in (Wang et al. 2011) shows that the failure modes observed are a) excessive

plastic shear deformation of panel zone (Figure 2.8a), b) local buckling of column wall above the connection (Figure 2.8b), c) local distortion of outer diaphragm c) weld crack between column and diaphragm, and d) fracture at the junction between diaphragm and beam flange. The authors report that failure modes were mainly dependent on the column wall thickness and specimens with a thin or thick wall failed in significantly different modes. Furthermore, the specimens where the panel zone failed, demonstrated better ductility.

a)  b) 

Figure 2.8 Failure modes observed in exterior diaphragms pure-steel connections: a) shear panel deformation, and b) buckling of the column wall (Wang et al. 2011)

Additional stiffeners were proposed in the past researches to improve the mechanical behavior of the beam-to-column joint. These stiffeners are assumed to be welded to the column face and to the outer sides of the diaphragms (Figure 2.9) and lead to the elimination of the strain concentrations in the diaphragm plate and in the column welding interfaces, as demonstrated through numerical simulations in (Bagheri Sabbagh et al. 2013).

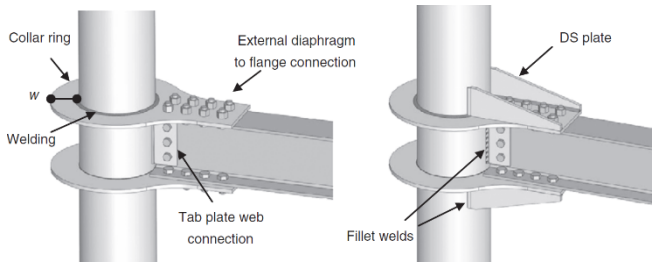

Figure 2.9 Connections studied in (Bagheri Sabbagh et al. 2013)

In conclusion, although economic benefits may arise from the adoption of exterior diaphragms, comparing to the joints with the interior ones, several welding processes

should be performed anyhow. Furthermore, in case of filled column, the composite behavior is not improved by the presence of steel elements embedded in the concrete core, and the concrete strength in the panel zone cannot be enhanced by the confinement due to the presence of diaphragms, resulting in higher web panel deformation. Moreover, the presence of big external stiffeners spoil down the aesthetic of the whole building.

2.2.3 Connections with passing-through elements

To overcome the main mechanical problems previously exposed with the direct connections and the diaphragms connections, solutions with elements continuous inside the column, which pass by limited slots made on the column wall, without having the complete discontinuity of the column wall, may be adopted. The passing-through elements can lead to the advantages that arise from the adoption of interior diaphragms, such as the improvement of the composite behavior, in case of filled column, the improvement in the stiffeners of the column wall, the well redistribution of forces from beams to column. Moreover, the column results to be continuous through the connection and the joint require less cutting and welding operations, resulting in lower overall cost and more ductile mechanical nonlinear behavior.

I-beam-to-CHS-column connections may be realized by passing, through the column, vertical plates. The vertical plates allow the development of a composite behavior and increase the stiffener of the web panel zone and column wall. Moreover, they do not require the complete discontinuity of the column through the column. Possible solutions were presented and analyzed in (Alderighi 2007). The first solution includes six passing-trough embedded vertical plates that connect the beams to the column wall and the concrete-core (Figure 2.10a). The six vertical plates are placed inside the steel tube on shop whereas they are connected to the main steel beam profile by in-situ welding. A good performance of this joint typology is strictly related to the precision of the cuts to be realized in the steel tube, considering its influence also on the construction phase, when the plates have to pass through the slots. The second solution proposed is made by two horizontal external diaphragm plates and one vertical embedded passing-through plate, as shown in Figure 2.10b. The presence of the vertical embedded continuous plate allows the transmission of shear forces from the beam to the column in the external joints and from one beam to the other in the internal joints, resulting in an improvement of the mechanical behavior.

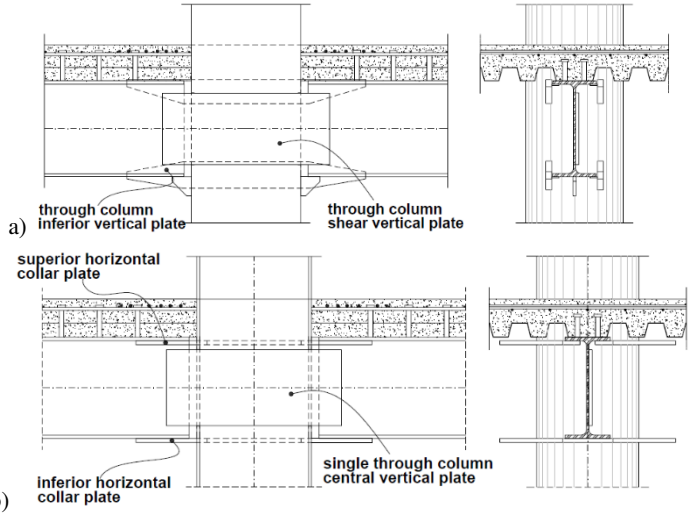

Figure 2.10 Connection with additional passing-through elements: a) six vertical passing-through plates (Alderighi 2007), and b) one vertical passing-through plate and two external collar plates (Alderighi 2007)

Steel and composite joints with passing-through horizontal plates, which do not require the total discontinuity of the column wall (Figure 2.11), were experimentally studied in (Schneider and Alostaz 1998; Ou et al. 2015) showing significant panel zone shear yielding and shear deformation for all specimens. In the test, failure of the specimens was caused by the fracture of the column tube near the through-flange plates and crushing of concrete in the panel zone, if concrete infill was present. Significant crushing and cracking of concrete was observed for specimens with concrete infill. Tests showed that the use of concrete infill increased the peak applied load by 156% and helped control the shear distortion of the panel zone. Despite of the increased strength, the fillet weld that attached the connection-stub flanges to the pipe wall exhibit premature fractures. The authors suggest that the large tolerances applied in the cutting operations to make the tube slots caused the problems in the mechanical behavior of the welds. The resulted flexural strength at the column face is higher than the plastic bending strength of the girder. However, cyclic tests highlight that this strength is not sustained upon subsequent same-amplitude cycles.

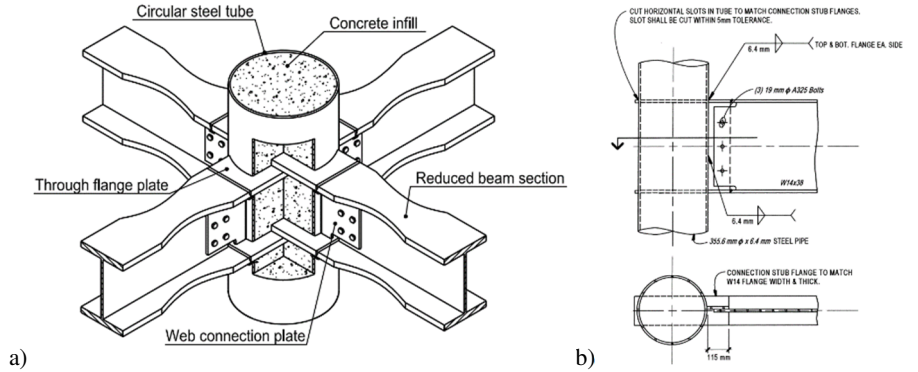

Figure 2.11 Connection with passing-through horizontal plates studied in a) (Ou et al. 2015) and b) (Schneider and Alostaz 1998)

The combination of the previously exposed solutions consists in the adoption of a beam stub that passes through the column (Figure 2.12) or, similarly, one vertical and two horizontal passing-through plates (Figure 2.13). In these cases, practically, a steel beam portion is continuous across the column wall and the connection to be realized in-situ is a beam-to-beam type, instead of beam-to-column. Even if this connection represents at best the ideal rigid connection condition, some problems may be caused by the tolerances adopted in the structural element production and the precision of the cutting processes, lead to difficulties in the assembly and welding processes. In fact, the correct assembly of the connection requires a shaped slot to be cut in the tube wall to firstly allow the passage of the web and flanges plates, or the beam portion, through the column and then the correct realization of the welds around the slots.

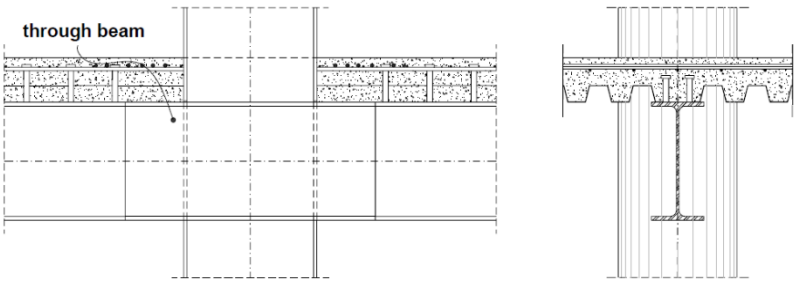

Figure 2.12 Connection made by a passing-through beam portion (Alderighi 2007)

This I-beam-to-CHS-column connection type is very advantageous from a mechanical point of view. In fact, the passing-through plates, or beam, allow the

redistribution of the flange stress to the concrete core and the reduction of the high shear demand on the tube wall. Nevertheless, the correct realization of welds requires precise cutting operations, in order to have the right welds mechanical behavior. Moreover, in case of filled column, the concrete casting operations result to be difficult, and special concrete has to be adopted.

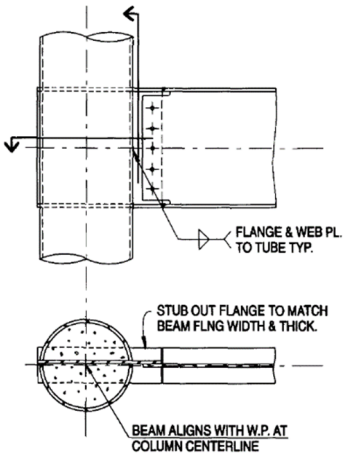

Figure 2.13 Connection made by passing-through plates (Alostaz and Schneider 1996a)

The mechanical behavior, under gravity and seismic loads, of I-beam-to-CHS-filled-column connections, made by passing-through beam stub, was studied by both numerical and experimental investigation (Alostaz and Schneider 1996a; Schneider and Alostaz 1998; Minouei and Mirghaderi 2009), showing that the elastic stiffness of the present connection type is the most close to the ideal rigid connection. Furthermore, results clearly indicate that the strength of this connection is limited by the capacity of the steel girder and not the joint region (Figure 2.14). Moreover, in case of filled column, the concrete core is not near crushing, thanks to the lateral confinement offers by the passing-through steel plates.

Therefore, researches confirm that this connection type, with passing-through flanges and web plates or beam portion, is the best one from a mechanical point of view. In fact, load transfer, from the beam to the column, takes place by the weld between the connection plate and the steel tube and, moreover, the bearing action and the friction force between the through elements and the concrete core. Furthermore, this type of connection increases the confinement of the column concrete core in the node region, improving thus the mechanical behavior of the connection. Nevertheless, problems arising from a fabrication and constructional point of view did not allow the

development of this construction technique, favoring more practice solution. Difficulties are mainly due to the problems in implementing cutting processes with high precision and in casting the concrete inside the column.

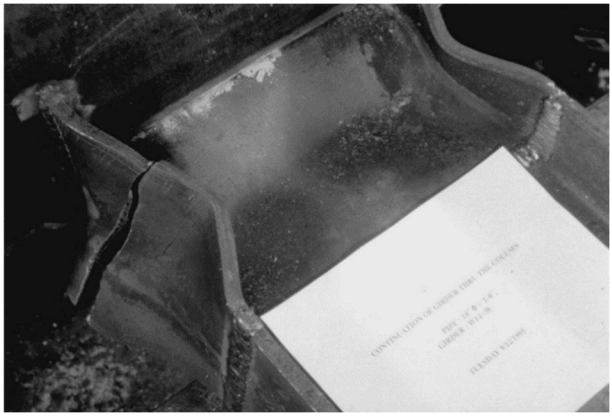

Figure 2.14 Girder failure exhibited in the experimental test (Schneider and Alostaz 1998)

3 Open problems, objectives and methodology

Even though tubular columns can lead to economic benefits, thanks to their optimized mechanical behavior and high aesthetic value, their use in building construction market is presently limited mainly due to the complexity of the beam-to-column connections. Nowadays the realization of I-beam-to-CHS-column steel and composite joints implies the direct connection of the beam to the column, with several problems due to the buckling od the column wall, or the introduction of a discontinuity in the column, with an increase of costs due to the necessity of restoring it, or the introduction of a great number of stiffeners, spoiling the aesthetic of the joint and increasing also in this case the costs and the realization time.

The present research aims at studying the possibility and the potentiality of using modern laser cutting techniques to exploit the potential advantages of passing-through I-beam-to-CHS-column joints, overcoming all the shortcomings highlighted by the current state of art.

3.1 Open problems

Nowadays I-beam-to-CHS-column steel and composite joints are realized in two practical solutions: the direct connection or the adoption of supplemental stiffeners. A third way with continuous elements that pass through the column have been studied recently but it has never been introduced in the market as practical solution due to the several realization shortcomings. All these solutions exhibited several and relevant disadvantages.

The direct connection can be considered the most convenient solutions in terms of rapidity and facility of fabrication. Nevertheless, several studies highlighted that in this case the joint cannot develop the ideal mechanical behavior of a rigid full-strength beam-to-column connection, due to the significant local distortions of the tube-

column wall, limiting therefore this solution in the realization of steel moment resisting frame structures.

The adoption of supplemental components (stiffeners) designed to allow the correct transfer of the axial forces from the beam flanges to the column wall can improve the mechanical behavior of the joints. However, these joint typologies generally require extensive additional cutting and welding processes, resulting in a reduction of the construction speed and increasing the overall building cost. In addition, the presence of big external stiffeners spoils down the aesthetic of the structure, limiting the appeal of the CHS columns.

The use of continuous elements that pass through the column was studied with the aim of overcoming the main problems of the two practical solutions depicted above. The researches executed on this type of joint highlighted that its mechanical behavior is quite promising and the best solutions are the one with passing-through flanges and web plates or the one with a stub passing through the column. However, from a fabrication point of view, this joint typology presents several issues, strongly limiting its effective use in the steel construction market. These issues can be identified as follows.

- The effective dimensions of the beams that need to pass through the column are characterized by tolerances that need to be considered when performing the laser cutting on the tube wall. Small gaps result in difficulties in the assembly process, whereas big gaps affect the effectiveness of the welding.
- The laser cutting machines currently need several cutting phases to obtain the correct shape of the slot, especially to assure the penetration of the welding.
- The experimental results on the actual behavior of these joints are currently quite limited and the few studies available are mainly focused on the behavior of the I-beam-to-CHS-column under vertical loads.
- The influence of the composite components on the global behavior of the I-beam-to-CHS-column joint is not properly quantified.
- There are no indications or provisions available for the design and characterization of these joints.

3.2 Objectives of the Thesis

The main scope of the present PhD research program is to study the connections between tubular columns and open section beams, realized by passing beam stubs or plates through fitted slots, made on the tube wall by laser cutting machines.

The present research deals with several aspects, associated with the possible benefits that can arise from the adoption of LCT in realizing the proposed connection

types and facing the issues that limited the use of this structural solution in the past. In particular, the following aspects are accounted for:

1. the feasibility of the LCT processes on structural steel profiles;
2. the appropriate fabrication process;
3. the possible solutions for two-way and four-way rigid full-strength or pinned beam-to-column connections;
4. the obtainable mechanical behavior in case of pure steel and composite structures;
5. the practical design of the joint elements.

From the mechanical and technological point of view, the expected advantages regarding the realization processes and the global and local mechanical behavior of the proposed connection should be confirmed and the critical aspects should be analyzed and preliminary solutions should be accounted for. Moreover, new joint typologies for the passing-through I-beam-to-CHS-column should be proposed, considering the practical and mechanical analyzed aspects and including the variation of the traditional realization process. The proposed passing-through tubular column joint solutions require the experimental assessment to obtain first indications on the mechanical behavior in case of steel and composite structures subjected to both gravity and horizontal actions.

On the base of the experimental tests results, tools for the mechanical characterization of the proposed joints shall be developed allowing the engineers and designers to efficiently design this type of joint. The development of mechanical models for steel and composite joints, which can be useful in the linear and non-linear design of the proposed joints, requires the definition and characterization of steel and concrete components, on the basis of the experimentally exhibited mechanisms. Finally, the mechanical models should aim at developing practical methods for the definition of the global elastic stiffness and strength of the joints, together with the definition of design forces acting on the singular components, allowing their correct design.

3.3 Methodology and organization of the Thesis

The achievement of such objectives is developed in four main connected steps, briefly described in the following.

The **first step** describes the characteristics of the LCT processes on steel parts, considering the advantages and disadvantages with respect to the other cutting

techniques from different point of views, such as the obtainable precision and the characteristics of the worked-pieces, and the cost and environment impacts.

The **second step** executes preliminary studies on the potential of the adoption of such technology for the realization of the proposed joints. This part studies the application of LCT in cutting operations on steel structural tubes and open profiles analyzing the researches performed in the past. Then, possible solutions for the fabrication, assembly and erection processes are presented and discussed and, together with the results of preliminary theoretical and numerical studies, all the evaluation done are used to propose different joint typologies with passing-through elements that are able to accomplish with the necessities that can arise in the steel and composite structures, either moment resisting and braced frames.

The **third step** aims at assessing the mechanical behavior of specifically designed connection through numerical and experimental analyses. The whole experimental campaign is designed to assess the global behavior of different I-beam-to-CHS-column joints with passing-through elements, and furthermore to obtain detailed information on the local performance of the singular components, which can be useful in the mechanical characterization of the connections. The whole program includes tests to be carried out on substructure of steel and composite steel-concrete buildings, characterizing I-beam-to-CHS-column connections. These experimental tests are performed to characterize the monotonic behavior of the proposed connections under vertical gravity loads on the structure, and both the monotonic and cyclic behavior under horizontal loads, such as wind or earthquake. All the tests shown in this thesis were performed within the LASTEICON research project (Castiglioni et al. 2016) in two laboratories at the INSA Rennes University and the University of Pisa. In the latter, composite specimens are tested with two main configurations and the design of the specimens and the test setups is presently exposed, since it is part of the present work.

The **fourth step** deals with the analytical interpretation of the mechanical behavior of the proposed connections. Considering the results of the experimental tests, joint components are defined and analyzed. Afterwards, considering the final objective of developing mechanical models for steel and composite joints, which can be useful in the linear and non-linear design of the proposed joints, steel and concrete components are studied in order to define for each one the elastic stiffness and the strength. Finally, preliminary mechanical models, which can appropriately simulate the real behavior of the proposed joints, are developed considering, as an example, the component based model described EN1993-1-8 (CEN 2004a), which is currently the most adopted characterization method for open section beam to tubular column joints.

4 Laser Cutting Technology

Laser Cutting Technology (LCT) is a modern technology, which make possible the realization of high precision cutting processes on steel part, such as tubes and plates. Although this technology is nowadays typically adopted for industrial manufacturing applications, the application of the LCT to the steel construction industry is made possible thanks to the use of laser cutting machines that, adopting the CO_2 and fiber technology, allow the realization of any type of accurate cutting in open-section elements and tubes with the typical structural dimensions.

Laser cutting operations may be fully programmed, without any intervention of an operator, allowing the reduction of possible human error on several processes of fabrication and thus a safer work environment. In addition, (BLM Group 2012) reported that laser cutting processes can be up to thirty times faster than standard cutting methods and therefore, in spite the initial investment is higher with respect to other traditional type cutting machines, this technology can lead to the reduction of the overall life cycle costs.

4.1 Laser cutting processes

In the laser cutting thermal process, the focused laser beam energy is absorbed by the hit surface of the workpiece and converted into heat, producing the melting of the metal, with the support of a pressurized assist gas (e.g. oxygen). The laser beam is in part absorbed by the workpiece, reflected and transmitted through the workpiece. This is schematically shown in Figure 4.1. The three parts: absorbed, reflected and transmitted depend on several factors. Some factors regard the laser beam, such as the wavelength, polarization and incidence angle. Other factors regard the workpiece to be cut, e.g. material characteristics, temperature, geometry, and surface conditions. As reported in (Caristan 2003), unlike the parameters above listed, the mechanical characteristics of metals, such as yield strength, hardness and ductility, do not significantly influence the laser cutting process.

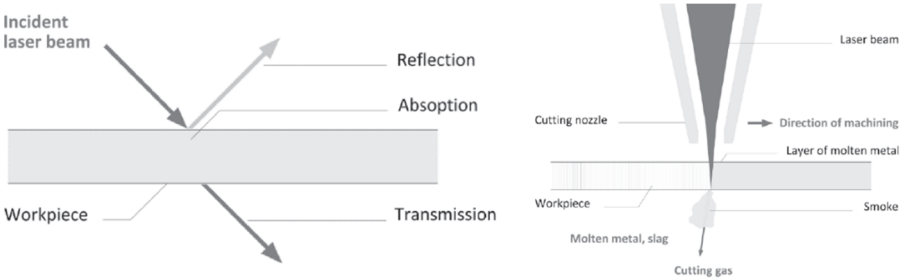

Figure 4.1 Interaction between laser beam and material in the laser cutting process (Kanyilmaz 2019)

Laser cutting mainly differs from other cutting techniques, namely water jet, plasma, oxygen cutting, for the following points: a) three-dimensional (3D) processing is feasible, which is not recommended in water-jet and plasma cutting methods; b) all metals can be processed (e.g. mild, stainless steel, aluminum, brass, copper), whereas plasma can cut only conductive metals; c) the heat-affected zone is very limited; d) the cutting has higher precision and is faster than others techniques.

The laser cutting processes can be done through two operation modes of the laser head: continuous and pulsed mode (Figure 4.2). The laser head constantly operates in the continuous mode, whereas the pulsed mode operates in an intermittent manner to reduce the accumulated heat on the workpiece. However, in the pulsed mode the overall cutting speed is decreased.

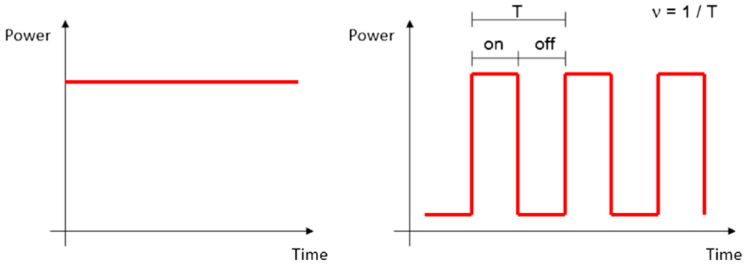

Figure 4.2 Continuous (left) and pulsed (right) mode of the laser cutting

Water jet and oxygen cutting are mostly used to cut plates, rather than profile sections. For hollow section profile cutting, laser cutting is the most effective option thanks to the possibility of automatic loading/unloading/handling systems. Most of the plasma cutting machines are dedicated to rather simple processing, without loading/unloading automation, and usually they work with a single piece at a time

with limited geometries. The quantified benefits of LCT compared with other cutting technologies are summarized in Table 4.1.

Table 4.1 Comparison between cutting methods (Aloke et al. 1997; Caristan 2003; Harničárová et al. 2010)

	Water-jet	**Plasma**	**Oxy-fuel**	**Laser**
Maximum thickness (carbon steel)	250 mm	50 mm	250 mm	30 mm
Heat Affected Zone	No	Large	Very Large	Small
Cutting speed	Moderate-fast	Very fast	Low	Very fast
3D processing	Difficult/not feasible	Difficult	Difficult	Easy/feasible
Metals processed	All	Only conductive	Only non-alloyed	All
Cut-edge quality	High	Moderate	Moderate	Very high
Dross	No	Moderate	High	Very small
Kerf width relative to laser-cut kerf width	3:1	4:1	3.5:1	1:1
Precision	Low-to-moderate (0.2 mm)	Very low (0.5 mm)	Very low (0.75mm)	Very high (0.05 mm)
Hollow section profile cutting	Not common	Possible but not efficient	Not common	Highly efficient

4.1.1 Influence of the surface properties on the laser cutting processes

There are three common surface issues related to the structural steel profiles: lubrication, coating and environmental effects (Caristan 2003). Lubrication does not affect the laser cutting process since a thin film of lubrication oil evaporates rapidly around the cutting surface before the melting of the metal. Zinc-based coatings, used for the improvement of the corrosion resistance, have a boiling temperature lower than steel (900 K vs 1800 K), but they may reduce the efficiency of laser cutting, reducing the cutting speed, due to the shielding of the zinc vapors. Oil mist, gasoline, dusts, rust and humidity adversely affect the laser cutting performance.

4.2 Heat Affected Zone induced by laser cutting operations

Heat Affected zone (HAZ) can significantly reduce the structural integrity of cut parts. HAZ is the non-melted area that undergoes micro-structural and mechanical variations due to the heat exposures during thermal processes on the workpieces, such as laser cutting processes. In the HAZ, ductility and fatigue resistance become lower, with problems in the cyclic behavior of the metal.

In (Caristan 2003), the author reports that the dimensions and the mechanical characteristics of the HAZ caused by LCT processes depend on the parameters applied during the cutting operations, such as laser power, wave-length, pulse types and assist-gas type. In comparison with the other cutting techniques, LCT induces smaller HAZ width, due to the application of heat in a very small area, which is normally extended to less than half of the workpiece thickness.

In (Harničárová et al. 2010), the previously exposed indications are confirmed. Authors report that the Heat Affected Zone (HAZ) induced by laser cutting beams is much smaller in comparison with other cutting methods and plasma cutting caused some micro cracks for the induced volume variations.

In (Andrés et al. 2016) a characterization of the HAZ produced by different thermal cutting processes (oxy-fuel, plasma and laser cutting), performed on the S640M structural steel of 15mm thickness, is presented. The study shows that the most reduced HAZ is achieved by laser-cutting. Plasma and laser cutting resulted in significantly higher yield and tensile strength with respect to oxy-fuel cutting.

The reduction of the HAZ obtained with laser cutting processes avoids material distortion and micro cracks that are unavoidable using plasma and oxygen cutting methods.

4.3 Influence on the fatigue strength of laser-cut workpieces

In (Bursi et al. 2017) authors performed a comparison of the mechanical cutting effects on the cut-edge properties of S355 plates, machined by traditional and laser cutting technologies. This study showed that mill and drill cutting techniques result in superior mechanical properties. However, material and high cycle fatigue properties of the edges obtained by laser cutting satisfied the code requirements provided by EN 1090-2:2018 (CEN 2018).

(Meurling et al. 2001) showed the results of an investigation on the fatigue properties of steel sheet made of carbon steel cut by laser and conventional mechanical methods. Lower fatigue strength was observed on the mechanical-cut specimens in comparison with laser cutting, due to the larger surface defects on the cut-edges.

In (Moazed and Fotouhi 2012) a study concerning welded square hollow-section T joints was presented. Authors compared the fatigue strength between T joints obtained by mechanical and laser cutting processes. Experiments with cyclic loading showed that the fatigue strength of the laser-cut specimens was higher with respect to those obtained with mechanical cutting. The authors also concluded that the hollow section profiles can be feasibly cut using LCT for an efficient joint assembly.

4.4 Cost and environment impact

Laser cutting machines requires initial investment cost higher than other traditional cutting methods. However, the overall costs and time spent for welding can be reduced in the whole life-cycle of manufacturing. In (Aloke et al. 1997) authors underlined the benefits of LCT in terms of eliminating human error on the cutting process, cost efficiency and quickness, manufacturing efficiency thanks to interface of laser machines with CAD/CAM tools, and quantified economic benefits of laser cutting for a wide range of industrial applications.

Environmental performance of the LCT also suppresses the other cutting methods. Laser cutting operations release much less noise and pollution. Besides, thanks to its high precision cutting, welding becomes simpler in the joint fabrication phase, releasing much less amount of slag. This improves considerably the workplace safety thanks to reduced use of welding.

5 Laser Cutting Technology for the realization of I-beam-to-CHS-column joints

In the previously exposed researches (Alostaz and Schneider 1996b, a; Schneider and Alostaz 1998; Alderighi 2007; Minouei and Mirghaderi 2009) the authors agree in saying that the best solution, from a mechanical behavior point of view, is the one with passing-through flanges and web plates or the through beam stub. Indeed, the continuity of the elements inside the column make possible the correct load transfer, from the beam to the column, and moreover the simultaneous stiffness of the column wall around the passing regions. Furthermore, in case of concrete filled column, the through elements interact with the concrete core, allowing a more satisfactory composite behavior. Nevertheless, this joint typology has not been successful in the steel construction market, due to the problematic fabrication and assembly processes. In fact, the difficulties in implementing cutting processes with high precision, which make possible the realization of fitted slots, did not allow the development of this construction technique, favoring more practice solution.

The application of the modern Laser Cutting Technology (LCT) to the fabrication and assembly of the I-beam-to-CHS-column joints, makes possible the realization of the connection with passing-through elements, reducing the fabrication and assembly problems. Indeed, laser cutting machines have the potential of performing high precision cutting processes on steel tubes and open sections with the typical structural dimensions. Although the laser cutting machines can realize slots with the nominal shape of the elements to be passed, some difficulties arise in the passage of them, due to the tolerances adopted in the realization of structural elements. In fact, the slot may be too small, nullifying the passage of the connecting elements, or may be too big, causing uncertainties in the mechanical behavior of the welds. Therefore, the realization of the presently studied joint with passing-through elements, require an

appropriate fabrication process, in order to reduce the problematics that spoiled the development of this construction technique.

For this purpose, the laser cutting machines have the intrinsic advantage of directly providing measuring instruments that can be used to measure the elements to be passed. Therefore, the whole fabrication process can start with the simultaneous cutting and measuring process of the I-beams and plates. Subsequently, slots can be realized on the tube-wall considering the previously taken and recorded measurements and applying a defined strict tolerance margin. In this way the correct passage of the beam portions or plates through the column is guaranteed and followed by the execution of the welds between the column wall and the beam. Furthermore, thanks to possibility of cutting with different inclination with the tube-face, the realization of penetration welding processes may be realized without performing any additional preparation on the worked-pieces.

LCT make thus possible the realization of the CHS-column-to-I-beam connection type that exhibited the better mechanical behavior in the past researches. Preliminary numerical and theoretical studies performed in the presently exposed work, confirm the advantages previously reported and allow the understanding of the global and local behavior of the connection in case of both vertical and horizontal loading on the structure. These studies allowed the obtaining of preliminary information on the global and local behavior and therefore the identification of the components that influence the behavior of the connection.

Considering the analyzed aspects inherent the practical realization and the mechanical behavior of the I-beam-to-CHS-column with passing elements, new joint solutions are presently proposed and described. These proposed solutions allow the realization of beam-to-column connections which have the purpose of behaving as rigid-full-strength joints or as nominally pinned connections. Furthermore, different typologies make possible the realization of interior and exterior beam-to-column joints with the beam connected in both the main directions.

5.1 Potential of LCT in the fabrication of I-beam-to-CHS-column connections

The application of the laser cutting to the steel construction industry is made possible thanks to the adoption of two different types of technology: CO_2 and fiber (Kanyilmaz 2019). Laser cutting machines adopting these technologies are capable of making any type of accurate cut in open sections elements and round tubes from 10 up to 508 mm in height or diameter, with wall thickness up to 20 mm and lengths up to 14 m. This make possible the realization of the I-beam-to-CHS-column

connection type with passing-through elements, which exhibited the best mechanical behavior in the previously exposed researches.

In fact, modern laser cutting machines, generally equipped with laser measuring instruments, can be firstly used to cut beam portions to be passed through the column, measuring simultaneously the actual dimensions, case by case, of these elements. Subsequently, two or more slots are realized in tube column wall, considering the previously taken and recorded measurements and applying a defined tolerance margin. In this way the correct passage of the beam portions through the column is guaranteed and followed by the execution of the welds between the column wall and the beam. Furthermore, steel profiles cut by LCT are also clean enough to go directly to the welding operation without additional processes.

These innovative I-beam-to-CHS-column connections, realized by using LCT, in addition to improve the mechanical behavior of structures, can reduce the overall cost and increase the aesthetics of buildings.

5.1.1 Laser cutting of tube and open section profiles

In (Kanyilmaz and Castiglioni 2018; Kanyilmaz 2019) advantages and disadvantages of the adoption of LCT for processing steel structure profile were discussed. Authors assert that, for the mild steels and low-alloy steels used in the hollow and I beam section profiles, the most currently adopted technology is the CO_2 laser cutting, which can cut up to 20 mm thicker plates with powers of up to 3,5 kW (25 mm, with 4,5 kW). Cutting speed is indeed influenced by the workpiece thickness (when the workpiece is thicker, the cutting speed is lower) and surface condition (rusted and painted surfaces require more cutting time and energy).

Disadvantages arise in the tube cutting, where the presence of the opposite wall should be considered when the parameters are fixed. Higher power cutting may cause the spraying of the inner tube wall with slag and melting and the overheating of the opposite wall. Thus, cutting of tubes often requires reduced power, with consequent longer processing time and reduced cutting quality. Furthermore, deviations of the laser beam may occur.

Different to standard cutting machines, laser cutting operation for structural profiles consists of the movement of both the cutting head and the work-piece. Laser cutting machines can be used for cutting round tubes and open section profiles from 10 Up to 508 mm in height or diameter, with wall thickness up to 20 mm and lengths up to 14 m. Whereas in tube-cutting the machine is able to cut the members from the exterior, in the cutting operation of open profiles, such as I-beams, the machine is able to cut flanges and web beam going in both sides of the element, allowing the cutting

of thicker elements. On the other hand, a problem arises in the cutting of the connection area between flange and web, where the thickness is higher and, consequently, the cutting speed has to be reduced.

A difference on the cutting geometry arises from the use of LCT instead of other conventional cutting techniques: both 2D and 3D geometries can be cut, thanks to the different positions that the laser tilting head can assume, as shown in Figure 5.1. In case of 2D cutting, the laser beam is guided in a horizontal plane, whereas the tube is rotating around its longitudinal axis (Figure 5.2-a). Consequently, the beam is always perpendicular to the surface of the processed tube.

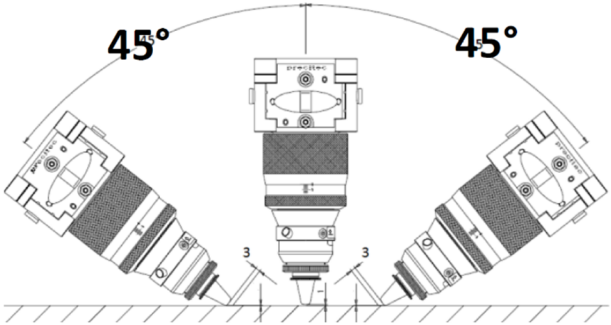

Figure 5.1 Possible positions of the laser tilting head (Castiglioni et al. 2016)

In case of 3D cutting, the laser beam is guided in a variable plane, whereas the tube is rotating around its longitudinal axis (Figure 5.2-b). In this case, it is possible to orientate the laser beam according to the required shape of the cut. A 3D laser-cutting machine can thus perform inclined cutting that allow the realization of partial and full-penetrating welding without other preliminary operations, such as realization of weld grooves. This operation reduces significantly the time spent during the joint shop assembly (welding preparation operations). However, according to (Kanyilmaz 2019), cutting speed in 3D cutting has to be reduced due to increment of the angle between the laser beam and the tube surface. In fact, the material thickness changes during the cutting process and the cutting parameters must be constantly adjusted to obtain good cutting results. In addition, the laser beam is inclined and does not flow exclusively into the cutting edge, due to the possible divergence of the gas.

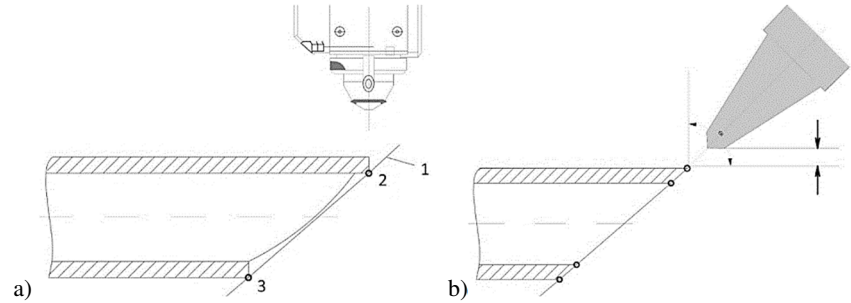

Figure 5.2 Laser cutting possible geometries: a) 2D cutting VS b) 3D cutting (Castiglioni et al. 2016)

In order to reduce problems, inclined cutting of the CHS profiles can be achieved in two steps sequentially steps: a) cutting of the 2D geometry with a standard projection rule (laser beam perpendicular to the surface), and b) cutting of the 3D geometry. 30° inclination can be obtained two times faster with respect to the 45° inclination since the thickness in the cutting direction was smaller and there is a lower reflection of the laser beam and the gas flux, which also increased the effective cutting power efficiency (Castiglioni et al. 2016).

5.1.2 Cutting tolerances

Laser cutting equipment allows cutting in steel profile with an accuracy of 10 µm (micro-meters) and repeatability of 5 µm. LCT machines are also able to recognize the differences between the expected profile and the real profile and the necessary compensation is automatically applied. As mentioned, the slot in the CHS column cannot be cut "a priori", taking into account the nominal sizes of the beam profile. In fact, steel structural elements are affected by geometric imperfections. EN 10034:1993 (CEN 1993) provides the allowable size scatters for the nominal dimensions of the profiles (e.g. flange thickness, flange width, depth, web thickness, out of square, web off center). This tolerance issue can be dealt in two ways: a) slots sized on the real dimensions of the beams, measured case by case, or b) the slots are oversized with respect to the nominal dimensions.

Each dimension of the I shaped slots, (e.g. the width of the flanges and web slots, the distance between the flanges slots) require a tolerance to make possible the beam passage through the column. The general scheme of the tolerances to be adopted can be seen in Figure 5.3. Tolerances influence, as well as the easiness of the assembly process, the quantity and the quality of the welding. In fact, strict tolerances can delay the joint assembly, leading to further manufacturing operation. On the other hand,

large tolerances can lead to a larger amount of welding and to a worse mechanical behavior of the connection. In order to reduce the gap, the beam cross-section geometry can be measured in detail, and then the column slot can be cut based on this geometry with very low tolerances (e.g. 1 mm). In this way, the cutting and the required welding quantity can be optimized.

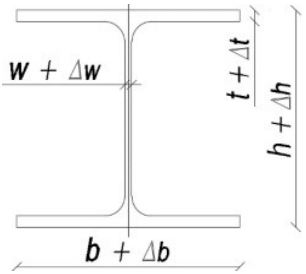

Figure 5.3 Nominal dimensions and tolerances

Several tests were performed in shop to study the influence of the tolerances adopted in the cutting process on the assembly one. The results were exposed in (Kanyilmaz and Castiglioni 2018). In the tests, each beam specimen was inserted through the two fitted slots made by laser cutting on the opposite sides of the CHS-column wall, as shown in Figure 5.4.

Figure 5.4 Pictures from the assembly tests (Kanyilmaz and Castiglioni 2018)

The CHS profiles used for the column and the corresponding beam profile adopted in the tests are reported in Table 5.1.

Table 5.1 CHS-column and I-beam or H-beam profiles adopted in the assembly test (Kanyilmaz and Castiglioni 2018)

Column profile	Column length	Beam profile	Beam length
CHS 355/9	900 mm	IPE 200	800 mm
CHS 355/9	700 mm	HEB 120	800 mm
CHS 406/18	1600 mm	IPE 400	800 mm
CHS 503/13	1100 mm	HEA 240	800 mm
CHS 503/13	1800 mm	IPE 500	800 mm

Each fitted slot has been created five times for each profile, with different tolerances applied to the nominal dimensions, as displayed in Figure 5.3. Table 5.2 shows the tolerances used for each slot (S1, S2, S3, S4, S5). Starting from 2 mm tolerance used for the cutting "S1" (Δt, Δw, Δb, Δh), slots were cut with increasing tolerances up to 6 mm for "S5", with respect to the nominal beam dimensions (t, w, b, h). For each beam profile, five specimens were tested and each specimen was ordered from a different steel supplier. Moreover, each specimen was inserted through the five different slots by both the external cross section. As result, 50 tests were performed for each beam profile.

For each tolerance, the number of specimens able to pass are reported analytically in Table 5.2 and graphically in Figure 5.5. As shown, a tolerance of 6 mm (S5) was necessary to allow the passage of all the specimens. However, a tolerance of 4 mm allowed the passage of all the specimen for HEB 120, HEA 240 and IPE 500 beams. Furthermore, a tolerance of 3 mm allowed only the passage of all the HEA 240 beam specimens, whereas the lower tolerance (2 mm) did not allow the passage of all the specimens for each beam profile. None of the cross sections could pass through the nominal dimensions of the cross section. Some specimens needed only the S1 tolerance (16%) and others needed all the way up to the S5 (10%). Nevertheless, the wide majority of cross sections fell in the midrange S2-S3-S4 tolerances (36%, 20% and 18% respectively). Table 5.2 and Figure 5.5 show a summary of the assembly tests.

Table 5.2. Tolerances adopted in the slot cutting and number of specimens able to pass through each slot type (Kanyilmaz and Castiglioni 2018)

Column section	Beam section	Number of specimens able to pass				
		S1: 2 mm	S2: 3 mm	S3: 4 mm	S4: 5 mm	S5: 6 mm
CHS 355/9	IPE 200	0	0	4	9	10
CHS 355/9	HEB 120	0	5	10	10	10
CHS 406/18	IPE 400	0	2	2	6	10
CHS 503/13	HEA 240	1	10	10	10	10
CHS 503/13	IPE 500	7*	9	10	10	10

* Six of these fail just because of the cutting imperfection of the rolling radius

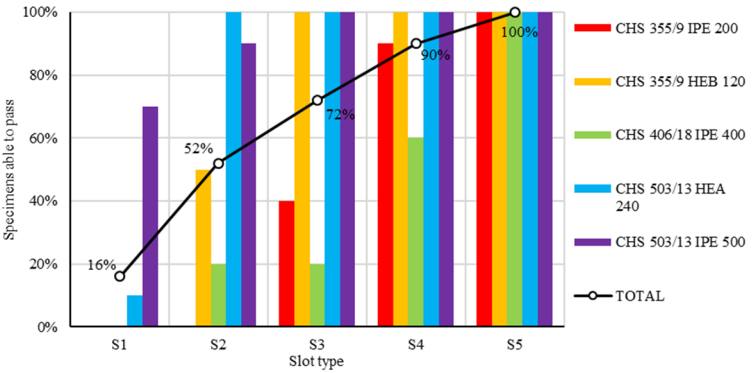

Figure 5.5. Specimens able to pass through the column by the different slot type

5.2 Fabrication, assembly and erection processes

The entire construction process for buildings equipped with the presented joints, realized using the LCT, needs three different main steps. The first step includes the laser cutting processes: I-beams and CHS-columns are cut by laser machine to provide the right element lengths and to execute the necessary slots, such as bolt holes and slots for the passage of plates and beams. The second step includes the shop-fabrication of column with beam stubs: I beam portions and plates are inserted inside the CHS-column through the laser-cut slots. Then, welding processes are performed to connect the passing-through beam portions and plates to the tubular column wall around the slot holes. The last step includes the transportation to the site of the shop-assembled parts and the erection of the building.

5.2.1 Laser cutting processes

The previously exposed tolerance study, shows that some of the beam specimens required slots made by very low tolerances (2-3 mm), whereas some others required slots with large tolerances (5-6 mm or even more). Therefore, it seems difficult to set a general optimized tolerance that can be valid for all the commercial profiles and can simultaneously satisfy the assembly and welding mechanical behavior purposes. A straight-forward solution would be to order beam profiles with strict tolerances from the supplier. An investigation made within the LASTEICON project (Castiglioni et al. 2016), shows that, in tubular profile sector, clients can order for stricter tolerances with an increased cost in the order of 10%. For the open section profiles, this is only possible for a significant amount of order for the same cross-section profile. The steel profile suppliers can guarantee a 15% improvement based on the code-requested tolerance values, if the order for one single type of profile is more than 100 tons. Thus, considering the common building construction tradition, such a request does not seem feasible. Another solution could be to set large tolerances to guarantee sufficient slot size for all profiles. However, this would increase the amount of welding in the cases of profiles having small geometry variations with respect to their nominal sizes. Moreover, the fatigue and seismic performance of such a welding solution with large gaps are expected to be poor.

Consequently, the most feasible solution is to cut the profiles based on their measured dimensions. This means the beam profiles should be measured in detail before or during the slot cutting operations, so that the column slots can be made almost according to the measured nominal dimensions with very small tolerances. This would optimize the welding quantity and increase the joint quality with minimum gaps. Modern laser cutting machines are generally equipped with measuring instruments Figure 5.6a. Therefore, they can be firstly used to cut beam portions and plates to be passed through the column, as shown in Figure 5.6b, and to measure simultaneously the nominal dimensions, case by case, of these worked-elements. The measurement results are stored and then, thanks to the fast marking capabilities of the laser machines, the part identifications will be marked on each beam. External girders may be also cut by laser cutting machines. Final result is an integrated approach merging the measurement and cutting during one single process with a single, automatically operated machine.

a) 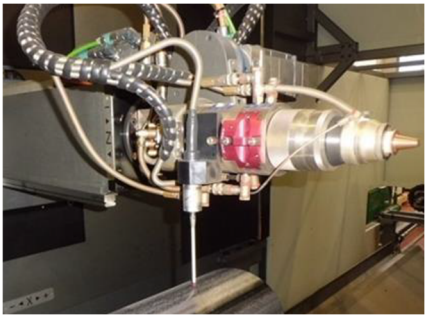 b) 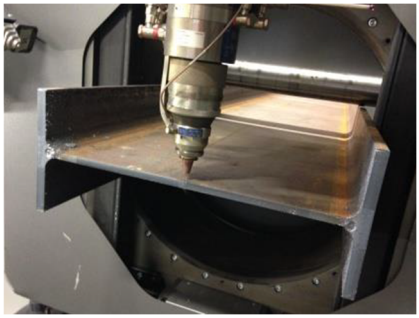

Figure 5.6 Laser cutting operations on beams: a) measurement probe integrated in a laser cutting machine, and b) laser cutting of an I-beam (Castiglioni et al. 2016)

After the cutting operations on beams and plates, in the case of the adoption of the described method based on automatically measured dimensions, a strict cutting tolerance, e.g. 1 mm, can be adopted in the column cutting operations. Indeed, two or more slots are realized in tube column wall, considering the previously acquired and recorded nominal dimensions and applying the defined tolerance margin (Figure 5.7a). The part identifications will be marked on each column (Figure 5.7b), in order to correctly couple beam stubs, plates and columns during the fabrication. In this way, the correct passage of the beam portions and plates through the column is guaranteed and followed by the execution of the welds between the column wall and the through elements.

a) 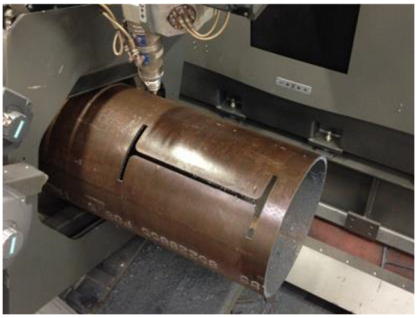 b) 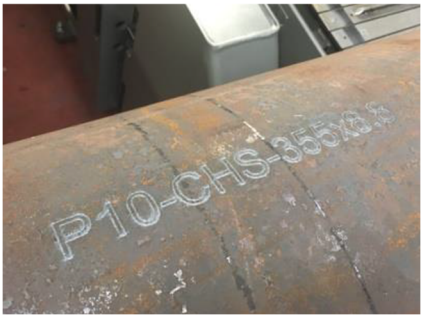

Figure 5.7 Laser cutting operations on column: a) slots realization on CHS-column, and b) part identification made by the laser cutting machine (Castiglioni et al. 2016)

5.2.2 Shop-fabrication operations

Considering the part identification made by the laser cutting machine, the column marks, composed by the CHS-column, I-beam-stubs and, eventually, plates, are

assembled on shop, as well as done in the prototype assembly shown in Figure 5.8. The elements are passed through the column and then tack welds are made in order to keep the correct positions during welding operations.

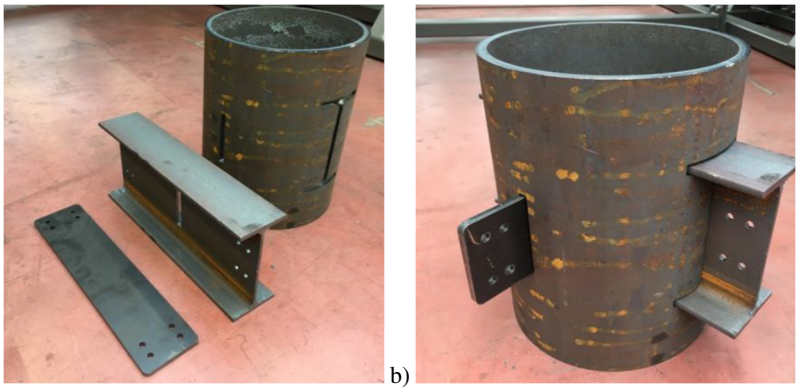

Figure 5.8 Assembly operations on a joint prototype: a) CSH-column with slots, beam stub and plate, and b) joint prototype assembly before welding operation (Castiglioni et al. 2016)

To connect the column face and the beam flange, fillet and full penetration welds are required all around the perimeter of the I-beam section slot. For the fillet welding, the column slots can be cut orthogonally with the smallest possible gap tolerance, e.g. 1 mm (Figure 5.9a).

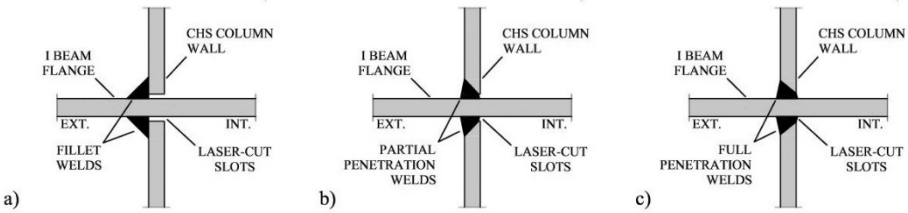

Figure 5.9 Welding possibilities for passing-through elements: a) fillet, b) partial penetration, and c) full penetration welding

Thanks to the 3D cutting process, partial and full penetration welding can be adopted as an alternative to the fillet one, as shown respectively in Figure 5.9b-c. Although welding penetration is allowed, welding is possible only from one side (back welding from inside the CHS profile is not feasible) and the weld quality can be verified by means of the penetrant and ultrasonic tests. The latter show if a full penetration is obtained in the case of tubular thickness up to 10 mm. On the contrary,

in case of thickness larger than 10 mm, it is not possible to qualify the joint as “full penetration”. Therefore, if the column profile thickness is more than 10 mm, the welded joint type should be downgraded to “partial penetration”. To obtain full penetration in such cases, there are two possibilities. Firstly, it is possible to increase the chamfer angle from 30° to 45°, with a double time and energy consuming, since the thickness in the cutting direction increases and the laser beam suffers higher reflection. Secondly, it is possible to increase the slot size, causing an increase of the welding amount.

5.2.3 On-site construction of the structure

The column marks and the external girder prepared in the workshop can be then transported to the construction site. Afterward, following the erection of the column marks, the bolted connections between external girder and beam stubs can be made, as shown for the prototype in Figure 5.10.

Figure 5.10 Assembly operations on a structure prototype (Castiglioni et al. 2016)

5.3 Preliminary studies on the mechanical behavior

Preliminary numerical studies are performed to investigate the mechanical behavior of the I-beam-to-CHS-column joint realized with the through stub. Attention is given to the mechanical behavior in case of vertical and horizontal loads on structures characterized by the presence of rigid full-strength beam-to-column connections, as required in order to develop a Moment Resisting Frame (MRF).

In case of vertical gravity loads on the structure, thanks to the continuity of the beam inside the column, it is possible to suppose that a great part of the bending moment on the girders is directly transmitted between the two sides and the beam-to-column joint need to transmit only the shear forces from the beams to the tubular column wall. In this case, the welds are designed to resist the shear forces and the connection may also rely on the direct contact between beam flanges and column wall. However, the direct contact and frictional forces cannot be considered in the design,

because it is very difficult to assess their real contributions. Obviously, if the welds are not designed to transmit the bending moment, beams must be designed considering them as a continuous beam on multiple supports, without considering the contribution to the rotational stiffness provided by the columns. This results in a higher positive bending moment in the external beams, whereas the central beams are not affected by significant changes.

In case of horizontal loads on MRF structures, connections are required to transmit bending moment between beams and column. In particular, considering the distribution of the moment of inertia of an I profile, the welding around the flanges transmits the majority of bending moment, and it can be designed to resist to the resultant axial force, which the flanges are subjected to, assuming the web absence.

5.3.1 Preliminary studies on the mechanical behavior under vertical gravity loads

Numerical feasibility studies are performed in the past to assess the mechanical behavior of the proposed joints when subjected to the action of gravity loads. These studies gave positive indications on the structural performances of tubular column joints realized by passing the beam through the column. Finite element models of two-way and four-way interior joints were developed to investigate the strength, stiffness, and stress distribution characteristics of some joint typologies subjected to gravity loads (Campolunghi 2012).

Finite element simulations include both material and geometrical non-linearity. Main beams are IPE300, secondary beams are IPE180 and columns are CHS355/-8 sections. The steel grade used was S275, and it does not play any important role in the present preliminary research, which is focusing mainly on the design and assembly procedures, tolerances, global and local behavior, rather than on the joint performance levels in terms of stiffness and strength correlated to the adopted steel grade.

The two-way connection consists in the IPE300 beam passing through the column, as shown schematically in Figure 5.11. The results in terms of normal stresses are shown in the contour plot shown in Figure 5.12. The development of the stress fields on the beam portion inside the column, highlights that there is an effective transmission of bending moments from one side to the other. Moreover, the deformed configuration shows that local buckling phenomena of the tubular column wall are excluded, thanks to the direct transmission of forces. This fact leads to a failure mechanism completely developed outside the node, with the girders that are able to develop plastic hinges, without leading to the node failure.

a) 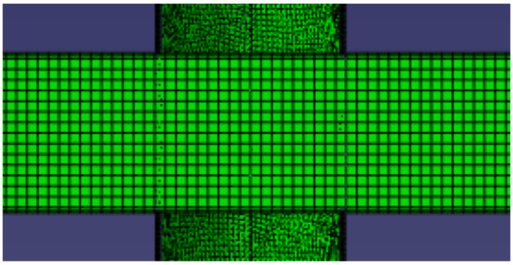 b) 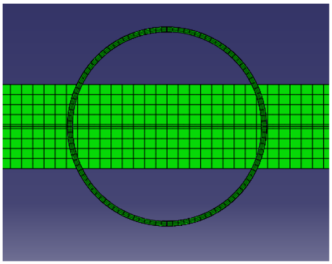

Figure 5.11 Finite element model of a two-way joint (Campolunghi 2012): a) Lateral view, and b) view from above

The four-way connection analyzed consists in one IPE300 beam passing through the column in the main direction, and three plates passing through the column in the secondary direction, externally connected to the IPE300 girders (Figure 5.13a). In Figure 5.13b, the normal stress distribution is shown under a joint rotation of 60 mrad.

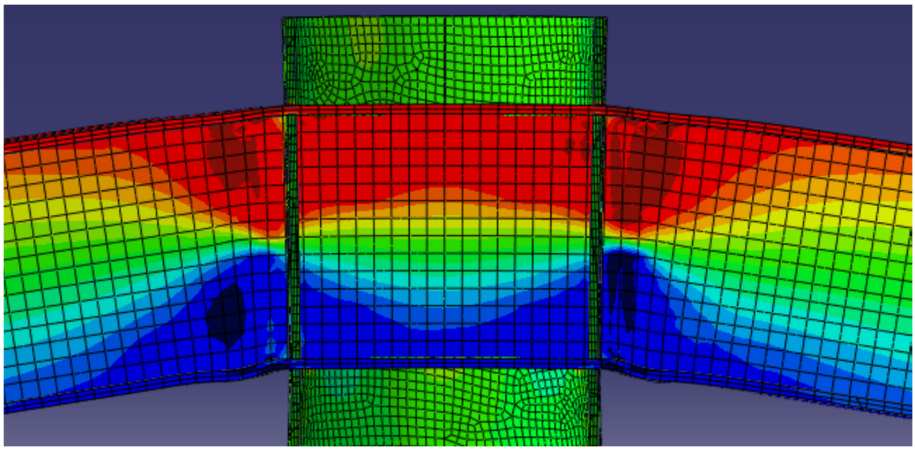

Figure 5.12 Von Mises stresses (red in tension and blue in compression) in the deformed configuration (Campolunghi 2012)

The girders are able to develop plastic hinges outside the node, until the local buckle of the lower flanges occurs, due to the development of high compressive stresses. Such as for the two-way joint analyzed, the column face does not suffer high stress concentrations and local buckling phenomena.

In Figure 5.14 the strength classification of passing-through joints, realized according to EN1993-1-8 (CEN 2005a), is reported. The limits for full-strength and pinned joints were defined considering the capacities of the connected beams and

columns (Campolunghi 2012). The passing-through joint with the continuous beam inside the node resulted to be able to transmit the bending moments efficiently, such as the node with T-flange passing-through plates. The joint realized by passing-through flange plates resulted able to reach the capacities of a full-strength joint but suffer a sudden drop of the capacities without developing ductile plastic hinges.

a) b)

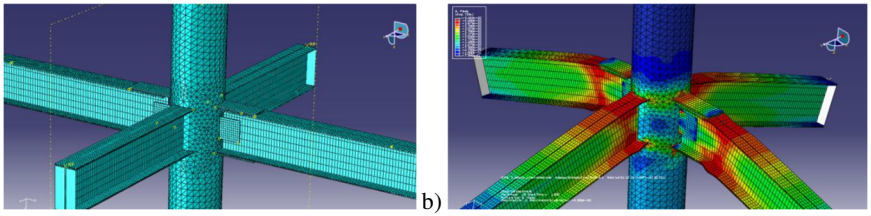

Figure 5.13 Finite element model of a four-way joint (Campolunghi 2012): a) 3D view, and b) Von Mises stresses at a rotation of 60 mrad

Although these studies gave significant indications about the behavior ogf the proposed joints under gravity loads, the connections analyzed are interior beam-to-column joints and the load configurations adopted are perfectly symmetric. Therefore, possible different behaviors may develop in case of asymmetric configurations, for both the geometry of the node and the applied gravity loads.

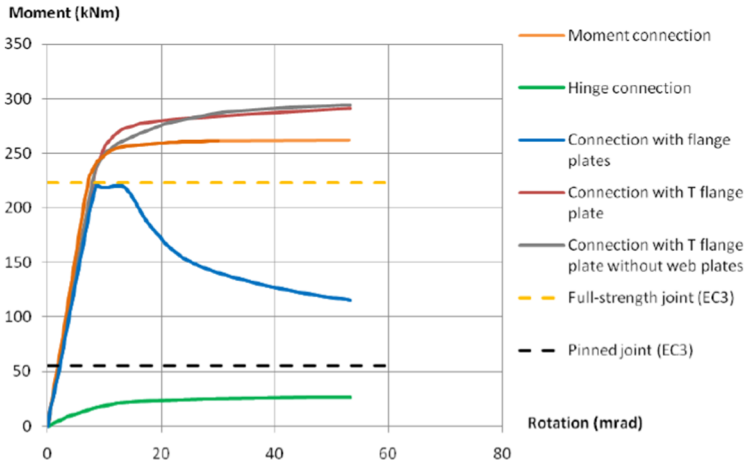

Figure 5.14 Strength classification of the joints (Campolunghi 2012)

5.3.2 Preliminary studies on the mechanical behavior under horizontal loads

Considering the lack of numerical studies about the behavior of the proposed passing-through joints under horizontal loads, an analytical Finite Element Model (FEM) was developed. The FE model, developed in ABAQUS, represents a connection between a CHS 355.6/10 column and IPE400 beam, and was used to perform monotonic analysis in order to confirm the theoretical predictions and to have further information on the mechanical behavior of passing-through joints under horizontal loads, such as wind or seismic actions.

The beam and the column were modelled as schematically shown in Figure 5.15. The cutting tolerance adopted is 2 mm on each side. The fillet welds around the slot are sized considering the current practical method, verifying that the lateral leg length of the welds z is higher than the 75% of the minimum thickness of the connected elements. Therefore, the resulting throat thicknesses were 6 mm for the flange welds and 4 mm for the web welds.

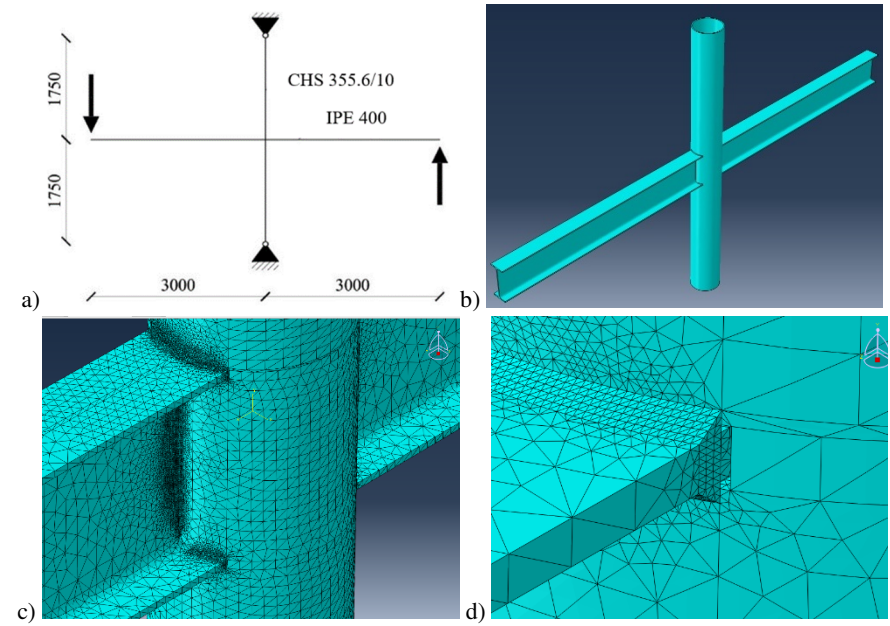

Figure 5.15 Preliminary numerical model of the proposed connection: a) geometrical and mechanical characteristics, b) global 3D view of the model, c) mesh adopted in the connection, and d) mesh adopted in the weld region

Homogeneous material properties were assumed, without considering the different mechanical characteristics of the main material, the welds and the Heat Affected Zones (HAZs). S355 steel properties were adopted whit reference to the results obtained in the OPUS research project (Finetto et al. 2007). The multi-linear true-stress-true-strain diagram of the steel was defined starting from the corresponding engineering values. The 4-node isoparametric tetrahedral elements were used, with a different size for the various element, as shown in Figure 5.15c, whit a minimum size of 2 mm used in the welding zone (Figure 5.15d). The top and the bottom of the column were constrained with hinges, whereas the loads were applied as imposed opposite vertical displacements in the beam-ends (Figure 5.15a).

The analysis performed highlights that the first damage occurred in the flange welds, as shown in Figure 5.16 and Figure 5.17. In these figures, blue elements are undamaged, whereas the black ones reached the critical deformations, and were therefore deleted during the simulations. The element deletion was performed through the application of the damage criterion for ductile materials, based on the deformations. The damage initiation points and the damage evolution criteria were defined to have a behavior close to the one of the steels provided by the database of the previously mentioned OPUS project.

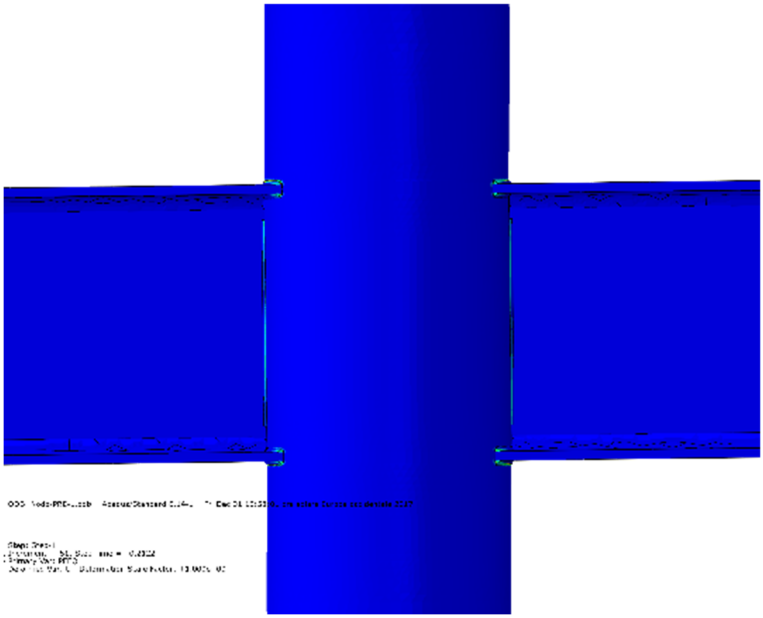

Figure 5.16 Equivalent Deformations in the final step

In addition, the behavior curve in terms of bending moment and relative rotation, defined with the FE model and reported in Figure 5.18, showed that the joint lost its rigidity before the first yielding of both beam and column. Moreover, taking into account the classification of beam-to-column joints by strength and stiffness, proposed by EN1998-1-8:2005 (CEN 2005a), the connection analyzed resulted as semi-rigid joint in the elastic range.

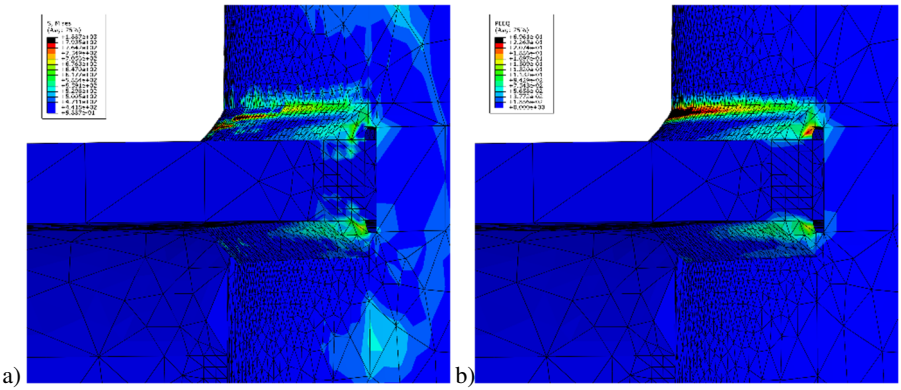

a) b)

Figure 5.17 End step of the preliminary numerical simulation: a) Von Mises stresses and b) equivalent deformations in the welds in tension in the beam flange

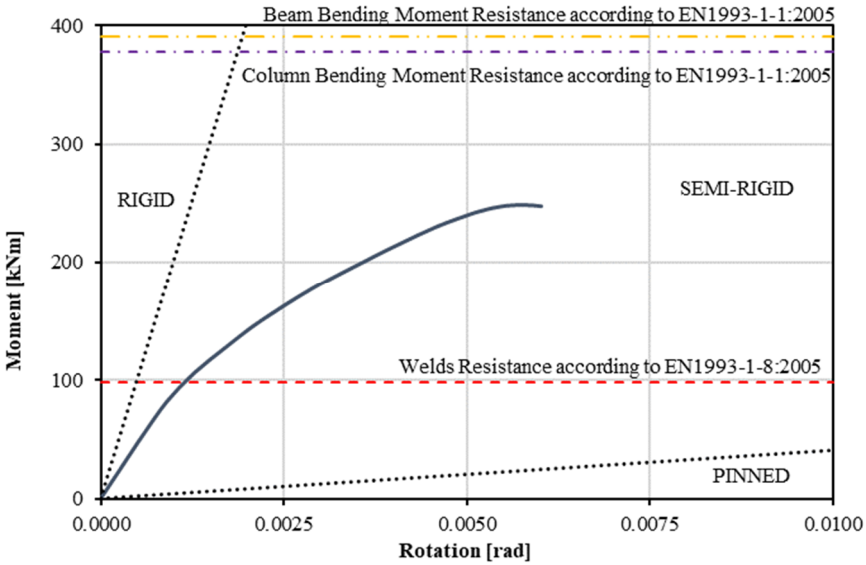

Figure 5.18 Moment-Rotation behavior of the connection FE model

Although these results are due to the sizing of the welds, this preliminary study confirmed the leading role of the flange welds in the mechanical behavior of the connection, in case of horizontal loads on MRF structures. Clearly, the beam continuity inside the column provide benefits as, for instance, the contribution to the rigidity of the column wall against local buckling and the better distribution of the flange axial force on the column wall.

The analysis results showed the influence of the column bending moment on the behavior of the welds. In fact, due to the presence of the bending moment, the column wall is subjected to compression and tension in the opposite welded side, as shown in Figure 5.19 (with the column also subjected to compression due to the gravity load) and Figure 5.20. Thus, the welds are subjected to shear stresses perpendicular to its axis and normal stresses perpendicular to the throat, according to EN1998-1-8:2005 (CEN 2005a) and considering the overturning effective section.

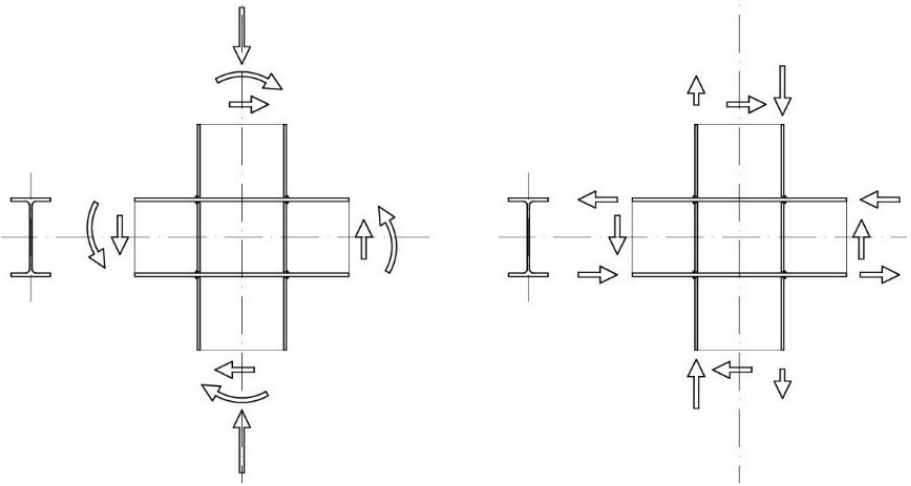

Figure 5.19 Beam and column stress components under horizontal loads on the structure

Furthermore, the stresses in the column wall turn out to be eccentric with respect to the welds, probably resulting in problems concerning the formation of cracks, especially under cyclic loads. Therefore, full and partial penetration welds may be preferred, instead of fillet, from a mechanical point of view.

Numerical preliminary analyses confirm that studying the mechanical behavior of the proposed connection, under horizontal load on the structure, is very close to studying the mechanical behavior of the beam-flange welding region under alternatively tension and compression axial loads. In the presented analysis, only fillet

welds are analyzed. In fact, other welding typologies are less susceptible to the tolerance adopted, thanks to the penetration of the welding which leads to fill the gap between beam flanges and column wall. Moreover, to ensure the welding penetration, the gap should be higher than a minimum value, otherwise the 3D laser cutting process should be adopted.

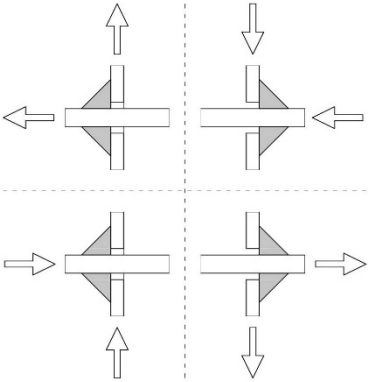

Figure 5.20 Schematic representation of the forces acting on the welds in case of opposite bending moment in the beams, such as under horizontal load on the structure

5.3.3 Preliminary numerical analyses on the weld mechanical behavior

According to the results of the previously reported studies, when horizontal loads act on MRF structures, joints between columns and beams must ensure the transmission of the bending moment. Furthermore, in case of exterior beam-to-column joints or interior joints subjected to asymmetric gravity loads, part of the bending moment has to be transmitted to the column and it is not possible to consider the complete direct transmission of loads. In this fields, the welds between beam flanges and column wall should provide the transmission of the consequent axial load in the flanges to the column wall.

Thus, preliminary numerical monotonic analyses were performed in ABAQUS to study the flange welds mechanical behavior and the influence of the cutting tolerance on this behavior. Fillet weld connections between two orthogonal plates (Figure 5.21), simulating the CHS-column wall and the H-beam flange, were numerically analyzed, whit different slot dimensions. Due to this configuration, the study does not consider the influence of the curvature of the column wall and relative welds.

For each model, different total tolerances between 1 mm and 8 mm (Table 5.3) were adopted, in order to study the influence of the slot width on the strength and

stiffness of the welds. Table 5.3 reports all the geometric characteristics. The effective throat thicknesses were assumed equal to 4 mm.

a) 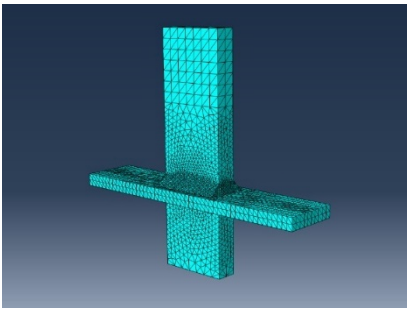 b) 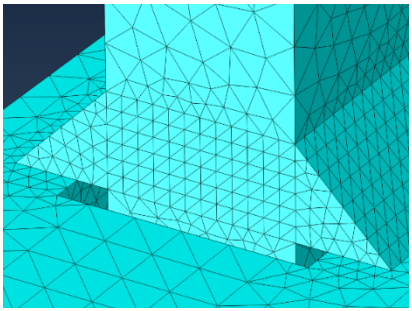

Figure 5.21 Preliminary numerical model of the welds for the "2C" model (Table 5.3): a) global 3D view and b) particular of the mesh adopted in the model

Homogeneous material properties were assumed, with S355 steel properties already mentioned. The 4-node isoparametric tetrahedral elements were used, with different sizes for the various element, as shown in Figure 5.21.a, whit a minimum size of 1 mm used in the welds (Figure 5.21.b). The lateral faces of the horizontal plate were constrained with full connections, whereas the load was applied as vertical displacement in the bottom part of the vertical plate. Both push and pull cases were analyzed in order to study the difference in the behavior and start to understand the cyclic behavior of the welds, in case of different slot widths.

Table 5.3 Denomination and tolerance of the models

Denomination	Vertical plate width	Slot width	Tolerance
2A	12 mm	13 mm	1 mm
2B	12 mm	14 mm	2mm
2C	12 mm	16 mm	4mm
2D	12 mm	18 mm	6 mm
2E	12 mm	20 mm	8 mm

An example of the damage occurred in the welds is reported in Figure 5.22. All the analyses highlighted that under both pulling and pushing force in the vertical plate, the strength of the welds is influenced by the width of the slot, instead the elastic

stiffness of the welds is not particularly influenced by the gap adopted, as shown Figure 5.23.

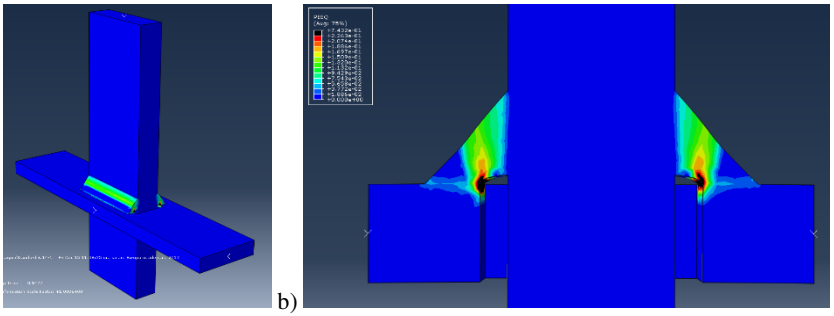

Figure 5.22 Von Mises deformations in the welds ("2C" model) whit pulling force in the vertical plate; the blue parts are undamaged, whereas the black ones reached the critical deformations

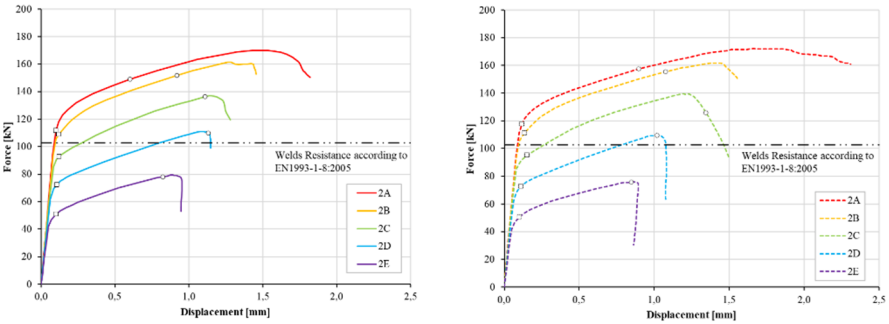

Figure 5.23 Mechanical behavior of the welds obtained by the preliminary numerical analyses for different slot widths (Table 5.3) in case of pulling (left) and pushing load (right)

In Table 5.4 are reported the values of the pulling or pushing force which corresponding to the first damage in the weld elements. As showed, the welds were able to develop their design resistance, calculated according to EN1993-1-8:2005, just for low tolerances ("2A", "2B"), whereas in case of higher dimensions of the slot the welds become damaged before reaching the design strength, equal to 102.58 kN.

Although these preliminary results are not exhaustive, due to the simplification adopted in the models, they confirmed that the tolerances adopted in the laser cutting process influenced the mechanical behavior of the fillet welds between beam flanges and column wall and may influence the mechanical behavior of the proposed connection in case of horizontal loads on an MRF structure.

Table 5.4 Denomination and tolerance of the models

Denomination	Pulling force at the first damage	Pushing force at the first damage
2A	111.69 kN	117.71 kN
2B	108.83 kN	111.17 kN
2C	92.90 kN	95.21 kN
2D	72.23 kN	72.70 kN
2E	50.99 kN	50.50 kN

5.4 Proposed design solutions

Considering both the practical and mechanical aspects inherent the I-beam-to-CHS-column connections with passing-through elements, joint solutions are proposed and described. These solutions allow the realization of beam-to-column connections which have the purpose of behaving as rigid-full-strength joints or as nominally pinned connections. Furthermore, different typologies make possible the realization of interior and exterior beam-to-column joints with the beam connected in both the main directions and with different restrains configurations.

5.4.1 Rigid full-strength connections

Two type of rigid full-strength beam-to-column connections between open beams and tubular columns may be realized by passing-through elements. The first type (Type R1) is realized by passing a beam portion through the CHS column (Figure 5.24). The beam portion is welded around the slots where it is passed and then connected by beam-to-beam connections to the external beams, which have the same section. For this beam-to-beam joint, a bolted connection with horizontal flange plates and vertical web plate is one of the most practical solution; others solution may be realized, such as a welded connection.

The second solution (R2) allows the rigid connection of the secondary beam in case of concurrently passing-through main beam. In this case the continuity of the beam is made by passing-through the column three plates (Figure 5.25). Two plates are horizontal and passing on the bottom and on the top of the main beam, whereas the third plate is vertical and passing-through the column and the main beam web. For this reason, one vertical slot has to be realized on the web of the passing-through main beam portion. Plates are then welded around the slots on the column wall and connected to the flanges and the web of the external beam. In order to allow this

solution, secondary beam need to have the same or higher height, in comparison with the main beam. As for the joint type R1, in the joint type R2 the connection with the external beam may be made in different way. The most practice solution is bolting the plates to the web and flanges of the beams.

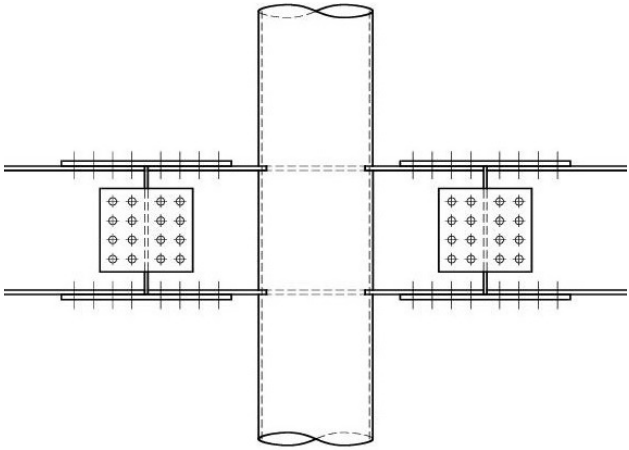

Figure 5.24 I-beam-to-CHS-column proposed rigid connection with the passing-through beam portion R1

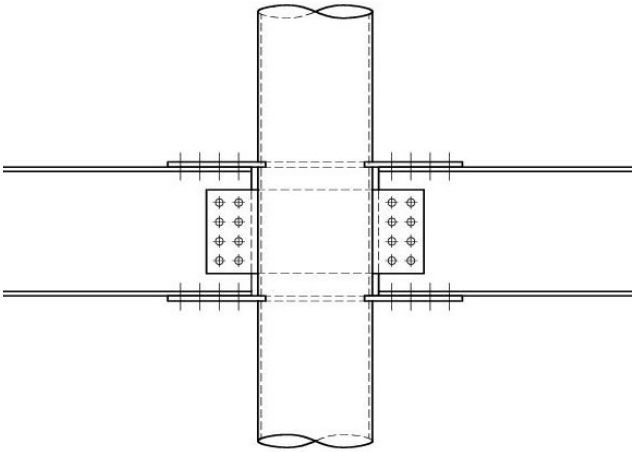

Figure 5.25 I-beam-to-CHS-column proposed rigid connection with three passing-through plates, one vertical and two horizontals R2

5.4.2 Nominally pinned connections

Besides the realization of rigid full-strength joints, two type of pinned connection, made by passing-through elements, are possible. The first type (P1) is made by using a passing beam portion welded around the slots and then bolted by web plates to the external beam, as shown in Figure 5.26. In this case the section of the passing-through beam portion may have different dimensions in comparison with the external beam.

The second solution (P2) is realized by passing, through the CHS column, one vertical plate welded around the slots and bolted to the external beam webs (Figure 5.27). Pinned connection P2 allows the realization of four-way joints characterized by passing-through beam portion in the main direction, with external hinged or fixed bolted connection. Solutions are possible by realizing an additional vertical slot in the main beam portion web and then by passing-through three slots the vertical plate. Obviously, the welding is not achievable around the slot made on the beam web.

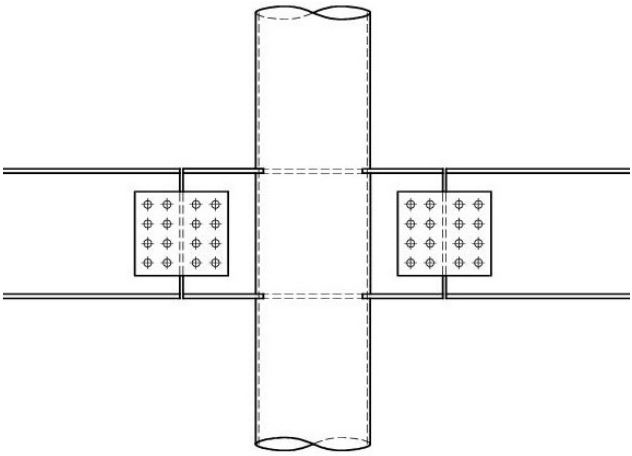

Figure 5.26 I-beam-to-CHS-column proposed pinned connection with a passing-through beam portion P1

Pinned connection P1 is required only when a double hinged connection has to be realized in a four-way joint. In fact, in this case, is not possible to pass two perpendicular vertical plates, otherwise the slot made in one of the plates, to pass the other plate, reduces considerably the resistance area.

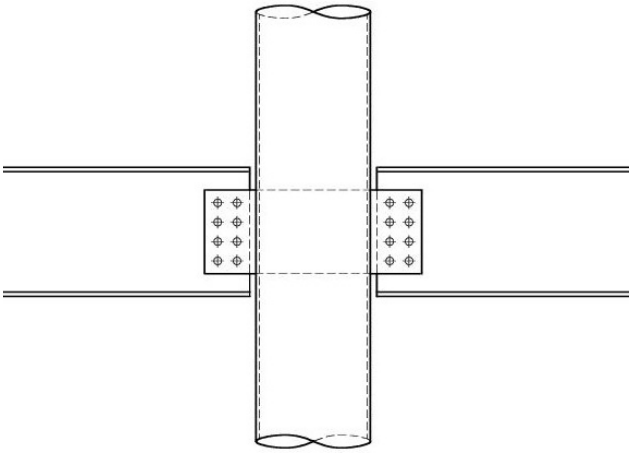

Figure 5.27 I-beam-to-CHS-column proposed pinned connection with one vertical passing-through plate P2

5.4.3 Four-way joints

Three different solutions of four-way joint are possible. The first type is nominally pinned in both transverse and longitudinal directions with the main external beams connected to a beam portion that pass through the CHS column in the longitudinal direction, as exposed for the connection type P1, whereas in the transverse direction, external beams are connected to a vertical plate, which is passed through the CHS column and through the web beam, as shown for pinned type P2.

The second type of four-way connection is nominally pinned in the secondary direction and rigid full-strength in the main one. External main beams are connected to an I-beam portion passing-through the CHS column in the longitudinal direction, as for the R1 type, whereas in the secondary direction beams are connected to a vertical plate passing-through the CHS column wall, as well as through the beam portion web, similar to P2 type.

The last four-way connection type is a double full-strength beam-to-column joint. Main beams are connected to a beam portion as for R1 type, whereas secondary beams are connected to the three plates, such as for the R2 type. The two horizontal plate are passed through two slots made on the CHS column wall, whereas the vertical plate has to pass through the web of the main passing-through beam portion.

6 Preliminary experimental tests on two-way steel joints

Considering the final objective of developing mechanical models for both steel and composite I-beam-to-CHS-column joints, a testing program is defined, including tests on pure steel and composite steel-concrete substructures specimens. The preliminary experimental tests on steel joint are performed not only to assess the global behavior of the different previously presented types of joints, in case of steel structures, but mainly to obtain detailed information on the local performance of the singular components, which can be useful in the mechanical characterization of both steel and composite connections.

In fact, tests on the pure-steel substructures allow the acquisition of information on the overall performance of the connections, in case of not filled tubular steel columns and steel I-beams without a compound behavior with the concrete slab. Furthermore, the information obtained from these tests on pure-steel substructures are useful for the development of the mechanical models for both the steel and composite connections. Pure-steel tests allow the acquisition of simpler information on the behavior of the steel components which can be also used in the mechanical models of the composite joints.

In the following paragraphs, the configurations adopted, the specimens tested and the results obtained are briefly reported and described. The design of specimens and of the testing setups is not part of the present work and therefore these parts are not herein reported.

The whole program includes tests carried out to characterize the monotonic behavior of the proposed connections under vertical gravity loads on the structure, and both the monotonic and cyclic behavior under horizontal loads, such as wind or earthquake. All the tests are performed within the LASTEICON research project (Castiglioni et al. 2016). Experimental investigation on two-way specimen of pure-steel substructures are performed in the “Laboratory of Civil and Mechanical

Engineering" (LGCGM) of the INSA Rennes University (Institut National des Sciences Appliquées Rennes).

6.1 Description of the experimental campaign on steel joints

In the experimental campaign, the mechanical behavior of steel beam-to-column connection is assessed by performing experimental simulation on full-scale substructures, simulating the action of both vertical gravity and horizontal load on the main structure. In the first type of test, only monotonic loads are applied, whereas the tests with the horizontal loading configuration are carried out applying both monotonic and cyclic loads. Monotonic horizontal tests are firstly performed to get information useful in the definition of the cyclic test loading procedures, in particular the yielding load and the yielding displacement. Moreover, monotonic tests highlight the impact of cyclic loadings on the ductility and resistance and show the degradation of the mechanical behavior.

The experimental simulations are carried out on two-way specimens. Tests on steel specimens are useful in order to have information more easily interpretable on the performance of the joints and the individual components. All the steel joint type to be tested are summarized in Table 6.1. Two type of rigid full-strength two-way connection are tested. All the tested specimens are full-scale substructure representing interior beam-to-column joints. Column height and beam lengths are different, case by case, according to the laboratory features and loading conditions.

Table 6.1 Steel connections tested in the experimental campaign

Den.	Specimen type	Connection type
C3	two-way	Passing-through beam stub R1
C4	two-way	Passing-through vertical web plate and horizontal flange plates R2

The first rigid full-strength beam-to-column connection, C3, is realized by passing a beam portion through the CHS column, as shown in Figure 6.1a. The second tested solution, C4, is characterized by three passing plates, as shown in Figure 6.1b. This latter solution can be useful to allow the rigid connection of the secondary girders in case of concurrently passing-through main beam, and it is characterized by the presence of two horizontal plates that pass on the bottom and on the top of the main beam, and one vertical plate that pass through three slots, two on the column wall and one on the main beam web.

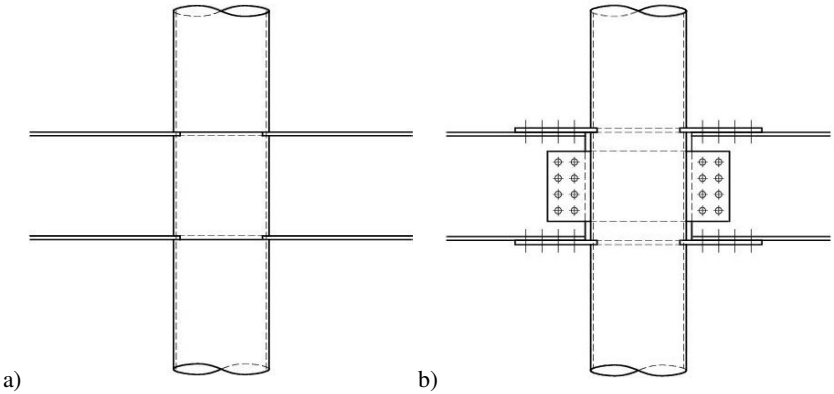

a) b)

Figure 6.1 Two-way beam-to-column rigid full-strength connections: a) C3, and b) C4

Steel two-way specimens are tested two different setups. The first one is used to simulate the action of gravity loads, whereas the second configuration simulates the action of horizontal loads. In the latter configuration, displacements are applied with both monotonic and cyclic history, whereas the vertical loads are simulated only with a monotonic displacement history.

Several two-way configurations are tested in the "Laboratory of Civil and Mechanical Engineering" (LGCGM) of the INSA Rennes University (Institut National des Sciences Appliquées Rennes). The execution of tests on pure-steel substructures allow the acquisition of information on the overall performance of the connections in case of steel buildings. Furthermore, the acquired results on pure-steel substructures are useful for the development of the mechanical model for both the steel and composite connections. Indeed, pure-steel tests allow to obtain simpler information on the behavior of the steel components which can be also used in the mechanical models of the composite joints.

6.1.1 Substructure specimens

In these tests, moment resisting full-strength connections, are defined and designed to be tested. Both C3 and C4 specimens are 2D steel substructure characterized by the presence of the beam-to-column two-way joint. All the beams have IPE400 section and the CHS-columns have the external diameter equal to 355.6 mm in each case, whereas the thicknesses are different case by case. The total height of the column is 2.40 m, and the total beam length is 5.40 m. In case of passing-through beam (C3) the external beam-to-beam bolted joints are excluded in order to reduce the uncertainties related to the bolted connection in the experimental test results. For practical issues,

mainly regarding the logistic of specimens, in this case beams are break off 1.20 m far from the joint and the continuity is replaced by full-strength beam-to-beam joints (Figure 6.2), characterized by bolted flanged connections designed to remain in elastic range during the execution of tests, in order to avoid any yielding/failure in these connections and clearly observe the failure in the node region. Specimens characterized by the three passing plates (C4) have the same overall dimensions of C3 but do not present the external flanged joints (Figure 6.3).

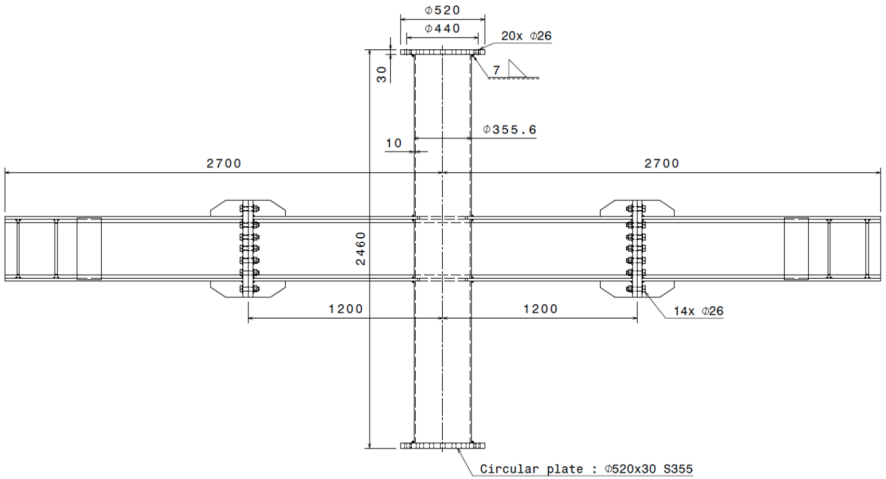

Figure 6.2 Overall dimension of the C3 specimen type tested at INSA-Rennes

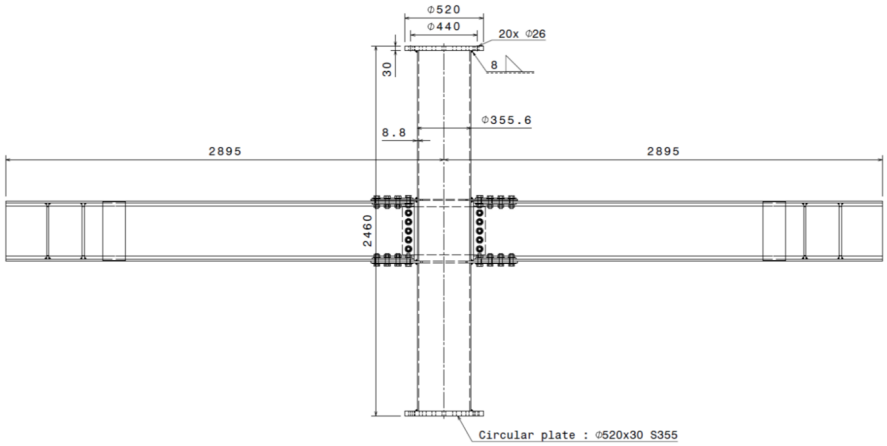

Figure 6.3 Overall dimension of the C4 specimen type tested at INSA-Rennes

The geometry of specimens C3 are presented in Table 6.2. These substructures mainly differ for the tube wall thickness, which is equal to 8.8, 10.0 and 12.5 mm respectively for connections C3-1, C3-2 and C3-3. C3-1 is characterized for the use of full penetration welding to connect the beam to the tube wall, whereas C3-2 is characterized by the presence of both fillet (C3-2A) and full penetration (C3-2B). For the last type of specimen, C3-3, only fillet welds are considered.

Table 6.2 Details of C3 specimens tested at INSA-Rennes

Den.	Loading Config.	Loading Type	Column Thick.	Welding	Axial Load on the Column
C3-1B-1	Sym.	Monotonic	8.8	Full penetration	No
C3-1B-2	Asym.	Monotonic	8.8	Full penetration	No
C3-1B-3	Asym.	Cyclic	8.8	Full penetration	No
C3-2A-1	Sym.	Monotonic	10	Fillet	No
C3-2A-2	Asym.	Monotonic	10	Fillet	No
C3-2A-3	Asym.	Cyclic	10	Fillet	No
C3-2B-1	Sym.	Monotonic	10	Full penetration	No
C3-2B-2	Asym.	Cyclic	10	Full penetration	No
C3-2B-3	Asym.	Cyclic	10	Full penetration	Yes
C3-3A-1	Sym.	Monotonic	12.5	Fillet	No
C3-3A-2	Asym.	Monotonic	12.5	Fillet	No

Table 6.3 reports the details of C4 specimens. These specimens differ for the thickness of the tube wall and plates. C4-1 and C4-2 have 8.8 mm thick tube wall, C4-3 and C4-4 have 10 mm thick tube wall, and C4-5 and C4-6 have 12.5 mm thick tube wall. Furthermore, C4 specimens differ for the plates thicknesses, which are equal to 10 mm (flanges) and 8 mm (web) for C4-1, C4-3 and C4-5, and equal to 12 mm (flanges) and 10 mm (web) for C4-2, C4-4 and C4-6. Full penetration welding is used in C4-1, C4-2, C4-3 and C4-4 substructures, whereas in the C4-5 and C4-6 cases, fillet welding is applied. The bolted plate-beam connections are designed to avoid as soon as possible yielding or failure in this part of the joint. For this purpose, additional plates are welded to flanges plates and beam flanges to limit net section/block shear failure. The bolts will be preloaded.

Table 6.3 Details of C4 specimens tested at INSA-Rennes

Den.	Loading Config.	Loading Type	Column Thick.	Flange Plates	Web Plate	Welding	Axial Load on the Column
C4-1B-1	Symmetric	Monotonic	8.8	180x10	320x8	Full penet.	No
C4-2B-1	Asymmetric	Monotonic	8.8	180x12	320x10	Full penet.	No
C4-2B-2	Asymmetric	Cyclic	8.8	180x12	320x10	Full penet.	No
C4-3A-1	Symmetric	Monotonic	10	180x10	320x8	Fillet	No
C4-3B-1	Symmetric	Monotonic	10	180x10	320x8	Full penet.	No
C4-4B-1	Symmetric	Monotonic	10	180x12	320x10	Full penet.	No
C4-4B-2	Asymmetric	Monotonic	10	180x12	320x10	Full penet.	No
C4-4B-3	Asymmetric	Cyclic	10	180x12	320x10	Full penet.	No
C4-5A-1	Symmetric	Monotonic	12.5	180x10	320x8	Fillet	No
C4-5A-2	Symmetric	Monotonic	12.5	180x10	320x8	Fillet	No
C4-6A-1	Asymmetric	Monotonic	12.5	180x12	320x10	Fillet	No
C4-6A-2	Asymmetric	Cyclic	12.5	180x12	320x10	Fillet	No
C4-6A-3	Asymmetric	Cyclic	12.5	180x12	320x10	Fillet	Yes

6.1.2 Testing setups

Specimens are tested with two loading conditions: a) vertical gravity loads, where the beams transmit opposite bending moments to the column, and b) horizontal loads, simulating the action of wind or earthquake, where the beams apply equal bending moments to the column. For the two load cases, the same test setup is used and only the loads apply by the hydraulic jacks are different. For the gravity loads, the two hydraulic jacks apply loads in the same direction, as shown in Figure 6.4, whereas in Figure 6.5 is shown the setup for the second case, where the load-jacks apply forces in opposite directions, in order to simulate the action of horizontal loads on the structure.

In the test setups, the specimen, composed of the beam and the column, is pinned at each extremity of the CHS column by roller. The roller on the bottom is fixed by bolts to the strong floor. The upper roller is fixed on a HEB 400 beam. This beam is connected to a frame composed of two HEA 300 column and 4 lateral bracings HEA 200, which does not allow the out-of-plane displacements of the column. Two 1500 kN hydraulic jacks apply vertical loads to the beams at each extremity at 2.50

(Symmetric load case, Figure 6.4) or 1.70 m (asymmetric load case, Figure 6.5) from the axis of the CHS column. Lateral-torsional bracings are placed in both cases to limit the lateral torsional buckling of the beam.

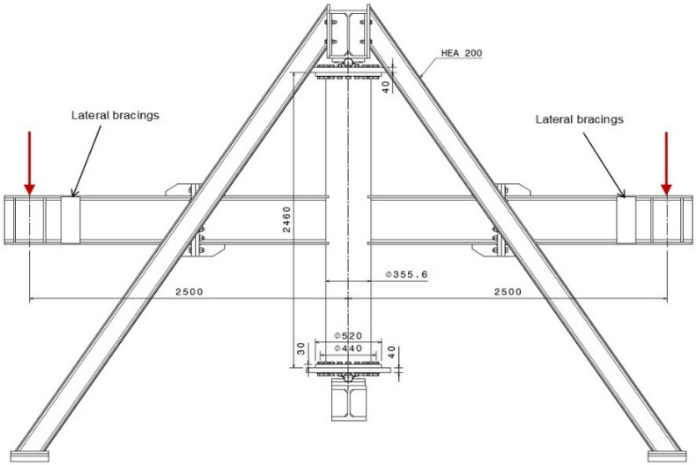

Figure 6.4 "Symmetric" test setup for the execution of tests with gravity load condition in the INSA-Rennes laboratory

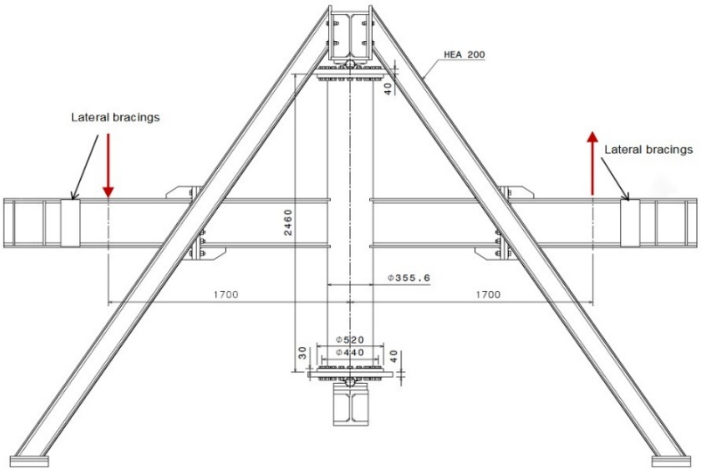

Figure 6.5 "Asymmetric" test setup for the execution of tests with horizontal load condition in the INSA-Rennes laboratory

Some tests are performed on beam-to-column specimens where an initial compression force of 800 kN is applied to the column, representing the compression due to gravity loads. The value of the axial force corresponds to 15-20 % of the compression resistance of the tubes tested. The compression is applied by preloading the column with eight steel rods anchor to circular end plates bolted to the top and the bottom of the column. Linear strain gauges are used to estimate the preloading in the steel rods.

6.1.3 Adopted instrumentation

The instrumentation used during the tests is made by inclinometers, inductive displacement transducer, strain-gauges and load cells, disposed on the whole substructure and test setup, in order to characterize opportunely both the monotonic and cyclic global behavior of the specimens, in terms of external reactions and global displacement, and to acquire information on the local mechanism. Data deriving directly from the experimental output are in fact useful to investigate the transfer mechanism of the internal forces.

In particular, inductive displacement transducer, inclinometers and strain gauges can provide information about the kinematics of the specimens and the deformations in some points opportunely chosen. The load cells allow the calculation of the imposed forces and, considering the statically defined scheme of the test, it is possible to obtain the distribution of the bending moment and shear force in each beam and column section. The total bending moment can be used to confirm the results obtained by strain gauges, by calculating the axial forces acting locally on the singular components, with the decomposition of the moment and the consequent deformations.

The instrumentations used in the tests of C3 and C4 specimens are represented in Figure 6.6, Figure 6.7, Figure 6.8 and Figure 6.9 for the “symmetric” and “asymmetric” configurations.

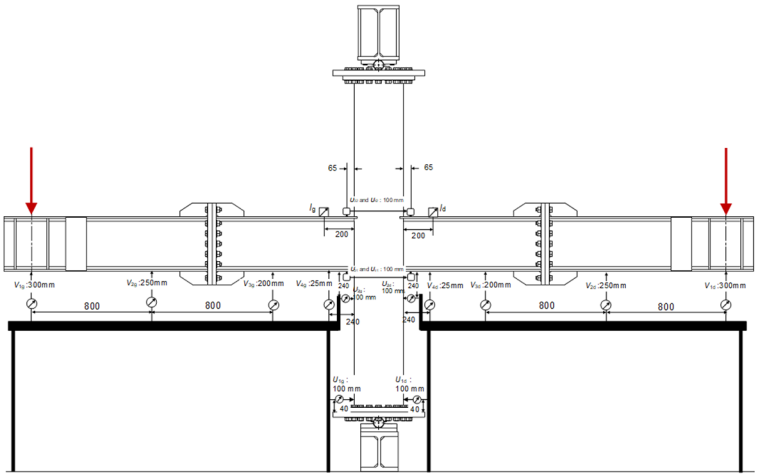

Figure 6.6 LVDTs and inclinometers in the "symmetric" configuration for C3 specimens

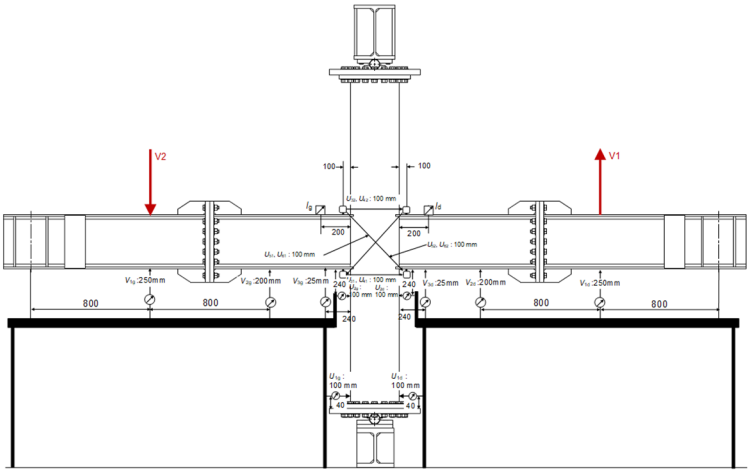

Figure 6.7 LVDTs and inclinometers in the "asymmetric" configuration for C3 specimens

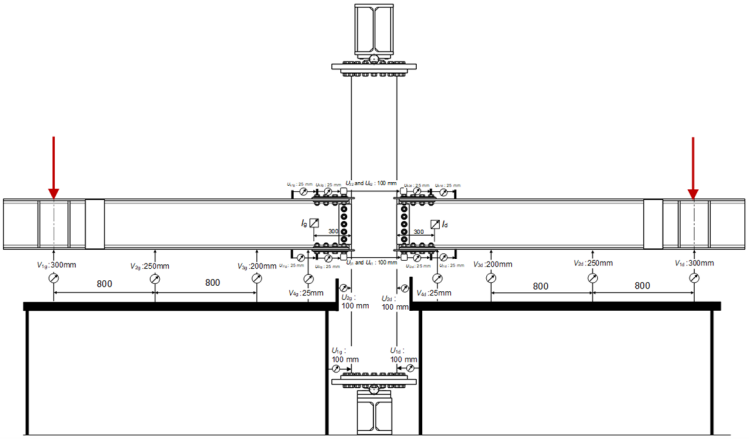

Figure 6.8 LVDTs and inclinometers in the "symmetric" configuration for C4 specimens

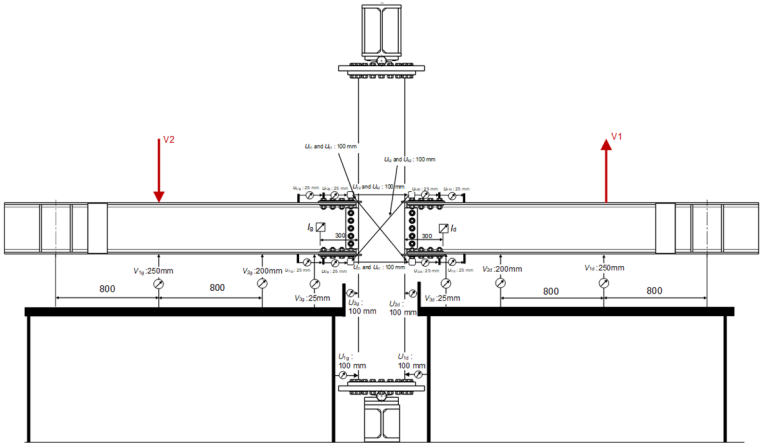

Figure 6.9 LVDTs and inclinometers in the "asymmetric" configuration for C4 specimens

Axial (*J*) and rosette (*R*) strain gauges are applied to beams and column in the connection region. Specimens are tested with different configurations of strain deformation sensors. In Figure 6.10 and Figure 6.11, some examples of specimens are shown for the types C3 and C4. Linear strain gauges are applied to the beam flanges to obtain local deformations and forces. Rosette are used on the column wall at 20 mm from the flanges to investigate the local stress distribution. In Figure 6.11a-c configurations where the linear strain gauges are inserted inside the column on the beam flanges of specimens C3 and C4 are presented. In these cases, internal linear

strain gauges are applied on the beam flanges before the assembly of the specimens, in order to determine the part of flange stresses transmitted by the welds to the column wall and the part that are directly transmitted by the two sides of the beam through the continuity inside the column.

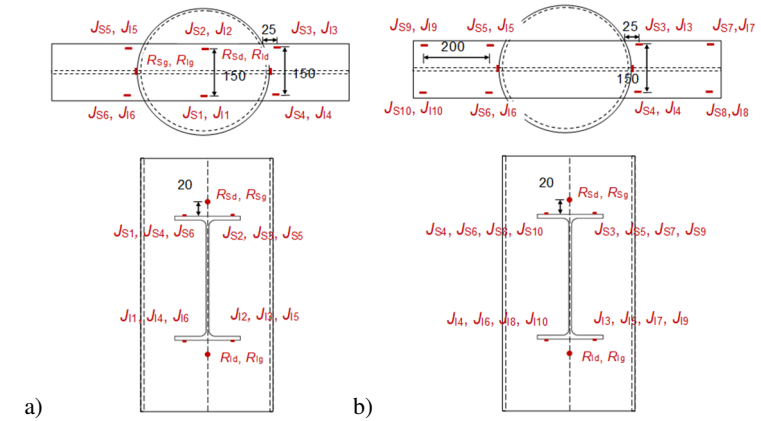

a) b)

Figure 6.10 Strain gauges applied to beams and column of C3 specimens: a) with internal strain gauges, and b) without internal strain gauges,

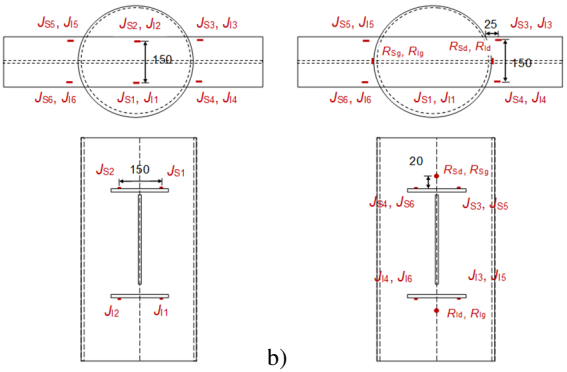

a) b)

Figure 6.11 Strain gauges applied to beams and column of C4 specimens: a) with internal strain gauges, and b) without internal strain gauges,

6.1.4 Loading procedure

Monotonic loads are applied in both the symmetric and asymmetric configurations, whereas Cyclic loads are applied in the asymmetric configuration, where the action of horizontal load on structures is simulated.

The monotonic loads are applied in three steps: a) applications of the 50% of the design resistance evaluated with nominal mechanical characteristics, and unloading, b) application of the design resistance and unloading, and c) loading until failure of the joint or the beam.

The loading procedure for the cyclic tests is based on the quasi-static procedure for the testing of components of steel structures provided in the ECCS-45 "Recommended Testing Procedure for Assessing the Behaviour of Structural Steel Elements under Cyclic Loads" (ECCS 1986). In the complete testing procedure, the cyclic displacement history is defined starting from the results obtained by the monotonic test, in particular the yielding load F_y and the yielding displacement d_y of the specimen. The cyclic test is carried out by applying increasing imposed cyclic displacements: firstly, four cycles are completed at the 25%, 50%, 75% and 100% of the yield displacement d_y; then the test provides groups of three cycles with the following amplitude:

$$\pm 2 \cdot (1 + n)\, d_y \qquad \text{Eq. 6.1}$$

where $n = 0, 1, 2, 3, etc$ until complete failure of the specimen.

6.1.5 Material characterization

In parallel with the execution of experimental tests on full-scale substructures, tensile tests for the mechanical characterization of steel are defined. The results of this characterization are useful for the definition of the material property to be used, for the individual components, in the mechanical models.

Therefore, tests were performed on specimens directly extracted from the IPE400 beams, the CHS355.6 columns and the plates of the substructures. The tensile tests allow the definition of the stress-strain curves for the singular specimen. Moreover, they allow the definition of the yielding stress, ultimate stress and elongation for the ultimate stress, for each tested specimen. The mean values of these mechanical characteristics are reported in Table 6.4 for each member type.

Table 6.4 Mean value of the mechanical characteristics for the different tested elements

Member	Type	Mean Yielding Stress [MPa]	Mean Ultimate Stress [MPa]	Mean Elongation for Ultimate Stress [%]
IPE400	Flange	366	527	17.9
IPE400	Web	371	538	17.1
CHS 355.6/8.8	Tube Wall	371	510	18.3
CHS 355.6/10	Tube Wall	382	519	18.1
CHS 355.6/12.5	Tube Wall	371	507	18.4
Plate 6 mm	Plate	338	430	16.8
Plate 10 mm	Plate	294	425	21.3
Plate 12 mm	Plate	434	513	12.8

The obtained stress-strain curves are represented for instance in Figure 6.12, for the IPE400 beam web and flanges, and the CHS355.6 column profiles (8.8 mm and 10.0 mm thick).

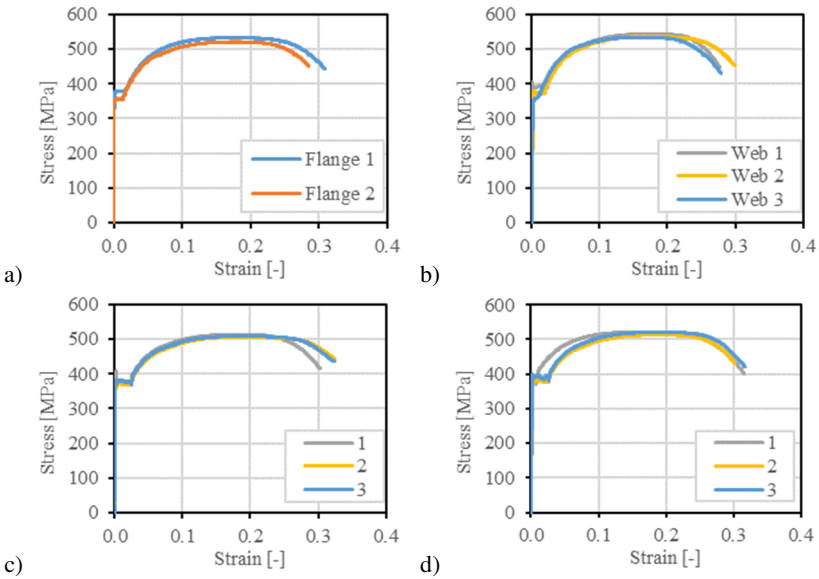

Figure 6.12 Stress-strain curves for: IPE400 a) flange, and b) web; and CHS355.6 c) 8.8 mm, and d) 10 mm thick

6.2 Vertical loading experimental results

In this paragraph, the experimental testing results for the two-way steel substructures subjected to monotonic vertical loads are reported. The action of vertical loads on the structure is simulated by applying vertical forces to the beam ends, according to the testing setup previously described (Figure 6.4). The tests are performed in displacement control.

6.2.1 Tests on C3 two-way joints

Specimens C3 are characterized by the full-strength beam-to-column connections realized by the passing through beam, as shown in Figure 6.2. All the beams have IPE400 section and the CHS-columns have the external diameter equal to 355.6 mm in each case, whereas the thickness is equal to 8.8, 10.0 and 12.5 mm respectively for connections C3-1, C3-2 and C3-3. C3-1 is characterized for the use of full penetration welding to connect the beam to the tube wall, whereas C3-2 is characterized by the presence of both fillet (C3-2A) and full penetration (C3-2B) welds. For the last type of specimen, C3-3, only fillet welds are considered.

In these tests, the action of vertical gravity loads on the structure is simulated by applying monotonically two equal forces to the beam-ends. The tests are performed in displacement-control. Details of the C3 specimens tested in this phase are reported in Table 6.5 with the obtained maximum moment transmitted by the singular beams to the column connection.

Table 6.5 Details and results of C3 specimens tested in the symmetric configuration; the design resistances are calculated according to EN1993-1-1:2005 (CEN 2005b), considering the mean yielding stresses previously reported

Den.	Column Thick.	Welding	Beam design resistance	Column design resistance	Maximum beam and column bending moment
			[kNm]	[kNm]	[kNm]
C3-1B-1	8.8	Full penetration	482	394	568
C3-2A-1	10	Fillet	482	456	582
C3-2B-1	10	Full penetration	482	456	576
C3-3A-1	12.5	Fillet	482	546	581

The moment-rotation curves are reported in Figure 6.13. The ultimate bending moment and initial rotational stiffnesses are themselves closed. Results highlight that

the behavior of the connections is not particularly influenced by the tube-wall thickness and welds type. Indeed, the failure is obtained in each case by the development of the plastic hinges on the beam (see the dot line in Figure 6.13) until the bottom compressed beam flanges exhibit local buckling phenomena (Figure 6.14).

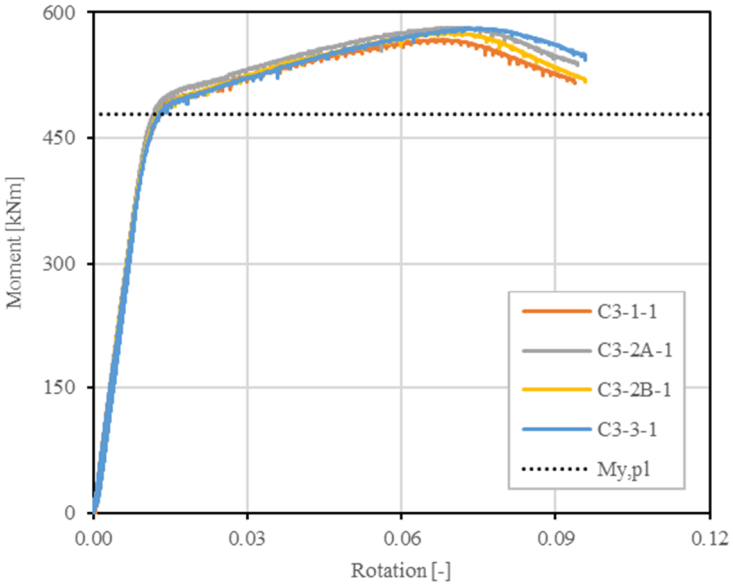

Figure 6.13 Results of monotonic test on C3 specimens in the symmetric configuration (vertical loading configuration); the dot line represents the beam design resistance

a) b)

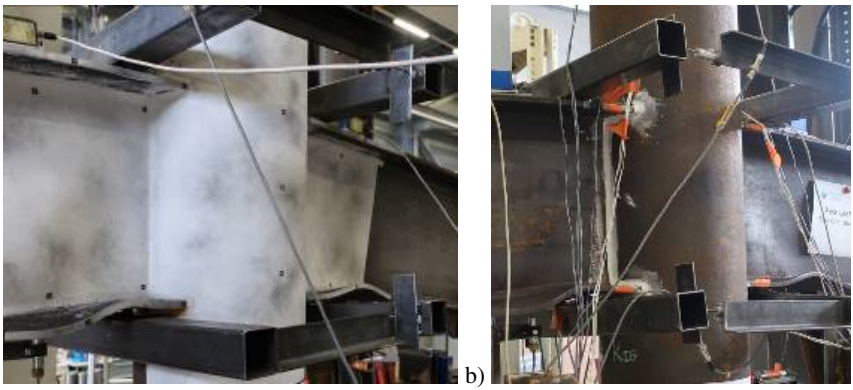

Figure 6.14 Failure mode exhibited in the C3 specimens under symmetric vertical loads: local buckling of the compressed beam flanges of specimen a) C3-1B-1, and b) C3-3A-1

This aspect is mainly due to the continuity of the beam inside the column that has the double effect of directly transferring the forces between the two side of the connection, and increase the stiffness of the tubular column wall in the connection region. Therefore, these joints can be classified as full-strength joints with respect to the vertical loads on the structure.

6.2.2 Tests on C4 two-way joints

Specimens C4 are characterized by the full-strength beam-to-column connections realized by three passing through plates externally bolted to beams, as shown in Figure 6.3. All the beams have IPE400 section and the CHS-columns have the external diameter equal to 355.6 mm in each case, whereas C4-1 and C4-2 have 8.8 mm thick tube wall, C4-3 and C4-4 have 10 mm thick tube wall, and C4-5 and C4-6 have 12.5 mm thick tube wall. Furthermore, C4 specimens differ for the plates thicknesses, which are equal to 10 mm (flanges) and 8 mm (web) for C4-1, C4-3 and C4-5, and equal to 12 mm (flanges) and 10 mm (web) for C4-2, C4-4 and C4-6. Full penetration welding is used in C4-1, C4-2, C4-3 and C4-4 substructures, whereas in the C4-5 and C4-6 cases, fillet welding is applied. The bolted plate-beam connections are designed to avoid as soon as possible yielding or failure in this part of the joint. For this purpose, additional plates are welded to flanges plates and beam flanges to limit net section/block shear failure.

In these tests, the action of vertical gravity loads on the structure is simulated by applying monotonically two equal forces to the beam-ends. The tests are performed in displacement-control. Details of the C4 specimens tested in this phase are reported in Table 6.6 with the obtained maximum moment transmitted by the singular beams to the column connection.

The six moment-rotation curves are reported in Figure 6.15. The initial rotational stiffnesses are themselves closed, whereas the specimen resistances appear different. Results highlight that the behavior of the connections in the first stage is not particularly influenced by the tube-wall thickness and welds type. Indeed, specimen C4-1B-1, with 8.8 mm thick column exhibits a higher maximum bending moment in comparison with the specimen C4-5A-2, characterized by a 12.5 mm thick column. Besides, the effect of the type of welding is not clear and it seems that the welds do not influence the global behavior. Conversely, the thickness of the plates clearly influences the behavior of the connection. In fact, C4-4B-1 specimen, which is the only one with 12 mm thick flange plates and 10 mm thick web plate (instead of 10 and 8 mm respectively), exhibits a differentiated behavior with greater resistance and stiffness.

Table 6.6 Details and results of C4 specimens tested in the symmetric configuration; the design resistances are calculated according to EN1993-1-1:2005 (CEN 2005b), considering the mean yielding stresses previously reported

Den.	Column Thick.	Flange and web plates thick.	Welding	Beam design resistance [kNm]	Column design resistance [kNm]	Maximum beam and column bending moment [kNm]
C4-1B-1	8.8	10-8	Full p.	482	394	431
C4-3A-1	10	10-8	Fillet	482	456	415
C4-3B-1	10	10-8	Full p.	482	456	318
C4-4B-1	10	12-10	Full p.	482	456	496
C4-5A-1	12.5	10-8	Fillet	482	546	462
C4-5A-2	12.5	10-8	Fillet	482	546	412

The tube-wall thickness has a clear impact on the post-buckling stage. In fact, for the thinner tube-wall thickness (8,8 mm for C4-1), a decrease of the applied forces is obtained because the tube-wall is not able to transmit the force in the compression area. For the intermediate tube-wall thickness (10 mm for C4-3 and C4-4) almost constant applied forces are observed after the flange plate buckling. However, a final decrease of the force appears. For the thicker tube-wall thickness (12,5 mm for C4-5) an increase of the applied forces on the load-jack is obtained followed by a slight decrease. For two specimens (C4-3A-1 and C4-5A-1), an increase of the forces is observed due to the fact that the buckled flange plates came in contact with the web plate inside the column.

In the test of C4-1B-1 specimen, which is the only one with 8.8 mm thick column wall tested under vertical loads, the behavior is linear until the first bolt sliding starts for a bending moment of almost 230 kNm (Figure 6.16). The stiffness decreases after the sliding of the bolted connection. A sudden drop of the applied forces occurs for a bending moment of 431 kNm probably due to the buckling of the flange plate in compression inside the tube. Then the bending moment continue to decrease and the local buckling of the tube-wall in the compression area can be clearly observed.

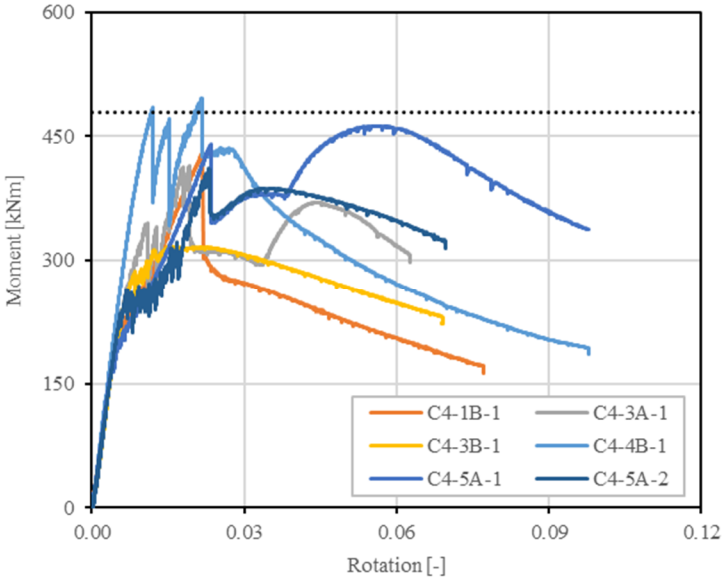

Figure 6.15 Results of monotonic test on C4 specimens in the symmetric configuration (vertical loading configuration); the dot line represents the beam design resistance

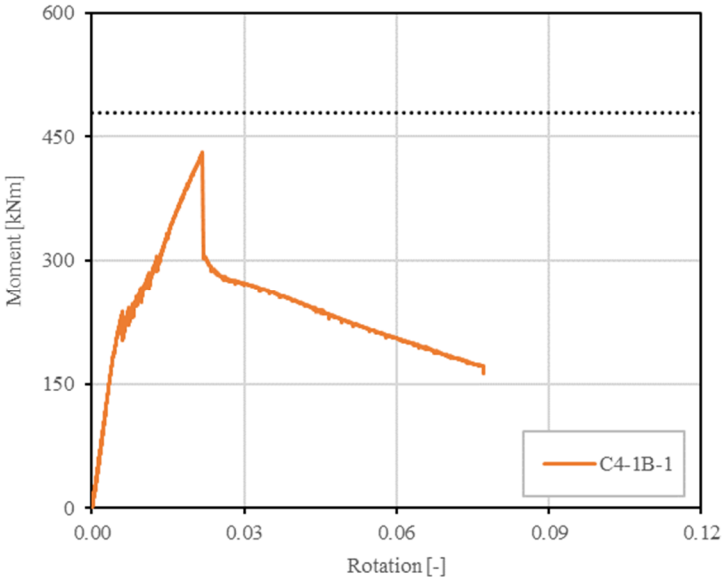

Figure 6.16 Moment-rotation curve for the C4 specimen with 8.8 mm thick column

In the tests of specimens with the 10 mm thick column wall, the behavior is linear until the bolted connections start to slid (Figure 6.17). The initial stiffness is not influenced by type of column, welding and plates, whereas after the sliding the behavior differ themselves. In all the cases the stiffness decreases.

The sliding of the bolted connection is influenced by the thickness of the plates. Indeed, for specimens with the thinner plates (C4-3A-1 and C4-3B-1) it happens at almost 300kNm, whereas for the specimen with the thicker plates (C4-4B-1) bolted connections start to slide for a bending moment of 480 kNm which is almost equal to the beam resistance.

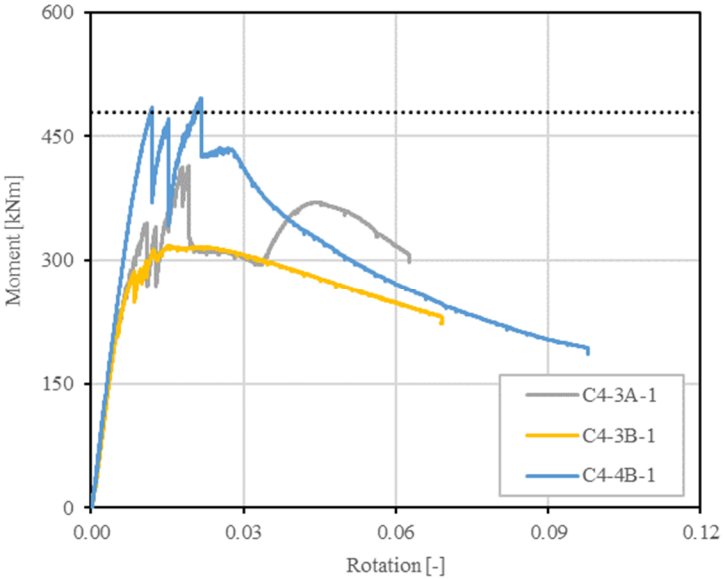

Figure 6.17 Results of monotonic test on C4 specimens, with 10 mm thick column, in the symmetric configuration (vertical loading configuration); the dot line represents the beam design resistance

Sudden drops of the applied forces occur, probably due to the buckling of the flange plate in compression inside the tube. Then the bending moment continue to decrease and the local buckling of the tube-wall in the compression area can be clearly observed (Figure 6.18). Afterwards, in the test of specimen C4-3A-1 the applied loads restart to increase, because the buckled lower flange comes in contact with the web plate inside the column (Figure 6.19).

The role of the different type of welding in the specimens C4-3A-1 and C4-3B-1 is not clear. Indeed, it seems that the differences in the behavior in these two cases are due to other effects, such as the different sliding mechanisms of the bolted connections and the absence or presence of contact inside the column. These phenomena should not be influenced by the welding behavior.

Figure 6.18 Specimen C4-4B-1 at failure

Figure 6.19 Specimens C4-3A-1 (left) and C4-3B-1 (right) after the tests

In the tests of specimens with the 12.5 mm thick column wall, the behavior is linear until the bolted connections start to slid (Figure 6.20). After the sliding the stiffnesses decrease. The sliding of the bolted connection happens at almost 225 kNm.

Sudden drops of the applied forces occur, probably due to the buckling of the flange plate in compression inside the tube. Then, the bending moment increases until the tube-walls start locally to buckle in the compression area. This aspect is not highlighted in the other tests, where the thinner tube-walls cannot allow to obtain the further resistance exhibited in these cases.

Afterwards, in the test of specimen C4-5A-1 the applied loads restart to increase, probably because the buckled lower flange comes in contact with the web plate inside the column. This specimen reaches thus a higher value of the bending moment. The specimen C4-5A-2 did not exhibit the increase of forces because the passing-through compressed flange plate buckles to the bottom without come in contact with the web passing-through plate.

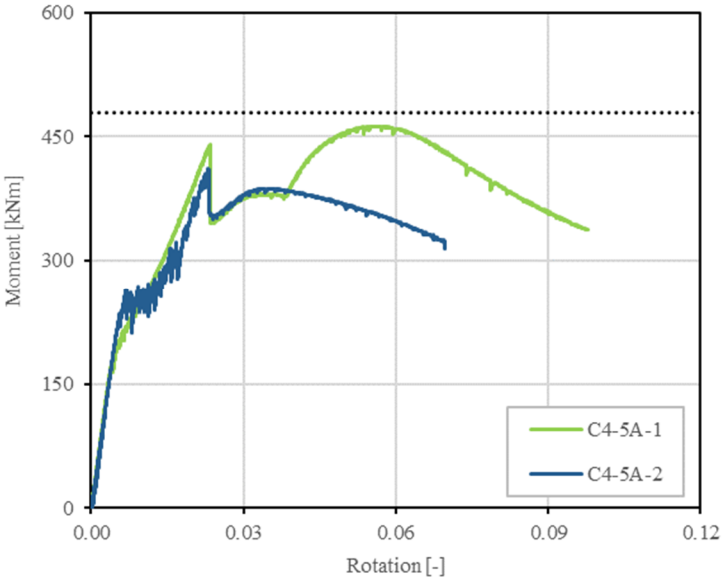

Figure 6.20 Results of monotonic test on C4 specimens, with 12.5 mm thick column, in the symmetric configuration (vertical loading configuration); the dot line represents the beam design resistance

6.3 Horizontal loading experimental results

In this paragraph, the experimental testing results for the two-way steel substructures subjected to monotonic and cyclic horizontal loads are reported. The action of horizontal loads on the structure is simulated by applying vertical opposite forces to the beam ends, according to the testing setup previously described (Figure 6.5). The tests are performed in displacement control.

6.3.1 Monotonic tests on C3 two-way joints

In these tests, the action of horizontal loads on the structure is simulated by applying monotonically two equal opposite forces to the beam-ends. The tests are performed in displacement-control. Details of the C3 specimens tested in this phase are reported in Table 6.7.

Table 6.7 Details and results of the C3 tested specimens; the design resistances are calculated according to EN1993-1-1:2005 (CEN 2005b)

Den.	Column Thick.	Welding	Beam design resistance	Column design resistance	Maximum beam and column bending moment
			[kNm]	[kNm]	[kNm]
C3-1B-2	8.8	Full penetration	482	394	260
C3-2A-2	10	Fillet	482	456	400
C3-3A-2	12.5	Fillet	482	546	481

The moment-rotation curves are reported in Figure 6.21. The ultimate bending moments and initial rotational stiffnesses highlight that the behavior of the connections is clearly influenced by the tube-wall thickness. Besides, the ductility of the specimens appears to be influenced by changing parameters.

The failure modes exhibit in the present configuration differ from the ones reported for the vertical loading condition. Weld tearing in the tensioned flange zones, tube wall local buckling in the compression region and shear panel deformation are reported for each specimen.

The initial stiffness is lower in comparison with the symmetric loading because joints components are activated. The reduction of the specimen stiffnesses are due to the shear panel deformation. A clear column web panel deformation in shear is observed for the specimen with the column thickness of 8.8 mm (Figure 6.22a).

Besides, 10 mm (Figure 6.22b) and 12.5 mm thick column specimens also exhibit a shear panel deformation.

First cracks appear in all the tests in the welds between the column walls and the tensioned beam flanges, as shown in Figure 6.23. Even if the tube-wall cracking appears quite early, immediately after the reduction of the specimen stiffnesses, the C3-1B-2 specimen, with the lowest column thickness, is able to develop major rotation capacity without clear loss of loading in comparison with the other two specimens.

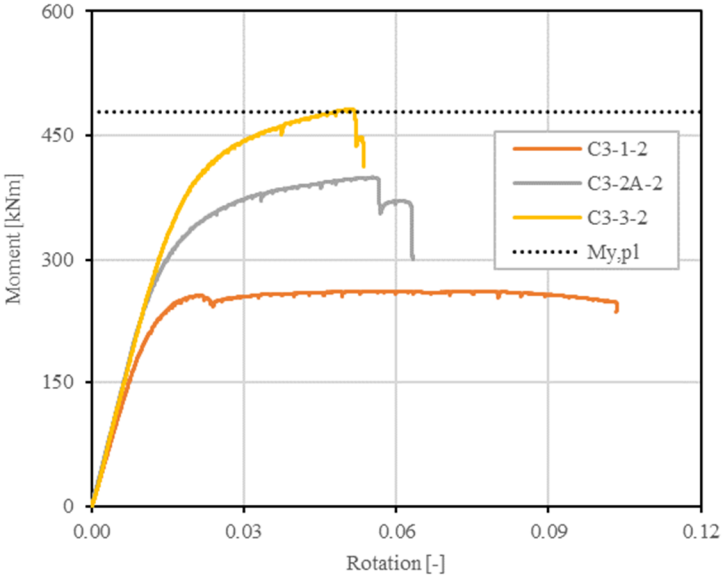

Figure 6.21 Results of monotonic test on C3 specimens in the asymmetric configuration (horizontal loading configuration); the dot line represents the beam design resistance

The reduction of the applied loads started when the welds and the column wall exhibited the tearing in the tension region (Figure 6.24) and the column wall exhibit buckling phenomena where the compressed flanges are connected (Figure 6.25).

C3-1B-2 specimen, made with full penetration welding, has an ultimate resistance equal to the 66% of the design resistance of column, whereas specimens C3-2A-2 and C3-3A-2, made with fillet welding, exhibit a resistance equal to the 88% of the design resistance of the column. In the last case, the resistance is equal to the design resistance of the beam, which is lower than the column design resistance. Besides, in

the first case the design resistance of the beam is higher than the column design resistance and, in the second case, the resistance are almost equal (Table 6.7).

a)  b) 

Figure 6.22 Shear panel deformation: a) C3-1B-2 specimen with 8.8 mm thick column, and b) C3-2A-2 specimen with 10 mm thick column

a) 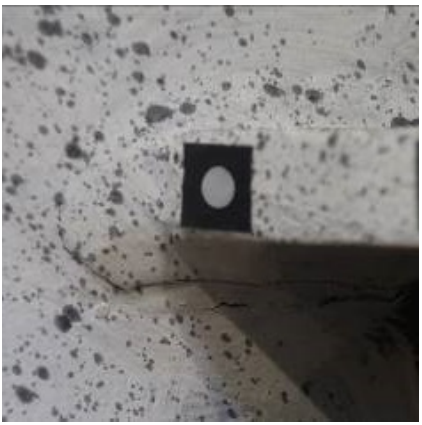 b) 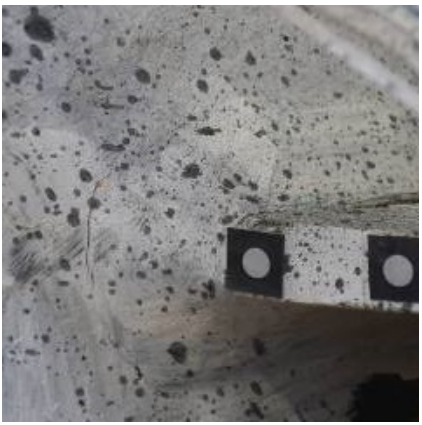

Figure 6.23 First crack in the weld between column wall and beam flange under tension axial forces: a) C3-1B-2 specimen with 8.8 mm thick column and full penetration welding, and b) C3-2A-2 specimen with 10 mm thick column and fillet welding

Therefore, is not clear if the higher reduction of resistance exhibited in the first specimen test is due to the type of welding or to the different failure mode of the welds. Indeed, for the 8.8 mm thick column with and full penetration welds, the tearing of the welds appears in the vertical direction, parallel to the column wall

(Figure 6.25a), whereas in the 10 and 12.5 mm thick column with fillet welds the weld tearing happens in the horizontal direction (Figure 6.25b). Moreover, the absence of tests with the same beam and column dimensions and different type of welding do not allow the clear understanding of the role of the welding type.

a)  b) 

Figure 6.24 Weld tearing in the tension region: a) C3-1B-2 specimen with 8.8 mm thick column and f. p. welding, and b) C3-3A-2 specimen with 12.5 mm thick column and f. welding

a)  b) 

Figure 6.25 Local buckling of the column wall where compression forces are transmitted by the flanges: a) a) C3-1B-2 specimen with 8.8 mm thick column and full penetration welding, and b) C3-3A-2 specimen with 12.5 mm thick column and fillet welding

6.3.2 Cyclic tests on C3 two-way joints

In these tests, the action of horizontal loads on the structure is simulated by applying cyclically two equal opposite forces to the beam-ends. The tests are performed in displacement-control with the loading procedure previously exposed. Details of the C3 specimens tested in this phase are reported in Table 6.8.

Table 6.8 Details and results of C3 specimens tested in the asymmetric configuration with cyclic loads; the design resistances are calculated according to EN1993-1-1:2005 (CEN 2005b), considering the obtained mean yielding stresses

Den.	Column Thick.	Welding	Beam design resistance	Column design resistance	Maximum beam and column bending moment
			[kNm]	[kNm]	[kNm]
C3-1B-3	8.8	Full penetration	482	394	291
C3-2A-3	10	Fillet	482	456	394
C3-2B-2	10	Full penetration	482	456	343
C3-2B-3*	10	Full penetration	482	456	323

* tested with additional compression on the column

A comparison of the moment-rotation curves obtained by the monotonic and cyclic tests is reported in Figure 6.26, for the specimens C3-1 with 8.8 mm thick column and full penetration welding. Specimen C3-1B-3 exhibits an almost linear behavior in the first cycles with the amplitude lower or equal to the yielding rotation.

Cracks start to develop on the welds in tension when the cycles reach two times the yielding rotation and non-linear behavior is highlighted. The bending moment gets, during these cycles, the maximum value, which does not decrease in the three equal repetitions.

For cycles with a maximum displacement equal to four times the yielding one, tearing of the welds and tube-wall in the tension region is clearly observed. During these cycles the maximum applied moment start to decrease in the subsequent repetitions. For the following cycles, tearing and crushing of the tube-wall in the tension region increase. The maximum forces applied decrease due to a huge tearing of the tube-wall (Figure 6.27). The maximum moment in the last cycle is around the 70% of the maximum load obtained in the first cycles.

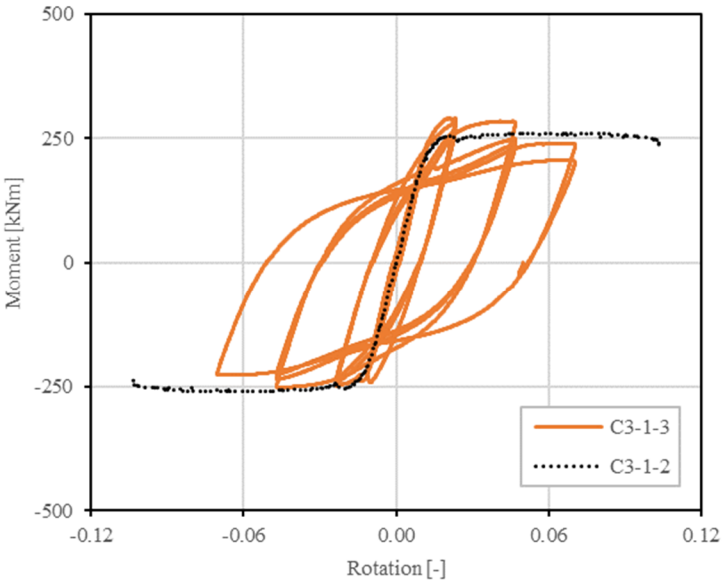

Figure 6.26 Comparison of the results of the monotonic and cyclic tests performed on C3-1 specimens, 8.8 mm thick column and full penetration welding, in the asymmetric configuration (horizontal loading configuration)

a) b)

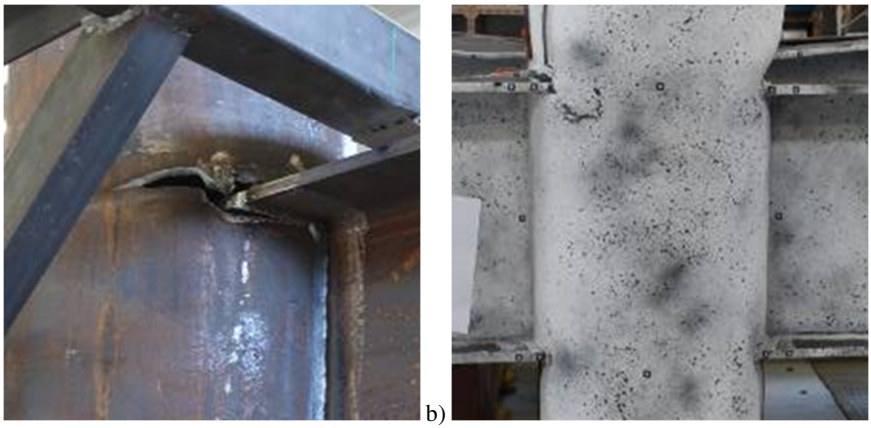

Figure 6.27 Failure modes observed in the cyclic test of C3-1B-3 specimen: a) tearing of the flange welds and tube wall, and b) local buckling and tearing in the flange weld regions

A comparison of the moment-rotation curves obtained by the monotonic and cyclic tests is reported in Figure 6.28 for the specimens C3-2 with the 10 mm thick column and fillet (C3-2A-2 and C3-2A-3) or full penetration welding (C3-2B).

Specimen C3-2A-3 exhibits an almost linear behavior in the first cycles before the monotonic yielding point. Unlikely, the specimen C3-2B-2, where full penetration welding is used, the first cracks in the welds appear already for the cycles for the amplitude equal to the yielding displacement.

Cracks start to develop also on C3-2A-3 specimen on the fillet welds in tension when the cycles reach two times the yielding rotation. Non-linear behavior is highlighted but the repetitions exhibit a constant shape. For specimen C3-2B-2, with full penetration welds, the moment gets, during the first cycle, the maximum value and decreases around the 10% in the subsequent equal repetitions. The sudden drop of the forces is caused by cracks of the weld all along the flange in tension on each side of the beam.

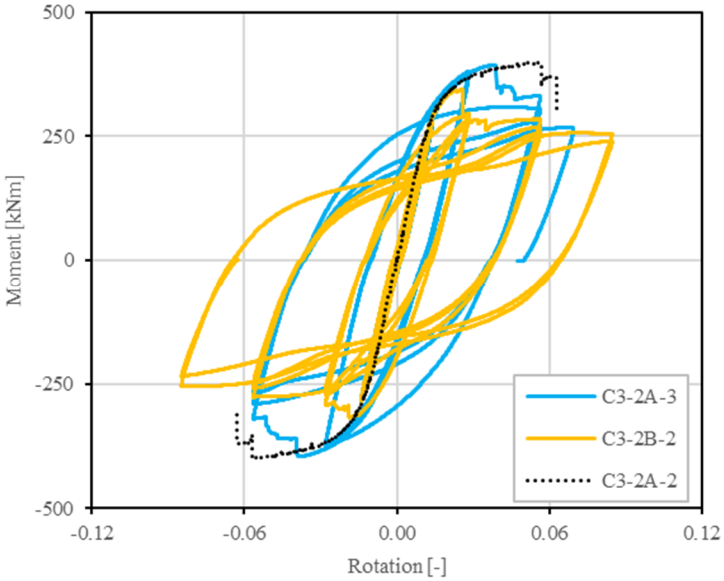

Figure 6.28 Comparison of the results of the monotonic and cyclic tests performed on C3-2 specimens, 10 mm thick column with fillet welding (C3-2A) or full penetration welding (C3-2B) in the asymmetric configuration (horizontal loading configuration)

For cycles with a maximum displacement equal to four times the yielding one, cracking of the welds due to tension and crushing due to compression are clearly

observed on specimen C3-2A-3. In the first cycle the loads rapidly drop due to the complete tearing of the tube-wall all along the fillet welds (Figure 6.29). In the following cycles the forces attain the 60% of the maximum ones. In the end of the repetitions, upper and lower parts on the right side of the column are completely teared all along the welds, whereas the left side is deformed by cracks and crushing of the tube-wall. Therefore, the test ended. On specimen C3-2B-2 cracks develop until the welds of the flanges cracked on both sides of the joint (Figure 6.30). The repetitions exhibit a pinching effect due to the transferring of forces only in the compressed parts by contact due to the absence of connection in tension parts.

Cycles with six times the yielding rotation were performed only on C3-2B-2 specimen, which exhibits a more constant and ductile behavior, with a decrease of the load of about the 25%. However, the maximum load achieved in the whole test is lower.

a)  b) 

Figure 6.29 Failure modes observed in the cyclic test of C3-2A-3 specimen: a) tearing of the flange welds, and b) local buckling and tearing in the flange weld regions

The Comparison of the test results for specimens C3-2B-2 (without axial load on the column) and C3-2B-3 (with axial load), represented in Figure 6.31, shows that the compression on the column has slight effect on the mechanical behavior of the specimen. The maximum obtained bending moment with axial load is equal to the 92% of the corresponding value obtained without compression. The cyclic behavior does not show great differences.

a)  b) 

Figure 6.30 Failure modes observed in the cyclic test of C3-2B-2 specimen: a) tearing of the flange welds, and b) local buckling and tearing in the flange weld regions

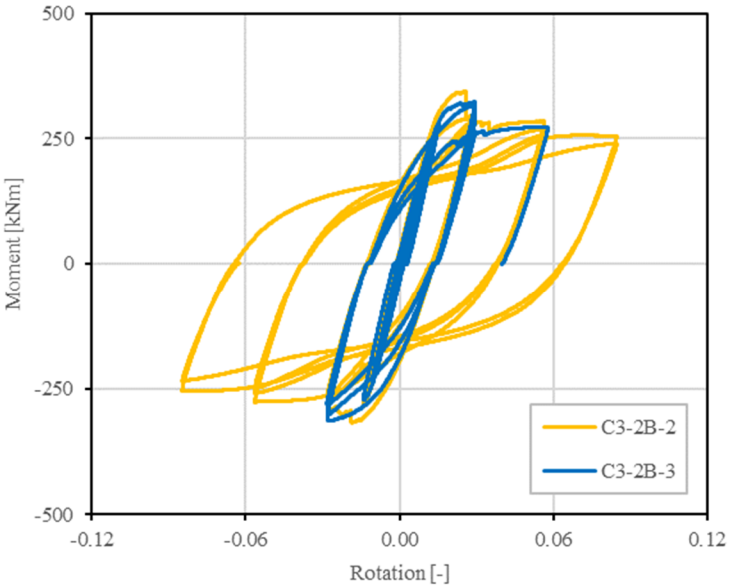

Figure 6.31 Comparison of the results of the cyclic tests performed on C3-2B specimens, 10 mm thick column and full penetration welding, with (C3-2B-3) and without (C3-2B-2) axial compression load on the column

6.3.3 Monotonic tests on C4 two-way joints

In these tests, the action of horizontal loads on the structure is simulated by applying monotonically two equal opposite forces to the beams. The tests are performed in displacement-control. Details of the C4 specimens tested in this phase are reported in Table 6.9 with the obtained maximum moment transmitted by the singular beam to the column connection.

Table 6.9 Details and results of C4 specimens tested with monotonic horizontal loading; the design resistances are calculated according to EN1993-1-1:2005 (CEN 2005b), considering the mean yielding stresses previously reported

Den.	Column Thick.	Flange and web plates thick.	Welding	Beam design resistance [kNm]	Column design resistance [kNm]	Maximum beam and column bending moment [kNm]
C4-2B-1	8.8	12	Full p.	482	394	207
C4-4B-2	10	12	Full p.	482	456	237
C4-6A-1	12.5	12	Fillet	482	546	419

The moment-rotation curves are reported in Figure 6.32. Results highlight that the behavior of the connections is clearly influenced by the tube-wall thickness. C4-2B-1 (8.8 mm) and C4-4B-2 (10 mm) specimens exhibit an equal initial stiffness, whereas C4-6A-1 (12.5 mm) exhibits a higher stiffness. Moreover, the more the thickness is, the more the resistance is.

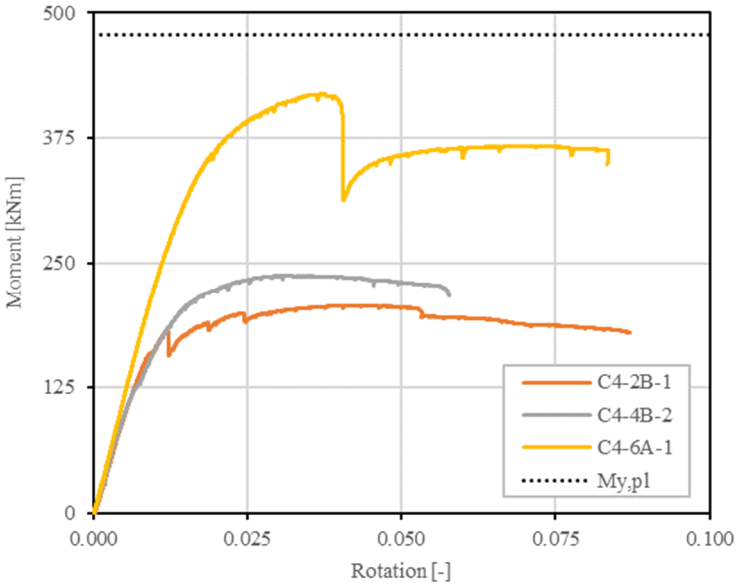

Figure 6.32 Results of monotonic test on C4 specimens in the asymmetric configuration (horizontal loading configuration); the dot line represents the beam design resistance

The first two specimens reach maximum bending moments equal to the 52% of their column design resistances, whereas the last one, with the thicker wall, attain the 77% of his column design resistance. Besides, the ductility of the specimens appears to be influenced by changing parameters. It is not clear if this difference is due to the type of welding or other factors.

The failure modes exhibited by C4 specimens in the present configuration are weld and column wall tearing in the tensioned flange zones and tube wall local buckling in the compression region. Moreover, the specimen with the thinner tube wall (C4-2B-1) is subjected to the sudden sliding of the bolted connections in the end of the linear stage, and finally, failure of the bolts in shear is obtained on the web plates. These phenomena were not observed in the other tests.

The first crack in the tensioned welds of specimen C4-4B-2 (Figure 6.33a) is already observed in the elastic range and causes a first decrease of the stiffness. However, in all the tests, significant decrease of the stiffnesses comes when the local buckling of the tube wall in the compressed area is registered. Afterwards, this latter phenomenon and tearing in the tensile part develop (Figure 6.33b) and the applied forces continually decrease.

In the test of specimen C4-2B-1 an important drop of the applied forces is registered. The causes are the tearing of the weld in tension and the tube-wall local buckling of the compressed part, both on the upper flange, as shown in Figure 6.33. Afterwards, forces register a little increase and then appear almost constant till the end of the test.

a) b)

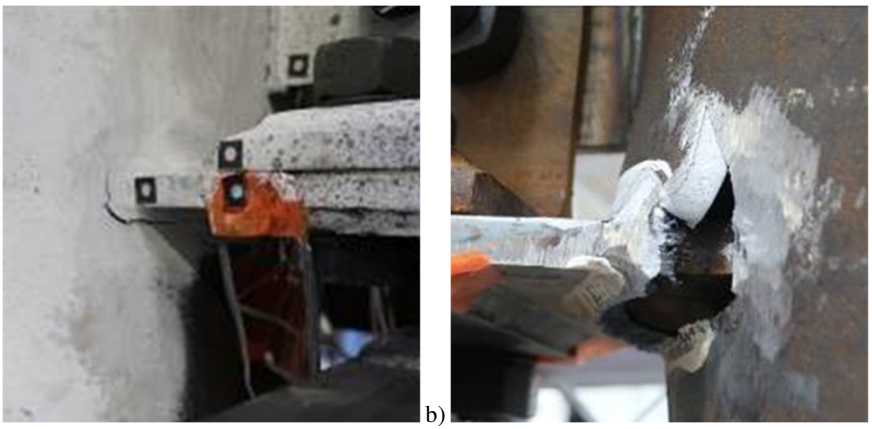

Figure 6.33 Failures of welds in tension: a) first crack in the specimen C4-4B-2, and tearing of the weld and tube wall in the end of the test on specimen C4-2B-1

6.3.4 Cyclic tests on C4 two-way joints

In these tests, the action of horizontal loads on the structure is simulated by applying cyclically two equal opposite forces to the beams. The tests are performed in displacement-control with the loading procedure previously exposed. Details of the C4 specimens tested in this phase are reported in Table 6.10 with the obtained maximum moment transmitted by the singular beams to the column connection.

Table 6.10 Details and results of C4 specimens tested in the asymmetric configuration with cyclic loads; the design resistances are calculated according to EN1993-1-1:2005 (CEN 2005b), considering the obtained mean yielding stresses

Den.	Column Thick.	Flange and web plates thick.	Welding	Beam design resistance [kNm]	Column design resistance [kNm]	Maximum beam and column bending moment [kNm]
C4-2B-2	8.8	12	Full p.	482	394	202
C4-4B-3	10	12	Full p.	482	456	244
C4-6A-2	12.5	12	Fillet	482	546	380
C4-6A-3	12.5	12	Fillet	482	546	375

A comparison of the moment-rotation curves obtained by the monotonic and cyclic tests is reported in Figure 6.34, for the specimens C4-2B with 8.8 mm thick column, 12 mm and 10 mm thick passing-through plates and full penetration welding.

Specimen C4-2B-2 exhibits an almost linear behavior in the first cycles with the amplitude lower or equal to the yielding rotation. Cracks start to develop on the welds in tension when the first cycle reach two times the yielding rotation (Figure 6.35a), and then non-linear behavior is highlighted. The bending moment gets, during this cycle, the maximum value, and decreases in the following equal repetitions of 10%.

For cycles with a maximum displacement equal to four times the yielding one, tearing of the welds and tube-wall, in the tension region, is clearly observed, cracking of the tube-wall near the web-plates starts and beam web starts to buckle near the bolted connection (Figure 6.35b). During these cycles the maximum applied moment and stiffness start to decrease in the subsequent repetitions.

For the following cycles, tearing and crushing of the tube-wall in the tension region increase but the connections were able to still dissipate energy. The maximum applied forces decrease and the maximum moment in the last cycle is around the 55% of the maximum registered value in the first cycles.

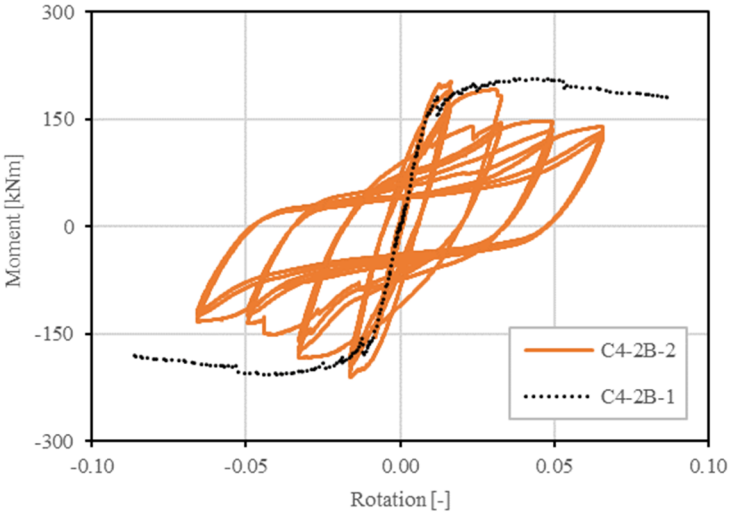

Figure 6.34 Comparison of the results of the monotonic and cyclic tests performed on C4-2B specimens, with 8.8 mm thick column, thicker plates, and full penetration welding, in the asymmetric configuration (horizontal loading configuration)

A phenomenon of closing and opening of the gap between the flange plate and the tube-wall is clearly observed (Figure 6.35c). Therefore, even if the tensile part is not able to transfer force, the compressive part on the other connection transfer the load. In the end, the web plate transfers an important part of the bending moment as yielding of the bolts in shear have been observed after tests (Figure 6.35d).

The comparison of the moment-rotation curves obtained by the monotonic and cyclic tests is reported in Figure 6.36, for the specimens C4-4B with 10 mm thick column, 12 mm and 10 mm thick passing-through plates and full penetration welding.

Specimen C4-4B-3 exhibits an almost linear behavior in the first cycles with the amplitude lower or equal to the yielding rotation. Cracks start to develop on the welds in tension when the first cycle reach two times the yielding rotation (Figure 6.37a), then non-linear behavior is highlighted. The bending moment gets, during this first cycle, the maximum value, and decreases in the following equal repetitions of almost the 15%.

For cycles with a maximum displacement equal to four times the yielding one, tearing of the welds and tube-wall, in the tension region, is clearly observed, cracking of the tube-wall near the web-plates starts and beam web starts to buckle near the bolted connection. During these cycles the maximum applied moment and stiffness start to decrease in the subsequent repetitions and tearing and crushing of the tube-

wall in the tension region increase (Figure 6.37b). However, the connections were able to still dissipate energy.

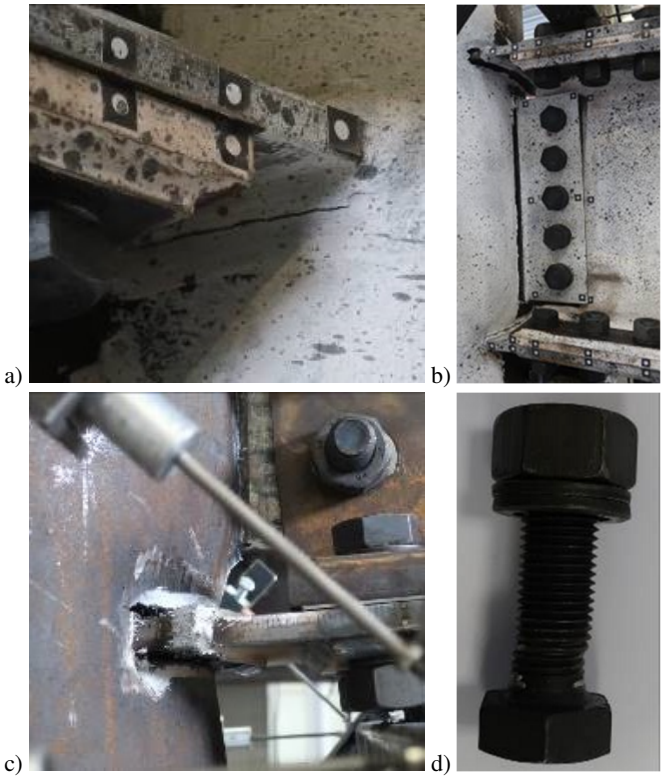

Figure 6.35 Specimen C4-2B-2: a) first crack opening, b) beam web local buckling, c) gap opening due to crushing of the tube wall, and d) yielding of the bolt

In the last two cycles at six times the yielding rotation, the maximum applied forces applied quickly decrease and the maximum moment in the last cycle is equal to the 60% of the maximum registered value in the first cycles.

The teared parts which get in contact in compressive area again are able to transmit part of the forces which can be observed as the post increase of stiffness of the joint at each cycle (Figure 6.36).

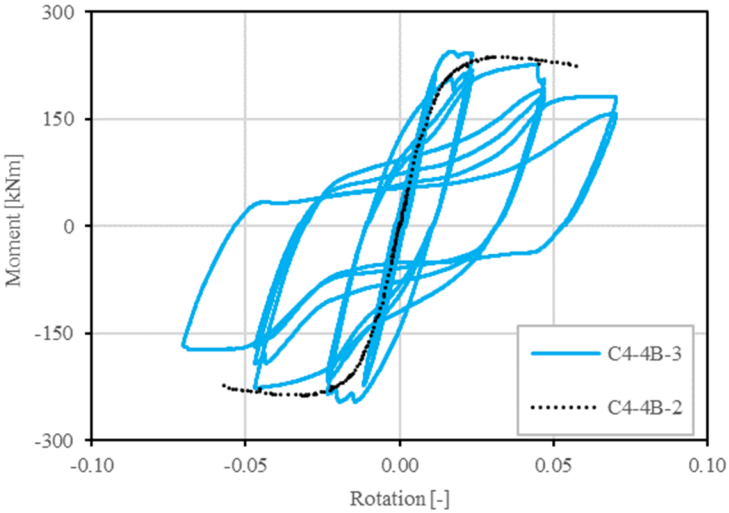

Figure 6.36 Comparison of the results of the monotonic and cyclic tests performed on C4-4B specimens, with 10 mm thick column, thicker plates, and full penetration welding, in the asymmetric configuration (horizontal loading configuration)

a) b)

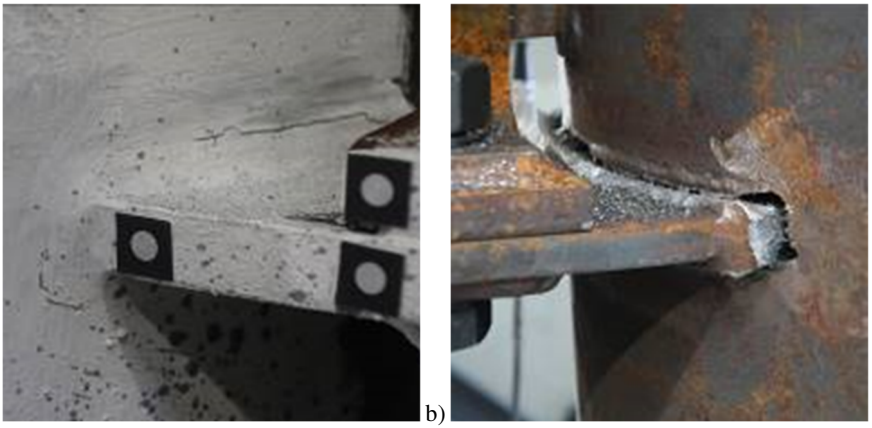

Figure 6.37 Specimen C4-4B-3: a) first cracks opening, b) welds tearing and gap opening

Comparison of the results of the monotonic and cyclic tests performed on C4-6A specimens, with 12.5 mm thick column, thicker plates, and fillet welding, without (C4-6A-1 and C4-6A-2) or with compression on the column (C4-6A-3) is reported in Figure 6.38. Results show that the compression on the column has minor effect on the mechanical behavior of the specimen. The maximum obtained bending moment with

axial load is equal to the 88% of the corresponding value obtained without compression. The cyclic behavior does not show great differences.

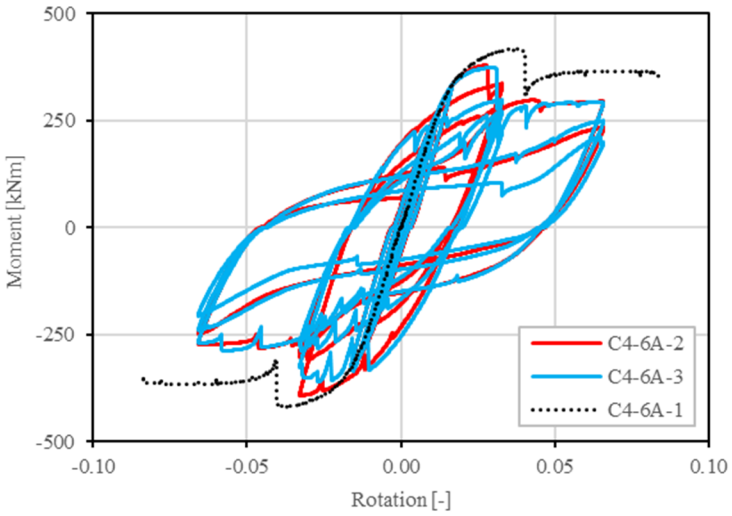

Figure 6.38 Comparison of the results of the monotonic and cyclic tests performed on C4-6A specimens, with 12.5 mm thick column, thicker plates, and fillet welding, in the asymmetric configuration (horizontal loading configuration) without (C4-6A-1 and C4-6A-2) or with compression on the column (C4-6A-3)

Both the cyclically tested specimens, already exhibited the first crack on the welds in tension in the first cycles with the amplitude equal to the yielding rotation. When the first cycle reaches two times the yielding rotation, a significant drop of the force is highlighted, due to a crack propagation in the welds on tension side of the joint. The bending moments get, during this first cycle, the maximum value, and decreases in the following equal repetitions. Specimen with compression on the column exhibit several bolts sliding at each following cycle.

For cycles with a maximum displacement equal to four times the yielding one, tearing of the welds in the tension region is clearly observed and tube walls start to buckle in the compressed regions. The drop of the applied forces corresponds to a crack on the welds of the web plate (Figure 6.39). During these cycles the maximum applied moments and stiffnesses start to decrease in the subsequent repetitions and tearing and crushing of the tube-wall in the tension region increase. However, the connections were able to still dissipate energy. Indeed, the teared parts which get in contact in compressive area again are able to transmit part of the forces.

a)  b) 

Figure 6.39 Tearing of the weld between column wall and web passing-through plate: a) specimen C4-6A-2, without compression on the column, and b) specimen C4-6A-3, with compression on the column

6.4 Critical analysis of the experimental results

In the experimental studies, the proposed joints behaved in a significantly different way from those most currently adopted and for which the Eurocode 3 (CEN 2004a) proposed the component method for the mechanical classification. In fact, in case of beam-to-column connections made with horizontal elements passing through the column, the latter is not is continuous in the node, in particular in case of four-way joints, which represent the most real configuration.

In the proposed cases the beam can be assumed as the continuous element and the column results to be divided in three parts, the node panel stub and the two external elements. Therefore, the welds between the beam and the column walls allow the parts to be reconnected. Such welds, or in any case the area of interaction between through flanges and the column wall, are those that suffered the most problems in the experimental tests, as also emerged in the preliminary studies.

6.4.1 Steel connections with passing-through beam

In the experimental tests with vertical load on C3 steel specimens, the failures are obtained in each case with the development of the plastic hinges in the beam until the bottom compressed beam flanges exhibit local buckling phenomena. This aspect is mainly due to the continuity of the beam inside the column that has the double effect of directly transferring the forces between the two side of the connection, and increase

the stiffness of the tubular column wall in the connection region. Therefore, this joint type can be directly classified as full-strength connection with respect to the vertical loads on the structure.

In case of horizontal loads on the structure, the experimental tests highlighted that the behavior of the connections is clearly influenced by the tube-wall thickness. The failure modes exhibited in this loading configuration differ from the ones reported for the vertical loading condition. Weld tearing in the tensioned flange zones, tube wall local buckling in the compression region and shear panel deformation were reported in each tested specimen. Moreover, a clear column web panel deformation in shear was observed. First cracks appear in all the tests in the welds between the column walls and the tensioned beam flanges. The reduction of the applied loads started when the welds and the column wall exhibited the tearing in the tension region and the column wall exhibit buckling phenomena where the compressed flanges are connected. Therefore, these two components, acting in parallel thanks to the continuity of the beam flanges, are the ones that mostly influence the connection behavior. Furthermore, for the 8.8 mm thick column, with a full penetration welds, the tearing of the welds appears in the vertical direction, parallel to the column wall, whereas in the 10 mm and 12.5 mm thick columns with fillet welds the weld tearing happens in the horizontal direction. In the cyclic test, the repetitions exhibit a pinching effect due to the transferring of forces only in the compressed parts by contact due to the absence of connection in the tension parts, since the welds are completely teared.

6.4.2 Steel connections with passing-through plates

In case of vertical loads on C4 specimens, the results exhibited that the thickness of the column wall influences the behavior of the connection. The maximum applied loads were reached when the lower horizontal plate in compression start to buckle inside the column. At this point, for the thinner tube-wall thickness (8,8 mm), a decrease of the applied forces is obtained because the tube-wall is not able to transmit the force in the compression area and the local buckling of the tube-wall in the can be clearly observed. For the intermediate tube-wall thickness (10 mm) almost constant applied forces are observed after the flange plate buckling. However, a final decrease of the force appears. For the thicker tube-wall thickness (12,5 m) an increase of the applied forces on the load-jack is obtained followed by a slight decrease. After the buckling of the plate, in some case a later increase of the stiffness was registered due to the internal contact between the through vertical and horizontal buckled plate.

As well as in the vertical loading configuration, in case of horizontal loading, test results highlighted that the behavior of the connections is clearly influenced by the

tube-wall thickness. The failure modes exhibited by C4 specimens in this configuration are weld and column wall tearing in the tensioned flange zones and tube wall local buckling in the compression region. Moreover, the specimen with the thinner tube wall is subjected to the sudden sliding of the bolted connections in the end of the linear stage, and finally, failure of the bolts in shear is obtained on the web plates. These phenomena were not observed in the other tests. The crack in the tensioned welds of specimen caused the first decreases of the stiffness. However, in all the tests, significant decrease of the stiffnesses comes when the local buckling of the tube wall in the compressed area is registered. Afterwards, this latter phenomenon and tearing in the tensile part continuing develop and the applied forces continually decrease. In the cyclic tests, a phenomenon of closing and opening of the gap between the flange plate and the tube-wall was clearly observed. Therefore, even if the tensile part is not able to transfer force, the compressive part on the other connection transfer the load.

7 Design of the experimental tests on composite joints

The present chapter describes the tests on composite steel-concrete substructure, showing detailed information about the definition and design of specimens and test setups and the fabrication process for the realization of specimens. The experimental assessment of the proposed connections in case of steel-concrete composite structures is performed on both two-way and four-way substructure specimens, characterized by the presence of the R.C. slab and concrete-filled column. Tests are executed in the University of Pisa Official Lab for the Experiences on Construction Materials (Centro Dipartimentale "Laboratorio Ufficiale per le Esperienze sui Materiali da Costruzione").

The composite specimens are tested with two main configurations. The first is used to simulate the action of horizontal loads on the structure on either two-way and four-way composite specimens. The second is used to test four-way composite specimens under vertical gravity loads. Tests in the horizontal loading configuration are carried out by applying cyclic and monotonic displacement histories, whereas tests in the vertical loading configuration are performed applying monotonically the load till the failure of the specimen.

Tests on two-way substructures are meant to provide more clear information about the performance of the joints and the individual components, not being influenced by the presence of the secondary beams. On the contrary, tests on 3D substructures are useful to assess the behavior of the connections in the real configuration and to study the influence of the transversal passing-through elements.

7.1 Definition of the experimental campaign

In the whole experimental campaign on composite joints, the mechanical behavior of steel-concrete beam-to-column connection is assessed by performing experimental simulation on full-scale substructures, simulating the action of both vertical gravity

and horizontal load on the main structure. In the first type of test, only monotonic loads are applied, whereas the tests with the horizontal loading configuration are carried out applying both monotonic and cyclic loads.

Although, tests on the pure-steel substructures allow the acquisition of information on the overall performance of the connections, in case of not filled tubular steel columns and steel I-beams without a compound behavior, tests on composite substructures with filled columns and R.C. slabs are performed to analyze the overall connection behavior in case of composite structures, which correspond to the nowadays most commonly adopted solution when tubular columns are used. Moreover, information on the composite components can be acquired in these last tests and can be joined with the information obtained from the tests on pure-steel substructures for the development of the mechanical models for both the steel and composite connections. Indeed, pure-steel tests allow to obtain simpler information on the behavior of the steel components which can be also used in the mechanical models of the composite joints.

Furthermore, the experimental simulations are carried out on both two-way and four-way specimens. Tests on 2D substructures are useful in order to have information more easily interpretable on the performance of the joints and the individual components. Besides, tests on 3D substructures are useful to assess the behavior of the connections in the real configuration and to study the influence of the transversal passing-through elements in the performance of the joint in the longitudinal direction and vice versa.

Tests are performed on composite specimens that are characterized by the presence of composite steel-concrete beams, realized with a R.C. slab, and a concrete-filled CHS steel column. The steel part of the composite specimens has the same dimensions of the pure-steel specimens, in order to verify the influence of the concrete part on the behavior of the proposed connection. All the tested specimens are full-scale substructure representing interior beam-to-column joints. Column height and beam lengths are different, case by case, according to the laboratory features and load conditions.

Two types of two-way rigid full-strength beam-to-column connection, and three substructures characterized by four-way beams-to-column joint are tested in the experimental campaign (Table 7.1). The two-way rigid full-strength beam-to-column connections, C3 and C4, have the same characteristics of the relative steel specimens. C3 joints are realized by passing a beam portion through the CHS column, as shown in Figure 6.1a. The C4 solution is characterized by three passing plates, as shown in Figure 6.1b. The first type of four-way joint, C5, is nominally pinned in both

transversal and longitudinal directions, with a combination of two two-way joint types, as shown in Figure 7.1.

Table 7.1 Overview of the whole experimental campaign

Laboratory	Specimen type	Structure type	Specimen type	Loading type
University of Pisa	two-way	Composite	C3	Horizontal
University of Pisa	two-way	Composite	C4	Horizontal
University of Pisa	four-way	Composite	C5	Vertical
University of Pisa	four-way	Composite	C6	Vertical
University of Pisa	four-way	Composite	C7	Vertical
University of Pisa	four-way	Composite	C7	Horizontal

The second four-way joint type, C6 (Figure 7.2), has nominally pinned joints in the secondary direction and rigid full-strength in the main one, with the passing-through beam stub in the main direction, such as in the C3 type, and a passing-through vertical plate in the secondary one. The last four-way connection specimen, C7 (Figure 7.3), is a double rigid full-strength beam-to-column joint: main beams are connected to a passing-through beam portion, as for C3 type, whereas secondary beams are connected to three passing-through plates, such as the C4 type. The two horizontal plate are passed through two slots made on the CHS column wall, whereas the vertical plate has to pass also through the web of the main passing beam.

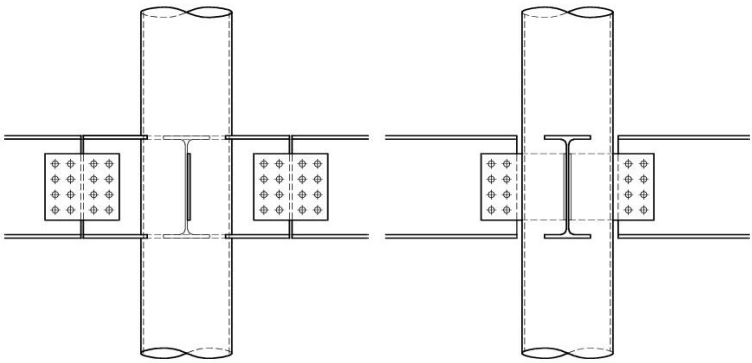

Figure 7.1 C5 four-way joint with pinned connections in both the main (through beam stub with external hinges) and secondary direction (through web-plate)

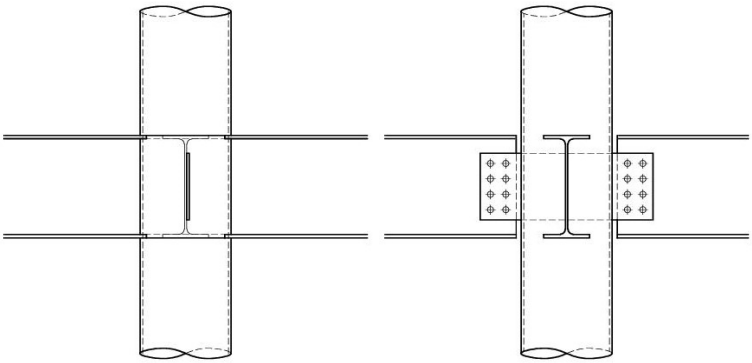

Figure 7.2 C6 four-way joint with rigid full-strength connections in the main direction (C3, through beam stub) and pinned connections in the secondary one (through web-plate)

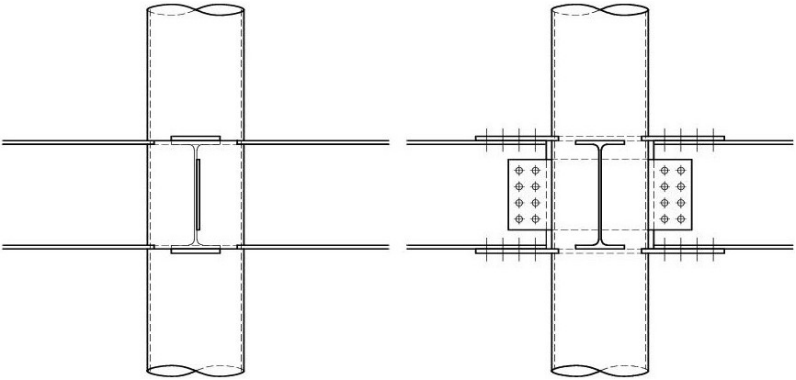

Figure 7.3 C7 four-way specimen with rigid full-strength connections in both the main (C3, through beam stub) and secondary direction (C4, through web-plate and flange-plates)

7.2 Design of the case study composite structures

The definition and design of case study structures are useful for the design of the composite specimens to be investigated in the University of Pisa laboratory. This paragraph refers to the definition and design of new four-story composite steel-concrete commercial buildings, characterized by the presence of CHS filled columns and composite beams with steel I-shaped members and R.C. slabs.

7.2.1 Definition of the case studies

Specimens are deduced from three types of structure, characterized by different horizontal load resisting systems, as reported in Table 7.2. The first case study

considered has Concentrically Braced Frames (CBFs) in both directions. Thus, the beam-to-column joints need to transmit only the shear and axial forces. The second case study has Moment Resisting Frames (MRFs) in the main direction and CBFs in the secondary one, whereas the third case study has MRFs in both directions. MRFs requires the transmission of bending moment from beam to column, thus is compulsory the adoption of rigid full-strength beam-to-column connections.

Table 7.2 Structural configuration of the case studies

Den.	Type	Main Direction	Secondary Direction
Case Study CS1	Composite Steel-Concrete	CBF	CBF
Case Study CS2	Composite Steel-Concrete	MRF	CBF
Case Study CS3	Composite Steel-Concrete	MRF	MRF

The case study structures are three four-story frame buildings with three 8.00 m bays in the main direction and 5.00 m bays in the secondary one. In the secondary direction, purlins are disposed with a wheelbase of 1.60 m. The floor height is 4.00 m. The gravity frames are composed of open beams and CHS columns, located at each structural axis. Lateral forces are resisted by the systems reported in Table 7.2. About that, beam-to-column joints and column bases are assumed as fully fixed, when acting a moment resisting frame and nominally pinned when a braced framed is acting. The floor plant and elevation of the buildings are illustrated in Figure 7.4, Figure 7.5 and Figure 7.6, respectively for Case Study 1, Case Study 2 and Case Study 3.

The gravity loads considered in the design of case studies are summarized in Table 7.3. For the horizontal loads, seismic action is considered with a suitable distribution of lateral loads defined according to Eurocode 8 (CEN 2004a) assuming a regular behavior for the constructions. The resulting base shear is derived from the seismic mass of the structure by considering the spectral acceleration corresponding to an estimated fundamental period. Usually, the design spectrum is reduced by a suitable behavior factor q in order to account for the over-strength and ductility of the system whereas designing the structure in the linear range. In this case, a unitary behavior factor is chosen, since the main objective of this study is the first assessment of the presented connections without consider the dissipation capacity, the ductility and the capacity design of structure.

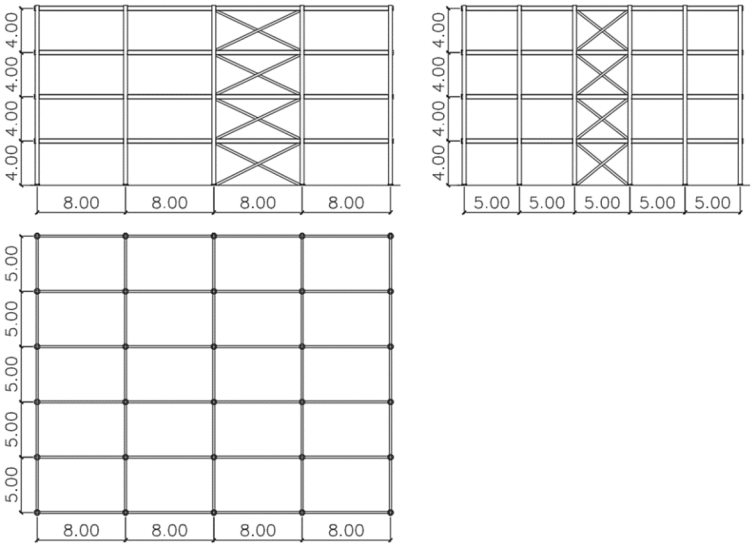

Figure 7.4 Configuration of Case Study CS1

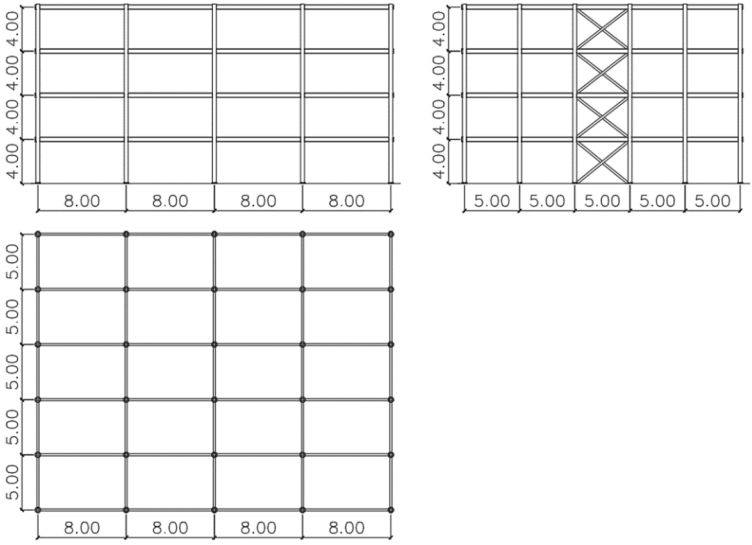

Figure 7.5 Configuration of Case Study CS2

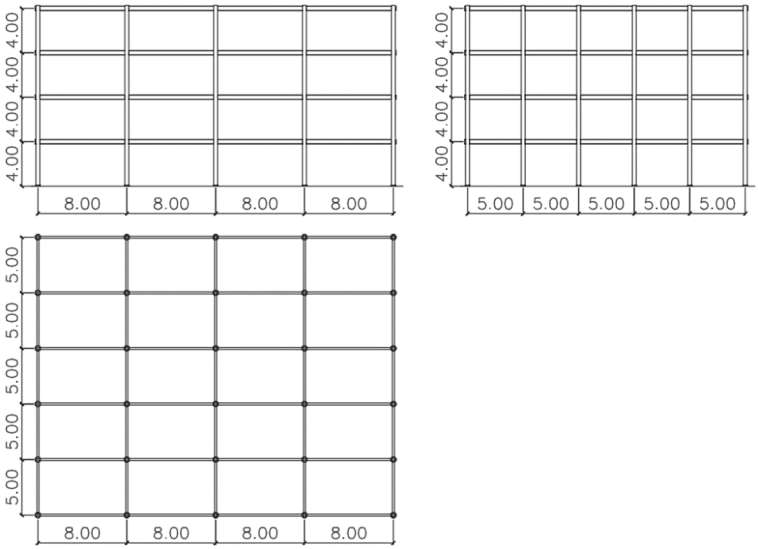

Figure 7.6 Configuration of Case Study CS3

Table 7.3 Loads considered in the design of case study structures

Load Class	Type of load	Value
Dead Loads	Composite slab with steel profiled sheeting (mean height 9.25 cm)	2.40 kN/m^2
Superimposed Loads	Services, celling and raised floors	1.20 kN/m^2
Live Loads	Commercial (Class D1)	4.00 kN/m^2
	Movable partitions	1.20 kN/m^2

7.2.2 Design of the composite beams

In the main direction, IPE400 (S275) beams with R.C. slab. In the secondary direction different solutions are possible: IPE270 (S275) with R.C. slab for Case Study 1 and Case Study 2, and IPE400 (S275) with R.C. slab for Case Study 3. In each case the slab is made with B450C re-bars and C25/30 concrete.

The resulting forces in the main and secondary beams, in case of the action of vertical gravity loads are the reported in Table 7.4.

Table 7.4 Forces for Ultimate Limit State

Case study	Main Beams			Secondary Beams		
	M_{Ed}^{-} [kNm]	M_{Ed}^{+} [kNm]	V_{Ed} [kN]	M_{Ed}^{-} [kNm]	M_{Ed}^{+} [kNm]	V_{Ed} [kN]
CS1	0	507	254	0	63	51
CS2	338	169	254	0	63	51
CS3	338	169	254	42	21	51

M_{Ed}^{-} is the maximum design moment for the beam in the connection region;
M_{Ed}^{+} is the maximum design moment for the beam in the center of the span;
V_{Ed} is the maximum design shear force for the beam.

The effective width of the composite main beam was defined according to EN 1994-1-1 (CEN 2004b), considering the geometry of the buildings. Results are shown in Table 7.5.

Table 7.5 Effective width of the beams

Case study	Main beam				Secondary beam			
	Lc ($b_{eff,1}$) [mm]	Lc ($b_{eff,2}$) [mm]	$b_{eff,1}$ [mm]	$b_{eff,2}$ [mm]	Lc ($b_{eff,1}$) [mm]	Lc ($b_{eff,2}$) [mm]	$b_{eff,1}$ [mm]	$b_{eff,2}$ [mm]
CS1	8000	-	2000	-	5000	-	1250	-
CS2	5600	4000	1400	1000	5000	-	1250	-
CS3	5600	4000	1400	1000	3500	2500	875	625

The geometric dimensions of the concrete slab are reported in Figure 7.7. The amount of general reinforcement in the beam in both directions should be not less than 80 mm^2/m, according to EN 1994-1-1 §9.2.1 (CEN 2004b). For this purpose, a welded mesh Φ6/150 mm is chosen in concrete slabs, providing an effective general amount of reinforcement of 188 mm^2/m in both directions.

According to EN 1994-1-1 §5.5.1 (CEN 2004b), for cross-sections in Class 1 and 2 with bars in tension, reinforcement used within the effective width should have a ductility Class B or C, as requested by EN 1992-1-1 (CEN 2004c).

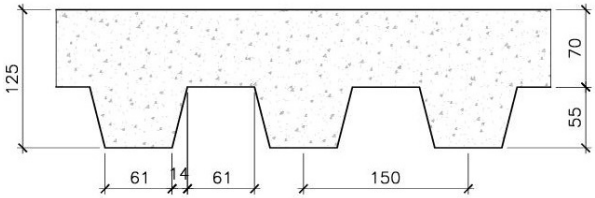

Figure 7.7 Dimensions of the composite slab

Additionally, a minimum area of reinforcement A_s, within the effective width of the concrete flange, should be provided to satisfy the following condition:

$$A_s \geq \rho_s \cdot A_c \qquad \text{Eq. 7.1}$$

where:

$$\rho_s = \delta \cdot \frac{f_y}{235} \cdot \frac{f_{ctm}}{f_{sk}} \cdot \sqrt{k_c} \qquad \text{Eq. 7.2}$$

The calculation made for the main and secondary beams, led to the following results:

$$\rho_{s,I} = 1.1 \cdot \frac{275}{235} \cdot \frac{2.56}{450} \cdot \sqrt{1} = 0.007 \qquad \text{Eq. 7.3}$$

$$A_{s,I} \geq 0.007 \cdot 1000\ mm \cdot 92.50\ mm = 680\ mm^2 \qquad \text{Eq. 7.4}$$

$$\rho_{s,II} = 1.1 \cdot \frac{275}{235} \cdot \frac{2.56}{450} \cdot \sqrt{1} = 0.007 \qquad \text{Eq. 7.5}$$

$$A_{s,II} \geq 0.007 \cdot 625\ mm \cdot 92.5\ mm = 405\ mm^2 \qquad \text{Eq. 7.6}$$

Considering the results of the calculation, the reinforcements to be used in the composite beams are defined. Thus, 6Φ16 B450C re-bars are provided in the beams rigidly connected to the column, supposed to have the concrete slabs in tension in the connection region.

In Moment Resisting Frames (CS2 and CS3), according to EN 1998-1, Annex C (CEN 2004a), in the slab of steel-concrete composite beams, in the beam-to-column joints region, an early crushing of the concrete of the slab shall be avoided (Figure 7.8).

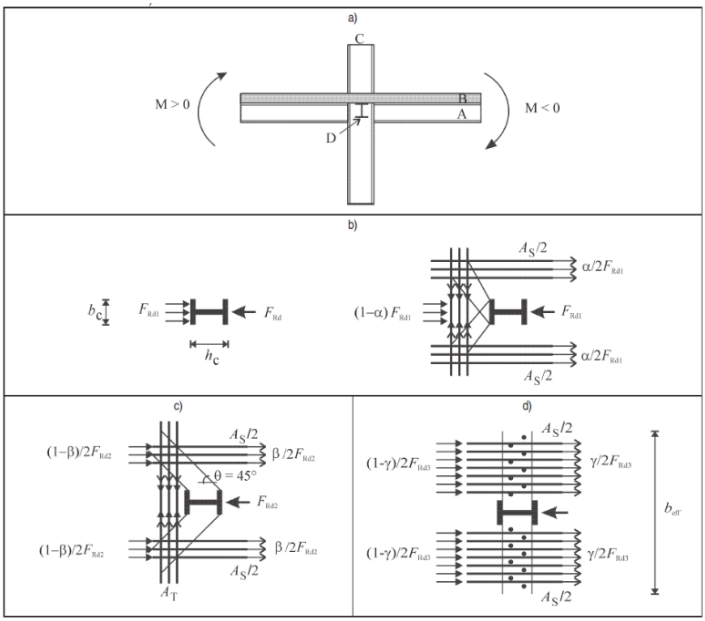

Figure 7.8 Possible transfer of slab forces in an interior composite beam-to-column joint with and without a transverse beam, under a positive bending moment on one side and a negative bending moment on the other side (EN1998-1 ANNEX C)

This condition imposes a lower limit of the transverse reinforcement in front of the column:

$$A_T \geq 0.5 \frac{F_{Rd,2}}{f_{yd}} \qquad \text{Eq. 7.7}$$

$$F_{Rd,2} = 0.7\ h_c d_{eff} f_{cd} \qquad \text{Eq. 7.8}$$

For the case study defined, characterized by the presence of CHS columns with an outside diameter of 355.6 mm, the following results are obtained:

$$F_{Rd,2} = 0.7 \cdot 355\ mm \cdot 65\ mm \cdot 14\ MPa = 229\ kN \qquad \text{Eq. 7.9}$$

$$A_T \geq 0.5 \frac{229\ kN}{390\ MPa} = 294\ mm^2 \qquad \text{Eq. 7.10}$$

On each side of the column, to avoid the early crushing of the concrete for the reversal of bending moment, 3Φ16 are placed, with a total area of 603 mm^2.

The results from the member verification for gravity loads, are reported in Table 7.6. Bending resistance of the composite beam is determined according to EN 1994-1-1, §6.2.1 (CEN 2004b), by using rigid-plastic theory, considering that the effective composite cross-section is in Class 2 and pre-stressing by tendons is not used. In the calculation, the composite cross-sections are assumed to remain plane, taking into account that the shear connection and the transverse reinforcement are designed considering appropriate distributions of design longitudinal shear force. Moreover, the tensile strength of concrete, such as the reinforcement in the compressed slab, are neglected, and a full interaction between structural steel, reinforcement, and concrete is considered. The presence of the profiled steel sheeting is neglected. Resistance of the composite beam to vertical shear is determined according to EN 1994-1-1, §6.2.2 (CEN 2004b), taking into account the resistance of the structural steel section, defined in accordance with EN 1993-1-1, §6.2.6 (CEN 2005b).

Table 7.6 Forces and capacity of beams in the ULS

	Case Study 1		**Case Study 2**		**Case Study 3**	
	Main Beam	**Secondary Beam**	**Main Beam**	**Secondary Beam**	**Main Beam**	**Secondary Beam**
Section	IPE400	IPE270	IPE400	IPE270	IPE400	IPE400
Steel grade	S275	S275	S275	S275	S275	S275
M_{Rd}^{+} **[kNm]**	609	236	571	236	571	571
M_{Rd}^{-} **[kNm]**	-	-	447	-	447	417
V_{Rd} **[kN]**	645	335	645	335	645	645
M_{Ed}^{+} **[kNm]**	507	63	169	63	169	21
M_{Ed}^{-} **[kNm]**	-	-	338	-	338	42
V_{Ed} **[kN]**	254	51	254	51	254	51
Ratio M^{+}	0.73	0.22	0.30	0.22	0.30	0.04
Ratio M^{-}	-	-	0.76	-	0.76	0.09
Ratio V	0.50	0.19	0.39	0.15	0.39	0.08

According to EN 1994-1-1 §6.6 (CEN 2004b), shear connection and transverse reinforcement shall be provided to transmit the longitudinal shear force between the concrete and the structural steel element, ignoring the effect of natural bond between

the two parts. For buildings, the number of connectors should be at least equal to the total design shear force for the Ultimate Limit State, determined according to EN 1994-1-1, §6.6.2 (CEN 2004b), divided by the design resistance of one single connector P_{Rd}. For stud connectors the design resistance should be defined according to EN 1994-1-1, §6.6.4 (CEN 2004b).

Considering the limitation provided in EN 1994-1-1, §6.6.1.2 (CEN 2004b), studs with a nominal diameter of 19 mm and height of 100 mm are chosen. The results of the shear connector design process are reported in Table 7.7.

Table 7.7 Design of the shear connectors

	CS1		**CS2**		**CS3**	
	Main Beam	**Secondary Beam**	**Main Beam**	**Secondary Beam**	**Main Beam**	**Secondary Beam**
Section	IPE400	IPE270	IPE400	IPE270	IPE400	IPE400
Steel grade	S275	S275	S275	S275	S275	S275
M_{Rd} **[kNm]***	609	236	447	236	447	417
$V_{l,Ed}$ **[kN]***	2214	876	451	876	451	300.6
P_{Rd} **[kN]**	73.10	57.09	73.10	57.09	73.10	57.09
L_C **[mm]***	8000	5000	2000	5000	2000	1250
p **[mm]**	150	150	200	150	200	150
Number of studs	53	33	10	33	10	8
$V_{l,Rd}$ **[kN]**	3874	1884	731	1884	731	457
Ratio	0.57	0.46	0.62	0.46	0.62	0.66

* Positive moment is used for beams without rigid connections, whereas negative moment was used for beams with rigid connections.

Longitudinal shear failure and splitting of the concrete slab due to concentrated forces applied by the connectors shall be prevented. As reported in EN 1994-1-1, §6.6.6 (CEN 2004b), transverse reinforcement in the composite beam with slab shall be designed to prevent premature longitudinal shear failure or longitudinal splitting. So that, the longitudinal shear stress for any potential surface of longitudinal shear failure within the slab, shall not exceed the longitudinal shear strength of the shear surface considered. The design shear strength of the concrete flange should be

determined in accordance with EN 1992-1-1, §6.2.4 (CEN 2004c) and the minimum area of transverse reinforcement should be determined considering EN 1992-1-1, §9.2.2 (CEN 2004c), using the following formula:

$$\rho_{w,min} = 0.08 \frac{\sqrt{f_{ck}}}{f_{yk}} = 0.08 \frac{\sqrt{25}}{450} = 0.00089 \qquad \text{Eq. 7.11}$$

In order to have the required area of transverse reinforcement between the concrete core of the composite beam, characterized by the presence of the shear connectors, and the lateral concrete slab, B450C Φ12/150 mm are disposed in both directions, obtaining the following results:

$$\rho_{w,main} = \frac{A_{sw}}{s\, b_w \sin\alpha} = \frac{2 \cdot 113\ mm^2}{150\ mm \cdot 1400\ mm \cdot 1} = 0.00108 \qquad \text{Eq. 7.12}$$

$$\rho_{w,sec} = \frac{A_{sw}}{s\, b_w \sin\alpha} = \frac{2 \cdot 113\ mm^2}{150\ mm \cdot 875\ mm \cdot 1} = 0.00172 \qquad \text{Eq. 7.13}$$

Transverse reinforcement re-bars have lengths such as to pass through all the any potential surface of longitudinal shear failure.

7.2.3 Design of composite columns

The concrete-filled steel tube column system has many advantages compared with the ordinary steel or the reinforced concrete system. One of the main advantages is the interaction between the steel tube and concrete: local buckling of the steel tube is delayed by the restraint of the concrete, and the strength of concrete is increased by the confining effect of the steel tube.

Concrete casting is usually done by Tremie tube or the pump-up method. However, difficulty in properly compacting the concrete may create a weak point in the system, especially in the case of passing-through. There is currently no way to ensure compactness or to repair this deficiency. To compensate, high-quality concrete with a low water-content and a superplasticizer for enhanced workability should be used in construction.

The design of the composite columns for the case studies is done by adopting the provision of the Eurocode 4 (CEN 2004b), which is also reported in the CIDECT Design Guide (Bergmann et al. 1995). The design guide provides different approaches for the calculation of the strength of concrete-filled tubular members. The first one is based on the AIJ Japanese standard (AIJ 2001) and it adopts the method of superposition which postulates that the ultimate strength of a member is given by the

sum of the ultimate strengths of the concrete part and steel part. The superposition method requires simpler calculations than the other method considering composite actions between the concrete and steel parts. According to the plastic theory, the superposition method gives a lower-bound solution for a structure made of ductile materials. However, this method may produce an error on the unsafe side if applied to composite members, because concrete is not sufficiently ductile. Therefore, the strength of composite members evaluated using the superposition method should always be verified by comparing it with experimental results. The second approach is based on the European code (CEN 2004b).

In case of axial loads on the column, the plastic resistance to compression $N_{pl,Rd}$ of a conlposite cross-section should be calculated by adding the plastic resistances of all its components: the steel tube and the concrete core. For concrete filled sections the coefficient 0.85 that reduces the stress strength of concrete is neglected.

In case of combined compression and uniaxial bending, the interaction between the two loading types must be consider. For this purpose, a plastic bending resistance is defined considering the normal force on the column. The resistance of the cross-sections to combined compression and bending and the corresponding interaction curve are calculated assuming rectangular stress blocks for the concrete stresses, neglecting the tensile strength of the concrete. The influence of transverse shear forces on the resistance to bending and normal force is considered if the shear ratio on the steel section exceeds 0.5. When higher, the influence of the transverse shear on the resistance in combined bending and compression is taken into account by a reduction of the design steel strength. The increase strength of concrete, caused by confinement, is also considered through the approach provided by Eurocode 4 (CEN 2004b).

The design led to the choice, for each case study, of CHS 355.6/10 concrete filled columns (S355 steel grade and C25/30 concrete).

7.2.4 Design of beam-to-column joints

Rigid and pinned beam-to-column connections are designed without consider the influence of the concrete. The design is carried out considering the provision of Eurocode 3, part 1-8 (CEN 2005a), by adopting C10.9 bolts with different nominal diameters. For the damage limitation limit states the design slip resistance is considered, whereas, for the ultimate limit states, the shear strength of the bolts is considered. Therefore, the bolts are considered preloaded as required in the code. All the bolted connections are partial-strength, since they are designed considering the forces that act in the sections and not the strength of the connected elements. All the

details are reported in Figure 7.9, Figure 7.10, Figure 7.11 and Figure 7.12, for the pinned and rigid connections types

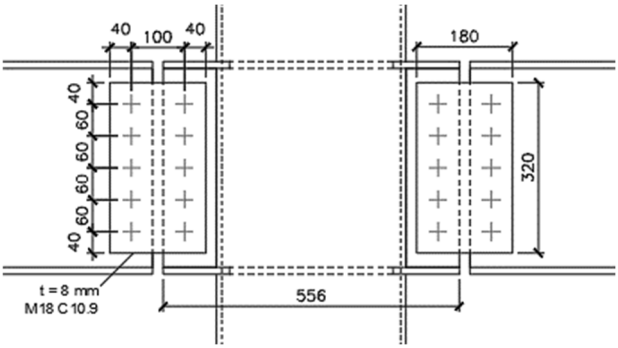

Figure 7.9 Details of the pinned connection with the through beam stub

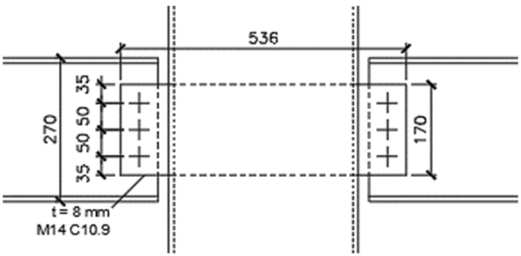

Figure 7.10 Details of the pinned connection with the through vertical plate

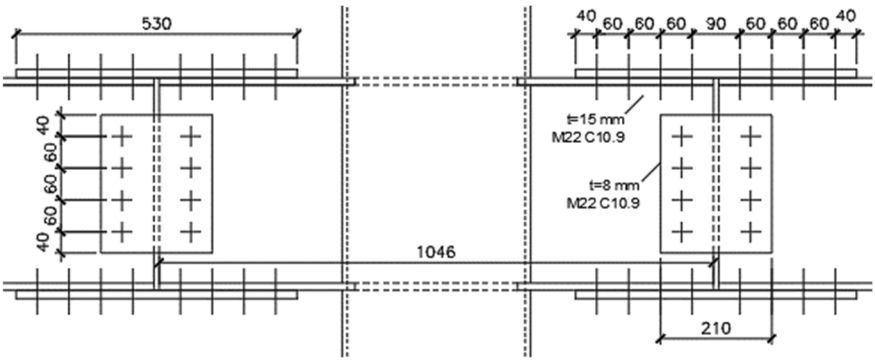

Figure 7.11 Details of the rigid connection with the through beam stub

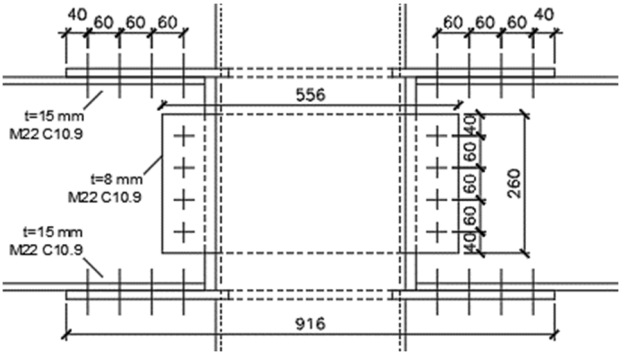

Figure 7.12 Details of the rigid connection with the three through

Welded connections between passing-through elements and columns are realized with fillet welds in case of pinned beam-to-column connection as reported in Table 7.8.

As the joints have the beams in both directions, appropriate combinations of the joint exposed are considered.

Table 7.8 Details of the bolted connections and welding

Den.	Beam	Welding	Flange plate	Flange bolts	Web plate	Web bolts
P1	IPE400	Fillet z = t	-	-	2 x 180 x 320 x 8	M18 C10.9
P2	IPE270	Fillet z =t	-	-	170 x 536 x 8	M14 C10.9
R1	IPE400	Full penet.	180 x 530 x 15	M22 C10.9	2 x 260 x 210 x 8	M22 C10.9
R2	IPE400	Full penet.	180 x 916 x 15	M22 C10.9	260 x 556 x 10	M22 C10.9

7.3 Definition of the testing program

The whole experimental program on composite substructures, summarized in Table 7.9, includes the execution of tests on two-way and four-way connection specimens. Six specimens are totally tested in the horizontal loading condition, whereas three specimens are tested under vertical loads. In addition to carry out tests on the specimens, the mechanical characterization of the materials is performed to obtain the mechanical characteristics of the steel used in the realization of members, columns, beams, and plates, the steel used in the fabrication of re-bars and the concrete casted in the slabs and infilled in the column.

Table 7.9 Overview of the experimental test performed in Pisa

Den.	Type	Main Direction	Secondary Direction	Loading type
C3-H-M	two-way	Through beam stub	-	Horizontal Monotonic
C3-H-C	two-way	Passing-through beam stub	-	Horizontal Cyclic
C4-H-M	two-way	Passing-through vertical and horizontal plates	-	Horizontal Monotonic
C4-H-C	two-way	Passing-through vertical and horizontal plates	-	Horizontal Cyclic
C7-1-H-M	four-way	Passing-through beam stub	Passing-through vertical and horizontal plates	Horizontal Monotonic
C7-2-H-M	four-way	Passing-through vertical and horizontal plates	Passing-through beam stub	Horizontal Monotonic
C5-V-M	four-way	Passing-through beam stub with external hinges	Passing-through vertical web plate	Vertical Monotonic
C6-V-M	four-way	Passing-through beam stub	Passing-through vertical web plate	Vertical Monotonic
C7-V-M	four-way	Passing-through beam stub	Passing-through vertical and horizontal plates	Vertical Monotonic

7.4 Design of the joint specimens for the vertical loading experimental tests

Tests with vertical load are performed on substructure specimens with four-way beam-to-column connections. Three specimens are totally tested under vertical loads. Each substructure is characterized by the presence of the beams in both directions, the concrete slab and the concrete filled tubular steel column. All the specimens have the same external dimensions.

The first specimen, C5, has all the beams pinned connected to the column. In the main direction, the pinned connections are made by one passing beam stub bolted to the external girders by two web plates (Figure 7.13a). In the secondary direction, one vertical passing-through plate is bolted to the beam webs (Figure 7.13b). The specimen is tested with a monotonic load applied from the bottom to the top, in order to have tension in the concrete slab (as expected for gravity load on the building).

The second specimen, C6, has the beams rigidly connected to the column in the main direction, whereas the beam in the secondary direction are pinned to the column. In the main direction the rigid connection is made by the continuity of the beam inside the column (Figure 7.14a). In the secondary direction, one vertical passing-through plate is bolted to the beam webs, realizing two external hinges (Figure 7.13b). The

specimen is tested with monotonic loads applied in the column, from the bottom to the top, and in the main beam-ends to the bottom, in order to have different loads applied in the main and in the secondary direction. The ratio between the load applied in the main and secondary planes is defined to have the 80% of the applied load in the main direction and 20% in the secondary one, as resulting from the analyses made on the case study structure CS2.

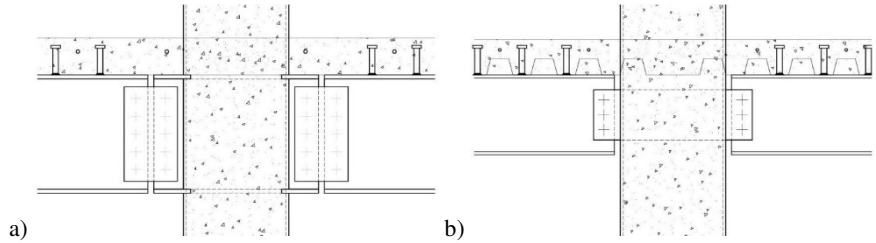

Figure 7.13 Pinned connection types: a) passing-through beam stub with external hinges, and b) one passing-through web plate

The third specimen, C7, has all the beams rigidly connected to the column. In the main direction the rigid connection is made by the continuity of the beam inside the column (Figure 7.14a). In the secondary direction, three passing plates are bolted to external beams (Figure 7.14b). The specimen is tested with monotonic loads applied, such as the C6 specimen, to have the right shear ratio between the main and secondary directions, 80% in the main direction and 20% in the secondary one, as resulting from the analyses made on the case study structure CS3.

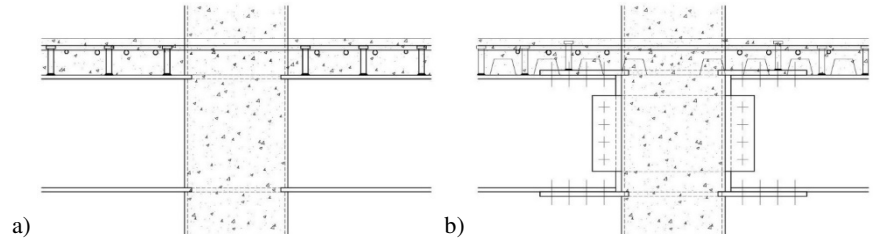

Figure 7.14 Rigid full-strength connection types: a) passing-through beam stub, and b) three passing-through plates

In Figure 7.15, Figure 7.16 and Figure 7.17 are respectively reported the details of C5, C6 and C7 specimens, which are tested in the vertical loading configuration. The total lengths of the main and secondary beams are respectively 3.82 and 3.24 m, as

well as the dimension of the slab. The columns have a total height of 1.86 m in each case. The overall dimensions of these specimens are defined to have moment-shear ratios in the beams according to the results of the design of the case study structures. The height of the column is chosen considering the laboratory features.

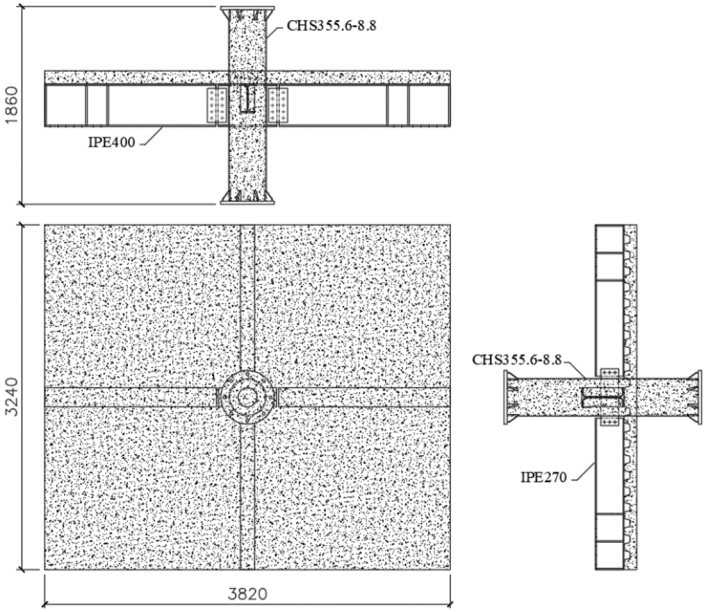

Figure 7.15 Details of specimen C5

All the specimens are designed according to the results obtained in the design of the case study structures. In this way, steel member sections, materials, dimensions of the concrete slab and reinforcement are defined. Some differences arise from the necessity of reduce the capacity of specimens to reduce the load to be apply in the tests.

Steel elements are chosen considering materials and sections defined in the case studies design and, furthermore, taking into account the geometry of the laboratory, the capacity of the equipment and the logistic necessities. The details of the steel parts of specimens are presented in Table 7.10.

CHS columns have in all the cases 355.6 mm external diameter and 8.8 thick wall. IPE400 is used in the main direction, either in fixed and pinned beams. In the secondary direction, IPE400 is used when the beam is rigidly fixed to the column, whereas IPE 270 is used when the beam is pinned to the column.

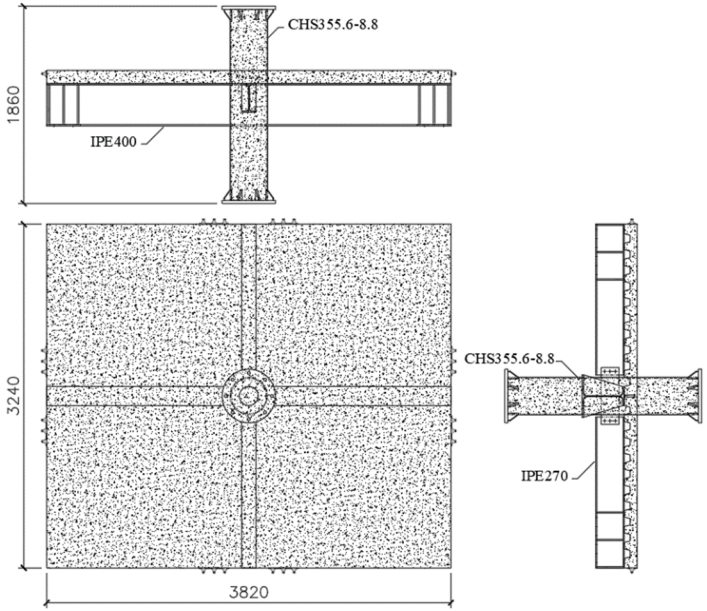

Figure 7.16 Details of specimen C6

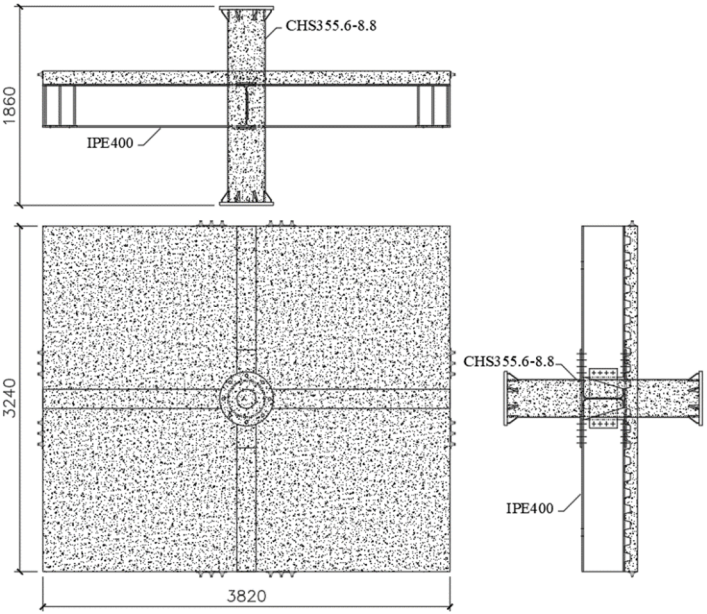

Figure 7.17 Details of specimen C7

C5 specimen has in the main direction a passing through beam stub (IPE400, which is connected by web plates to the external girders (IPE400), as done for the case study in the C1 connection (Figure 7.9). C10.9 M18 bolts and 8 mm thick plates are used. In the secondary direction, an 8 mm thick plate pass through the column wall and the web of the beam stub. The plate is connected by C10.9 M14 bolts to the girders (IPE270), as done in the C2 connection type in the case studies design (Figure 7.10).

C6 specimen is characterized by the presence of the passing-through beam (IPE400) without the external bolted connection, such as the C3 specimens, in the main direction. In the secondary one, an 8 mm thick plate pass through the column wall and the beam web. The plate is connected by C10.9 M14 bolts to the girders (IPE270), as done in the C5 specimen.

In the main direction, C7 specimens are characterized by the presence of the passing-through beam (IPE400) without the external bolted connection, such as the C3 specimens. In the secondary one, 15 mm thick passing-through flange plates and 8 mm thick passing-through web plate are used. The bolted connections are realized with C10.9 M22 bolts, such as the C4 specimen.

Adopted materials are steel S355 for columns and plates of the investigated connection and for flanges and diaphragm that allow the connection of the specimen to the test setups. Steel S275 is instead used for all the beams. All the connections, which are supposed to have a rigid full-strength behavior, are characterized for the use of full penetration welding to connect passing-through beams and plates to the tube wall, whereas passing-through elements are connected with fillet welds to the column wall in case of pinned connection.

Table 7.10 Passing-through elements of composite specimens tested under vertical loads

Den.	Welding type	Main direction			Secondary direction		
		Beam stub	Flange plates	Web plate	Beam stub	Flange plates	Web plate
C5-V-M	Fillet	IPE400	-	-	-	-	170x8
C6-V-M	Full penet.	IPE400	-	-	-	-	170x8
C7-V-M	Full penet.	IPE400	-	-	-	180x15	260x10

A R.C. slabs are realized and the column is filled by concrete, in order to test the behavior of the beam-to-column connection in case of composite beam and column. The required concrete strength-class is C25/30 for the casting of the slab and the filling of the column. Therefore, concrete is supposed to have, at 28 days, characteristic (5%)

cylinder strengths f_{ck} equal to 25 MPa and characteristic (5%) cube strengths R_{ck} equal to 30 MPa, in accordance with EN206:2013 (CEN 2013).

The concrete slab is casted by using a corrugated sheet with a height of 55 mm and a thickness of 0.8 mm. The corrugated sheet is not supposed to work together with the slab and the steel beam in the normal situation after the hardening of the concrete. The total height of the concrete slab is equal to 125 mm and shape is the same defined in the case studies design (Figure 7.7). In all the specimens to be tested with vertical loads (C5, C6 and C7), the corrugated slab is in parallel with the main direction.

In the specimen C5 tested with vertical loads, according to the case studies CS1, longitudinal and transversal anchored Φ16 Re-bars are not placed in the concrete slab, in order to assure the development of hinges. As shown in Figure 7.18. Φ12/150 mm are disposed perpendicular to the main direction and Φ12/150 mm perpendicular to the secondary direction to assure the shear connection between the core of the composite beam and the external sides. A welded mesh Φ6/150 mm is used in the concrete slabs. Welded studs, with a nominal diameter of 19 mm and height of 100 mm, are placed on the steel beam with a distance of 150 mm in both directions.

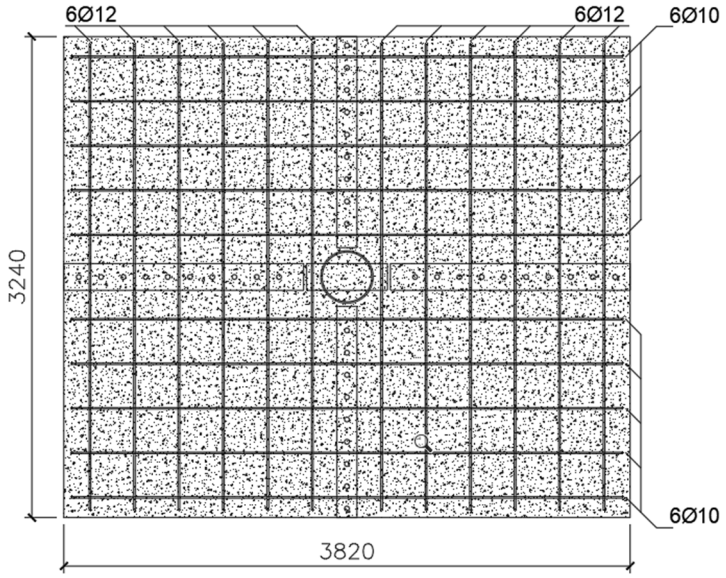

Figure 7.18 Concrete slab details for the specimen C5

Specimens C6 and C7, to be tested under vertical loads, are represented respectively in Figure 7.19 and Figure 7.20.

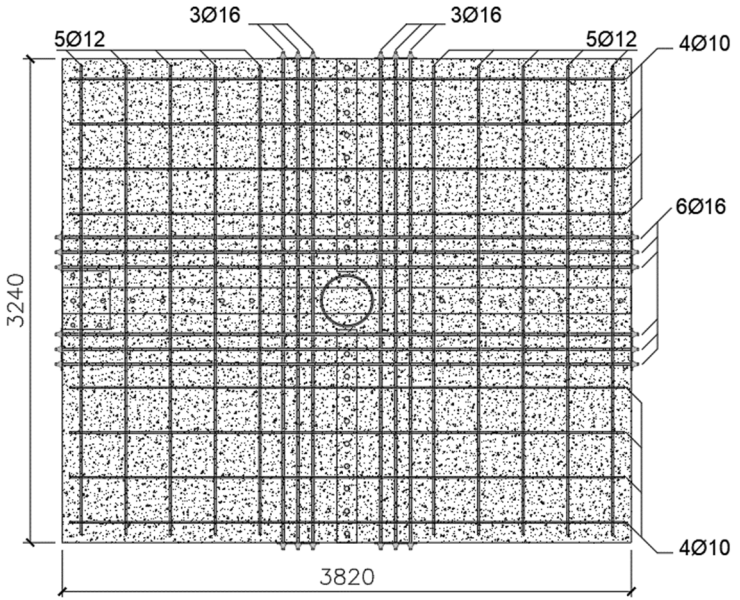

Figure 7.19 Concrete slab details for the specimen C6

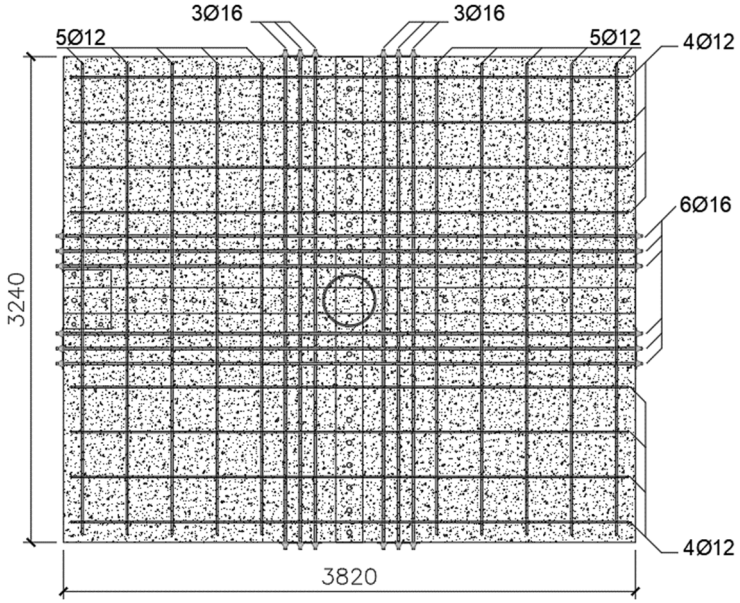

Figure 7.20 Concrete slab details for the specimen C7 to be tested under vertical loads

The reinforcements are disposed in the slab according respectively to the case studies CS2 and CS3. 6Φ16 longitudinal re-bars are inserted and, on each side of the column 3Φ16 transversal re-bars are placed. All these re-bars are anchored to the exterior of the slab by steel plates welded to the re-bars, in order to simulate the external anchorage. Φ12/150 mm are disposed in both the specimen in the main direction, whereas in the secondary one, C6 has Φ10/150 mm and C7 has Φ12/150 mm. Additionally, a welded mesh Φ6/150 mm is used in the concrete slabs. Welded studs, with a nominal diameter of 19 mm and height of 100 mm, are placed on the steel beam with a distance of 200 mm in the main direction and 150 mm in the secondary one.

7.5 Design of the joint specimens for the horizontal loading experimental tests

Tests with horizontal loading are performed on substructure specimens with two or four-way beam-to-column connections. Six specimens are totally tested. Four specimens are two-way composite joints with one steel beam in the main direction, the concrete slab and the concrete filled tubular steel column, whereas two specimens are four-way composite joints, with the beams in both directions, the concrete slab and the concrete filled tubular steel column. Two-way specimens are characterized by the presence of the rigid full-strength beam-to-column connections, one with the passing-through beam stub (Figure 7.14a) and one with the three passing-through plates (Figure 7.14b), respectively for C3 and C4. The two four-way specimens, tested with the horizontal loading setup, have in both the directions a rigid full-strength connection.

One two-way specimen, for both C3 and C4 types, is tested with monotonic loads, and the second one is tested with cyclic loads. The two four-way specimens, to be tested with horizontal monotonic loads, are C7 type and have the external dimensions equal to the two-way specimens, in order to use one test setup for the execution of all the test with horizontal loads. The difference between the two C7 specimens is the type of connection used in the load application direction. C7-1 specimen is investigated by applying the loads in the direction of the passing-through beam stub, whereas C7-2 is tested in the direction of the three passing-through plates, one vertical and two horizontals. In these last two tests, the influence of the passing-through elements in the transversal direction, on the behavior of the joint in the longitudinal direction, where the loads are applied, is investigated.

In Figure 7.21, Figure 7.22, Figure 7.23 and Figure 7.24 are respectively presented the details of C3, C4, C7-1 and C7-2 specimens to be tested under horizontal loads.

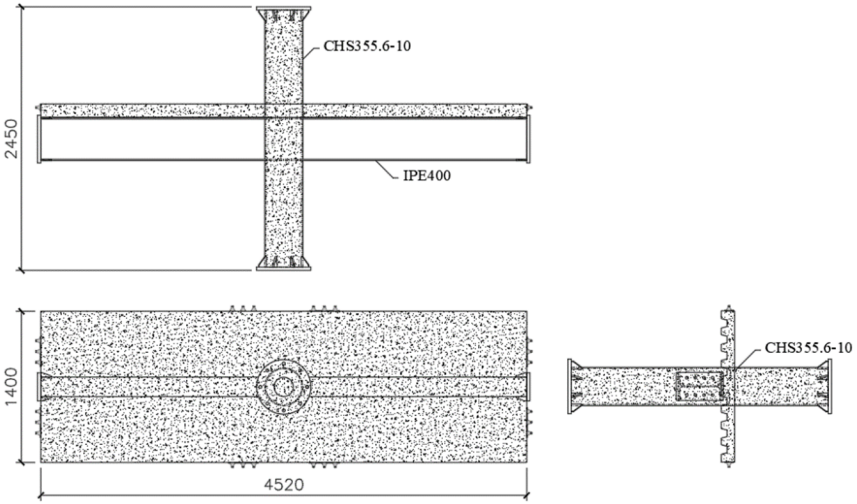

Figure 7.21 Specimen C3 to be tested under horizontal loads

All the specimens are designed according to the results obtained in the design of the case study structures. In this way, steel member sections, materials, dimensions of the concrete slab and reinforcement are defined. Some differences arise from the necessity of reduce the capacity of specimens and therefore reduce the load to be apply in the tests.

In each case the total beam length is equal to 4.52 m, the column height is 2.45 m and the width of the concrete slab in the secondary direction is 1.40 m. The length of the main beam is chosen to have a moment-shear ratio in the beam during the tests, according to the results of the analyses of the case studies under horizontal loads. The length of the secondary beams and the width of the slab are defined considering the effective width calculated for the case studies and reported in Table 7.5. The height of the column is fixed in order to have the moment-shear ratio similar to the one obtained in the case studies analyzed and considering the characteristics of the laboratory where the specimens are tested and the limitation that refer to the logistic necessities.

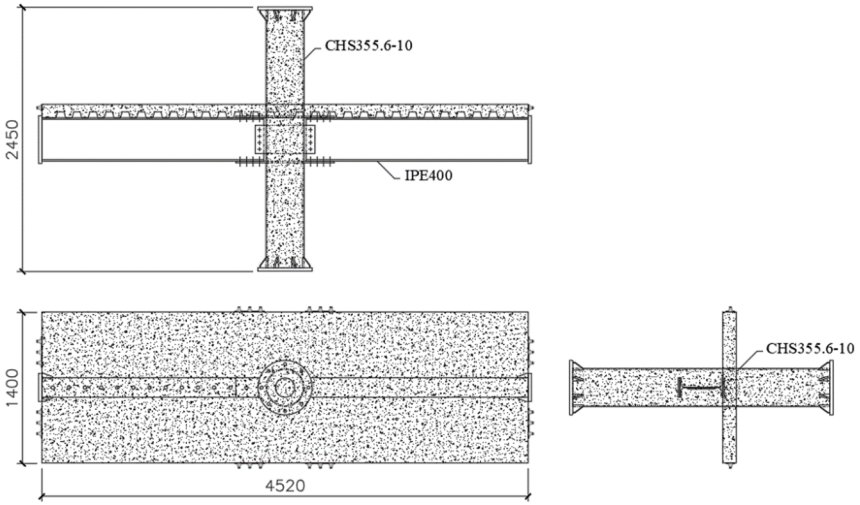

Figure 7.22 C4 to be tested under horizontal loads

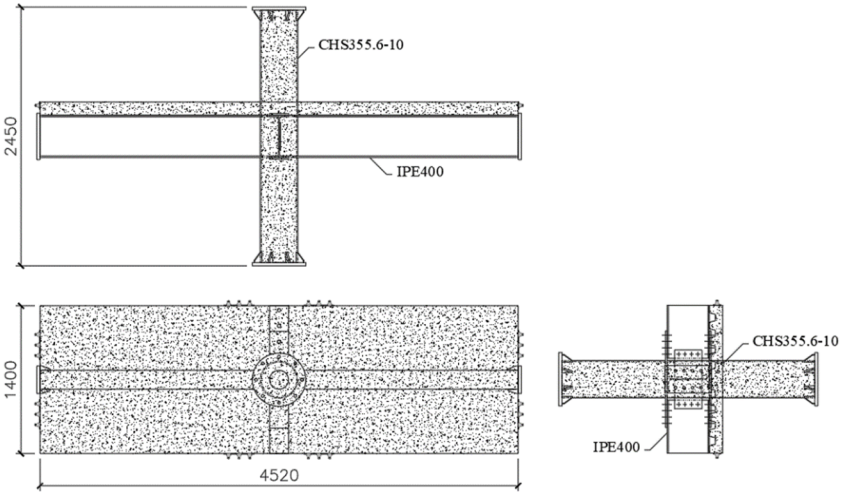

Figure 7.23 C7-1 to be tested under horizontal loads

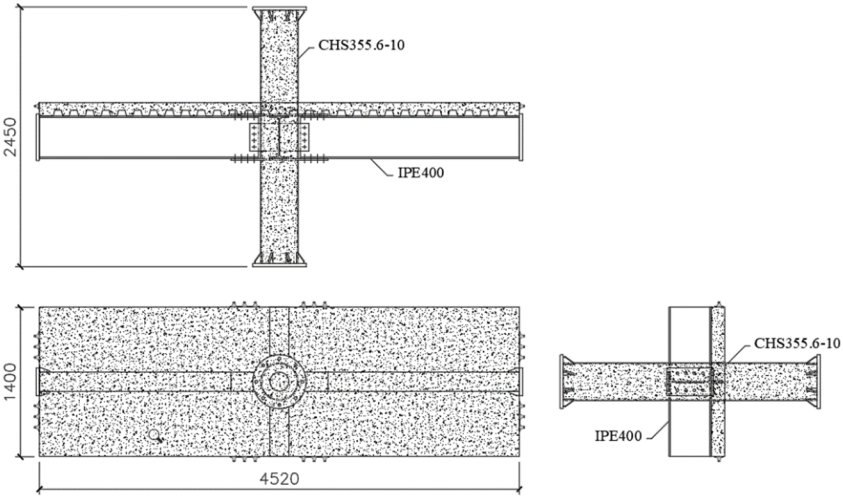

Figure 7.24 C7-2 to be tested under horizontal loads

Steel beams and columns, as well as connecting plates, are chosen considering materials and sections defined in the case studies design and, furthermore, taking into account the geometry of the laboratory, the capacity of the equipment and the logistic necessities. The details of the steel parts of specimens are presented in Table 7.11.

CHS columns have in all the cases 355.6 mm external diameter and 10.0 mm thick wall. IPE400 is used in the main and secondary directions.

C3 specimens have the passing-through beam. The external beam-to-beam bolted joint is excluded in order to eliminate possible mechanisms in these regions and more clearly understand the test results.

C4 connection is characterized for the presence of 15 mm thick passing-through flange plates and 8 mm thick passing-through web plate. The bolted connections are realized with C10.9 M22 bolts. The disposition comes from the connections designed for the case studies. Details are shown in Figure 7.12.

In the main direction, C7 specimens are characterized by the presence of the passing-through beam without the external bolted connection, such as the C3 specimens. In the secondary one, 15 mm thick passing-through flange plates and 8 mm thick passing-through web plate are used. The bolted connections are realized with C10.9 M22 bolts, such as the C4 specimen. C7-1 and C7-2 differ from the direction used for the load application. In the first case the loads are applied in the main direction. In the second one the loads are applied in the secondary direction.

Adopted materials are steel S355 for columns and plates of the investigated connection and for flanges and diaphragm that allow the connection of the specimen to the test setups. Steel S275 is instead used for all the beams. All the connections, which are supposed to have a rigid full-strength behavior, are characterized for the use of full penetration welding to connect passing-through beams and plates to the tube wall.

Table 7.11 Passing-through elements of composite specimens tested under horizontal loads

Den.	Welding type	Main direction			Secondary direction		
		Beam stub	Flange plates	Web plate	Beam stub	Flange plates	Web plate
C3-H-M	Full penet.	IPE400	-	-	-	-	-
C3-H-C	Full penet.	IPE400	-	-	-	-	-
C4-H-M	Full penet.	-	180x15	260x10	-	-	-
C4-H-C	Full penet.	-	180x15	260x10	-	-	-
C7-1-H-M	Full penet.	IPE400	-	-	-	180x15	260x10
C7-2-H-M	Full penet.	-	180x15	260x10	IPE400	-	-

In all the composite specimens, a R.C. slab is realized and the column is filled by concrete, in order to test the behavior of the beam-to-column connection in case of composite beam and column. The required concrete strength-class is C25/30 for the casting of the slab and the filling of the column. Therefore, concrete is supposed to have, at 28 days, characteristic (5%) cylinder strengths f_{ck} equal to 25 MPa and characteristic (5%) cube strengths R_{ck} equal to 30 MPa, in accordance with EN206:2013 (CEN 2013).

The concrete slab is casted by using a corrugated sheet with a height of 55 mm and a thickness of 0.8 mm. The corrugated sheet is not supposed to work together with the slab and the steel beam in the normal situation after the hardening of the concrete. The total height of the concrete slab is equal to 125 mm and shape is the same defined in the case studies design (Figure 7.7). The corrugated sheet is disposed in parallel to the main beam, which is the one that passes directly through the column.

In the specimens C3, C4, C7-1 and C7-2, to be tested in the horizontal loading configuration, the reinforcements are disposed in the slab according to the case studies CS3. All the specimens have the configuration represented in Figure 7.25. 6Φ16 longitudinal re-bars are inserted and, on each side of the column 3Φ16 transversal re-bars are placed, to avoid the early crushing of the concrete for the reversal of the

bending moment. All these re-bars are anchored to the exterior of the slab by steel plates welded to the re-bars, in order to simulate the external anchorage. Φ12/150 mm are disposed in both directions, in order to have the required area of transverse reinforcement between the concrete core of the composite beam, characterized by the presence of the shear connectors, and the lateral concrete slab. Additionally, a welded mesh Φ6/150 mm is used in the concrete slabs, providing an effective general amount of reinforcement equal to 188 mm^2/m in both directions. Welded studs, with a nominal diameter of 19 mm and height of 100 mm, are placed on the steel beam with a distance of 200 mm in the main direction and 150 mm in the secondary one. In the specimens C3 and C7-1 the corrugated slab is in parallel with the load-application direction, whereas in the C4 and C7-2 specimens it is perpendicular to the load-application direction.

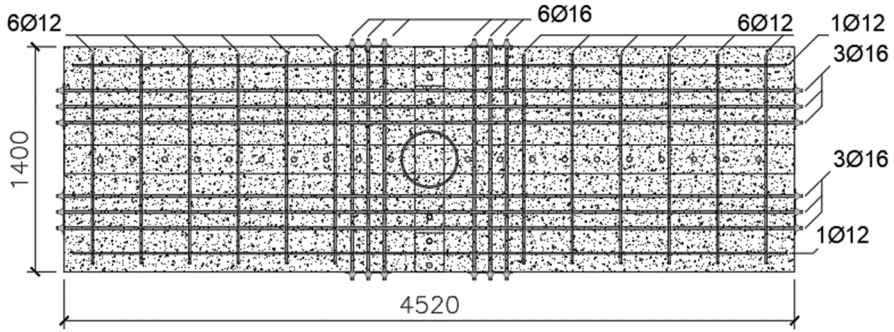

Figure 7.25 Concrete slab details for the specimen C3, C4, C7-1 and C7-2 to be tested under horizontal loads

7.6 Assembly and casting of the specimens

The cutting operations were performed in shop in the production center of ADIGE-SYS SpA. The assembly of the steel parts that requires welding operations was entirely realized in shop in the production center of OCAM Srl. These companies are two of the industrial partners of the RFCS research project LASTEICON (Castiglioni et al. 2016). The assembly of the steel parts with bolted connections, the preparation of the formworks and the concrete casting operations are carried out in the laboratory of the University of Pisa where the specimens are tested. Considering the characteristics of the laboratory and the specimens, a maximum of three specimens are processed simultaneously.

7.6.1 Assembly processes

The whole assembly process includes the cutting processes, the assembly of the steel parts of the specimens with the welding processes and the realization of the bolted connection.

The whole procedure starts with the laser cutting operations performed in the production center ADIGE-SYS SpA. Beams and columns are therefore processed in order to have the right slot dimensions. 3D cutting type is used to realize the slots, when the penetration welding is required. The cutting angle adopted is 30° and the dimensions of the slot were defined measuring the dimension of the beams and adding a gap of 3 mm, in order to allow the complete penetration of the welding.

Afterwards, the cut elements were delivered to the shop where the welding processes were carried out. In the production center of OCAM Srl, the passing-through elements were inserted through the slots and then the welds were realized (Figure 7.26a). Besides, the specimens are equipped with the diaphragms and plates required to connect the specimens to the test setups (Figure 7.26b).

a)  b) 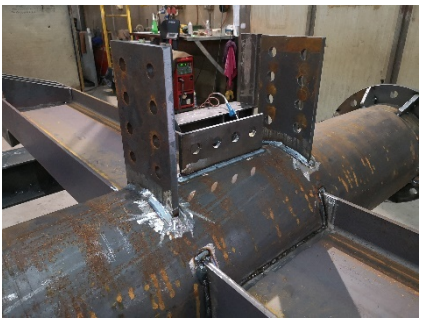

Figure 7.26 Welding processes on the specimens: a) welds realized in the flange passing-through plate region and b) C7 specimen completely assembled

Specimen marks were then delivered to the University of Pisa were the assembly of the steel parts with bolted connections are carried out in the laboratory where the specimens are tested. The specimens are assembled in three phases. In each phase three specimens are assembled and completely fabricated. All the specimens are assembled inserting the bottom part of the column inside the holes of the R.C. strong floor of the laboratory, as shown in Figure 7.27.

The assembly of the specimens C3 did not require the realization of bolted connections. The realization of the bolted connection of the external girders in the transversal direction of specimen C7-1 did not exhibited any problems, as shown in

Figure 7.27a. On the contrary, the assembly of C4 and C7-2 specimens, characterized by the three passing-through plates in the longitudinal tested direction, highlights some problems with the correct position of the external girders and bolts. Problems are due to the reduced distance between the two horizontal plates (Figure 7.27b) and the improper position of the holes on the plates with those on the flanges of the external beams.

a) 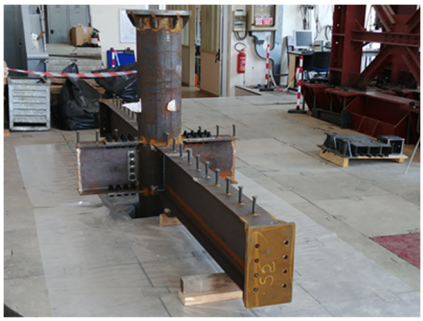 b) 

Figure 7.27 Assembly operations in the laboratory: a) specimen C7-1, and b) specimen C4

7.6.2 Casting operations

After the assembly of the steel parts, the preliminary operations for the realization of the concrete castings are carried out. First of all, the corrugated sheet is correctly positioned on support systems. The formwork is then prepared for the casting and the reinforcing re-bars are positioned. Preventively, the longitudinal and transverse re-bars are equipped with strain gauges. This process required the preparation of the controlled points on the re-bars, the application of the strain gauges (Figure 7.28a) and the complete protection of the sensitive parts before the castings (Figure 7.28b).

a)  b) 

Figure 7.28 Strain gauges on re-bars: a) application and b) protection of the parts

The preparation of the formworks did not exhibit additional difficulties comparing with the traditional I-beam-to-CHS-column composite connections (Figure 7.29 and Figure 7.30). The re-bars that require the external anchorage are passed through the formwork thanks to fitted slots.

Figure 7.29 Formworks of a two-way specimen

Figure 7.30 Formworks of a four-way specimen

The casting operations of the slab did not exhibit particular problems (Figure 7.31a). The filling of the column is made through a hole realized in the upper diaphragm welded to the column (Figure 7.31b) and highlights some problems with the correct passage of the concrete through the small free space in the connection region. In fact, where the plates or the beam pass through the column, reduced spaces remain free for the passage of the concrete, in particular for the four-way specimens (Figure 7.32). For this purpose, Self-Compacting Concrete (SCC) is used instead of normal concrete. However, the presence of air in the lower part of the column complicated the operations and only thanks to the manual handling of the concrete, the correct realization of the filling was reached.

a)  b) 

Figure 7.31 Fabrication of composite specimens: a) casting of the concrete slab, and b) filling of the tubular steel column

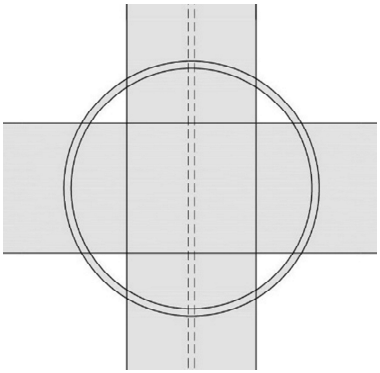

Figure 7.32 Schematic view of the reduced spaces that remain free for the passage of the concrete in the four-way specimens

7.7 Material characterization

In parallel with the execution of the experimental tests on the full-scale substructures, the mechanical characterization of the materials is carried out. Tensile tests on specimens directly extracted from the steel members, and on re-bars are defined, as well as compression tests on cube realized during the casting operation. The results of this characterization are useful for the definition of the material property to be used for the individual components in the mechanical models.

7.7.1 Steel members

Tests were performed on specimens directly extracted from the IPE400 beams, the CHS355.6 columns and the plates of the substructures, for each member, three specimens are extracted and worked to get the dimensions shown in Figure 7.33, in order to carry out tensile tests. The thickness of the specimens is equal to thickness of the base member. In case of thickness higher than 10 mm the specimens are worked to reach 10 mm of thickness.

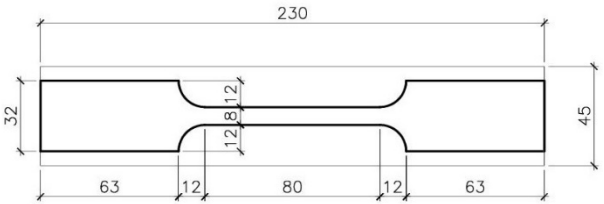

Figure 7.33 Geometric characteristics of the specimens

The tensile tests allow the definition of the stress-strain curves for the singular specimen. Moreover, they allow the definition of the yielding stress, ultimate stress and elongation for the ultimate stress, for each tested specimen. The mean values of these mechanical characteristics are reported in Table 7.12 for each member type.

Table 7.12 Mean value of the mechanical characteristics for the different tested elements

Member	Type	Mean Yielding Stress [MPa]	Mean Ultimate Stress [MPa]	Mean Elongation for Ultimate Stress [%]
IPE400	Flange	354	485	20.1
IPE400	Web	393	496	17.5
IPE270	Flange	314	432	17.8
IPE270	Web	313	436	19.3
CHS 355.6/8.8	Tube Wall	405	563	13.4
CHS 355.6/10	Tube Wall	390	555	14.3
Plate 8 mm	Plate	409	558	15.2
Plate 10 mm	Plate	347	500	17.1
Plate 15 mm	Plate	414	569	16.0

Some resulting stress-strain curves are reported in Figure 7.34, for instance, for the IPE400 and CHS355.5/10 profiles and for the 8 mm and 15 mm thick plates.

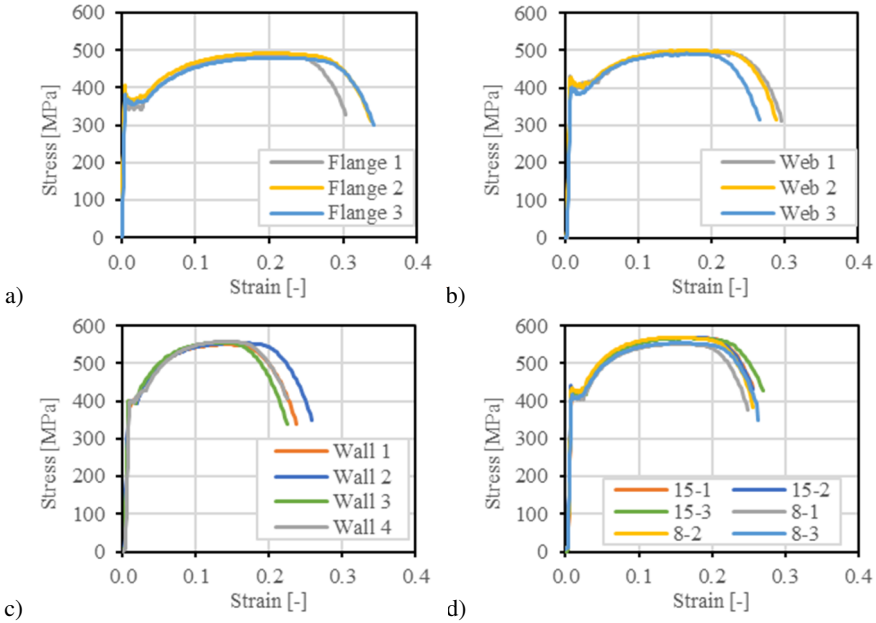

Figure 7.34 Stress-strain curves of: a) IPE400 flanges, b) IPE400 webs, c) CHS355.6/10 tube and d) 8 mm and 15 mm thick plates

7.7.2 Reinforcement

Tensile tests are also performed on re-bars specimens in order to obtain the stress-strain curves and to define the yielding stress, the ultimate stress and elongation for the ultimate stress, for the singular type of re-bar used. The mean values of these mechanical characteristics are reported in Table 7.13 for the ϕ10, ϕ12 and ϕ16 re-bars used in the R.C. slabs. The obtained stress-strain curves are represented Figure 7.35 for ϕ12 and ϕ16 re-bars used in the R.C. slabs of the specimens.

An additional test is performed on a ϕ16 re-bar equipped with two strain gauges in order to correlate the deformation obtained with the strain gauges and the axial load in the re-bar. The test shows a fine correlation of deformation calculated with the displacement obtained by LVDTs and one directly obtained by strain gauges (Figure 7.36a). Moreover, the axial load calculated considering the strain gauges deformation and the nominal characteristics of the re-bar, such as the steel Young's modulus and

the nominal resisting area, results to be almost equal to the one directly obtained from the testing machine in the elastic range (Figure 7.36b).

Table 7.13 Mean value of the mechanical characteristics for the different re-bars

Type	Mean Yielding Stress [MPa]	Mean Ultimate Stress [MPa]	Mean Elongation for Ultimate Stress [%]
ϕ12	463	565	7
ϕ16	561	618	6

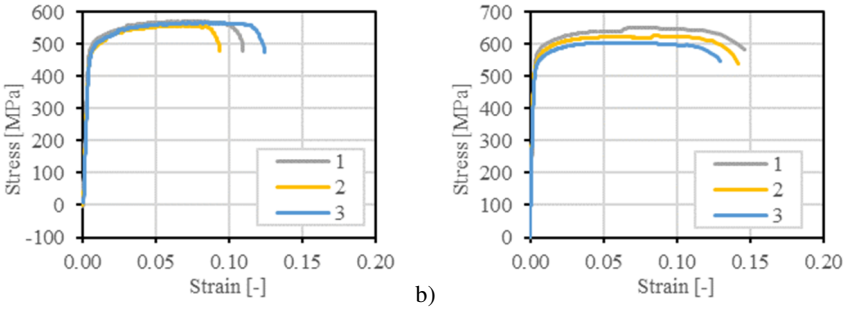

Figure 7.35 Stress-strain curves of a) φ12 and b) φ16 re-bars for the specimens

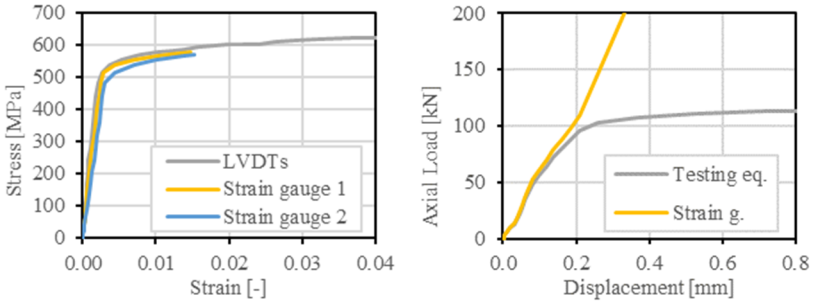

Figure 7.36 Comparison of the results obtained with the testing machine equipment and the strain gauges applied to the re-bar: a) stress-strain curves, and b) axial load-displacement

7.7.3 Concrete

Compression tests are carried out concrete cube specimens realized during the casting operation. For each specimen, two cubes where extracted and tested for either the slab and the column, realized with different concrete. The mean values of the cube strengths R_c are reported in Table 7.14 for the different elements and specimens.

The results exhibit a higher value of the cube strengths R_c, in comparison with the strength required. In particular, for the slab the mean value is 36 MPa and for the column is 44 MPa. In this latter case the concrete is a SCC type.

Table 7.14 Results of the compression test on cubes

Specimen	Element	*Ac*	*F* [kN]	*Rc* [MPa]	Curing days
C3-H-M	Slab	226.50	775	34.2	36
C3-H-M	Column	228.00	920	40.3	33
C7-1-H-M	Slab	222.00	757	34.1	65
C7-1-H-M	Column	225.73	985	43.6	62
C3-H-C	Slab	216.82	867	40.0	93
C3-H-C	Column	220.52	1010	45.8	90
C4-H-M	Slab	225.75	780	34.55	42
C4-H-M	Column	225.00	990	43.97	34
C7-2-H-M	Slab	228.00	785	34.43	42
C7-2-H-M	Column	225.75	1063	47.06	34
C4-H-C	Slab	228.75	863	37.70	97
C4-H-C	Column	225.00	1157	51.44	89
C5-V-M	Slab	223.50	815	36.37	39
C5-V-M	Column	222.51	890	40.00	34
C6-V-M	Slab	221.51	876.67	39.58	39
C6-V-M	Column	224.49	955	42.54	34
C7-V-M	Slab	228.25	853	37.35	72
C7-V-M	Column	225.00	1027	45.63	65

8 Experimental assessment of the composite-joint behavior under vertical gravity loads

All the tests on composite specimens with vertical loads are carried out in the University of Pisa Laboratory "Laboratorio ufficiale per le esperienze sui materiali da costruzione". A R.C. strong floor characterizes the laboratory. Three testing configurations are adopted in order to test three specimens under vertical loads. All the substructure specimens have a four-way composite beam-to-column joint.

Each type of four-way specimen is characterized by different joint types: specimen C5 with all the beams nominally pinned to the column, specimen C6 with the passing through continuous main beam (rigid full-strength) and the nominally pinned secondary beams, and the specimen C7 with the passing through continuous main beam and rigidly connected secondary beams (both joints are rigid full-strength).

The simulation of vertical loads acting on the deck is carried out with three configurations, opportunely defined and designed to apply the proper load ratios in the main and transversal directions, according to the results of the case study analyses.

C5 specimen, with the external pinned connection in both directions, is tested in the configuration shown in Figure 8.1. The vertical load is applied monotonically in the bottom of the column, directed to the top of the specimen. The beam lengths are defined in order to have a ratio between the main and secondary beam shear, according to the proper case study structure. Load is applied to the bottom in order to have sagging bending moment in the composite beams, with the concrete slab in compression, as expected for pinned beams. Clearly, the beams are connected by ideal pinned connections and, in the first phase of the test, hogging bending moment is present in the beam-to-column connection, until the plastic hinges develop. All the beam-ends are connected to the test setup by rigid full-strength connections.

C6 specimen, with rigid full-strength connections in the main direction and nominally pinned ones in the secondary direction, is tested in the configuration shown in Figure 8.2. Opposite vertical loads are applied on the bottom of the column (to the top) and on the main beam-ends (to the bottom). This configuration allows the application of different loads in the main and in the secondary beams. The ratio between these loads is defined according to the results of the analyzed case studies CS2. Besides, beam lengths are defined to have the right moment-shear ratio in the connection region. The direction of the load is chosen to have hogging bending moment in the main beam in the connection region. The beams in the secondary direction are connected in their ends to the test setup, by rigid full-strength connections.

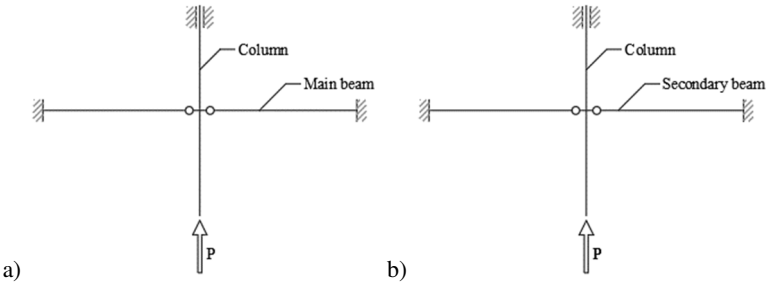

Figure 8.1 Testing configuration with vertical loads for specimen C5 in the a) main and b) secondary directions

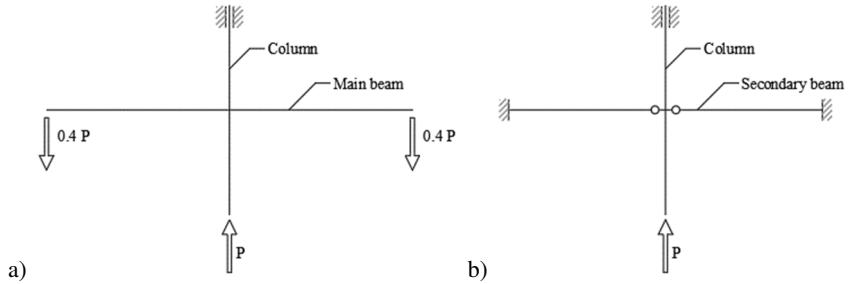

Figure 8.2 Testing configuration with vertical loads for specimen C6 in the a) main and b) secondary directions

C7 specimen, with rigid connection in both directions, is tested in the configuration exposed in Figure 8.3. As for the C6 configuration, opposite vertical loads are applied on the bottom of the column (to the top) and on the main beam-ends (to the bottom), in order to have different load in the main and in the secondary beams. Besides, beam

lengths (different from the C6 specimen) are defined to have the right moment-shear ratio in the connection region, as resulting from the results of the case study CS3. The direction of the load is chosen to have hogging bending moment in the beams in the connection regions. The beams in the secondary direction are connected in their ends to the test setup by pinned joints.

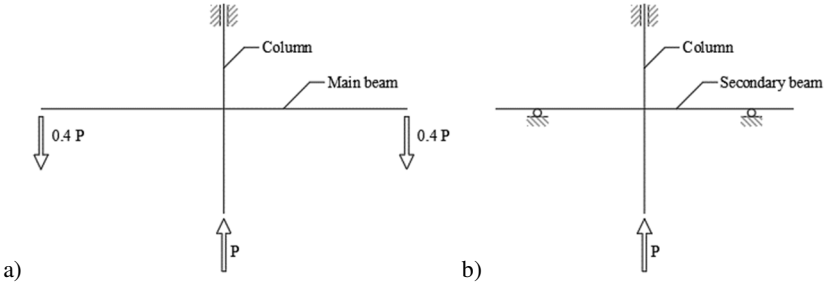

Figure 8.3 Testing configuration with vertical loads for specimen C7 in the a) main and b) secondary directions

Considering the difference between the testing configurations adopted for composite specimens, the comparison of the results of the vertical loading tests is made by calculating the total bending moment acting on the beam-to column connection in the main and secondary directions and by the rotation of the beams, obtainable respectively through the applied loads and the vertical relative displacements.

8.1 Testing setups

A steel basement, composed of HEB400 S355 profiles, is used in all the testing setups represented in Figure 8.4, Figure 8.5 and Figure 8.6 to applied the load to the specimens. One 1.5 MN single acting hydraulic jack applies the load (only in compression) in the bottom of the column (directed to the top) in all the testing setups.

In the tests with the loads applied in the beam-ends too, two 450 kN double acting hydraulic jacks are additionally used. In the main direction, these hydraulic jacks are connected in the lower side to the steel basement, and in the upper one to the beam-ends of the specimen. In the secondary direction the specimens are supported by columns. Contrast elements and steel rods rigidly connect the basement to the laboratory R.C. strong floor as shown in Figure 8.4, Figure 8.5 and Figure 8.6.

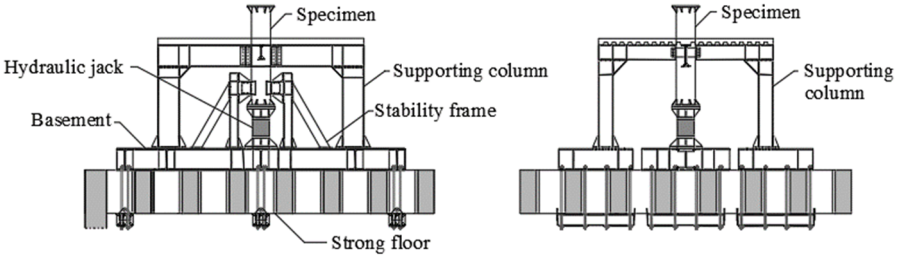

Figure 8.4 Frontal (left) and lateral (right) views of the testing layout for the specimen C5 under monotonic vertical loads

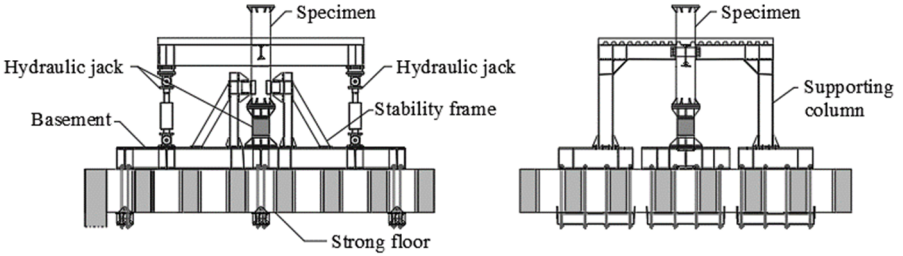

Figure 8.5 Frontal (left) and lateral (right) views of the testing layout for the specimen C6 under monotonic vertical loads

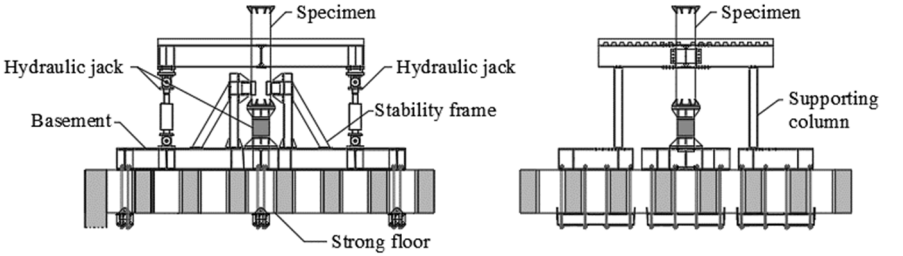

Figure 8.6 Frontal (left) and lateral (right) views of the testing layout for the specimen C7 under monotonic vertical loads

C5 specimen (Figure 8.4) is supported by two IPE400 columns in the main direction and by two IPE270 columns in the secondary one. The columns are fixed to the basements, and to the beams of the specimen, by rigid full-strength bolted joints. In the case of specimens C6 and C7, the additional load jacks are connected to the main beam by bolted connection and additional stiffeners. In the secondary direction, specimen C6 is supported by IPE270 columns rigidly fixed to the basement and the beam-ends (Figure 8.5), whereas the specimen C7 is supported by HEB160 column

pinned to the beam-ends (Figure 8.6). All the steel parts of the setup are made with S355 steel.

The lateral rotations of the column in the elastic and post-elastic phases are avoided by the stability frames, represented in Figure 8.6, composed of HEB160 columns and struts, and contrast movable elements put in contact with the column of the specimen.

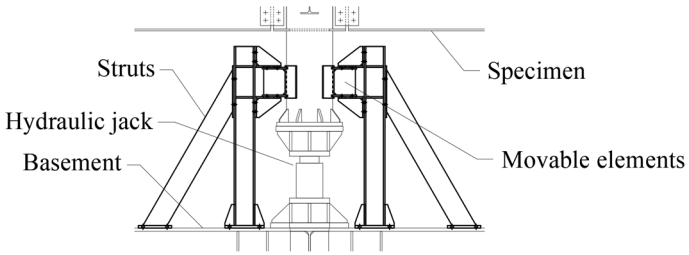

Figure 8.7Stability frame adopted to avoid lateral displacement of the column

8.2 Instrumentation

The instrumentation setups are defined considering the objectives of opportunely characterizing both the monotonic global behavior of the specimens, in terms of external reactions and global displacement, and the local mechanism of forces transferring from the composite beams to the filled column. The instrumentation used during the vertical loading tests is made by inclinometers, strain-gauges, inductive displacement transducer, load cells and pressure transducers. Inductive displacement transducer (LVDTs), inclinometers and strain gauges can provide data about the kinematics of the specimen and the deformations in some points opportunely chosen. The load cells allow the definition of the external applied forces during the test. Therefore, it is possible to obtain the distribution of the bending moment and shear force in each section of the beams in the main direction and of the column. Moreover, the data acquisition about the forces, makes possible the definition of the ratio between the load in the main and secondary directions. To examine the local mechanism in the specimen, strain gauges are used to measure the deformation of the rebars in the R.C. slab and of the beam flanges. Strain gauges make thus possible the evaluation of the deformation and transferred forces in the controlled sections of the composite beam. Strain gauges are also applied on the steel column wall in order to investigate the deformation and the stresses in the connection regions.

Where adopted, the two lateral hydraulic jacks are equipped with load cells and displacement transducers for monitoring the applied load and the global displacements. In each case the central hydraulic jack is equipped with a pressure and

displacement transducers to acquire data about force and elongation. In the C5 testing setup, the four lateral columns are equipped with strain gauges in order to acquire information about the load distribution in the main and secondary direction. Inclinometers and LVDTs displacement transducers are used to detect rotations and displacements during the tests, in both the directions. The inclinometers and LVDTs used in the C7 testing setup are for instance shown in Figure 8.8 and Figure 8.9 respectively.

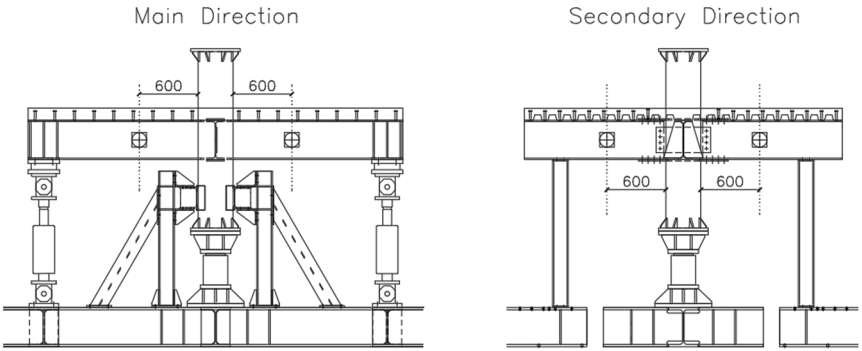

Figure 8.8 Inclinometers disposed on the specimen in each testing setup

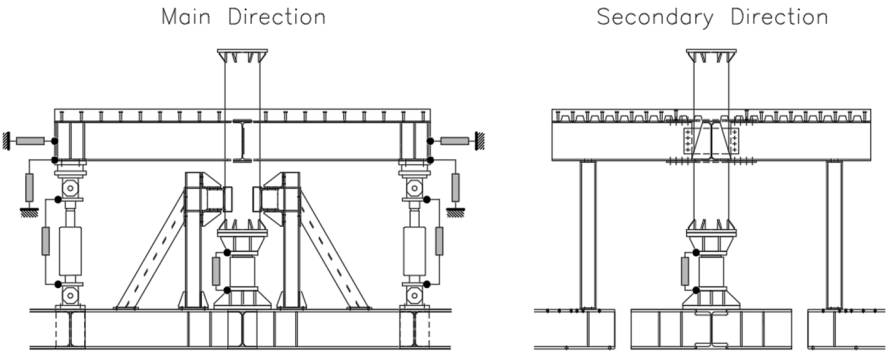

Figure 8.9 LVDTs displacement transducers disposed in the test setup and on the specimen in each testing setup

In each the test performed, strain gauges are applied to the steel parts of beams and column. The controlled beam sections (Figure 8.10) are furnished by four 6 mm linear strain gauges, disposed as shown for instance in Figure 8.11a. On the column wall, six 6 mm linear strain gauges are applied on each side of the specimen around the slots for the passing-through elements (Figure 8.11b).

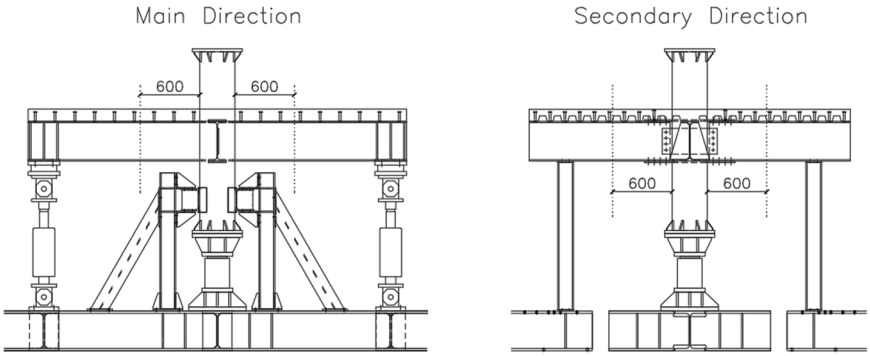

Figure 8.10 Beam sections controlled by strain gauges in the C7 testing setup

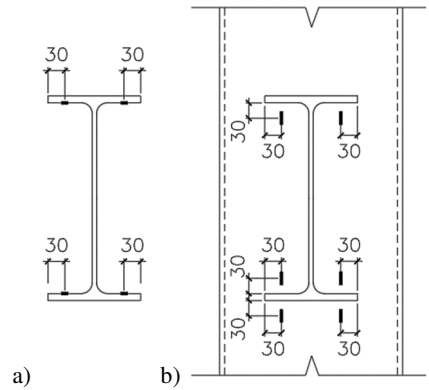

Figure 8.11 Position of the strain gauges on C7 specimen: a) beam flanges in each controlled section, and b) tubular column wall near the slot for the passage of the beam

Linear strain gauges are also applied to the longitudinal and transversal re-bars of the R.C. slab in each specimen (Figure 8.12). Each controlled point is provided by two 6 mm linear strain gauges disposed on the opposite sides of the bar.

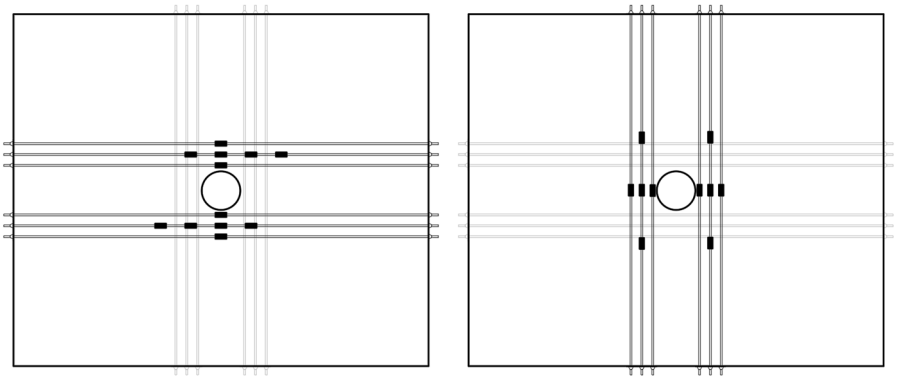

Figure 8.12 Disposition of the strain gauges on the longitudinal (left) and transversal (right) re-bars in the specimens C7 to be tested with monotonic vertical loads

8.3 Results of the tests on the four-way composite specimens

In this paragraph, the experimental testing results for the four-way composite substructures subjected to monotonic vertical loads are reported. These tests are carried out in the University of Pisa laboratory with the testing setup previously described.

The action of vertical loads on the structure is simulated by applying vertical forces to the bottom of the column and to the beam ends. The tests are performed in a mixed force-displacement control system, afterward described for each case.

8.3.1 Test on the four-way C5 specimen

The four-way specimen C5 is characterized by the passing-through beam stub in the main direction and by one vertical passing-through plate in the secondary direction. In the main direction the external girders are both connected by only vertical plates on the web, realizing pinned connections, as shown in Figure 8.13. The specimen is experimentally tested under monotonic vertical loading applied on the column from the bottom to the top, in order to have tension in the slab around the node.

The force-displacement curve, reported in Figure 8.14, highlights that in the initial elastic stage, the four-way specimen C5 shows a little higher stiffness. However, after the first drops, when the total load applied is almost 250 kN, probably due to the sliding of one external bolted connection and the cracking of the slab, the behavior is almost constant till the reaching of the highest value of the applied loads.

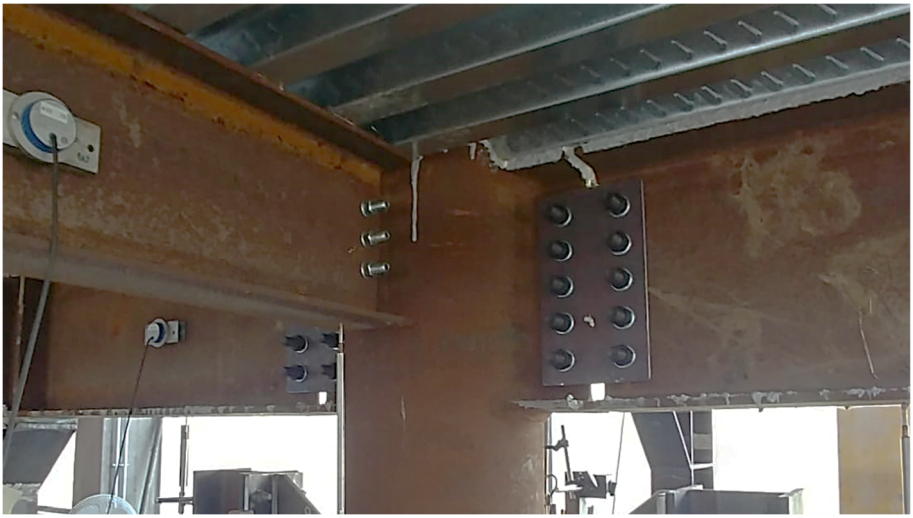

Figure 8.13 Four-way specimen C5 tested under vertical loads

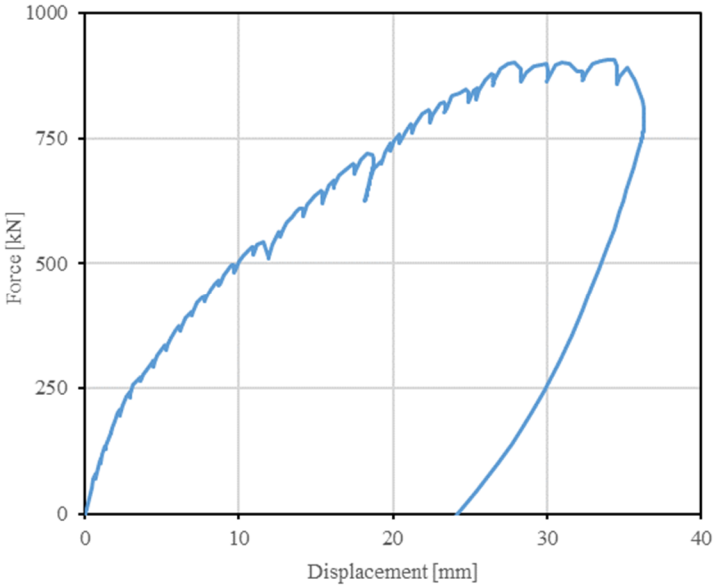

Figure 8.14 Total applied force VS central displacement for the test on C5 four-way specimen

The maximum applied load is around 900 kN and the test ended after the failure of the beam end joints in the main direction. These elements are not part of the specimen, which did not exhibit excessive damages in the node region.

In the end of the test, the C5 specimen exhibited the sliding of the bolted connections, with the consequent rotation of the external girders (Figure 8.15a), and the cracking of the concrete slab in tension (Figure 8.15b). The node, characterized by the passing-through elements in the main and secondary directions, did not exhibit failures and the welds resulted to be able to transfer the shear forces until the end of the test in both directions.

a)  b) 

Figure 8.15 Failure modes exhibited in the monotonic test of the four-way specimen C5: a) rotation of the external girders due to the sliding of the bolted connections, b) cracking of the slab in the tension

8.3.2 Test on the four-way C6 specimen

The four-way specimen C6 is characterized by the passing-through beam in the main direction and by one vertical passing-through plate in the secondary direction, as shown in Figure 8.16. The specimen is experimentally tested under monotonic vertical loads applied on the beams in both directions: the 80 % of the load is applied in the main direction and the remaining 20 % in the secondary direction.

The moment-rotation curves for the beam-to-column nodes in the main direction, reported in Figure 8.17, highlight an almost elastic behavior up to the reaching of the resistance of the composite main beam under a hogging moment. Afterward, the bending moment in the beams remains constant for the plasticity phenomena that involve the local buckling of the lower compressed flanges.

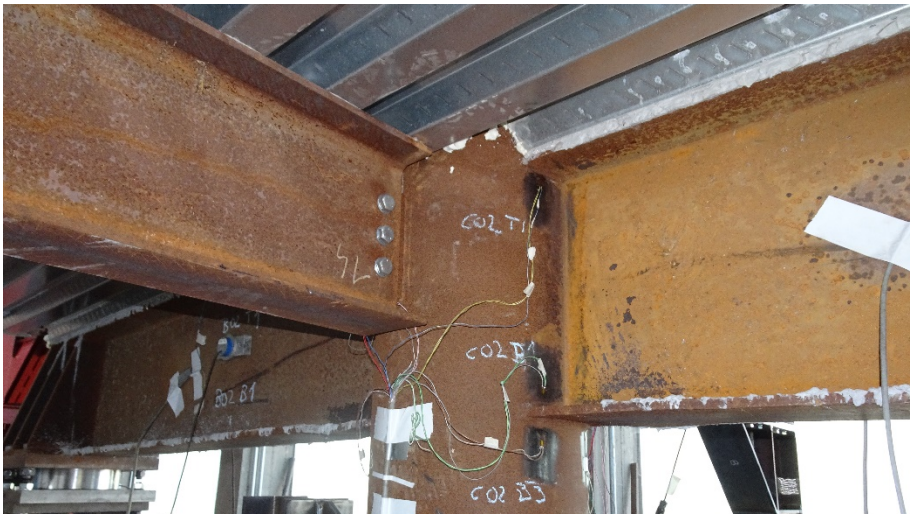

Figure 8.16 Four-way specimen C6 tested under vertical loads

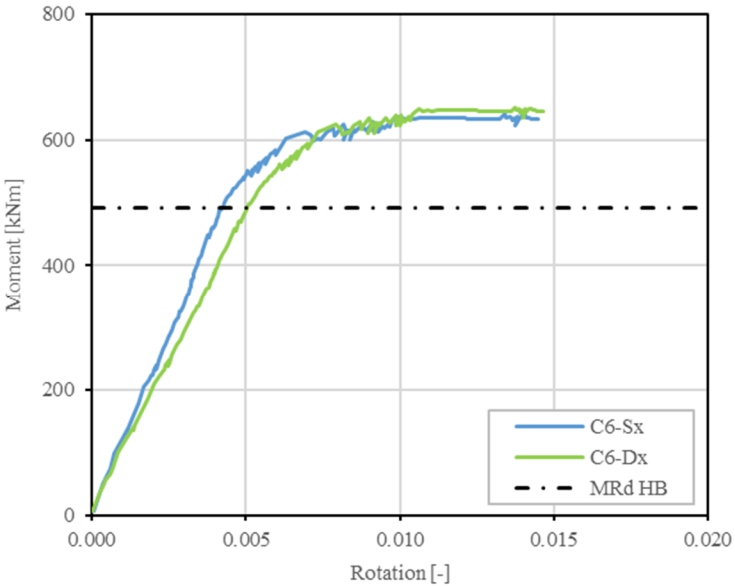

Figure 8.17 Moment-rotation curves for the main beams of specimens C6

In the end of the test, the C6 specimen exhibited the local buckling of the compressed lower flanges of the passing-through beam in the main direction (Figure 8.18), and the cracking of the concrete slab in tension. The node region, with the passing-through elements, did not exhibit damages, with the welds that resulted to be able to withstand the load till the reaching of the failure of the external girders. In the secondary direction failures were not highlighted.

Figure 8.18 Local buckling of the lower compressed flange of the passing-through beam in the main direction of specimen C6

8.3.3 Test on the four-way C7 specimen

The four-way specimen C7 is characterized by the passing-through beam in the main direction and by three passing-through plates in the secondary direction, as shown in Figure 8.19. The specimen is experimentally tested under monotonic vertical loads in both directions: the 80 % of the load is applied in the main direction and the remaining 20 % in the secondary direction.

As highlighted in the test of the specimen C6, the moment-rotation curves for the main direction of specimen C7, reported in Figure 8.20, highlight an almost elastic behavior with a hogging moment less to the resistance of the composite main beam. A low reduction of the stiffness was exhibited, probably due to the cracking of the tensioned slab. The final failure of the specimen is reached with the local buckling of the lower compressed flanges in the main direction in both the sides of the node.

Figure 8.19 Four-way specimen C7 tested under vertical loads

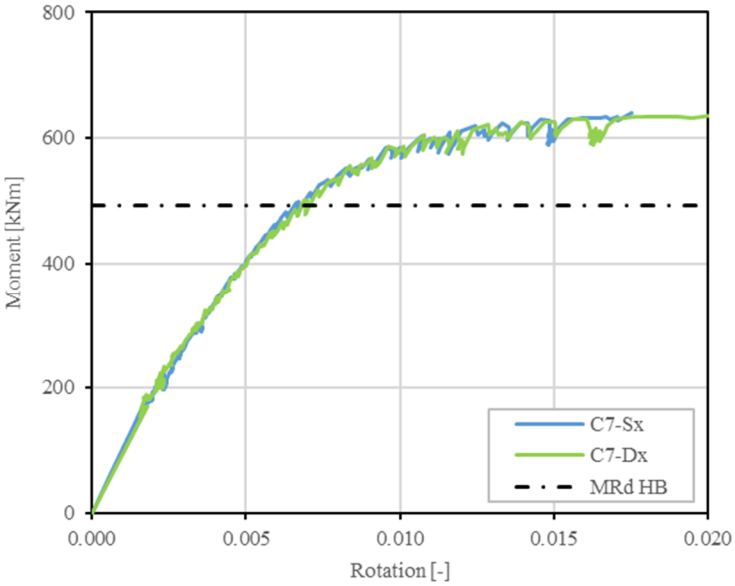

Figure 8.20 Moment-rotation curves for the main beams of specimens C7

A comparison of the curves for the test on four way C6 and C7 specimens is reported in Figure 8.21. These two specimens have the same characteristics in the main direction, whereas in the secondary direction the specimen C6 has pinned joints and the specimen C7 has two rigid full-strength joints. The external girders in the secondary direction are respectively IPE270 and IPE400. The comparison showed a similar behavior for a hogging moment lower than 200 kNm. After this value, the specimen C7 exhibited a drop of the stiffness, whereas the ultimate moment is almost the same for the two different specimens. Therefore, it seems that the different characteristics of the elements in the secondary direction have influence only on the stiffness of the joint. However, this information needs further studies to be confirmed.

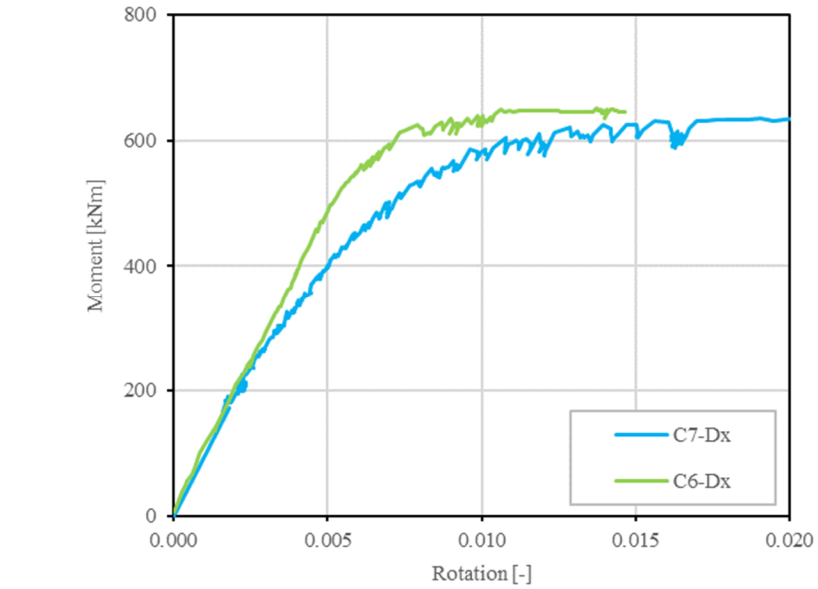

Figure 8.21 Moment-rotation curves for the C7 and C6 specimens tested under vertical loads

After the test, the C7 specimen exhibited the local buckling of the compressed lower flanges of the passing-through beam in the main direction (Figure 8.22), and the cracking of the concrete slab in tension. The node region did not exhibit damages, till the reaching of the failure of the external girders. In the secondary direction failures were not highlighted.

Figure 8.22 Local buckling of the lower compressed flange of the passing-through beam in the main direction of specimen C7

8.4 Critical analysis of the experimental results

The experimental tests conducted on the composite specimens, simulating the actions of vertical loads on the structure, provides significant information about the monotonic global behavior of the proposed joints and about the local mechanism of forces transferring from the composite beams to the filled column.

In the tests, damages were not exhibited in the node region. The welds resulted to be capable of withstanding the forces imposed by the vertical loads on the beams. Moreover, the nodes did not exhibit shear deformations or local buckling phenomena, due to the presence of the concrete cores, which avoided any failures.

In comparison with the experimental tests previously reported, performed on the pure steel two-way joints, the composite four-way joints guarantee better performances. In particular, for the C4 joints, characterized by the presence of three passing-through plates, the presence of the concrete core avoids the local buckling phenomena that involve the lower compressed horizontal passing-through plate inside the node. Moreover, the presence of the passing-through elements in both directions provides to the plates better restraining conditions inside the node.

The failure mechanisms exhibited in the composite tests regard in all the case the elements outside the nodes. In particular, the local buckling of the lower compressed flanges affects and characterizes the strength of the specimens.

The comparison of the experimental results, in terms of moment-rotation behavior, for the composite and steel C3 joints is reported in Figure 8.23. The C3 steel joint considered for the comparison is the C3-1B-1 type (Table 6.5), which has the same column wall thickness and the same welds type.

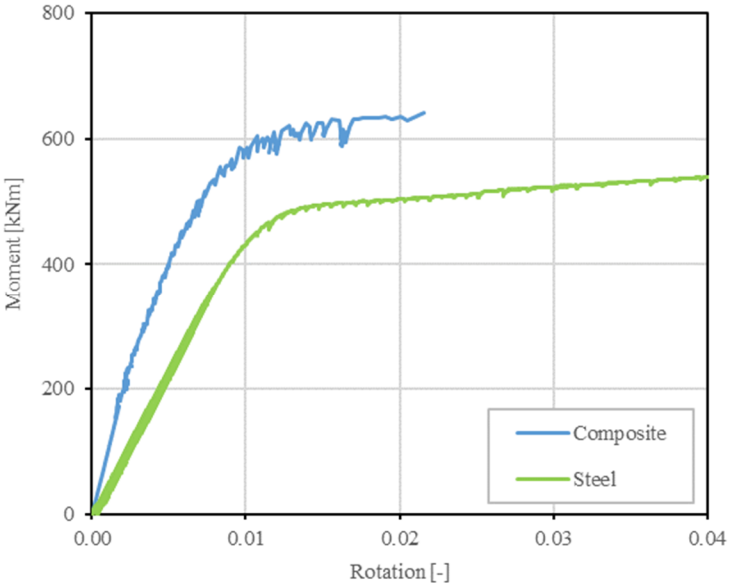

Figure 8.23 Comparison of the experimental tests for the steel and composite C3 joints

The composite joint showed higher stiffness and strength with respect to the steel specimen. The stiffness of the composite joint results to be more or less two times higher than the one of the C3 steel joint considered, whereas the yielding hogging moment results to be the 30 % higher than the one of the steel specimen. In both cases, the strength of the specimens is characterized and affected by the local buckling of the lower compressed beam flanges outside the node. In this perspective, the benefits in terms of strength are probably due to the higher stiffness of the node, which gives a higher restrain to the lower beam flanges, and to the presence of the RC slab, which gives to the beam sections a higher torsional moment of inertia, influencing the moment that induces the local buckling.

9 Experimental assessment of the composite-joint behavior under horizontal loads

Experimental tests with horizontal loads were conducted on substructures designed taking into account the results of the design of the case-study structures previously reported. The case-study structures were designed considering, as regards the seismic action, a non-dissipative behavior of the structure, thus not considering the capacity design of the structural elements. In this perspective, the structure and the individual structural elements do not have ductility requirements but only resistance and initial stiffness ones.

However, in the tests performed, attention was also paid to the ductility aspect of the substructures studied for two main reasons. Firstly, to research the sources of the fragility of the proposed connections, to identify possible improvements; secondly, to evaluate the ductility obtained in any case by designing in the elastic range. The latter aspect has been considered in the current framework of the updates provided for the seismic legislation at the European level, which considers low ductility classes that can be used to ensure less stringent ductility requirements than those required by current regulations.

Anyway, the current regulations provide for the exclusion of the beam-to-column connections from the elements involved in the global dissipative mechanism. Therefore, at the connection level, the strength assumes greater importance than ductility. The connection must be designed to remain in the elastic range during the development of the dissipative mechanisms in the other structural elements, regardless of the ductility possessed. However, it remains understood that a fragile crisis should be avoided with a higher safety level and it is therefore important to evaluate the type of crisis that involves the proposed joint under horizontal loads on the structures.

In terms of stiffness, the proposed beam-to-column connections require a rigid full-strength moment-rotation behavior with regards to the horizontal loads. This requirement is necessary in order not to have excessive rotations and therefore excessive displacements in the elastic range, especially concerning the design towards the limit states of exercise.

All the horizontal loading tests on composite specimens are carried out in the University of Pisa Laboratory "Laboratorio ufficiale per le esperienze sui materiali da costruzione". A R.C. strong floor, equipped with a steel rigid wall, useful to apply horizontal loads, characterizes the laboratory. A test setup is defined in order to perform experimental analyses on the beam-to-column connection specimens, simulating the action of horizontal loads on the structure, such as seismic and wind actions.

The tests are carried out with the test configuration represented in Figure 9.1. The action of horizontal loads on the structure is simulated by applying horizontal loads in the upper part of the column, in both horizontal directions. Beam-ends are constrained by sliding systems that allow only the longitudinal displacements, whereas the base of the column is fixed by a cylindrical hinge that allows the rotation around the transversal direction.

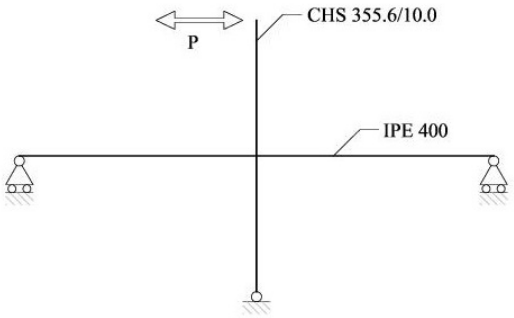

Figure 9.1 Testing configuration for the simulation of horizontal loads on the structure

Each specimen is a substructure that characterizes one interior beam-to-column connection, extracted from the case study structures, as well as reported in the example in Figure 9.2. Dimensions of the specimens are defined considering the designed case study structures, the laboratory features, and logistic limitations. In case of four-way joint the specimens have the beam in both the longitudinal and the transversal directions. Beam and column ends are constrained by elements of the test

setup or consist in the point of application of loads. Furthermore, beams are composed by the steel member and the R.C. slab, and the column is filled by concrete.

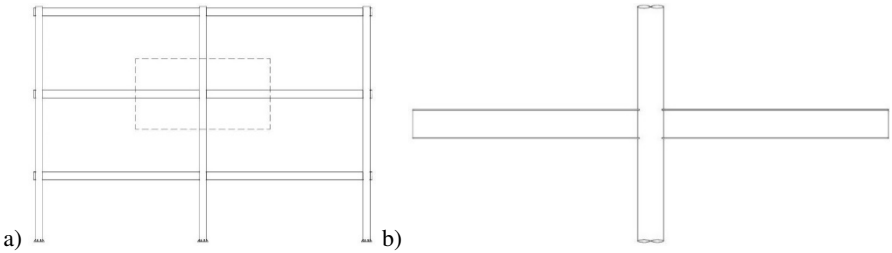

Figure 9.2 two-way joint specimen definition: a) example of case study structure, and b) substructure extrapolated from the case study with the CHS-column and the I-beam

9.1 Testing setup

The test setup represented in Figure 9.3 is designed to perform tests of two-way and four-way composite specimens under monotonic and cyclic horizontal loads. Two 450 kN double-effect hydraulic jacks, acting in parallel, apply the monotonic or cyclic horizontal load on the top of the column.

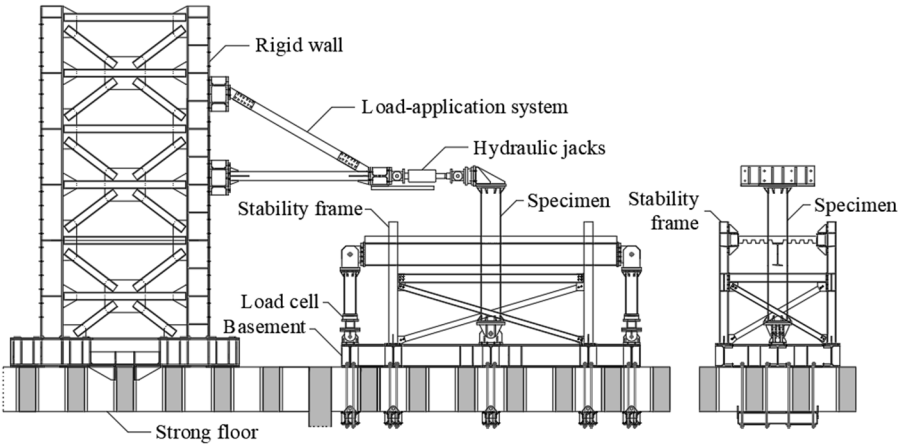

Figure 9.3 Lateral (left) and frontal (right) views of the testing layout for cyclic and monotonic horizontal loads

The Hydraulic jacks are connected in one side to the rigid wall, by a load-application system designed to have smaller deformations under the maximum capacity of the load jacks (Figure 9.4). The load-application system is composed by

HEB160 beams and struts and UPN100 braces. The load jacks are connected to this system through a strong HEM300 beam. In the other side, the load is introduced in the specimen by means of a connection element composed of 40 mm thick plates and designed to transfer the maximum applicable load by the two actuators to the column (Figure 9.4).

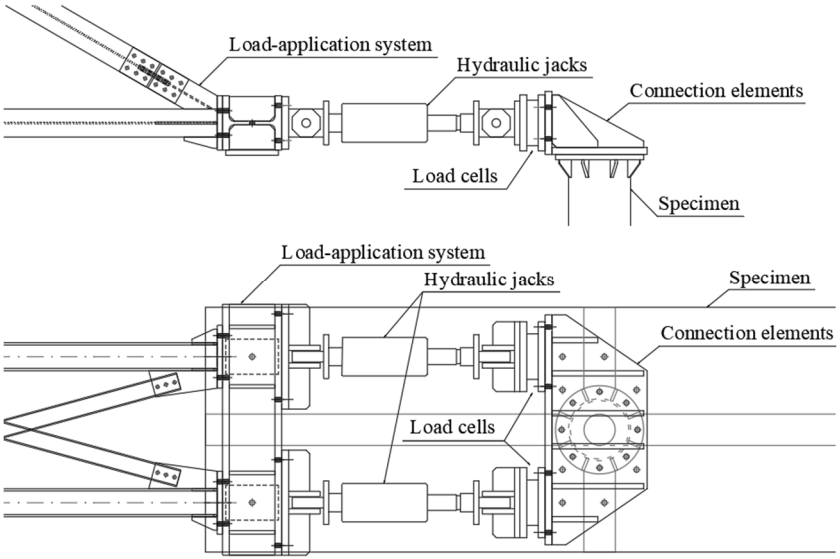

Figure 9.4 Frontal and plan views of the load-introduction system

The specimen is supported by a steel basement realized with HEB400 beams, which are rigidly connected to the R.C. strong floor by post-stressed M24 C8.8 steel rods and contrast elements made by three UPN200 beams and 20 mm thick plates. The steel basement is designed to be used in the tests with both horizontal and vertical loads. One cylindrical hinge, realized by a 60 mm diameter high strength steel pin, connects the bottom side of the specimen column to the steel base. Furthermore, two vertical steel tubular pendulums CHS219.1/12.5 are externally connected by cylindrical hinges, with 40 mm and 60 mm diameter high strength steel pins, respectively to the basement and to the beam-ends (Figure 9.5). Each pendulum is also composed by a load cell and a steel plug useful to connect the load cell to the lower hinge. The lateral displacement of the specimen is avoided by the cylindrical hinges and by a stability frame, composed of HEB160 columns and beams, UPN 160 and UPN100 braces, and contrast movable elements which are put in contact with the concrete slab of the specimen (Figure 9.6).

All the steel parts are made with S355 steel, except for the high strength steel pin made with S890QL steel.

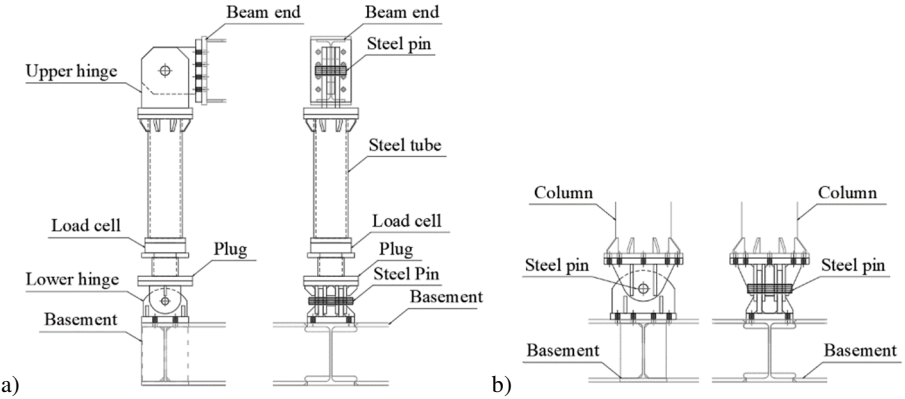

Figure 9.5 Frontal and lateral views of: a) the pendulum equipped with load cell, and b) the pinned connection of the column specimen to the basement

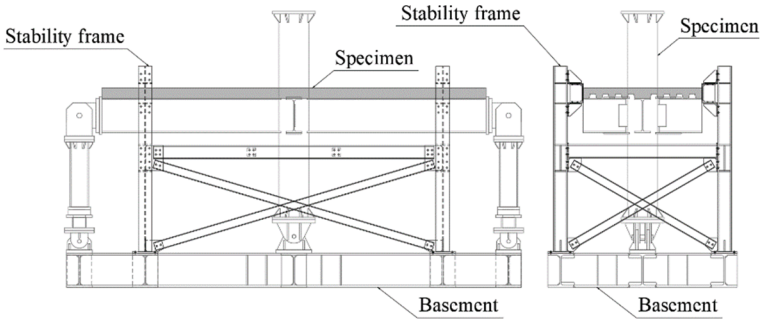

Figure 9.6 Stability frame designed in order to avoid lateral displacement

Differently from the test performed on the steel specimens, tested with opposite vertical loads applied to the beam-ends, for the composite specimens, the horizontal loading on the structure is simulated by applying the load horizontally to the top of the column.

In order to correlate results obtained in the two presented configurations, the interstory drifts and the story shear forces V are used. In the first exposed configuration, used in the steel tests, the vertical forces at the beam-ends F are acquired through load cells and the beam end vertical displacements δ by means of displacement transducer. In the second configuration, used in the composite tests, the

total shear force is recorded by the load cells of the hydraulic jacks, and the interstory drift is equal to the imposed displacement Δ, as shown in the schematic configuration in Figure 9.7a. Considering the schematic representation in Figure 9.7b, the interstory drift Δ and the story shear force V, can be related to δ and F, by the following equations:

$$R = \frac{2\delta}{L} = \frac{\Delta}{H} \quad \rightarrow \quad \Delta = \frac{2\delta}{L} \cdot H \qquad \text{Eq. 9.1}$$

$$V \cdot H = F \cdot L \quad \rightarrow \quad V = \frac{F}{H} \cdot L \qquad \text{Eq. 9.2}$$

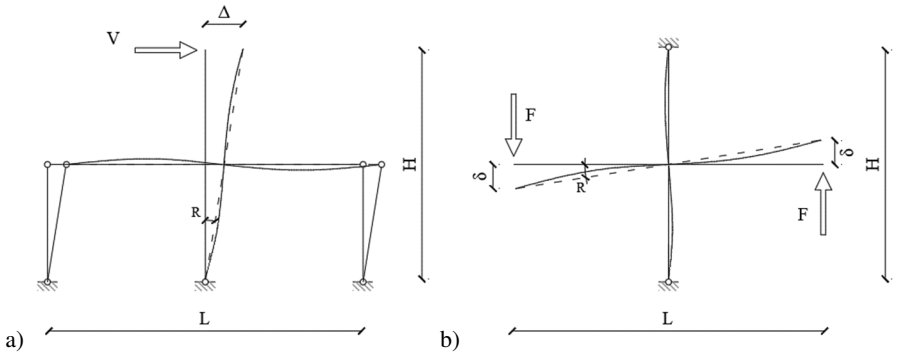

Figure 9.7 Equivalent transformation from force-displacement relationship at beam end to story shear-drift relationship at column top

9.2 Instrumentation

The instrumentation used during the tests with horizontal loads is made by inclinometers, strain-gauges, inductive displacement transducer and load cells, disposed on the whole substructure in order to characterize opportunely both the monotonic and cyclic global behavior of the specimens, in terms of external reactions and global displacement, and local mechanism of transferring of the forces from the composite beam to the filled column. Inductive displacement transducer (LVDTs), inclinometers and strain gauges can provide data about the kinematics of the specimen and the deformations in some points opportunely chosen. The load cells allow the definition of the external reactions acting on the substructure during the test. Therefore, it is possible to obtain the distribution of the bending moment and shear force in each section of the beams and of the column. To examine the local mechanism in the specimen, strain gauges are used to measure the deformation of the rebars in the R.C. slab and in the beam flanges. Strain gauges make possible the evaluation of

the deformation and transferred forces in the controlled sections of the composite beam. Strain gauges are also applied on the column wall to investigate the deformation and the stresses in the connection region.

Both the hydraulic jacks, as well as both the pendulums, are equipped with load cells for monitoring the applied load and the support reactions. The actuators are also provided by LVDTs displacement sensors in order to perform test in displacement control. Seven inclinometers (Figure 9.8) and ten LVDTs displacement transducers (Figure 9.9) are used to detect rotations and displacements during the tests. In each test performed, 28 strain gauges are applied to the steel parts of beams and column.

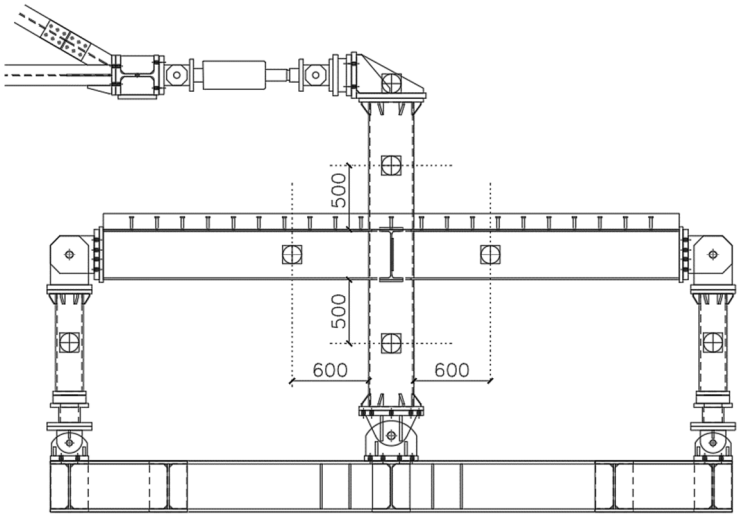

Figure 9.8 Inclinometers disposed on the specimen and on the setup elements

Four sections of the beam (Figure 9.10) are controlled by 16 strain gauges, disposed as shown in Figure 8.11a. On the column wall, six 6 mm linear strain gauges are applied on each side of the specimen around the slots for the passing-through elements, as represented in Figure 8.11b for the vertical loading specimens.

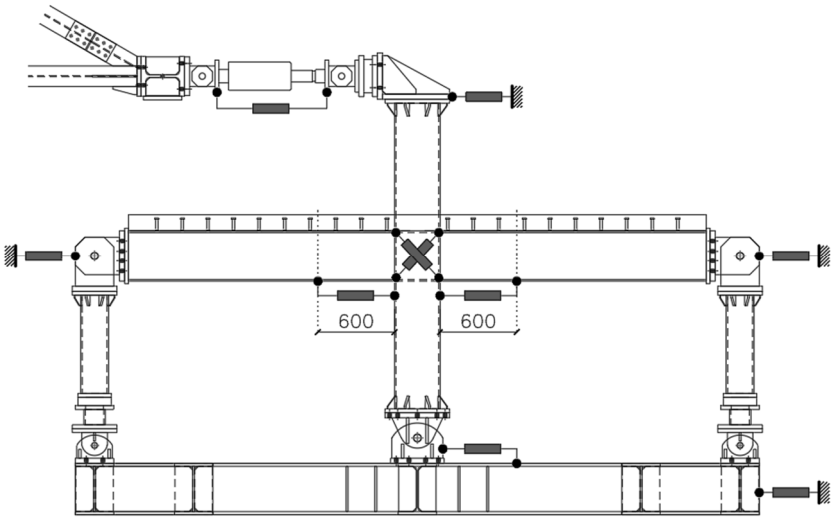

Figure 9.9 LVDTs displacement transducers disposed in the test setup and on the specimen

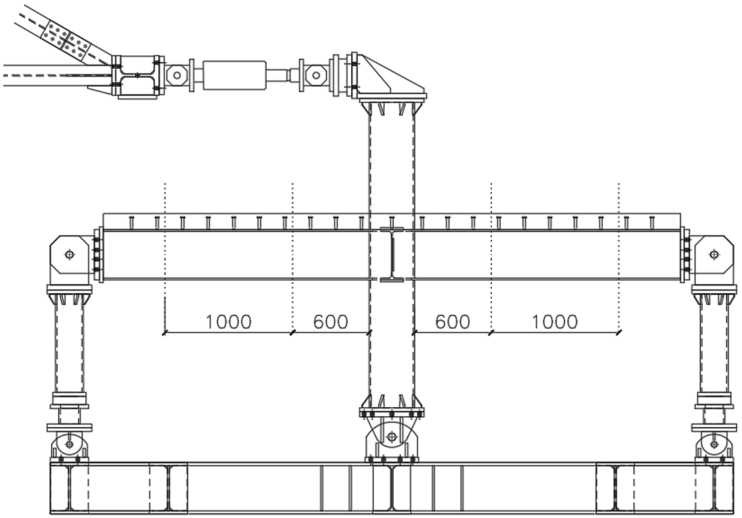

Figure 9.10 Beam sections controlled by strain gauges

Linear strain gauges are also applied to the longitudinal and transverse bars of the R.C. slab in each specimen. For example, 30 controlled points are defined in the re-bars of specimen C3 and C7-1 to be tested under monotonic loads (Figure 9.11) and

33 controlled points on the specimen C3 to be tested with cyclic loads (Figure 9.12). Each controlled point is provided by two 6 mm linear strain gauges disposed on the opposite sides of the bars.

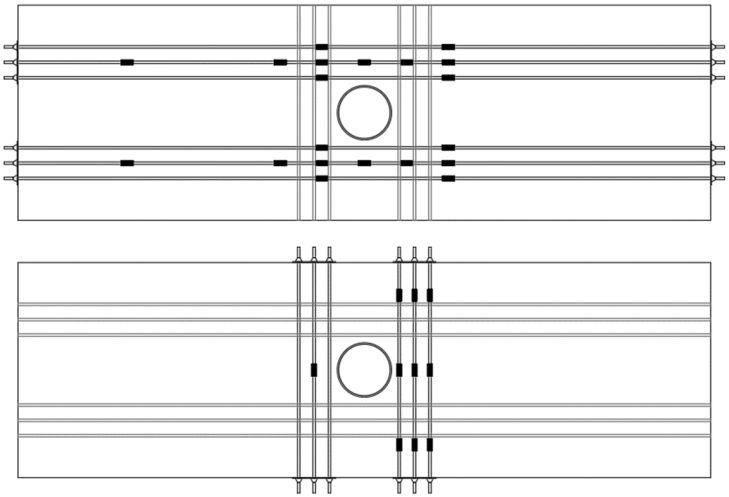

Figure 9.11 Disposition of the strain gauges on the longitudinal (up) and transversal (down) re-bars in the specimens to be tested with monotonic horizontal loads (C3 and C7-1); the slab on the left part is in tension and the right one is in compression

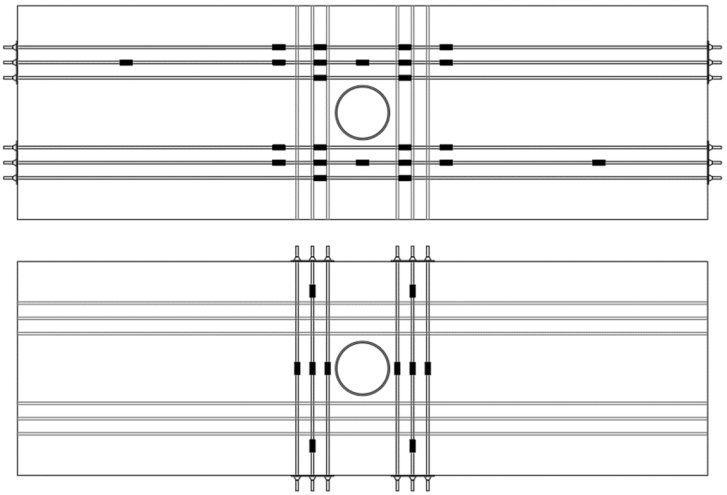

Figure 9.12 Disposition of the strain gauges on the longitudinal (up) and transversal (down) re-bars in the specimens to be tested with cyclic horizontal loads (C3)

9.3 Results of the tests on two-way composite specimens

In this paragraph, the experimental testing results for two-way and four-way composite substructures subjected to monotonic and cyclic horizontal loads, are reported. These tests are carried out in the University of Pisa laboratory, with the test setup previously described and represented in Figure 9.13.

The action of horizontal loads on the structure is simulated by applying horizontal forces to the top of the column. All the tests are performed in displacement control.

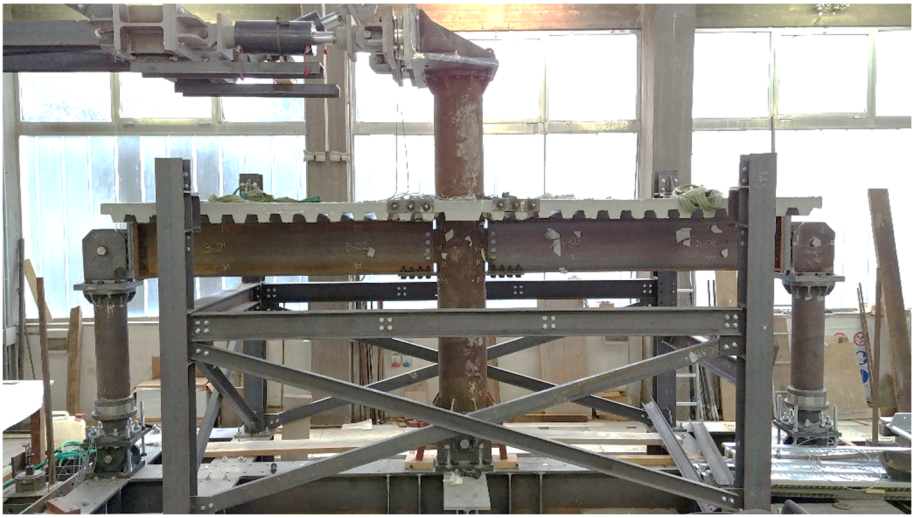

Figure 9.13 Horizontal loading test setup for composite specimens (University of Pisa)

9.3.1 Tests on C3 two-way joints

In this subsection the results of the tests performed on the two-way specimens C3 are presented. The presence of the passing-through continuous beam in the longitudinal direction characterizes the C3 specimens (Figure 9.14). For this type of specimen two tests were performed, the first with monotonic horizontal loading and the second with cyclic loading.

Figure 9.14 Two-way specimen C3 with the passing-through continuous beam

9.3.1.1 Monotonic loading

The monotonic test on the C3 two-way specimen was concluded since the maximum elongation capacity of the jacks was reached. In the end of the test, this specimen did not exhibit excessive damage on the welds and column wall. Therefore, it is reasonable to assert that it could resist greater rotations. However, the cracks on the tensioned welds could start propagating at any moment, leading to a brittle failure. The moment-rotation curve is reported in Figure 9.15.

Once the maximum load is reached, the specimen exhibits a slow reduction of the applied load. Then, it maintains a constant value, with some oscillations, until the end of the test. The bending moment in the lower column, calculated in the bottom section of the connection is almost equal to the design resistance for the bending moment of the composite column, as shown in Figure 9.16.

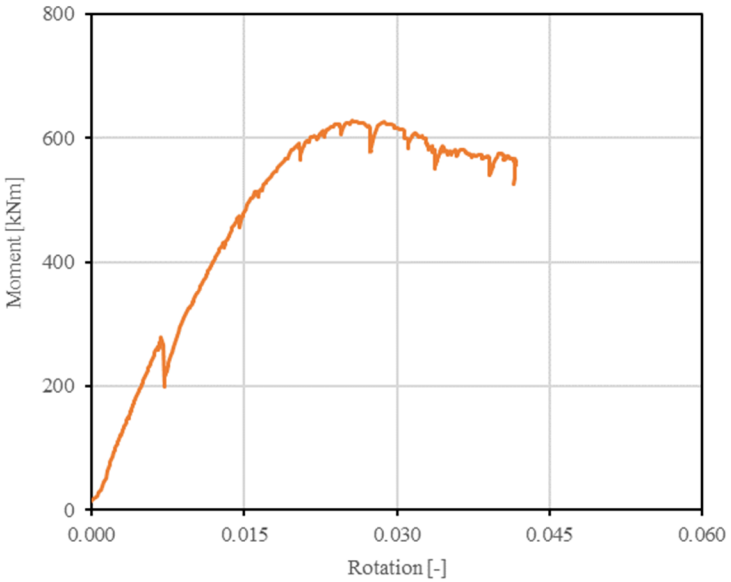

Figure 9.15 Moment-rotation monotonic behavior of specimen C3 under horizontal loads

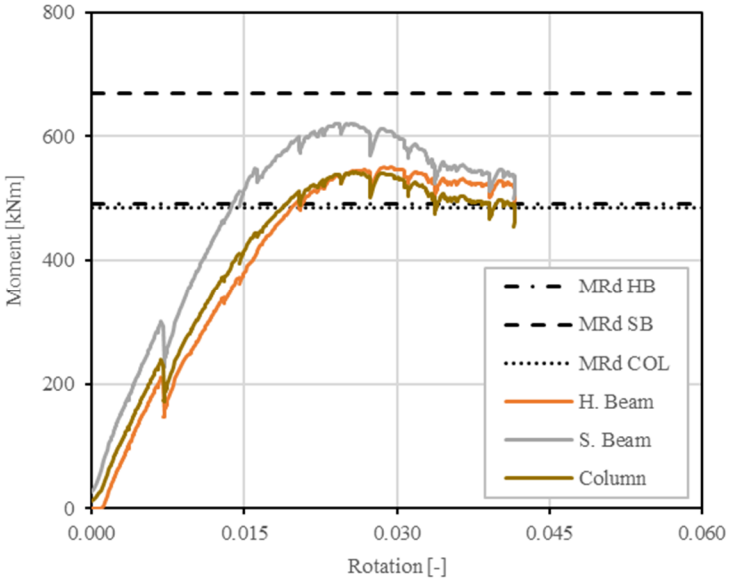

Figure 9.16 Moment-rotation curves for the C3 two-way specimen; the column bending moment is calculated in the sections on the top and on the bottom of the connection

In the end of the test, the C3 specimen exhibited the local buckling of the compressed upper and lower beam flanges (Figure 9.17a), the presence of cracks in the upper and lower welds (Figure 9.17b), the crushing of the compressed concrete slab in the contact area with longitudinal and inclined lesions (Figure 9.17c), and transversal lesions in the concrete slab in tension (Figure 9.17d). The node region did not exhibit a shear deformation.

Figure 9.17 Failure modes exhibited in the monotonic test of the two-way C3 specimen: a) local buckling of the compressed lower beam flange, b) cracks in the welds in the tension region, c) crushing and lesions in the compressed concrete slab, and d) lesions in the tensioned slab

9.3.1.2 Cyclic loading

In this test horizontal cyclic loads are applied on the specimen type C3, already tested with horizontal monotonic load. The tested substructure is the one with the continuous beam that passes through the tubular column, without transversal elements. The test is performed in displacement-control with a loading procedure based on the quasi-static procedure for the testing of components of steel structures provided in the ECCS-45 "Recommended Testing Procedure for Assessing the Behaviour of Structural Steel Elements under Cyclic Loads" (ECCS 1986). In the complete testing procedure, the cyclic displacement history is defined starting from the results obtained by the monotonic test, in particular the yielding load F_y and the yielding displacement d_y of the specimen.

To define the yielding displacement shown in the monotonic test of the specimen, the displacement that induces a maximum residual drift equal to 0.2 % is considered. The obtained residual drift is 1.39 % (Figure 9.18a), which corresponds to a displacement of the column top equal to 39.25 mm. Therefore, starting from a yielding displacement of 40 mm the cycles to be applied were defined. The cyclic test is carried out by applying increasing imposed cyclic displacements with some differences with the previously reported procedure. Firstly, instead of one cycle at each step, three cycles are completed at each step equal to the 25%, 50% and 100% of the yielding displacement d_y, without performing the step at the 75%. Then, the normal procedure, which provide three cycles to be performed at 2 d_y and 4 d_y, was slightly changed by adding some intermediate steps. Therefore, three cycles have to be completed at 1.5 d_y, 2 d_y 3 d_y and 4 d_y, i.e. at 60 mm, 80 mm and 120 mm (Figure 9.18b).

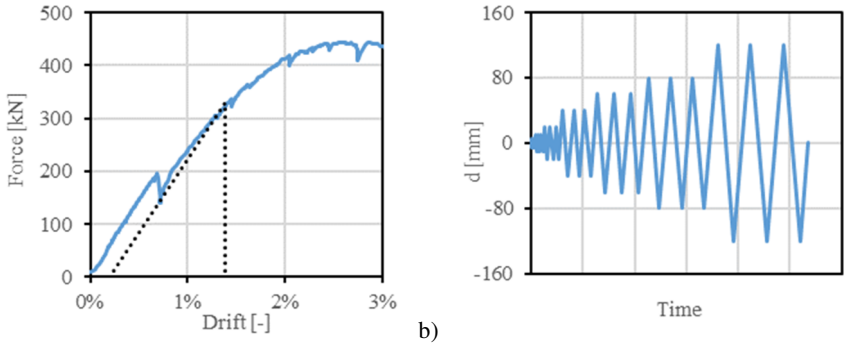

a) b)

Figure 9.18 Loading procedure for the cyclic test on C3 specimen: a) definition of the yielding drift exhibited in the monotonic test on C3 substructure, and b) displacement history

A comparison of the moment-rotation curves obtained by the monotonic and cyclic tests is reported in Figure 9.19. In the cyclic test, the specimen is not able to reach the maximum value of the load applied in the monotonic test. In fact, a strong degradation is highlighted in the second repetition of the cycle at 60 mm, equal to 1.5 times the yielding displacement. Afterwards, a drop of the applied load is shown at each following cycle. Therefore, the test was concluded in the inversion of the load in the third cycle at 80 mm (2 times the yielding displacement) where it is possible to see that the substructure was not able to withstand any load.

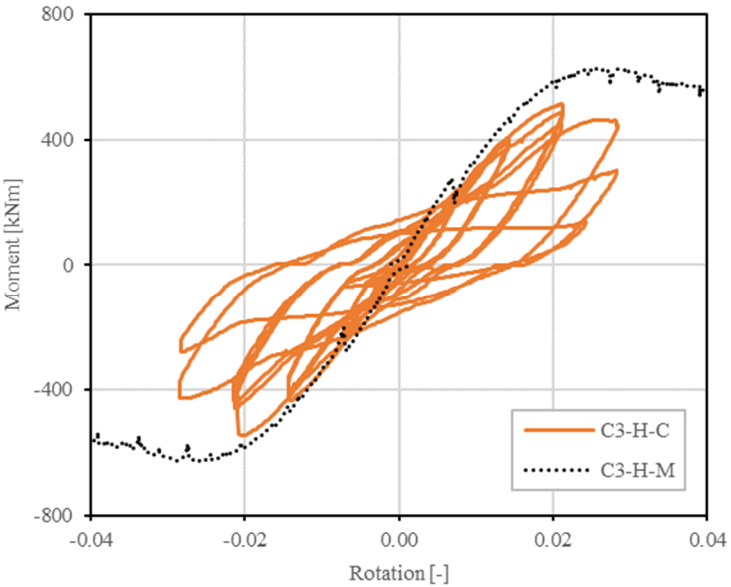

Figure 9.19 Comparison of the moment-rotation curves obtained with the monotonic and the cyclic tests on the C3 substructure type

Specimen exhibits an almost linear behavior in the first cycles with the amplitude lower to the yielding rotation (Figure 9.20a). Cracks start to develop on the welds in tension when the first cycle at the yielding displacement was performed (Figure 9.21a). However, in the repetitions at 40 mm the moment-rotation curve does not exhibit degradation (Figure 9.20b). At this amplitude, some transversal cracks appeared in the concrete slab in the following cycles.

When the first cycle at 60 mm (1.5 times the yielding rotation) was carried out, the lesion in both the lower welds completely opened and the column wall tearing was

exhibited (Figure 9.21b). In this cycle the maximum applied load is reached and then, in the repetition, a degradation is shown with subsequent drops of the maximum load (Figure 9.20c) and a clear non-linear behavior is highlighted. In this point, transversal tension cracks were present in both the side of the concrete slab, as well as the crushing of the concrete in contact with the steel tubular column.

For cycles with a maximum displacement equal to two times the yielding one (80 mm), tearing of the welds and tube-wall in the weld regions is clearly observed (Figure 9.21c-d). In the first repetition the maximum applied load decrease to the 60 % of the load applied in the first cycle at 80 mm, whereas in the second repetition it reaches just the 25 % of the maximum applied load in the first cycle at 80 mm (Figure 9.20d).

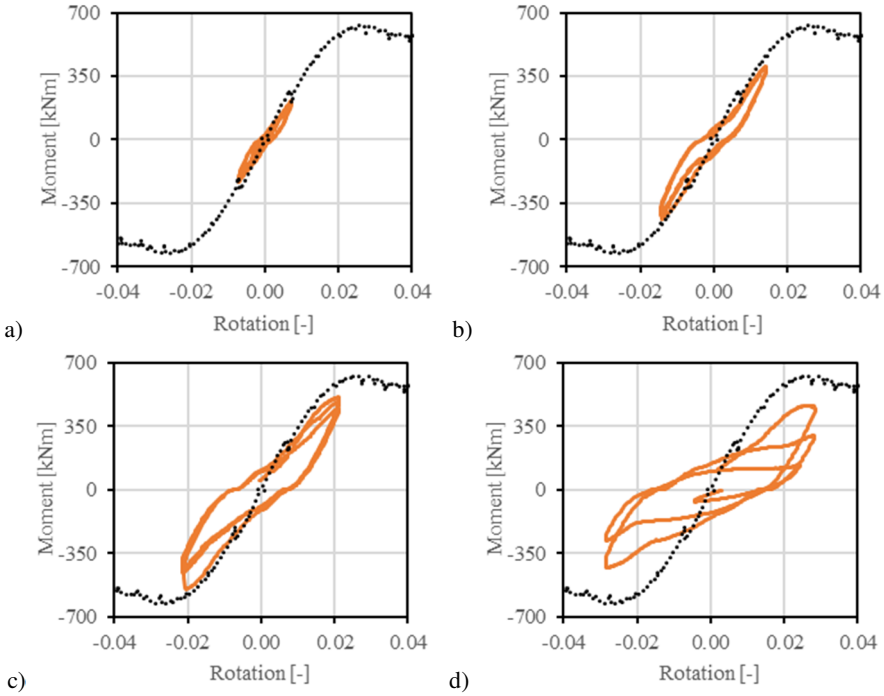

Figure 9.20 Steps of the cyclic test: a) cycles up to the 50 % of the yielding point, b) cycles at the yielding displacement, c) cycles at the 150 % of the yielding point, and d) cycles at two times the yielding displacement

The substructure experimentally tested with cyclic horizontal loads exhibited a huge degradation in the following cycles, mainly due to the failure of the welds in tension and the propagation of the lesions to the tubular column wall around the slots,

which were made by laser cutting in order to pass the beam. A phenomenon of closing and opening of the gap between the flange and either the tube-wall and the concrete filling, is clearly observed. Therefore, even if the tension part is not able to transfer forces, the compressive part on the other side transfers the loads. This fact determined the shape of the moment-rotation curves, characterized by the pinching effect typical in the R.C. elements (Figure 9.19).

Figure 9.21 Failures of the penetration welds: a) first lesion exhibited in the first cycle at 40 mm, b) propagation of the lesion to the column wall in the first cycle at 60 mm, c) and d) bottom weld regions in the end of the test

9.3.2 Tests on C4 two-way joints

In this subsection the results of the tests performed on the two-way specimens C4 are presented. The presence of the three passing-through continuous plates in the longitudinal direction characterizes the C4 specimens (Figure 9.22). As well as done for the previous specimens, for this type of specimen two tests were performed, the first with monotonic horizontal loading and the second with cyclic loading.

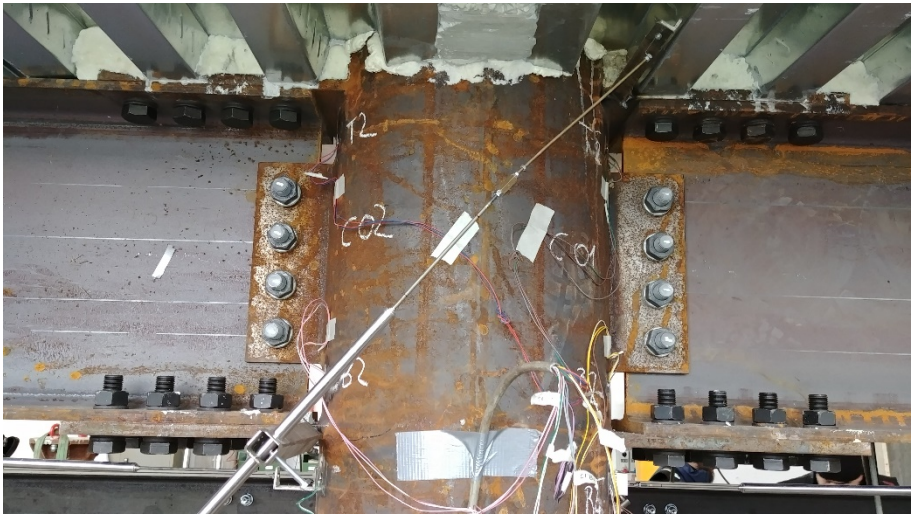

Figure 9.22 Two-way specimen C4 with the passing-through plates bolted to the girders

9.3.2.1 Monotonic loading

The monotonic test on the C4 two-way specimen was concluded since the maximum elongation capacity of the jacks was reached. In the end of the test, also this specimen did not exhibit the final failure. Cracks on the tensioned welds initiated after the reaching of the yielding. The moment-rotation curve is reported in Figure 9.23.

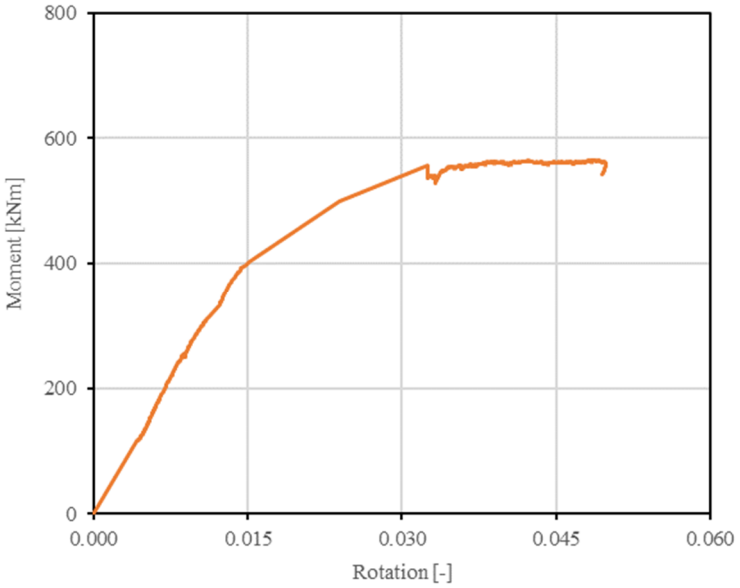

Figure 9.23 Moment-rotation monotonic behavior of specimen C4 under horizontal loads

Once the maximum load is reached, the curve exhibits an almost constant value of the applied load until the end of the test. The failures exhibited in the test are the formation of cracks in the tensioned welds (Figure 9.24a), the cracking of the concrete slab in tension (Figure 9.24b), the crushing of the concrete slab in the contact area with the steel tubular column (Figure 9.24c). The sliding of the external bolted connection is exhibited during the test, as reported in Figure 9.24d. The node region did not exhibit a clear shear deformation.

Figure 9.24 Failure modes exhibited in the monotonic test of the two-way C4 specimen: a) cracks in the tensioned welds, b) cracking of the concrete slab in tension, c) crushing of the concrete slab in the contact area, and d) sliding of the external bolted joints

9.3.2.2 Cyclic loading

In this test horizontal cyclic loads are applied on the two-way specimen with the three passing-through plates, already tested with monotonic load. As well as done in the previous reported test procedure for the cyclic test of the C3 joint, the cyclic test of specimen C4 is performed in displacement-control with a loading procedure based on the quasi-static procedure for the testing of components of steel structures provided in the ECCS-45 (ECCS 1986). To define the yielding displacement shown in the monotonic test of the specimen, the displacement that induces a maximum residual drift equal to 0.2 % is considered. The obtained yielding drift is 1.40 % (Figure 9.25a),

which corresponds to a displacement of the column top equal to almost 40 mm. The cyclic test is carried out by applying increasing imposed cyclic displacements with some differences with the standard procedure. Firstly, instead of one cycle at each step, three cycles are completed at each step equal to the 25%, 50% and 100% of the yielding displacement d_y, without performing the step at the 75%. Then, the normal procedure, which provide three cycles to be performed at 2 d_y and 4 d_y, was modified by adding some intermediate steps. Therefore, three cycles are completed at 1.5 d_y, 2 d_y, 2.5 d_y and 3 d_y, i.e. at 60 mm, 80 mm, 100 mm and 120 mm (Figure 9.25b).

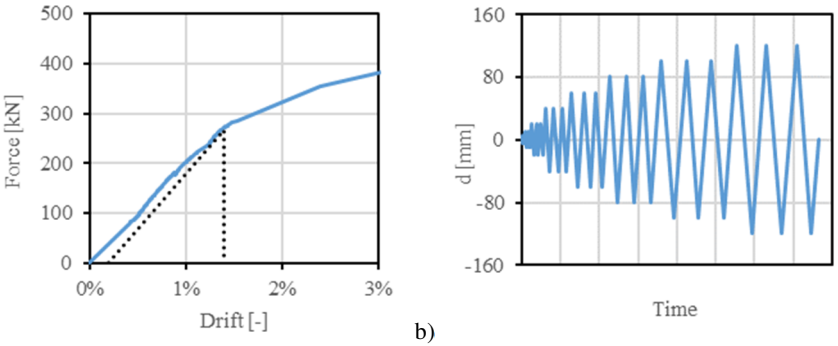

a) b)

Figure 9.25 Loading procedure for the cyclic test on C3 specimen: a) definition of the yielding drift exhibited in the monotonic test on C3 substructure, and b) displacement history

A comparison of the moment-rotation curves obtained by the monotonic and cyclic tests is reported in Figure 9.26. In the cyclic test, the specimen is able to reach the maximum value of the load applied in the monotonic test. Although, after the yielding, the specimen exhibited a low degradation in the following cycles, the specimen is able to withstand a higher load ratio in comparison with the specimen C3 (Figure 9.19). Whereas the specimen C3 hugely degraded in the cycles at 1.5 times the yielding displacement, the specimen C4 is able to reach the cycles at 3 times the yielding displacement. The test was concluded after these three cycles, where the maximum applied load is almost the 80% of the maximum applied load.

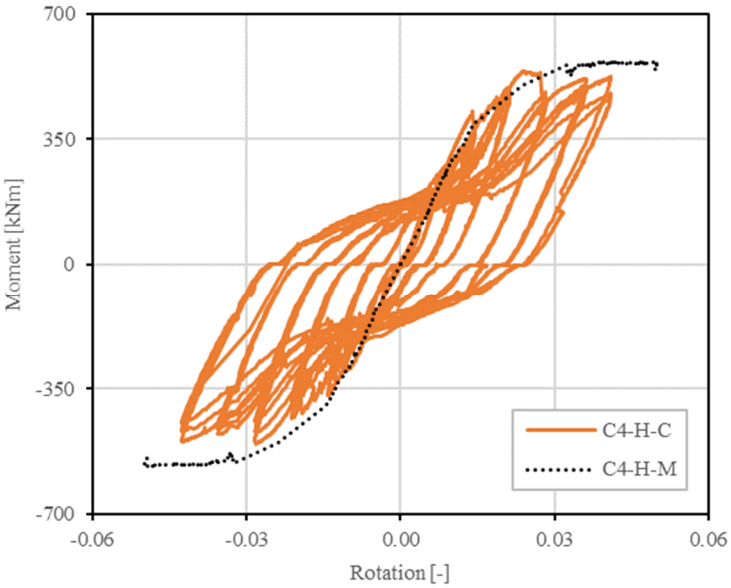

Figure 9.26 Comparison of the moment-rotation curves obtained by the monotonic and the cyclic tests on the C4 substructure type

Specimen exhibits a linear behavior in the first cycles up to the 50% of the yielding rotation (Figure 9.27a). In these cycles cracks start propagating in the concrete slab in tension, whereas the steel parts did not exhibit damage. Others cracks start to develop in the concrete slab in the cycles at the yielding amplitude; in the repetitions the moment-rotation curve does not exhibit degradation (Figure 9.27b). The welds did not show failures.

When the first cycle at 60 mm (1.5 times the yielding rotation) was completed, the lower welds showed cracks on the lateral sides, as shown in Figure 9.28a. In the following equal cycles, the maximum applied load was more or less the same.

In the first cycle at two times the yielding displacement, the cracks in the welds propagate to the central part (Figure 9.28b) and the maximum applied load is reached (Figure 9.27c). In the first repetition, a clear pinching phenomenon and a degradation of the applied load are. However, the second and third cycles are almost equals. In these cycles the concrete slab starts to exhibit the crushing in the compression regions.

In the cycles at 2.5 times the yielding amplitude, the cracks in the welds propagated and the continuous passing-through lower plates resulted to be almost completely detached in the upper and lateral sides, as shown in Figure 9.28c.

For cycles with the maximum defined amplitude (120 mm), equal to three times the yielding one, the complete tearing of the welds was observed (Figure 9.28d). In the third repetition, the applied load is almost the 83% of the load withstand in the first cycle at 120 mm (Figure 9.27d).

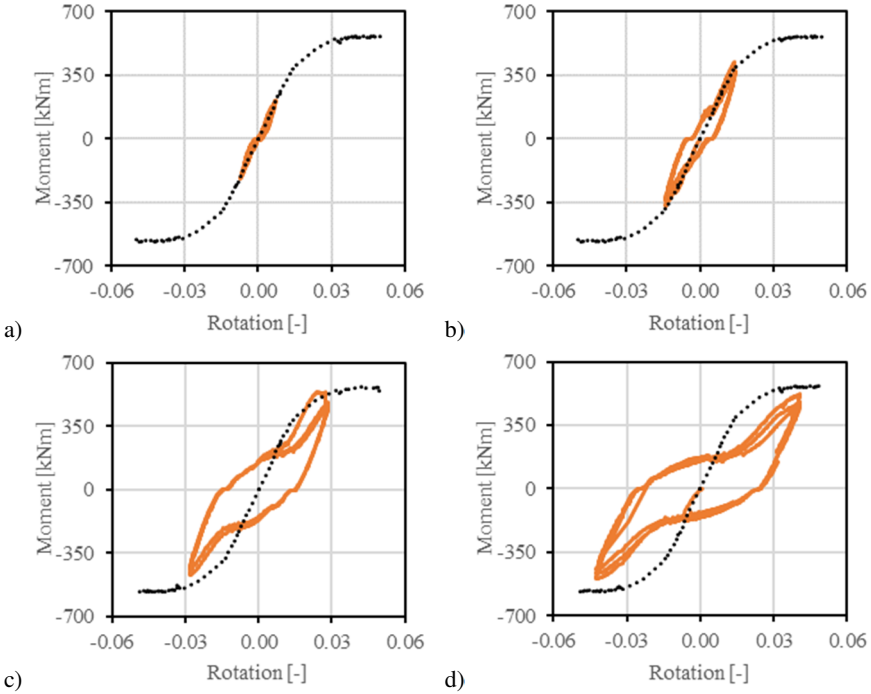

Figure 9.27 Steps of the cyclic test of specimen C4: a) cycles up to the 50 % of the yielding point, b) cycles at the yielding rotation, c) cycles at the 200 % of the yielding rotation, and d) cycles at three times the yielding rotation

In comparison with the substructure with the passing-trough beam, which exhibited a huge degradation in the following cycles (Figure 9.19Figure 9.26), with the propagation of the cracks to the tubular column wall around the slots (Figure 9.21), the substructure with the passing-through plates exhibited a more stable following cycles, with a reduced degradation (Figure 9.26), and it was able to withstand cycles at three times the yielding rotation without the propagation of the cracks to the steel column wall (Figure 9.28).

This difference is mainly due to the continuity of the column around the slots in the specimen C4 with the passing-through singular plates, whereas in the C3 specimen

the passage of the beam stub requires the realization of slots that completely interrupt the continuity of the column wall in the node, resulting in the brittle behavior.

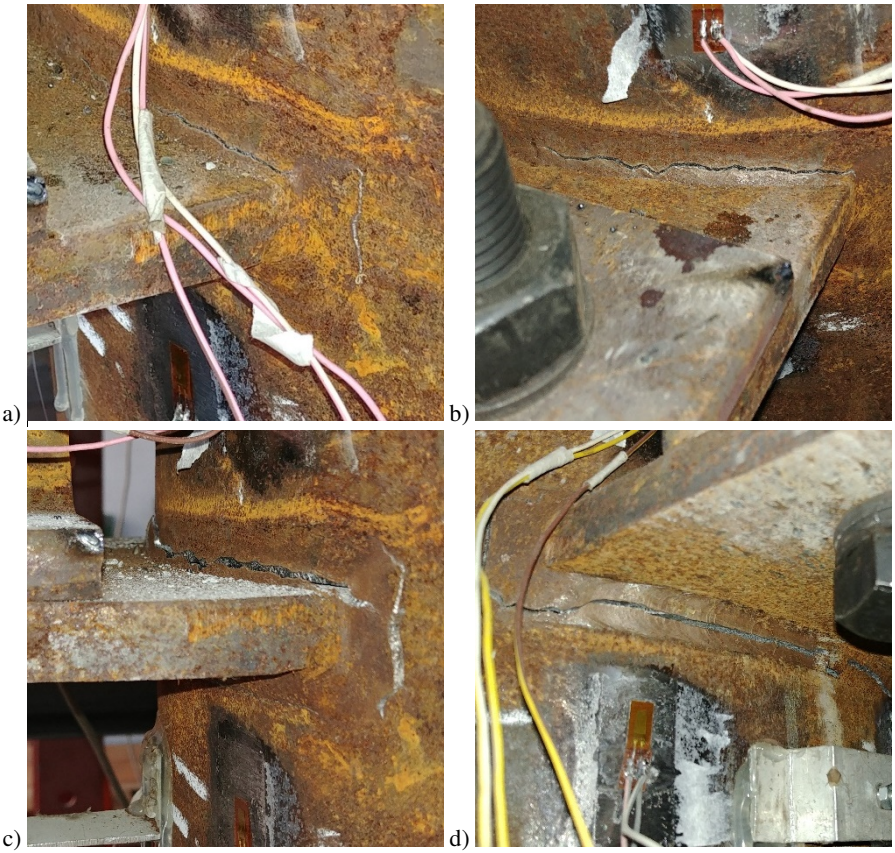

Figure 9.28 Failures of the penetration welds: a) first lesion exhibited in the first cycle at 60 mm, b) propagation of the lesion to the column wall in the first cycle at 80 mm, and c) in the cycles at 100 mm, and d) welds in the end of the test

9.4 Results of the tests on four-way composite specimens

In order to investigate the influence of the passing-through transversal elements on the behavior of the proposed rigid full-strength proposed joint typologies under horizontal loads in the longitudinal direction, monotonic tests were performed on two four-way specimens.

The four-way specimens are characterized by the presence of the passing-through continuous beam in the main direction and the three passing-through plates in the secondary one. The test of the first specimen (C7-1) is performed by applying the horizontal load in the main direction, i.e. by applying the horizontal load in the plane with the passing-through beam, similarly to the two-way C3 specimen test. The second four-way specimen (C7-2) is tested by applying the horizontal load in the plane with the three passing-through plates (the secondary direction), as done for the C4 two-way specimen test.

The tests were performed with the same testing setup and with specimens characterized by the same global dimensions.

9.4.1 Tests on C7-1 four-way joints

The four-way specimen C7-1, characterized by the passing-through beam in the tested direction, as shown in Figure 9.29, is experimentally tested under monotonic horizontal load.

Figure 9.29 Four-way specimen C7-1 with the passing-through beam in the tested direction

The comparison with the monotonic test performed on the two-way C3 specimen, reported in Figure 9.30, highlights that the ultimate bending moment and the initial rotational stiffnesses are not influenced by the presence of the passing-trough transversal elements (in this case represented by the three passing-through plates), whereas the ductility is clearly different for the two-way and four-way specimens. In

fact, the two-way specimen did not exhibit the brittle failure during the test, whereas the four-way specimen C-7-1 exhibited the brittle failure, which causes the collapse of the substructure.

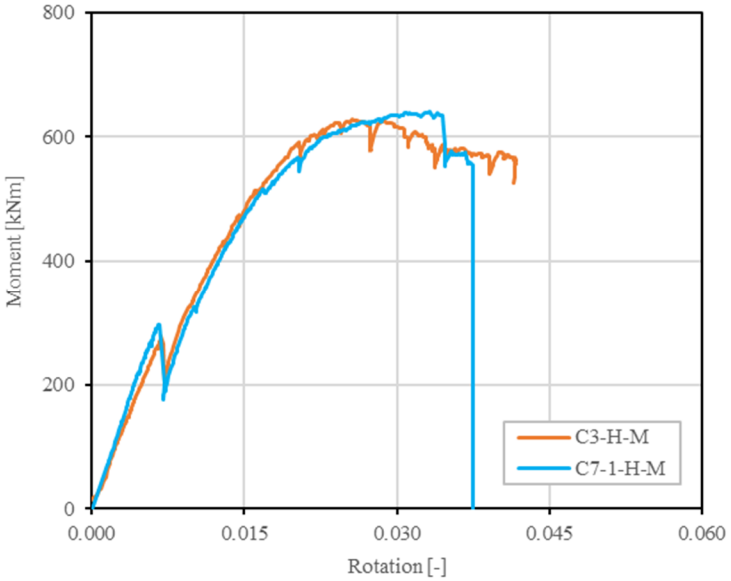

Figure 9.30 Moment-rotation curves for the monotonic tests of specimens C3 (two-way) and C7-1 (four-way) in the horizontal loading configuration

In the initial elastic stage, the four-way specimen shows a little higher stiffness. However, after the first drops probably due to the sliding of one external bolted connection, the behaviors are almost the same till the reaching of the highest value of the applied loads.

The four-way specimen reaches the maximum load for a little higher rotation, in comparison with the two-way specimen, but suffers a sudden drop of the bending moment in the elements (Figure 9.31) due to the propagation of the weld cracks (Figure 9.32a-b). The complete tearing of the passing-through welds is followed by the ones of the welds of the lower horizontal plate that passes through the column in the transversal direction (Figure 9.32c), with the propagation of the cracks to the column wall.

In the section where the welds are realized, the column wall was interrupted by the laser cutting to allow the passage of the beam flange and plates. Consequently, after the welds tearing, the load on the tension side of the lower composite column is

completely withstand by the only part of the tubular-column wall that is continuous in this section. In the end, the complete tearing of the continuous part of the column wall is observed, corresponding to the final brittle failure (Figure 9.32d).

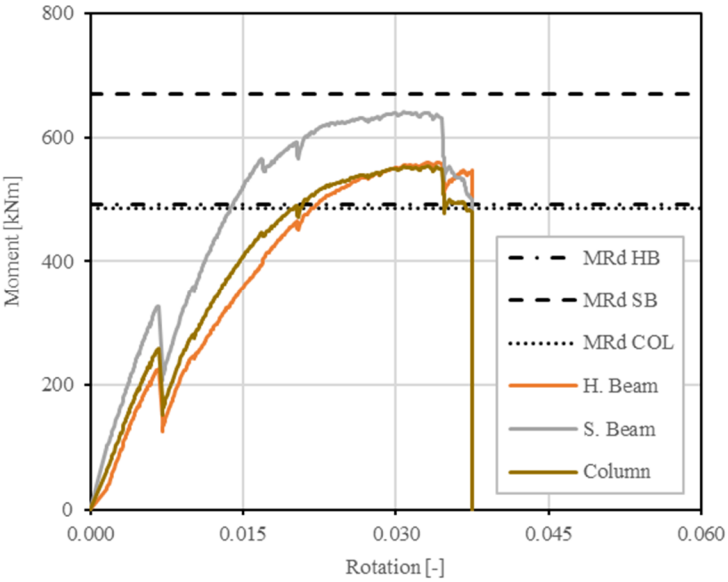

Figure 9.31 Moment-rotation curves for the C7-1 four-way specimen elements

In the end of the test, the C7-1 specimen also exhibited the local buckling of the compressed lower beam flanges, the presence of cracks in the upper tensioned welds, the crushing of the compressed concrete slab in the contact area with inclined lesions, and transversal lesions in the concrete slab in tension. The node region did not exhibit a clear shear deformation.

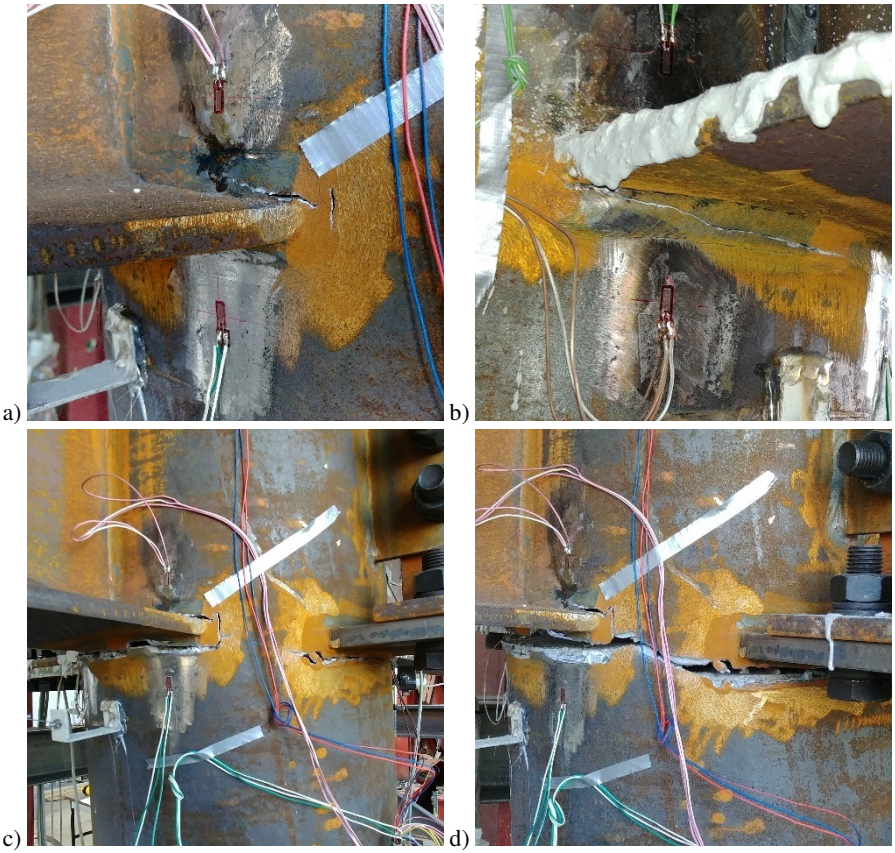

Figure 9.32 Tearing of the welds and column wall: a) and b) crack propagation in the lower beam flanges weld in tension, c) complete tearing of the flange weld and propagation to the transversal plate welds and column wall, d) final tearing of the column wall welds

9.4.2 Tests on C7-2 four-way joints

The four-way specimen C7-2 is characterized by the three passing-through plates in the tested direction, such as the C4 specimen.

The comparison of the monotonic test results of the two-way specimen C4 and the four-way specimen C7-2 is reported in Figure 9.34. The presence of the passing-through elements in the transversal direction elements (in this case represented by the passing-through beam) did not afflict the behavior of the joint. In fact, the strength and stiffness of the two specimens are almost the same. In the same way, the ductility of the four-way specimen is not compromised by the transversal elements. In fact, the

test was concluded when the maximum elongation of the jacks was reached, without any brittle failures and maintaining a constant applied load.

Figure 9.33 Four-way specimen C7-2 with the passing-through plates in the tested direction

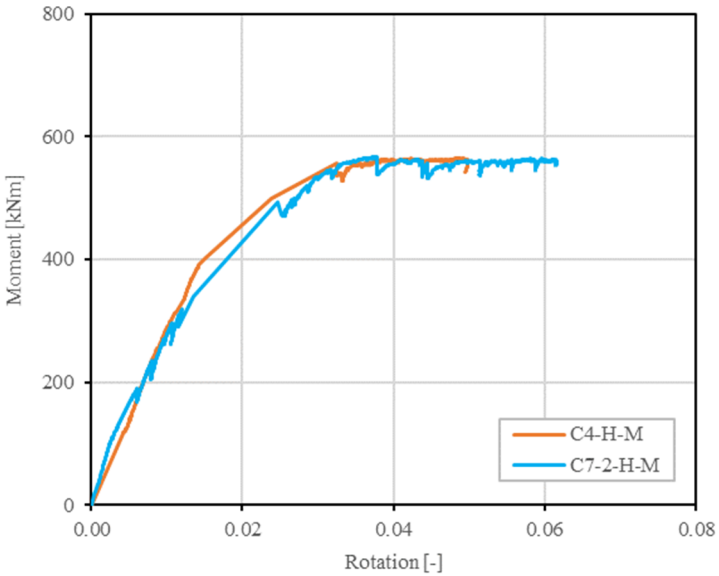

Figure 9.34 Moment-rotation curves for the monotonic tests of specimens C4 (two-way) and C7-2 (four-way) in the horizontal loading configuration

The failure mode observed in the end of the test are the sliding of the bolted joints that connect the web and the bottom flange of the external girders to the passing-through-plates (Figure 9.35a), the crushing of the concrete slab in the contact area and the cracking in the tensioned side (Figure 9.35b), and the tearing of the welds around the bottom plate in tension (Figure 9.35c) with the opening of the gap (Figure 9.35d), which was due to the tension force applied by the column wall in tension.

In the end of the test, the C7-2 specimen also exhibited the local buckling of the compressed lower passing-through plate, and the presence of cracks in the upper tensioned welds. The node region did not exhibit a clear shear deformation.

Figure 9.35 Failure modes exhibited in the test of the four-way specimen C7-2: a) sliding of the bolted connection of the flanges and web external girders, b) cracking of the concrete slab in tension, c) tearing of the welds around the bottom plate in tension, and d) opening of the gap due to the tension force applied by the column wall in tension

9.5 Critical analysis of the experimental results

The experimental tests conducted on the composite specimens, simulating the actions of horizontal loads on the structure, provides significant information about the monotonic and cyclic global behavior of the proposed joints and about the local mechanism of forces transferring from the composite beams to the filled column.

In the monotonic and cyclic tests, the specimens exhibited similar failure mechanisms. In all the specimens, the RC slabs showed crushing phenomenon in the compressed region around the steel tubular columns, and transversal cracks in the tensioned sides.

The main mechanisms exhibited in the tests were the failures of the welds around the passing-through beam flanges or the passing-trough horizontal plates. These damages occurred when the passing-through elements were subjected to tension forces due to the bending moments in the girders and in the column, and in the cyclic tests, degradation was exhibited and, in some cases, brittle failure occurred due to the sudden propagation of the cracks to the steel column wall. In particular, in the monotonic test of the C7-1 four-way specimen, the complete tearing of the passing-through welds is followed by the ones of the welds of the lower horizontal plate that passes through the column in the transversal direction, leading to the complete tearing of the tubular column wall. In fact, in the section where the welds are realized, the column wall was interrupted by the laser cutting to allow the passage of the lower beam flanges and horizontal plates. Consequently, after the welds tearing, the load on the tension side of the lower composite column is completely withstand by the only part of the tubular-column wall that remain continuous after the laser cutting processes.

The complete breakdown of the specimen allowed the close observation of the weld lesions. A first analysis permits to notice that the penetration welding was not been able to completely melt the base material of the column wall in some points. In fact, it was still possible to see the laser cutting-worked surface (Figure 9.36). Chemical analyses on samples directly extracted from the weld failure surfaces were carried out, showing that the failure of the welds was ductile. Therefore, the brittle failure was caused by the local discontinuity of the material that causes hotspot points with high stresses.

Figure 9.36 Region of lesion formation in the welds; it is possible to notice that, in the welding process, the base material did not melt on the laser cutting-worked surface

In all the tests, the node regions did not exhibit clear shear deformations and, outside the node, the lower beam flanges in compression were subjected to buckling phenomena. In the specimens where the external girders are connected by bolted joints, sliding mechanisms were shown during the test, whereas the bolts did not suffer any damage.

The comparison of the results of the horizontal monotonic loading tests performed on the two-way and four-way specimens is reported in Figure 9.37. Although the specimens with the passing-through beam (C3 and C7-1) exhibited higher stiffness and strength, the specimens with the three-passing through plates (C4 and C7-2) did

not show the reduction of the applied load after the reaching of its maximum values and showed more ductile behaviors.

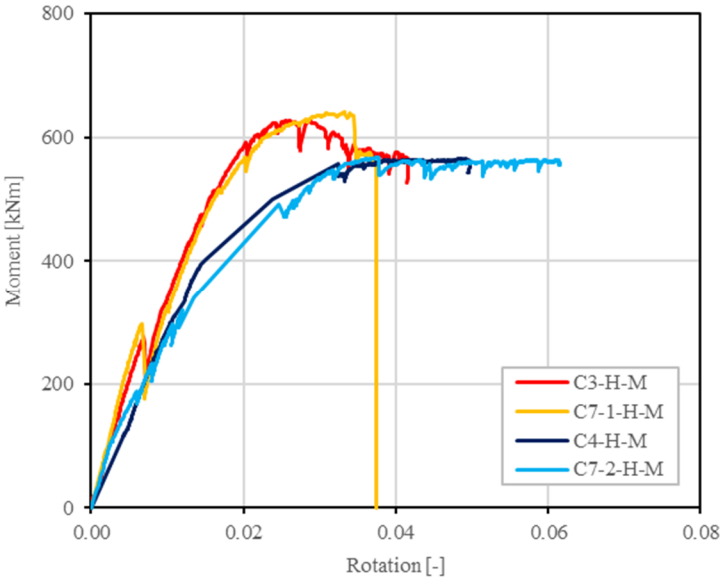

Figure 9.37 Comparison of the curves representing the behavior of the specimens with the passing-through beam in the tested direction (C3 and C7-1) and the specimens with the three passing-through plates in the tested direction (C4 and C7-2)

Moreover, in the case of passing-through beams in the tested direction, the presence of elements in the transversal direction (in this case represented by the three passing-through plates) did not influence the ultimate bending moment and the initial rotational stiffnesses, whereas the ductility is clearly different for the two-way and four-way specimens (C3 and C7-1). In fact, the two-way specimen did not exhibit the brittle failure during the test. When the specimens were tested in the direction with the passing-through plates, the presence of the passing-through elements in the transversal direction (in this case represented by the passing-through beams) did not afflict the behavior of the joint. In fact, the strength and stiffness of the two specimens (C4 and C7-2) are almost the same. In the same way, the ductility of the four-way specimen is not compromised by the transversal elements.

In the cyclic test, after the yielding, the specimen C4 exhibited a low degradation in the following cycles (Figure 9.26), and it is able to withstand a higher load ratio in

comparison with the specimen C3 (Figure 9.19). Whereas the specimen C3 hugely degraded in the cycles at 1.5 times the yielding displacement, the specimen C4 is able to reach the cycles at 3 times the yielding displacement.

In comparison with the experimental tests performed on the pure steel two-way joints, the composite two-way joints guarantee better performances in terms of stiffness and strength. In particular, for both the C3 and C4 connections, the presence of the concrete inside the tube avoids two of the main failure mechanisms of the steel joints: the local buckling that involve the tubular column wall around the welds, and the shear deformation of the node. The steel and composite specimens suffer the damages on the welds in the tensioned regions and the buckling of the compressed beam flanges. However, thanks to the presence of the RC slab, the upper beam flanges cannot buckle in the composite specimens.

The comparison of the experimental results, in terms of moment-rotation behavior, for the composite and steel C3 and C4 joints is reported in Figure 9.38. The steel joint specimen considered for the comparison is the C3-2A-2 and C4-4B-2 (Table 6.2 and Table 6.3Table 6.5), which have the same column and beam characteristics.

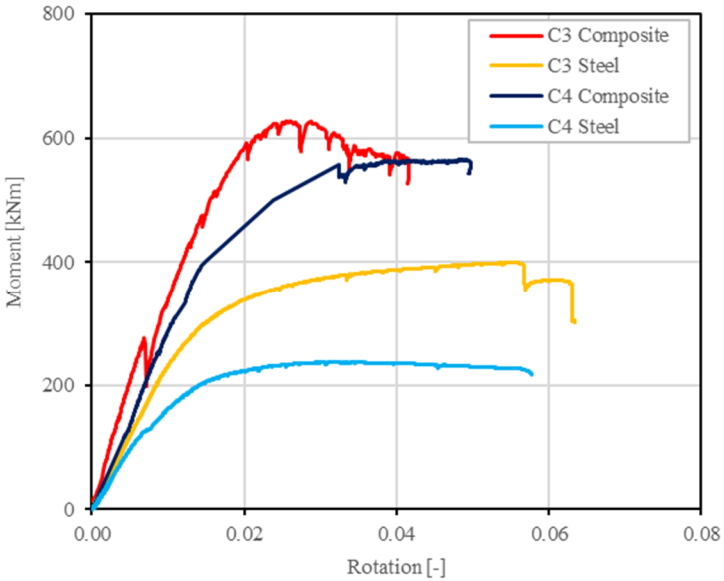

Figure 9.38 Comparison of the experimental test results for the steel and composite C3 and C4 joints under horizontal loads

The composite joints showed higher stiffness and strength with respect to the steel specimens. The stiffness of the C3 composite joint results the 60 % higher than the one of the C3 steel joint considered, whereas the strength results to be the 80 % higher. For the C4 specimens, the composite specimen had more than two times the steel joint stiffness and a strength the 40 % higher than the steel specimen. The benefits in terms of strength are in part due to the higher strength of the connected composite elements and in part due to the lack of failure mechanism avoided by the concrete parts.

In terms of ductility, the composite joints exhibited lower capacities in terms of post-elastic rotation, due to the brittle failures that involve, in particular the specimens tested in the direction with the passing-through beam.

10 Mechanical characterization of the proposed beam-to-column connections

The mechanical behavior of the proposed connections is analyzed considering the results obtained in the experimental tests on steel and composite joints. Considering the test results, in the present chapter, tools for the mechanical characterization are presented and discussed.

The characterization is accomplished with the development of mechanical models. Such models are composed of an assembly of rigid elements and translational and/or rotational springs, properly connected.

Spring elements can have linear or non-linear constitutive laws and can represent all the joint components. For this purpose, several analytical models can be developed for each functional element (component). All the components are assembled in suitable mechanical functioning schemes, which can represent the mechanical behavior of the beam-to-column connections and can be useful in the linear and non-linear design of the proposed joints.

In this context, steel and concrete joint components are defined and analyzed considering the failure modes exhibited in the experimental assessment and the theoretical and numerical analyses performed.

Afterwards, methods useful for the calculation of the elastic stiffness and strength of the components are developed. In the literature, many studies exist for the definition of the behaviors of joints components. However, the mechanical performance of some steel and composite components is nowadays still little studied, and therefore some appropriate classification methods are herein proposed, trying to adapt the researches already published on similar components and analyzing the test measurements obtained in the experimental campaign.

Finally, preliminary mechanical models, which can appropriately simulate the real behavior of the proposed joints, are developed considering, as an example, the component based model described EN1993-1-8 (CEN 2004a) for open section beam-to-column joints, which is currently the most adopted joint characterization method. The analysis of the preliminary mechanical models provides useful information on the aspects to be more deeply investigated in order to characterize the behavior of the proposed joints.

10.1 Characterization of beam-to-column connection behavior

A common beam-to-column joint is composed of two distinct regions: the connection, representing the set of elements that mechanically connect the beam to the column, and the node area, representing the element subjected to stresses by beams and column. In design practice, the behavior of beam-column joint is commonly schematized according to the two ideal fixed or hinged models (Figure 10.1). In reality, the beam-to-column connections have finite strength and deformability and their behavior is usually far to the ideal models. The connections that cannot be considered neither rigid nor hinged are called semi-rigid (Figure 10.2).

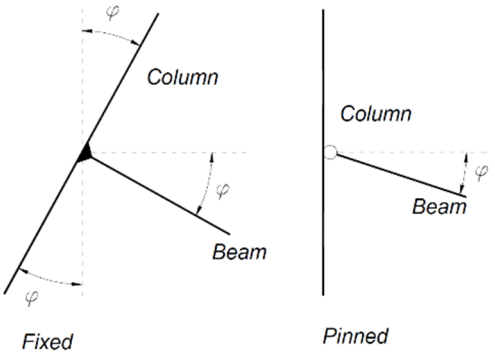

Figure 10.1 Fixed (left) and pinned (right) beam-to-column joint

Early studies on semi-rigid beam-to-column connections were conducted at the end of the 1980s in order to clarify the influence on the behavior of frame structures. Subsequent researches, have then refined the knowledge up to the modern design approach.

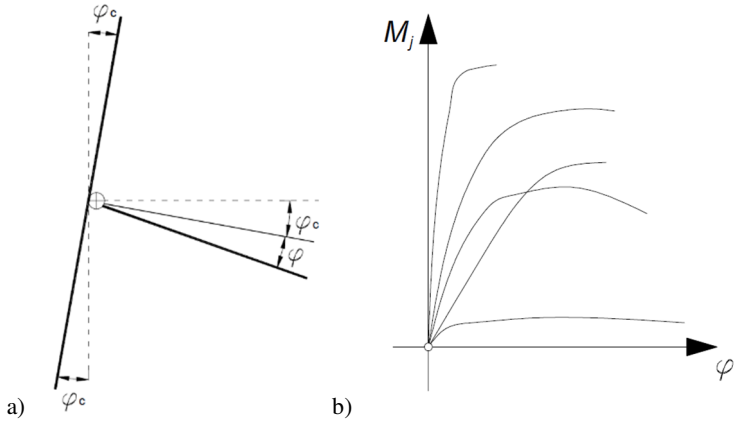

Figure 10.2 Semi-rigid beam-to-column connection: a) definition of relative rotation, and b) moment-rotation behavior

The classification by stiffness can be done considering the limits provided in the annex J of Eurocode 3 - Part 1-8, EN 1993-1-8:2005 (CEN 2005a). The limits for pinned and rigid connections are reported in the schematic representation in Figure 10.3.

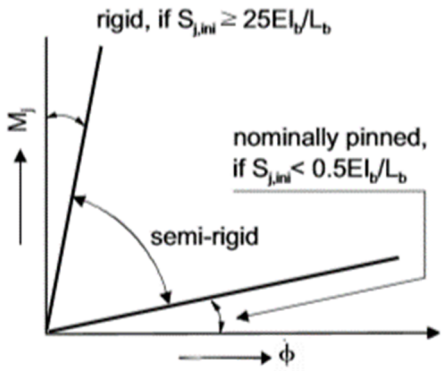

Figure 10.3 Limits for the stiffness classification of beam-to-column-connection

All the beam-to-column connections that have a stiffness in the zone marked with "semi-rigid" should be classified as semi-rigid. In the strength classification the connection is defined as full-strength if the moment design capacity is such that the plastic moment capacities are first reached in the connecting beams or columns. Instead, the beam-to-column connection is classified as pinned, if the design moment

capacity of the connection does not exceed the 25% of the design moment capacity required for a full-strength connection. If the connection moment capacities are between the above limits, is defined as partial-strength.

10.1.1 Semi-rigid beam-to-column connections

Different types of models were developed in order to describe the behavior of the semi-rigid connections. Generally, models can be divided in 4 classes: mathematical, analytical, numerical and mechanical models. These models predict, in a more or less accurately manner, the joint behavior of different construction types under monotonic and cyclic loading.

10.1.1.1 Mathematical models

More or less complex analytical functions are used in the mathematical models. These functions are defined with a certain number of constants calibrated considering experimental moment-rotation curves. The simplest models include linear models or even multi-linear models. Linear models use the following expression type:

$$M_j = K_{el} \cdot \varphi_j \qquad \text{Eq. 10.1}$$

where K_{el} represents the initial stiffness of the node, easily obtainable from experimental test results, M_j is the moment transmitted by the beam-to-column node and φ_j is its relative rotation. Continuous linear curves compose the multilinear model (Figure 10.4). Each linear interval is characterized by a different stiffness. This model is versatile and allows an approximation of the experimental curves the more accurate the greater is the number of intervals considered. On the other hand, a large number of intervals requires the calibration of many parameters.

Using polynomial and exponential equations, more complex models can be developed, in which the functions are defined by characteristic constants determined through numerical interpolation techniques, in order to approximate the experimental curves to be represented.

The mathematical models can accurately represent the behavior of the beam-to-column nodes. However, they are just employable for the joint typologies where the constants calibration has already been performed. Furthermore, some models need knowledge of a large number of parameters, that requires the use of complex techniques for interpolating experimental data. For these reasons, simplified analytical models have been developed.

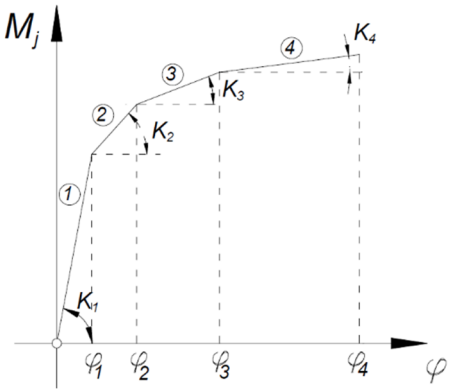

Figure 10.4 Parameters of the multilinear model

10.1.1.2 Analytical models

Analytical models can describe the structural behavior of the beam-to-column connections considering the mechanical properties of the materials, e.g. the initial stiffness, the post-elastic stiffness and the yielding stress, and the geometry of the elements. They can be realized considering numerical simulations, as well as experimental tests.

The analytical models represent a promising technique of representation of node behavior, since they allow the evaluation of fundamental mechanical characteristics, such as stiffness or resistance, generally providing values according to the experimental tests. On the other hand, it is not possible to obtain the entire moment-rotation curve without performing numerical interpolation procedures.

10.1.1.3 Numerical models

In numerical models, finite element models represent a general approach for studying the behavior of beam-to-column joints. However, the model complexity and the computational burden make the approach usefully applicable just to the field of research.

The level of accuracy achieved by today's calculation codes allows the analysis of complex three-dimensional structures in which all non-linear phenomena can be adequately considered. However, these numerical models require sufficiently powerful processors to easily deal with the computational burden.

10.1.1.4 Mechanical models

Mechanical models can be composed of an assembly of rigid elements and translational and/or rotational springs, properly connected. In general, spring elements have linear or non-linear constitutive laws.

The beam-to-column joint mechanical models can accomplish the representation of the behavior of such connection. In fact, the constitutive law of each elastic element is defined through experimental and/or numerical studies or with appropriate analytical models, and then the assembly of the model is performed. The use of a set of rigid and deformable elements can lead to consider the contributions of each part of the connection through an overall model similar to an analytical one.

10.1.1.5 Component method

The component method is nowadays the more useful structural design method for the beam-to-column joints. This method integrates several analytical models, developed for each functional element (component) of the beam-to-column connection, in a suitable mechanical functioning scheme, so that obtaining the initial stiffness and ultimate bending strength of the connection. This method for the characterization of joints was initially developed for the design of steel joints, and later extended to the design of steel-concrete composite connections (ECCS 1999; CEN 2005a). The approach proposed by the component method is the result of different numerical and research contributions, developed from the late 1970s to the early 1990s (Krawinkler et al. 1971; Krawinkler 1978; Witteveen et al. 1982; Jaspart and de Ville de Goyet 1988; Stark and Bijlaard 1988; Tschemmernegg and Humer 1988). In particular, the performed experimental tests highlighted the possibility of identifying elements in the beam-to-column connections, which are defined in terms of strength and stiffness. The complete design methodology with a subdivision in separated operational phases, is due to the studies conducted at the University of Liège and the University of Innsbruck (Huber 1999).

The component approach was firstly applied only to beam-to-column steel joints subjected to bending and shear stresses generated by static actions. More recent studies allowed the extension of the method to the modeling of different type of connections, such as column-to-foundation connections, other loading conditions, such as seismic action, and other materials, such as composite joints (Braconi 2004).

The method procedure can be briefly summarized in four phases: a) the identification of the functional elements (components) within the beam-to-column joint and their schematization (Figure 10.5a); b) the identification of the type of stress that characterized each component; c) the definition of their mechanical properties

(strength and stiffness); and d) the assembly of the components in a suitable mechanical operating scheme (Figure 10.5b), which can simulate adequately the kinematics of the connection.

Although correctly modeling the actual mechanical behavior of the node, a mechanical model similar to the one shown in Figure 10.5b is not easily applicable in commercial structural analysis programs, due to the large number of springs and rigid elements. Therefore, to make the use of the component method feasible with less sophisticated calculation programs, all the springs in the connection are combined in a few equivalent springs as shown in Figure 10.6.

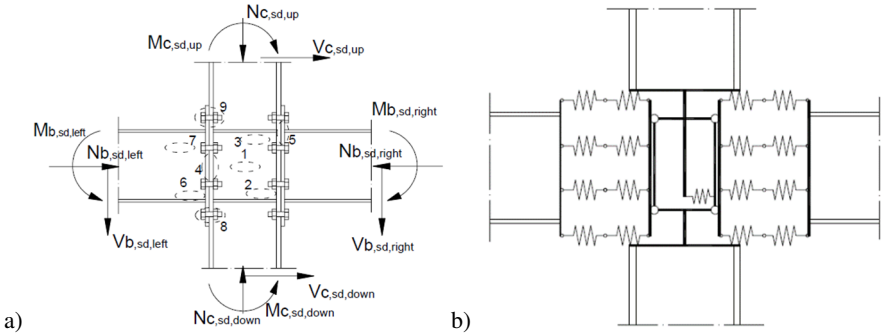

Figure 10.5 Component method applied to a beam-to-column bolted joint: a) definition of the components, and b) assembly of the mechanical model (Braconi 2004)

The effectiveness of the method depends on the precision of the mechanical description of each component behavior. Moreover, the presence of a high number of components can lead to an interaction between the behavior of different components, which can influence the simulation of the whole node. However, a proper description of the individual interacting components does not invalidate the efficiency of the component method.

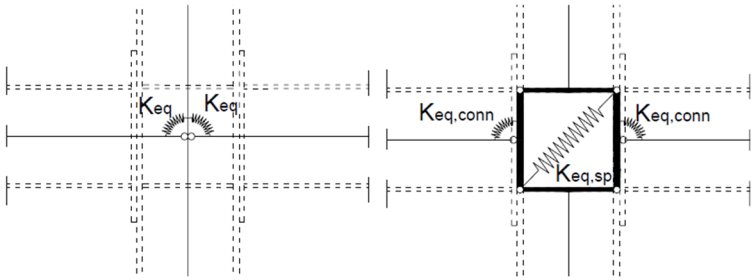

Figure 10.6 Simplified models used in static (left) and seismic design (Braconi 2004)

10.1.2 Characterization of I-beam-to-CHS-column connections

The first investigations on unstiffened connections between plates or I-beam and CHS hollow sections have been carried out in Japan and were published mainly in Japanese papers. The rigid diaphragm stiffened connections were also extensively studied in Japan. The mechanical characterization of joints between CHS-column an open-section beams can be realized considering formulae provided by the Eurocode 3, EN1993-1-8 (CEN 2005a) and CIDECT Guide Lines (Kurobane et al. 2004; Wardenier et al. 2008) for connection between tubes (columns or chords) and compressed or tensioned plates (disposed parallelly or perpendicularly to the longitudinal axes of the tube), or I-beams in tension, compression or bending. The semi-analytical formulae for the design of uniplanar and multi-planar hollow section joints reported in these codes were derived from the numerical simulations and the experimental assessment exposed in (Wardenier 1982; de Winkel 1998; Ariyoshi and Makino 2000; Kurobane et al. 2004).

For the joints between CHS profiles and open-section profiles or plates, the failure modes to be considered in the definition of the design strength and stiffness are the following.

- Tube face failure (or tube plasticization) in the connection region, with connected elements in tension, compression or bending.
- Tube side wall failure (or tube web failure) in the lateral side, by yielding, crushing or instability, with the connected member in compression.
- Tube shear failure.
- Punching shear failure of the hollow section wall.
- Connected open-section brace failure with reduced effective width.
- Local buckling failure of the open-section or plate connected element in the connection region.

Considering the reported failure mechanisms, the strength and the stiffness of the joint components are provided. In particular the strength and stiffness of directly connected I-beam to the tube wall are derived from the relative value of the connection of transverse plates in the flange region, without consider the beam web. The strength and stiffness of the single transverse plate-to-CHS T-connection in tension and compression considered to two limit states. CHS-profile plasticization and tube-wall punching shear. The first limit state refers to the transversal tube wall yielding or buckling in the connection regions, both in tension and compression, assuming that both the branch plate and the weld are adequately designed and are non-critical. Calculation of the two limit states depends significantly on connection geometry, particularly the dimensions of both the plate and the tube.

CIDECT Design Guide N.9 (Kurobane et al. 2004) also provides a method for the evaluation of the column web panel strength and stiffness. The shear strength of the node panel is defined considering the influence of the stress ratio in the tubular column wall. The node panel is able to develop a further increase in load, thanks to the strain hardening, showing a stable load vs. deformation curve (Kurobane et al. 2004). Furthermore, a beam-to-column joint in which the design moment resistance is governed by the design resistance of the column web panel in shear, may be assumed to have adequate rotation capacity for plastic global analysis (CEN 2005a). Thus, moderate yielding of the column web panel has a beneficial effect on enhancing the performance of moment-resisting frames, because it can participate in dissipating input energy and helps to prevent hinging of the column. Furthermore, yielding of the column web panel serves the same function as plastic hinges at the beam ends on both sides of the connection. However, excessive yielding of the column web panel should be avoided because large shear strain in the panel induces local bending of the column or beam flanges in the region adjacent to the groove welds, which may result in a premature development of tensile failures in these regions.

Regarding the component method for steel I-beam-to-CHS-column joints, in (Weynand et al. 2003; Jaspart and Weynand 2015) authors exposed studies on the extension of the traditional component method, developed for I-columns and I-beams, to joints between hollow and open sections. For the connection involving concrete filled columns, studies on the mechanical characterization of the node region are reported in (Li and Han 2011, 2012). In (Ou et al. 2015) a model that considers crushing of concrete in the panel zone, as failure mode, is proposed to calculate the panel zone shear strength contribution from concrete, considering confined and unconfined concrete.

For the mechanical characterization of the components involved in the composite beams, suitable information can be taken from the studies reported in (Braconi 2004; Braconi et al. 2007, 2010) where the development of refined component models for exterior and interior beam-to-column joints for composite structures is exposed.

10.2 Definition and characterization of the components

Joint components are defined considering the failure modes exhibited in the experimental assessment and the theoretical and numerical analyses. With the final objective of developing mechanical models for steel and composite joints, steel and concrete components are studied in order to develop methods for the definition of the component elastic stiffnesses and the strengths.

Vertical loading tests exhibited similar behaviors for all the studied joint typologies. In fact, in case of gravity loads on the structure such as the overload on the decks, the joints do not exhibit failures inside the node and all the damages are located on the external girders, except for the buckling of the compressed passing-through plates inside the column.

In the horizontal loading experimental studies, the joints characterized by the continuous beam behaved in a significantly different way from those most currently adopted and for which the Eurocode 3 (CEN 2004a) proposed the component method for the mechanical classification. In fact, in case of external girders connected to a beam stub that passes through the column, the column is not continuous in the node. In these cases, the beam can be assumed as the continuous element and the column results to be divided in three parts, the node panel stub and the two external elements, one on the top and one on the bottom.

On the contrary, when the connection of the external girders is realized with passing-through plates, the column can be assumed as continuous under horizontal load, since the slots to be realized are less impactive and do not result in the complete discontinuity of the tubular column wall.

In case of four-way joints, which represent the most actual configuration, the behavior under horizontal loads, should be discerned for the two directions. Moreover, the presence of passing-through elements in both directions causes the reduction of the continuous part of the column wall and the welds made around the laser-cutting slots between the beam and the column walls allow the reconnection of the elements. Such welds, and the area of interaction between through flanges or plates and the column wall, are those that suffered the most critical mechanisms in the horizontal loading experimental tests, as also emerged in the preliminary studies.

10.2.1 Steel components

To model the proposed joints in a way that closely reproduces the expected behavior, the most important areas are the regions where the beam flanges (C3) or the horizontal plates (C4) pass through the column and the web panel in shear. Phenomena were there observed in the experimental tests and, generally, the collapse of the joint substructures was due to the failure of the components in these regions.

The main components to be considered in the node are the passing-through elements, i.e. the I-beam flanges (Figure 10.7a) or the flange plates (Figure 10.7b), the tubular column wall above and below its (Figure 10.7c), and the welds that join these elements (Figure 10.7d). All the beam and column components are mainly

loaded by axial loads, whereas the welds are subjected to the resultants of the axial loads in the connected elements.

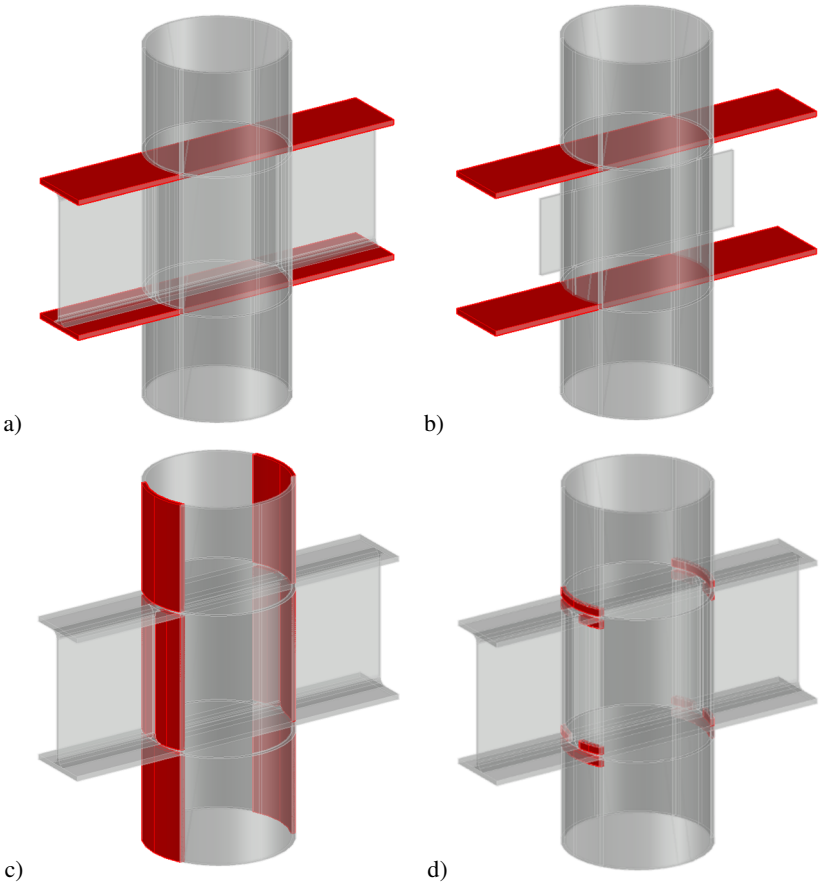

Figure 10.7 Axially loaded components: a) through beam flanges (type C3), b) through flange plates (type C4), c) tubular column wall, and d) flange welds

In addition to the above-described components, which are mainly subjected to axial forces, the other components that can be defined in the proposed steel beam-to-column connection are those subjected to shear forces and bending moment. Among these, it is possible to identify the internal and external beam web that passes through the column (Figure 10.8a), the vertical passing-through web plate (Figure 10.8b) and the

central part of the column wall, which is continuous in the node, in the simplified case without transversal passing-through elements (Figure 10.8c).

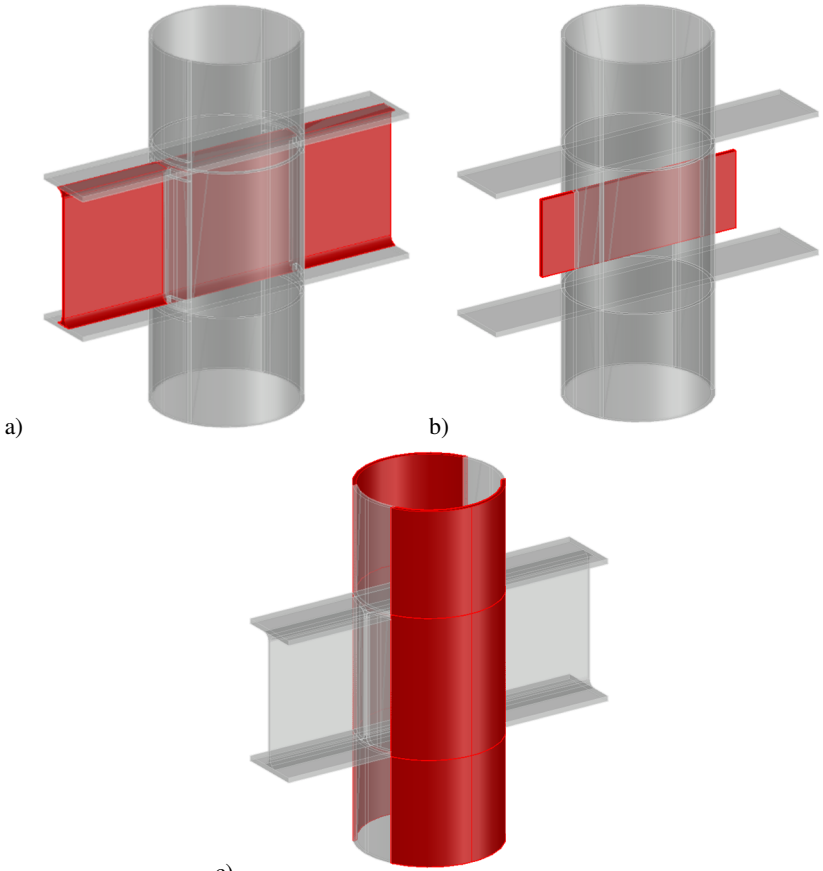

Figure 10.8 Components subjected to shear forces and bending moment: a) passing-through beam web (type C3), b) through vertical web plate, and c) tubular column wall

10.2.1.1 Axially loaded components

In case of vertical loads on the structure, the flange or the corresponding plate are subjected to opposite compression or tension forces, respectively for the upper and the lower region (Figure 10.9). For vertical loading, the tests showed that the load is not transmitted to the column wall and it is almost totally transmitted from one side to the other of the column through the internal continuity of the flanges. In fact, the

deformation, measured by strain gauges inside the joint, reported values almost equal to those recorded outside the column. Therefore, the external load is almost equal to the load inside the column. This occurs both in compression and in traction and, finally, the collapse of these components and of the joint substructures occurs due to plasticization of the flange in tension and compression, with the additional local buckling of the compressed flanges. The welds do not have to transmit loads and the joint can be classified as rigid and full-strength and the characterization of stiffness and strength is not necessary.

However, in the case of a through plate (connection C4), an additional limit state must be considered. In fact, the compressed through plate may buckle inside the column, considering the absence of internal stiffeners. The connection stiffness is not influenced by this mechanism in the elastic range. However, the buckling of the bottom plate lead to a brittle failure of the connection, before the development of the beam capacity. The thickness of the trough plate, as well as the diameter and the thickness of the column influence this failure mode. In case of internal local buckling of the passing through plate, the column wall in the connection regions start to locally buckle, as shown in Figure 10.9b. Therefore, the thickness of the column wall and the axial compression load in this element can influence the buckling load.

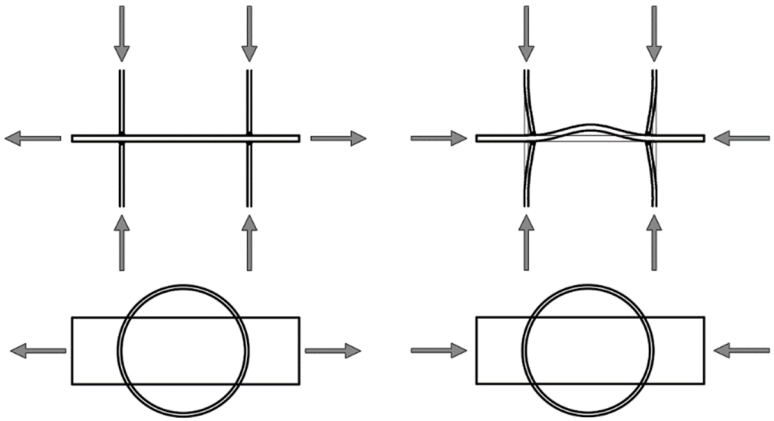

Figure 10.9 Axial load on the component in case of vertical loads on the structure: a) upper flange in tension, and b) lower flange in compression

This phenomenon can be characterized by assuming a beam element subject to compression with a section equal to the one of the through plate and an effective length equal to half the diameter of the tube, assuming fixed ended for the plate. The

capacity of the connection in terms of bending moment can be therefore calculated considering the Euler's formula for the determination of the critical load, with the following equation.

$$M_{cr} = P_{cr} \cdot h_{beam} = \frac{\pi^2 \cdot E \cdot J_{plate}}{(0.5 \cdot D_{column})^2} \cdot h_{beam} \qquad \text{Eq. 10.2}$$

The results of the application of this formula to the experimental tests conducted are reported in Table 10.1, for the tests with vertical loads on C4 specimens, i.e. C4-1B-1, C4-3A-1, C4-4B-1 and C4-5A-1. The comparison of the exhibited experimental capacities $M_{b,plate}$ with the analytical simulations M_{cr}, shows a fine correlation except for the third case. However, in the test C4-4-B-1, with the passing-through plate thickness equal to 12 mm, the local buckling of the passing through bottom plate happened in the end of the test, after the plasticization of the plates outside the column. In fact, in this case the external beam capacity was reached (Figure 6.17).

Even though the use of an effective length equal to half the diameter lead to satisfying results, the complete knowledge of the mechanism requires more in-depth studies and parametric analyses able to provide a methodology for the determination of the effective length to be used in the Euler's formula for the determination of the critical load.

Moreover, the buckling phenomena that afflict the passing-through compressed plate are probably influenced by the transversal elements inside the node. These elements can be assumed as restrains for the plates and can avoid this failure or increase the load that induces the mechanism.

Table 10.1 Comparison of the experimental results and analytical simulation

b	t	J	D_m	L_{eff}	P_{cr}	M_{cr}	$M_{b,plate}$
mm	mm	mm^4	mm	mm	kN	kNm	kNm
180	10	15000	346	173	1040	416	431
180	10	15000	346	173	1040	416	415
180	12	25920	346	173	1797	719	496
180	10	15000	346	173	1040	416	440

In case of horizontal loads on the structure, as predicted by the preliminary studies and numerical analyses, and confirmed through the execution of experimental tests, the moment-rotation behavior of the connection is particularly influenced by the

behavior of the axially loaded components, such as the beam flanges, the column wall above and below the flanges, and their connecting elements. Indeed, in case of horizontal loads, the opposite beam and column are subjected to equal bending moments. In this situation, each flange of the beam (or each horizontal plate), as well as the column wall above and below these elements, are mainly subjected to axial tension or compression forces (Figure 10.10), which can be defined by considering the geometry of the sections. Therefore, the axial behavior of these components, in terms of capacity and elastic stiffness, has a high influence on the moment-rotation behavior of the connection in case of horizontal loads. Furthermore, the connection elements, i.e. the welds realized around the passing-through elements, allow the transfer of the forces between these beam and column components.

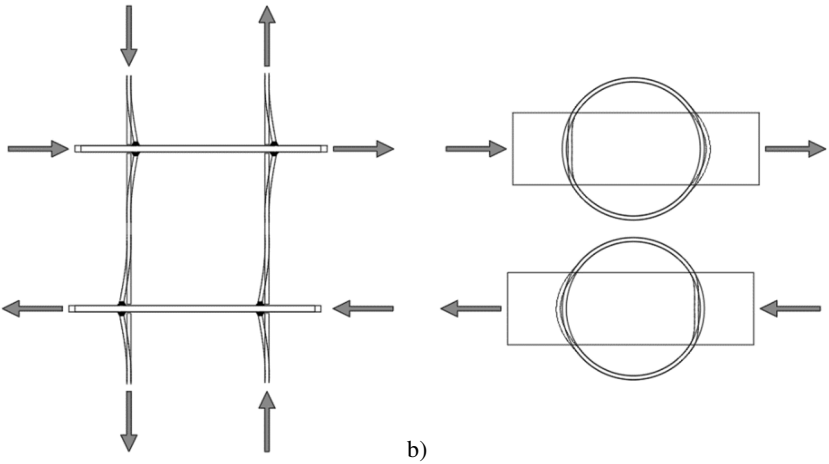

Figure 10.10 Behavior of the proposed connections in case of horizontal load on the structure: a) axial loads on beam flanges and column wall, and b) upper and bottom flanges with the corresponding axial loads

Two different main mechanisms can be described for the involved components: the first in the compression region, where the beam flange is subjected to a compression load, as well as the column wall, and the second one in the tension region, where the beam flange and the column wall are in tension. These two mechanisms act in parallel. In fact, the continuity of the through elements inside the column allows the transmission of the load to one side to the other.

For the definition of the global capacity of this mechanism, three limit states must be considered: a) the beam flange (or plate) and tube-wall plasticization in tension or

compression; b) the local transversal buckling of the column wall in the tension and compression regions (Figure 10.10); and c) the failure of the welds.

The beam flanges plasticization in tension or compression, as well as the plasticization of the through plates in case of C4 connection type, is an easily describable phenomenon. The axial load that leads to the plasticization can be calculated considering the area of the transversal section and the yielding stress of the through element. Besides, the capacity of the column wall sections that act mainly in tension or compression, can be calculated in the same way, considering the involved area and the yielding stress of the CHS column.

$$N_t = A \cdot f_y \qquad \text{Eq. 10.3}$$

The second limit state to be considered is the transversal tube wall yielding or buckling in the connection regions. Without considering the welds failure, which is separately described and analyzed, this phenomenon involves both the sides of the passing-through elements, and thus both the compressed and tensioned sides of the column wall. Considering that there are no precedents or theoretical models that can be used as a basis for the development of design recommendations, it is possible to consider the general behavior of the passing-through plate or beam flange T-connected to the CHS-column wall as approximately equivalent to the addition of tension and compression transverse plate-to-CHS T-connection (Figure 10.11) behaviors, as suggested in (Voth and Packer 2016). In this study, authors provide the following general formula for the definition of the axial strength of passing-through transversal plates directly welded to the tube-wall in compression or tension.

$$N_1 = f_{y,CHS} \cdot t_{CHS} \cdot \left[\mathrm{Q}_{U,90,C} + \mathrm{Q}_{U,90,T}\right] \cdot Q_F \qquad \text{Eq. 10.4}$$

The partial strengths in compression and tension $\mathrm{Q}_{U,90,C}$ and $\mathrm{Q}_{U,90,T}$ can be defined considering the limit state inducted by lateral tube-wall yielding or buckling, assuming that both the connected plate and the weld are adequately designed and are non-critical. In (Wardenier et al. 2008; Voth and Packer 2012) authors provide empirical formulae, considering existing CHS-to-CHS design guidelines to a limited set of experimental results for plate-to-CHS connections and using regression analyses. The partial design strength functions, expressed as an axial force in the plate, take the following general forms:

$$\mathrm{Q}_{U,90,C} = 0.85 \cdot 2.9 \cdot \left(1 + 3 \cdot {\beta_{eff}}^2\right) \cdot \gamma^{0.35} \qquad \text{Eq. 10.5}$$

$$Q_{U,90,T} = 0.85 \cdot 2.6 \cdot \left(1 + 2.5 \cdot {\beta_{eff}}^2\right) \cdot \gamma^{0.55}$$ Eq. 10.6

A lower-bound reduction factor equal to 0.85 was suggested, based on a regression analysis of the numerical results, for application to limit states design. In the formulae, β_{eff} and γ are equals to:

$$\beta_{eff} = \frac{b_p + 2 \cdot z}{D_{CHS}} \quad ; \gamma = \frac{D_{CHS}}{2 \cdot t_{CHS}}$$ Eq. 10.7

where b_p is the width of the through plate, z is the weld leg length along the tube, D_{CHS} and t_{CHS} are respectively the external diameter and the thickness of the tube.

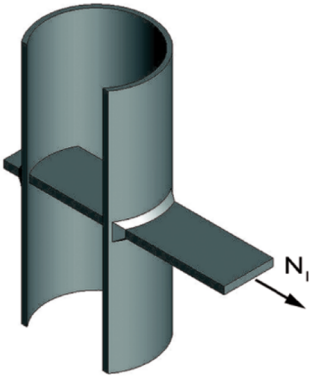

Figure 10.11 Schematic representation of the transverse through-plate-to-CHS T-connections studied in (Voth and Packer 2016)

In the formula for the definition of the axial strength N_1 of passing-through transversal plates, $f_{y,CHS}$ is the yielding stress of the tube and Q_F is a tube stress influence function that considers the stress level in the tube face by reducing the connection resistance. In fact, $Q_{U,90,C}$ and $Q_{U,90,T}$ are the partial design strength functions that predict the connection resistance without the tube axial stress. Q_F can be calculated with the following reported formulae provided in (Wardenier et al. 2008) respectively for the tube in compression ($Q_{F,C}$) or in tension ($Q_{F,T}$) (Figure 10.12):

$$Q_{F,C} = (1 - |n|)^{0.25} \; ; Q_{F,T} = (1 - |n|)^{0.20}$$ Eq. 10.8

where n is the stress ratio in the tube, calculated as the ratio between the demand and the capacity in compression or tension. Therefore, it is possible to consider the

influence of the bending moment acting in the column, on the strength of this component. Furthermore, considering that in the current situation the tubular column wall is compressed where the plate is in compression and tensioned where the plate is in tension, the new following formulae for $N_{b,C}$ and $N_{b,T}$ can be written starting from the previously reported equation provided in (Voth and Packer 2016).

$$N_{b,C} = f_{y,CHS} \cdot t_{CHS} \cdot Q_{U,90,C} \cdot Q_{F,C} \quad \text{Eq. 10.9}$$

$$N_{b,T} = f_{y,CHS} \cdot t_{CHS} \cdot Q_{U,90,T} \cdot Q_{F,T} \quad \text{Eq. 10.10}$$

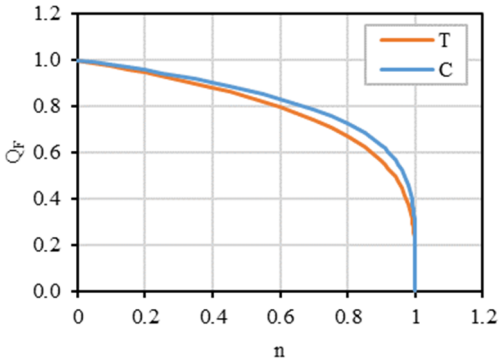

Figure 10.12 Tube stress reduction factors Q_F for the tube in compression or tension in function of the stress level in the tube face n

The reported equations are clearly empirical, and verified for a limited parameter range and with limited data. Therefore, the clear understanding of the phenomena requires larges studies, since in the reported and considered studies, only fillet welds and tube in compression or tension were investigated. Furthermore, the schematic representation of stand-alone passing-through transverse plate, is quite different from the actual one, where the web plate acts like a stiffener for the tube wall in one side of the components and, moreover, in one case is directly connected to the flange (C3 type) and involved in the bending moment resistance.

The using of separated equations, for the strength in the compression and tension regions, is useful in the mechanical characterization of the global behavior (Figure 10.13). In fact, different mechanism can happen in the tension and compression region, such as the welds failure only in tension exhibited in the experimental tests. Therefore, it is possible to separate these two strengths, which are then considered

together with the other limit states, i.e. the resistance of the welds and plates in tension and compression. At that point, the overall resistance of the whole component can be determined as the minimum resistance of the single components in each region.

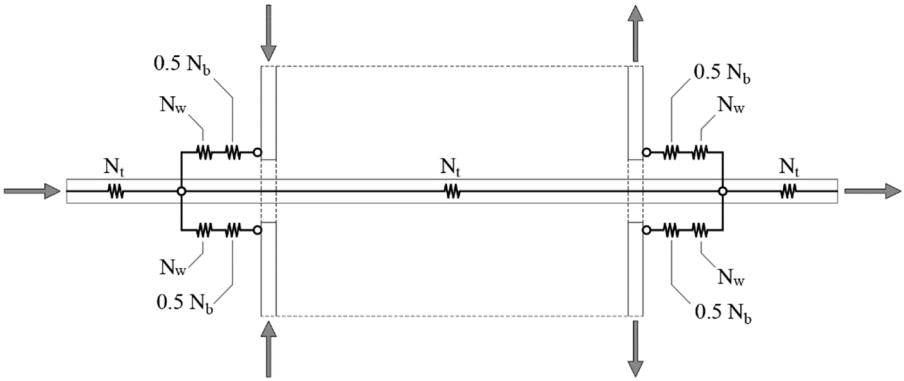

Figure 10.13 Assembly of the components in the flange region; each component can have different strength in compression and in tension

In terms of stiffness, in the elastic range the stiffness is mainly influenced by the one of the passing-through elements and by the lateral bending of the column wall in the connection region, followed by the transversal local buckling. This second effect cause a reduction of the axial stiffness of the whole flange component and thus of the connection in terms of rotation. On the contrary, the welds can be considered as rigid in comparison with the other components. In (Kurobane et al. 2004) the following formula for the initial stiffness of the flange plate directly connected to CHS-column wall is provided.

$$K = 1.9 \cdot E \cdot t_{CHS} \cdot \beta^{1.3} \cdot (2\gamma)^{-0.7} \qquad \text{Eq. 10.11}$$

However, the reported formula does not consider the fact that the element passes through the column, and further studies should be performed in order to have a fine calibration.

10.2.1.2 Weld components

Although the flange-connecting welds do not influence the stiffness of the connection, they substantially influence the strength of the connection, leading to a brittle failure in case of their failure, as reported in the experimental tests. These welds are realized between the through beam flange (or plate) and the tubular column wall,

in two different ways: fillet and partial/full penetration welding. Several factors make difficult the mechanical characterization of the weld performances. First of all, in fillet welds, the stress on the column wall is eccentric with respect to the weld, with the consequent appearance of additional normal stresses (Figure 10.14a). In penetration welds, this problem does not exist (Figure 10.14b). However, it is difficult to realize the full penetration by acting only from the outside of the tube. This problem is partly overcome by the possibility of applying a 3D laser cutting geometry.

The schematization of the flange welds as an axially loaded component can be realized by defining the influence of supposed secondary effects on the supposed main phenomenon. In fact, the stress state in the weld is at least biaxial, due to the simultaneous presence of tension or compression in the column wall and in the passing-through I-beam flange or plate (Figure 10.14). Considering the resistant section of the weld, overturned on the plane of the through element, there are both normal stresses and tangential forces that are mainly orthogonal to the welding axis. Therefore, it is possible to define the strength in one direction (e.g. parallel to the beam flange axis), considering the reduction due to the stress level in the other one (e.g. parallel to column axis).

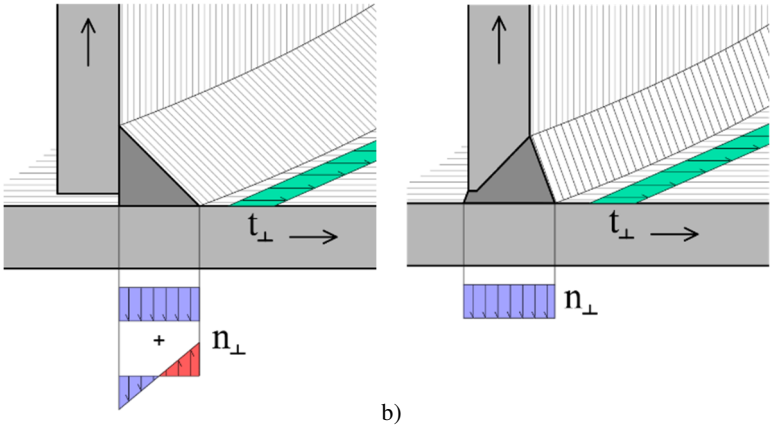

Figure 10.14 Welds between the through element and the column wall: a) fillet and b) full penetration welding

Experimental tests exhibited that the weld failure mainly happens in the tension region, whereas in the compression side, the welds did not exhibit particular problems and the failure mode exhibited is the local buckling of the column wall around the welds. In both cases, the stress distribution is not uniform due to the interaction between the tube wall and the plate, as highlighted in the experimental tests and

numerical simulations reported in (Voth 2010). The peak stress of the non-uniform stress distribution occurs adjacent to the connection stiff points, which develop in the outward points of the weld. This phenomenon is due to the lower stiffness of the cut CHS face in the central area, when subjected to transverse loads, and produces a shear stress concentration on the lateral sides of the weld (Figure 10.15).

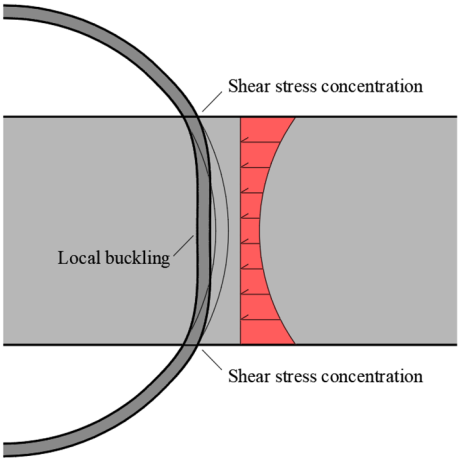

Figure 10.15 Force transmission in the compression region

The non-uniform stress distribution can be transformed into an equivalent uniform stress block with an effective reduced width. Furthermore, a redistribution of stress occurs when a portion of the through plate reaches the yield stress, resulting in an increased effective width. Nowadays, the influence of the non-uniform distribution on the strength and stiffness of the connection, is not completely clear, and the current design recommendations by CIDECT (Wardenier et al. 2008), do not include an effective width parameter.

However, the experimental tests and numerical simulations reported in (Voth 2010) demonstrated that this phenomenon is more evident in case of external transverse plate in tension or compression (Figure 10.16). In fact, in case of passing-through plate, the stress distribution on the plate surface resulted to be more uniform in comparison with the external plates (Figure 10.17). This result is probably due to whole redistribution of stresses in the two side of the tube, one in compression and the second in tension. Moreover, the past researches did not study the influence of the axial stresses in the tube wall on the stress distribution in the plate. Therefore, further studies are necessary to completely understand the mechanism.

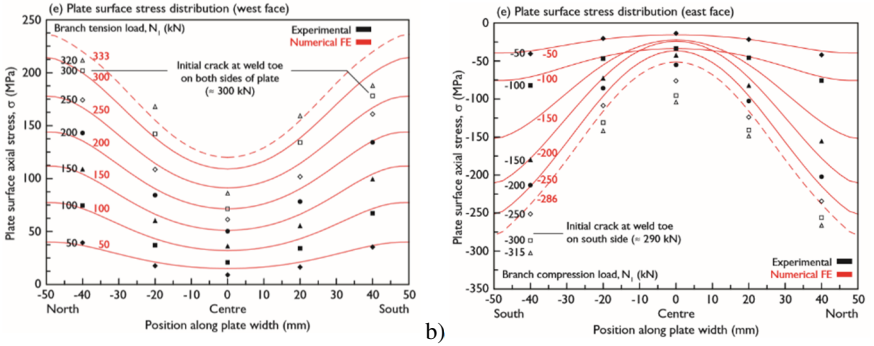

Figure 10.16 Plate surface stress distribution of a directly welded transverse plate: a) tension and b) compression (Voth 2010)

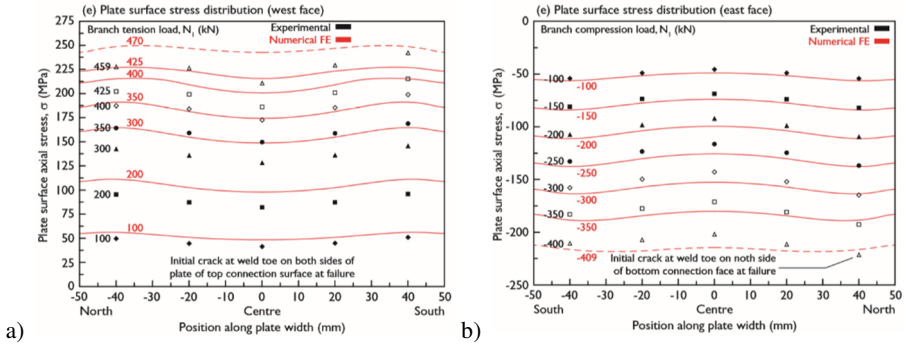

Figure 10.17 Plate surface stress distribution of a passing-through transverse plate: a) tension and b) compression (Voth 2010)

In conclusion, the mechanism has tridimensional characteristics that are not easily interpretable by 2D mechanical models. Therefore, the schematization proposed in Figure 10.13, where the in-series springs marked as N_w and N_b refers respectively to the behavior of the welds and the tube-wall, is not completely realistic. In fact, looking at the tridimensional mechanism, an in-parallel mechanism of the welds can be adopted, as shown in Figure 10.18, with the first spring traducing the lateral transmission of the load (N_{wL}) and the second one (N_{wC}), which acts in-series with the local buckling effect (N_b), the central transmission mechanism. Moreover, these two weld regions have completely different stress situation, due to their direction and to the stress distribution in the column wall, which has higher values in the central region than in the lateral one, and can rely in this latter area on the lateral continuity of the column wall.

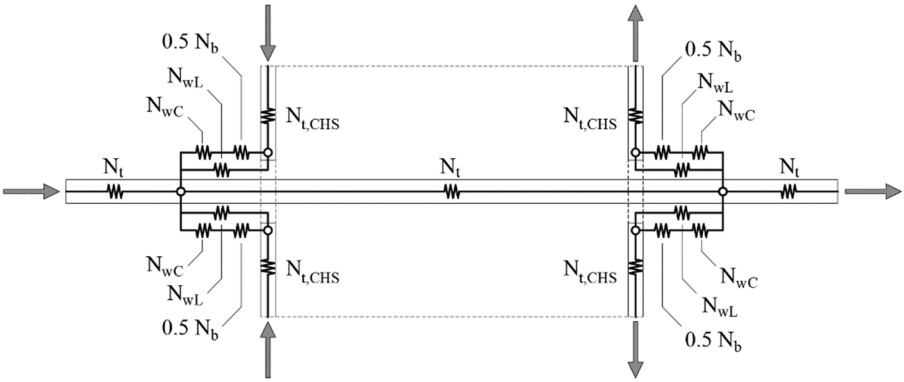

Figure 10.18 Assembly of the components in the flange region with the tridimensional effect of the welds resisting mechanism

In addition to the previously reported aspects, a comparison of the mechanical characterization of the connection welds and the results of the experimental tests cannot consider reliable. In fact, considering both the geometry and the material mechanical characteristics of the welds, there are considerable uncertainties, which do not allow a clear understanding of force transmission mechanisms. Therefore, more in-depth studies are necessary for a better knowledge of the phenomenon.

10.2.1.3 Components subjected to shear forces and bending moment

In case of vertical loads on the structure, the external beam web is subjected to the shear force, whereas inside the node the shear stress is not present due to the transmission of the vertical force from the beams to the column wall through the welds realized around the web slots and through the direct contact, which develops between the passing through elements and the tube-wall. However, in the experimental tests no evidence about shear failure was highlighted, and the failure mode exhibited are the yielding of flanges and the local buckling of the passing-through bottom plate. However, in case of asymmetric loads on the beams or horizontal loads on the structure, the shear stressed internal components must be considered. In fact, the shear deformation of the panel zone was exhibited in the tests on steel specimens under horizontal loading, suggesting that the behavior of this component influence that of the connection. For the definition of the global strength and stiffness of this component, three mechanisms must be considered a) the shear deformation and failure of the internal through beam web (or vertical plate); b) the shear deformation and fail of the tube-wall in the node region; and c) the failure of the connection elements

(welds) due to the shear stress. The first two mechanisms act in parallel and can be mechanically modelled by two axial spring with the effective stiffness and strength (Figure 10.19). The latter mechanism allows the in-parallel behavior of these two components. Indeed, the failure of the welds between the beam and the column cause relative displacements with consequent separated behaviors. In this case, the beam web is only subjected to shear stresses transmitted by the beam, as well as the panel zone of the column.

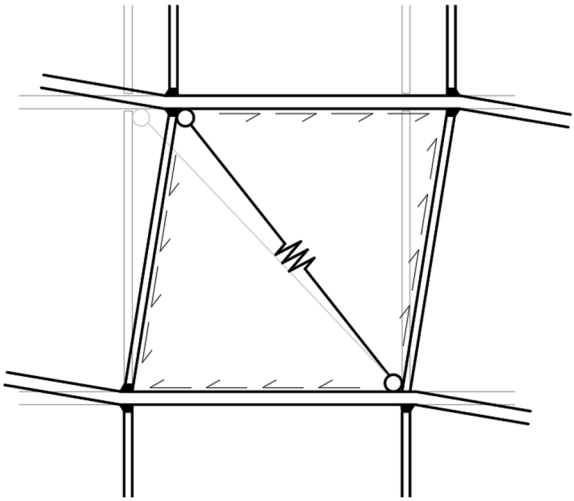

Figure 10.19 Mechanical model for the panel zone subjected to shear

The strength of the beam web panel or the web plate can be defined considering the two limit states described in the Eurocodes. Eurocode 3, part 1-8 (CEN 2005a) provides the following formula for the definition of the design shear resistance.

$$V_{wp,Rd} = \frac{0.9 \cdot f_{y,wc} \cdot A_{vc}}{\sqrt{3} \cdot \gamma_{M0}} \qquad \text{Eq. 10.12}$$

where the shear of the I-beam A_{vc} can be calculated considering the following equation reported in the Eurocode 3, part 1-1 (CEN 2005b).

$$A_{vc} = A - 2 \cdot b \cdot t_f + (t_w + 2 \cdot r) \cdot t_f \qquad \text{Eq. 10.13}$$

A, b, t_f, t_w and r are respectively the total area, the width, the flange and web thickness, and the root radius of the I-section. However, the formula refers to I-profile

webs not stiffened. In the proposed joints, the web panel of the continuous beam results instead to be stiffened by the tube-column wall in the node. The reported code provides further formulae useful to take into account the presence of stiffeners. In case of C4 joint type, with the passing-through web plate, which is disconnected to the flanges, the shear resistance can be calculated with the same formula by using the total transverse area of the section for A_{vc}, without consider the presence of stiffeners.

The second limit state to be considered for the web panel, is related to the shear buckling. Indeed, Eurocode 3, part 1-5 (CEN 2006) provides the following formula for the definition of the shear buckling resistance of the web panels.

$$V_{bw,Rd} = \frac{\chi_w \cdot f_{y,w} \cdot h_w \cdot t_w}{\sqrt{3} \cdot \gamma_{M1}} \qquad \text{Eq. 10.14}$$

where the factor χ_w can be defined with the provided tables for webs without stiffeners, such as the passing-through vertical plate, and for webs with transverse stiffeners at supports only, such as in the case of the passing-trough beam stub.

In-parallel, the node panel of the tube-column acts in shear. The referred shear strength for the tube-column panel in the node region can be calculated considering the previously reported equation provided by Eurocode 3, part 1-8 (CEN 2005a). The shear resistance area A_{vc} for tube-sections can be calculated with the following formula, reported in the Eurocode 3, part 1-1 (CEN 2005b) and in the CIDECT Design Guide N. 9 (Kurobane et al. 2004).

$$A_{vc} = 2 \cdot t_{CHS} \cdot (D_{CHS} - t_{CHS}) \qquad \text{Eq. 10.15}$$

CIDECT Design Guide N.9 (Kurobane et al. 2004) also provides a formula for the evaluation of the column web panel strength. In this case an additional factor is applied to consider the average stress ratio n in the tubular column. The shear strength of the node panel can be defined considering the following formula.

$$V_{wp,Rd} = \frac{\sqrt{1-n^2} \cdot f_{y,wc} \cdot A_{vc}}{\sqrt{3} \cdot \gamma_{M0}} \qquad \text{Eq. 10.16}$$

The shear deformation of the web panels should also be taken into account to correctly model the deformational behavior of the beam-to-column proposed joint. As well as in the case of the resistance, the whole stiffness can be defined by considering two in-parallel mechanisms. The first one refers to shear deformation of the beam web

and the second to the shear deformation of the panel node of the tubular column. In each case, the shear deformation can be calculated with the following formula:

$$K_{el,wp} = \frac{G \cdot A_v}{d} \qquad \text{Eq. 10.17}$$

where d is equal to the tubular column diameter in the case of the beam web, and it is equal to the height of the beam, when calculating the shear deformation of the tube. By adopting a single axial spring for each one of the single mechanisms, the modelling requires to define the relation between the axial component strength and stiffness and the shear stiffness and deformation of the real components.

The external elements subjected to shear and bending moment forces are not considered in terms of stiffness and shear strength in the mechanical characterization of the node. Therefore, a rigid shear connection is considered in the mechanical models of the semi-rigid proposed joints. The bending moment strength and rotational stiffness of these components can be considered in two ways. One possibility is to use for the previously described axially loaded elements, such as the beam flanges and the external parts of the tube, an effective area defined considering the contribution of the beam web and of the central parts of the tubular column. The second possibility is to consider separately the additional rotational stiffness and additional bending moment resistance.

10.2.2 Composite components

The composite connection can be simulated by a series of different components, which represent the behavior of the composite beam and the one of the composite columns. The behavior of the joints depends therefore on the basic components of the R.C. slab, reported in Table 10.2, and the mechanical behavior of the concrete-filled tubular steel column.

Table 10.2 Basic components in the composite beam

Sagging Bending Moment	Hogging Bending Moment
Concrete slab in conpression	Longitudinal slab re-bars in tension
Upper horizontal plate in compression	Upper horizontal plate in tension
Vertical plate in bending	Vertical plate in bending
Lower horizontal plate in tension	Lower horizontal plate in compression

In the development of the mechanical models, useful to characterize the behavior of the connection through the one of the singular components, the composite column

can be assumed to be infinitely rigid, due to the presence of the confined concrete core, as reported in the final report of the RFCS Project PRECIOUS (Bursi et al. 2009). In case of composite beam-to-column joints, with tubular filled column, the connection can be generally assumed as rigid.

For the region subjected to sagging bending moment, three different resultant actions are considered: a) the composite slab in compression, b) the upper horizontal plate assumed in compression, and c) the lower horizontal plate in tension (Figure 2.1). For the connection under hogging bending moment, the three resistant components taken into account were: a) the lower horizontal plate in compression, the upper horizontal plate assumed in tension, and c) the reinforcing bars in tension (Figure 2.1).

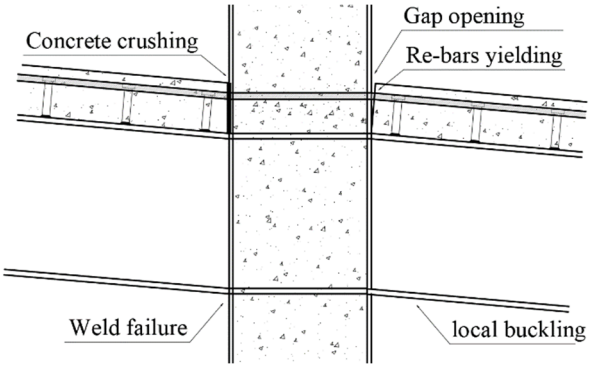

Figure 10.20 Deformed configuration of the proposed composite joints

10.2.2.1 Effects of concrete parts on steel components

Concrete filling of the CHS columns increases the stiffness and capacity considerably but limits the deformation capacity of the connections. Furthermore, the connection strength and stiffness can be significantly increased by using a composite floor. Although the stiffness and resistance increase, in general the rotation capacity decreases. The compression side of the connection at the column face will act as a stiff part since the loads are resisted by the concrete infill of the column. At the tension side the column face can only marginally deform and the deformations are generally not sufficient to allow a yield line pattern resulting in a small deformation capacity.

Regarding the strength of the axially loaded flange components, experimental tests reported in (de Winkel 1998) exhibited that plates directly welded to the tube face are able to resist to a higher axial load in tension in case of concrete filled column, however for tension loading, a punching shear failure occurred at a load just above

the yield load of the plate. Based on these investigations it was proposed to use for the definition of the strength of connections between I-beams and concrete filled CHS columns, the yield load of the flange in compression, whereas for the flange loaded in tension, the strength can be based on the punching shear strength.

In (Voth 2010), experimental tests conducted on axially loaded plate-to-tube connection, shown that the stress redistribution in the plate, due to the trasversal deformation of the tube wall, exhibited in case of unfilled tubes, is not instead higlighted in case of filled tube, as shown in Figure 10.21a-c. Furthermore, in case of passing-through transverse plate, the stress results to be constant along the width of the plate (Figure 10.21b).

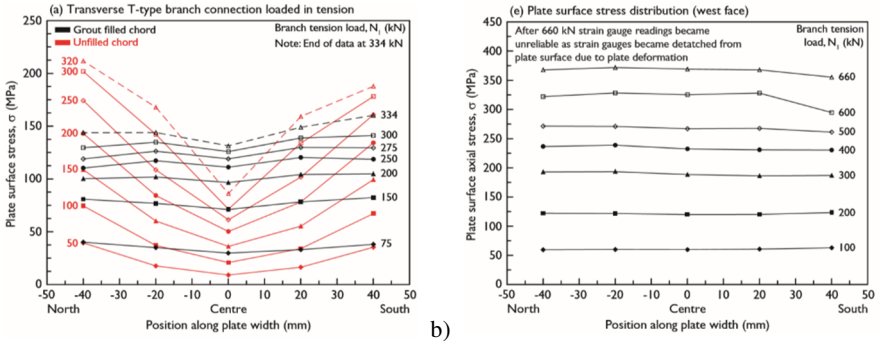

Figure 10.21 Plate surface stress distribution: a) comparison of filled and unfilled tube for the external plate in tension, and b) passing-through transverse plate in tension in case of concrete filled tube (Voth 2010)

The limit state design formula previously described for unfilled through plate connections are not applicable for passing-through plate in filled CHS-column. The grout core, combined with the through plate connection, provided resistance against yielding and ovalization of the tube wall, resulting in a connection strength that exceeded the capacity of the through element. The filling also increases the connection stiffness and move the failure away from the connection and into the connecting members, such as welds. Thus, connections between the flanges and concrete-filled columns are not to be considered critical.

10.2.2.2 Composite beam components

Composite beam-to-column connections transfer the hogging moment from the beam to the column through the longitudinal re-bars in the slab. A mechanical model able to describe the behavior of the slab in the tension region of the node, with hogging

moments, was developed by the adoption of a strut and tie schematization (ECCS 1999; Huber 1999; CEN 2004b). In this model the node is subjected to two typical loading conditions: the first one with equal hogging moments, which induce a tension force equal to $F_{1,Sd}$ in both sides, as shown in the example in Figure 10.22; the second one with different hogging moments, which induce different tension forces, $F_{1,Sd}$ and $F_{2,Sd}$, in the two sides, as shown in the example in Figure 10.23. The contribution of the concrete in tension can be neglected in the definition of both the strength and stiffness of the slab as suggested in (Huber 1999). However, for low value of the moments, the influence of the concrete on the stiffness of the slab is not completely neglectable, since the concrete make less deformable the re-bars, thanks to the developed adherence (Braconi 2004).

In the symmetric loading condition, Figure 10.22, the tension applied in the slab is entirely absorbed by the re-bars. The mechanical model is thus represented by just the longitudinal re-bars in the effective width of the composite beam. Therefore, the strength of each spring component can be evaluated by the following equation.

$$F_{t,Rd} = A_{bars} \cdot f_{sk} \qquad \text{Eq. 10.18}$$

where A_{bars} is the total area of the longitudinal re-bars in each side of the composite beam within the effective width, and f_{sk} the steel re-bars strength.

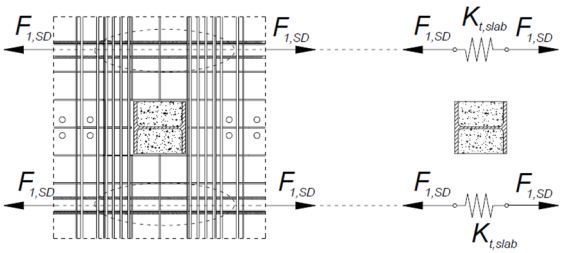

Figure 10.22 Mechanical representation of the slab in tension in case of symmetric loading condition (CEN 2004b)

The effective width of the composite beam can be defined following the criteria provided by Eurocode 4 (CEN 2004b). The stiffness of each spring component, in case of symmetric loading condition, can be calculated by the following equation.

$$K_t = \frac{A_{bars}}{h_c} \cdot E_s \qquad \text{Eq. 10.19}$$

where h_c is the height of the column section, in the proposed joint equal to the diameter D_{CHS} of the CHS-section, and E_s is the elastic is the Young modulus of the steel.

In the asymmetric loading condition, the tension forces in the two sides of the column are not in equilibrium. Therefore, their resultant force should be transfer to the column, through the compressed concrete in contact with the column in the side with the lower tension force, Figure 10.23. In this situation, a strut and tie mechanism can be defined in the slab, with the compressed concrete struts and tensioned re-bar ties. The position of the tensile components is defined by the geometric centers of the re-bars that effectively act in the mechanisms. According to Eurocode 8 (CEN 2004a) two slab mechanism can develop in the compressed region. The two slab mechanisms proposed by the code, include the central direct contact (Mechanism 1, Figure 10.24), and strut and tie system with the lateral contact to the tubular column (Mechanism 2, Figure 10.25). In the Mechanism 1, column compression forces are assumed to act within two cones of 30° with respect to the longitudinal axes of the beam, while for Mechanism 2 an inclination of 45° for the struts is assumed.

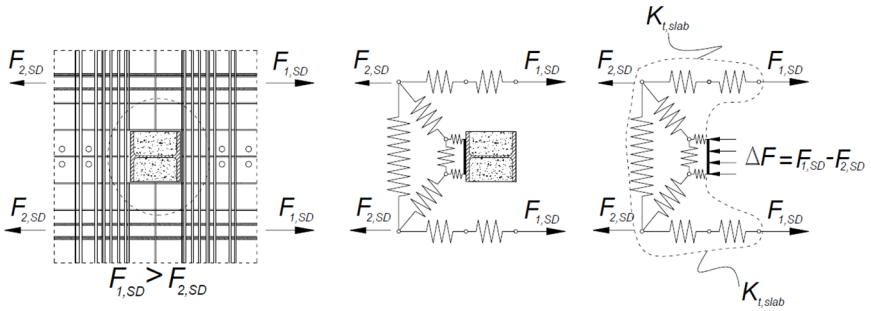

Figure 10.23 Mechanical representation of the slab in tension in case of asymmetric loading condition (CEN 2004b)

Each component is represented by an elastic spring characterized by a specific stiffness and strength, and the appropriate coupling in parallel and series of these springs provides the global stiffness of the mechanisms. The stiffness and resistance of each spring, that represents one component, are function of the mechanical characteristics of the material, such as the strength and Young modulus of the steel in tension f_{sk} and E_s, and the of concrete in compression f_{ck} and E_c, and the geometry of the elements, i.e. the area of the longitudinal A_{bars} and transversal A_{T-bars} re-bars in each side of the column, the average thickness of the slab h_{cls} and the diameter of the column D_{CHS}.

The strength and stiffness of each spring represented in Figure 10.24 for the Mechanism 1 can be calculated by the following equations, considering the total area $A_{bars,1}$ and $A_{T-bars,1}$ of the involved re-bars, and the effective and length of the singular components to be defined by the geometry of the slab, i.e. the length of the rebars components $L_{t,1}$ and $L_{T-t,1}$, and the length of the concrete strut $L_{c,1}$. For this mechanism the concrete cones develop with an angle α_1 equal to 30°.

$$F_{t,1,Rd} = A_{bars,1} \cdot f_{sk} \quad \text{Eq. 10.20}$$

$$F_{T-t,1,Rd} = A_{T-bars,1} \cdot f_{sk} \quad \text{Eq. 10.21}$$

$$F_{c,1,Rd} = D_{CHS} \cdot \sin \alpha_1 \cdot h_{cls} \cdot f_{ck} \quad \text{Eq. 10.22}$$

$$K_{t,1} = \frac{A_{bars,1}}{L_{t,1}} \cdot E_s \quad \text{Eq. 10.23}$$

$$K_{T-t,1} = \frac{A_{T-bars.1}}{L_{T-t,1}} \cdot E_s \quad \text{Eq. 10.24}$$

$$K_{c,1} = \frac{D_{CHS} \cdot \sin \alpha_1 \cdot h_{cls}}{L_{c,1}} \cdot E_c \quad \text{Eq. 10.25}$$

The distribution of the compression force develops within a distance equal to about half the effective width of the composite beam, generating a transverse tensile stress, to be absorbed by transversal reinforcements.

The different failure mechanisms can be identified and defined with the previously reported equations. Therefore, the minimum value of the failure loads can be assumed as the design resistance of the connection. The resistance of the first mechanism is thus provided by the resistances of the central strut in contact with the column and the tie rods, respectively $F_{c,1,Rd}$, $F_{t,1,Rd}$ and $F_{T-t,1,Rd}$. Considering the inclination β_1 for the two struts, it is possible to calculate the resistance associated to Mechanism 1, by considering the equilibrium of the internal force.

$$F_{H,1,Rd} = min\left\{2 \cdot F_{t,1,Rd}\ ;\ F_{c,1,Rd}\ ;\ 2 \cdot F_{T-t,1,Rd} \cdot \cot\ \beta_1\right\} \quad \text{Eq. 10.26}$$

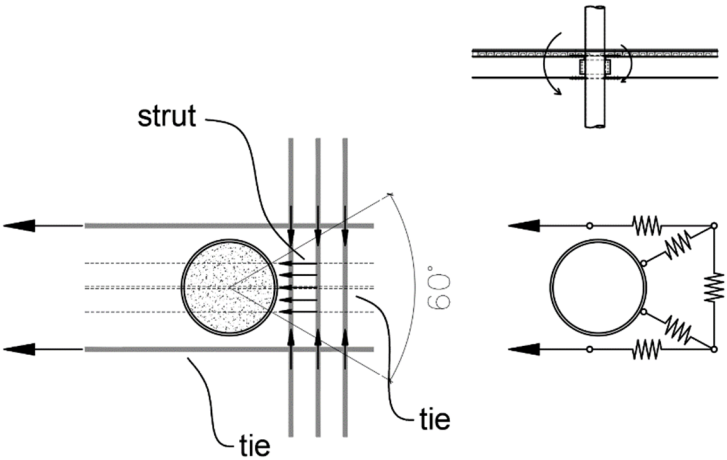

Figure 10.24 Mechanism 1 for hogging moment: central concrete strut

The strength and stiffness of each spring represented in Figure 10.25 for the Mechanism 2 can be calculated by the following equations, considering the above-mentioned quantities. For this mechanism the concrete cones develop with an angle α_2 equal to 30°, each one with an inclination of 45° with respect to the beam axes.

$$F_{t,2,Rd} = A_{bars,2} \cdot f_{sk} \quad \text{Eq. 10.27}$$

$$F_{T-t,2,Rd} = A_{T-bars,2} \cdot f_{sk} \quad \text{Eq. 10.28}$$

$$F_{c,2,Rd} = D_{CHS} \cdot \sin \alpha_2 \cdot h_{cls} \cdot \nu \cdot f_{ck} \quad \text{Eq. 10.29}$$

$$K_{t,2} = \frac{A_{bars,2}}{L_{t,2}} \cdot E_s \quad \text{Eq. 10.30}$$

$$K_{T-t,2} = \frac{A_{T-bars,2}}{L_{T-t,2}} \cdot E_s \quad \text{Eq. 10.31}$$

$$K_{c,2} = \frac{D_{CHS} \cdot \sin \alpha_2 \cdot h_{cls}}{L_{c,2}} \cdot E_c \quad \text{Eq. 10.32}$$

The coefficient ν, for the reduction of the concrete compression strength in case of transversal tensile stresses, can be defined considering the formula provided by Eurocode 2 (CEN 2004c).

$$\nu = 0.7 - \frac{f_{ck}}{200} \geq 0.5 \qquad \text{Eq. 10.33}$$

Considering the inclination of 45° for the two struts, it is possible to calculate the resistance associated to Mechanism 2, by considering the equilibrium of the internal force.

$$F_{H,2,Rd} = min\left\{2 \cdot F_{t,2,Rd}\ ;\ \sqrt{2} \cdot F_{c,2,Rd}\ ;\ 2 \cdot F_{T-t,2,Rd}\right\} \qquad \text{Eq. 10.34}$$

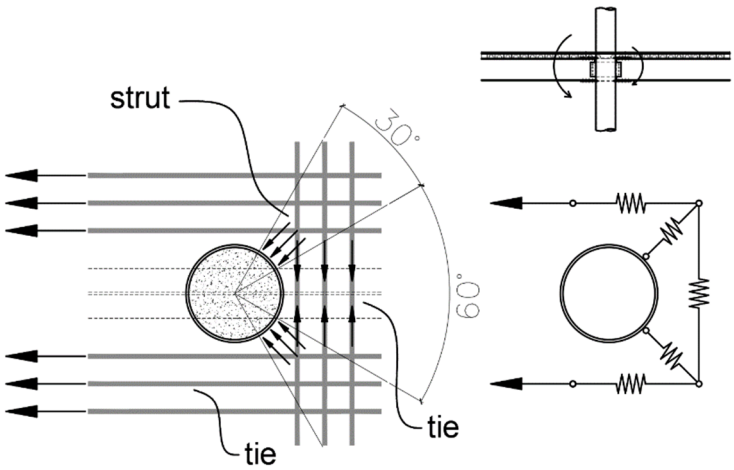

Figure 10.25 Mechanism 2 for hogging moment: lateral concrete struts

When the structure is subjected to horizontal loads, such as seismic action and wind, the beam-to-column nodes are subjected to both sagging and hogging bending moment. In the side where the sagging moment acts on the beam, the concrete slab has to transmit the compression action to the column. The interaction between the concrete slab and the column in the composite node, typically occurs through two mechanisms that are similar to the one previously described for the beam subjected to hogging moment in one side.

The first mechanism is characterized by the compressed strut that insists directly to the central part of the column wall, Figure 10.26, in a cone within an angle equal to 60°. In this case, transverse reinforcement is required to absorb the tensile stresses perpendicular to beam axes. The second mechanism is represented by a system of two compressed concrete struts inclined at 45°, which are in contact with the lateral sides of the tubular column (Alderighi 2007). For the formation of these struts, transversal

rebars are required to have the perpendicular tie and make possible the development of the mechanism, as shown in Figure 10.27.

The distribution of the compression force in the Mechanism 1 develops within a distance equal to about half the effective width of the composite beam, generating a transverse tensile stress, to be absorbed by transversal reinforcements. Therefore, the minimum value of the failure loads can be assumed as the design resistance of the connection. The resistance is provided by the strengths of the central strut in contact with the column and the tie rod, respectively $F_{c,1,Rd}$ and $F_{T-t,1,Rd}$. Considering the inclination β_1 for the two struts, it is possible to calculate the resistance associated to Mechanism 1, by considering the equilibrium of the internal force.

$$F_{S,1,Rd} = min\{F_{c,1,Rd}\ ;\ 2 \cdot F_{T-t,1,Rd} \cdot \cot\ \beta_1\} \qquad \text{Eq. 10.35}$$

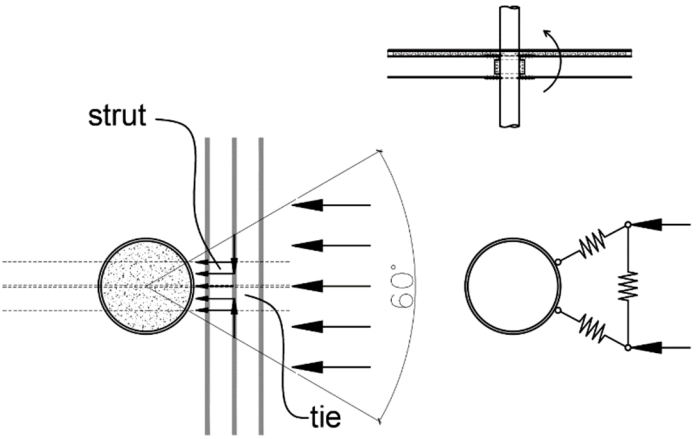

Figure 10.26 Mechanism 1 for sagging moment: central concrete strut

The resistance of the second mechanism is provided by the resistances of the equivalent struts and tie rods, respectively $F_{c,2,Rd}$ and $F_{T-t,2,Rd}$. Considering the inclination of 45° for the two struts, it is possible to calculate the resistance associated to Mechanism 2 by considering the equilibrium of the internal force.

$$F_{S,2,Rd} = min\{\sqrt{2} \cdot F_{c,2,Rd}\ ;\ 2 \cdot F_{T-t,2,Rd}\} \qquad \text{Eq. 10.36}$$

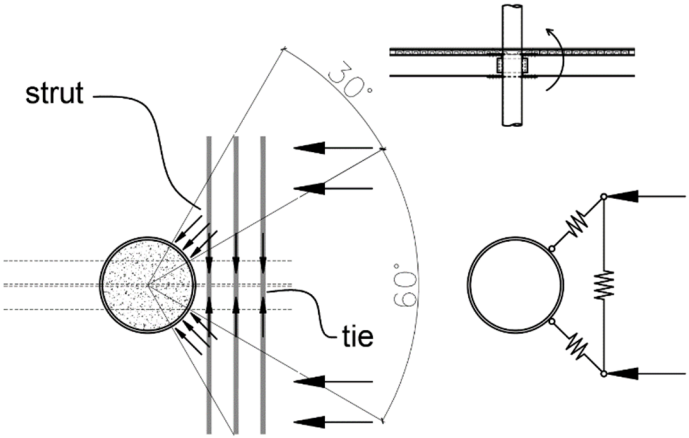

Figure 10.27 Mechanism 2 for sagging moment: lateral concrete struts

The two analyzed mechanisms act in parallel in the composite beam. However, the longitudinal shear connection can be represented through an additional spring. Indeed, the deformability of this interaction mechanism can reduce the stiffness of the Mechanism 2, which is characterized by the two laterals struts (Figure 10.28a). On the contrary the Mechanism 1 is described by the central strut, which is directly connect to the steel beam through the shear connectors (Figure 10.28b). The stiffness that characterized the interaction between the two mechanism can be defined as rigid, whereas the strength is defined by the shear strength of the two lateral vertical shear section characterized by the concrete and the transversal reinforcements.

The connection between the steel beam and the concrete slab is usually made through shear connectors, such as the Nelson stud use in the experimental campaign. The deformability of shear connectors can influence the behavior of the composite beam. The mechanical behavior of shear connectors can be represented by a multi-linear force-relative sliding diagram, such as the one shown in Figure 10.29a (Braconi 2004), in which it is possible to recognize a first elastic phase governed by the stiffness of the connectors. The elastic limit deformation γ_{el} can be calculated according to the following formula.

$$\gamma_{el} = \frac{F_{SC,el}}{K_{SC,el}} \qquad \text{Eq. 10.37}$$

$K_{SC,el}$ represents the stiffness of the beam-slab connection, which can be defined through the following equation (ECCS 1999; CEN 2004b).

$$K_{SC,el} = \frac{N \cdot K_{SC,el}}{\beta_{SC} - \left(\frac{\beta_{SC}{}^{-1}}{1+\alpha}\right) \cdot \frac{h_s}{d_s}} \qquad \text{Eq. 10.38}$$

with:

$$\alpha = \frac{E_s \cdot J_b}{E_s \cdot A_s \cdot {d_s}^2}; \beta_{SC} = \left[\frac{(1+\alpha) \cdot N \cdot K_{SC,el} \cdot l \cdot {d_s}^2}{E_s \cdot J_b}\right]^{0.5} \qquad \text{Eq. 10.39}$$

where l is the length of the tensioned cracked slab, J_b the moment of inertia of the steel beam, N is the number of stubs in the tension region, $K_{SC,el}$ is the shear stiffness of the singular connectors, d_s is the distance between the geometrical center of the longitudinal rebars and the one of the steel beam, and h_s is the distance between the geometrical center of the longitudinal rebars and the one of the compressed beam flange.

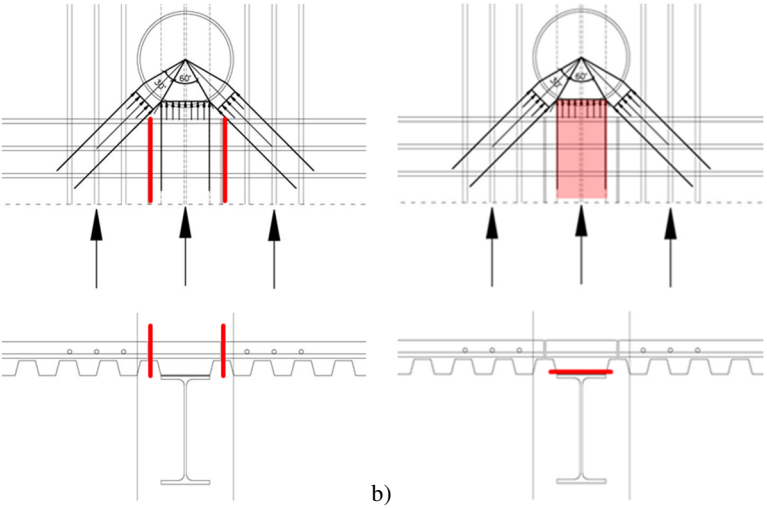

Figure 10.28 Shear connection mechanisms: a) interaction between the central and the lateral struts, and b) interaction between the steel beam and the concrete slab

The behavior is then limited by the maximum sliding γ_{pl}, which can be defined, as reported in (Braconi 2004), through the connection ratio.

$$\gamma_{pl} = \Psi \cdot \gamma_{el} \cdot \frac{F_{SC,el}}{F_{SC,pl}} \qquad \text{Eq. 10.40}$$

where Ψ is an empirical coefficient that can be set equal to 2 in case of full-strength shear connection, or equal to 3 in a partial-strength shear connection.

The plastic resistance of the shear connection $F_{SC,u}$ is defined as the addition of the singular resistance $P_{SC,Rd}$ of the stubs in the tensioned cracked slab.

$$F_{SC,u} = N \cdot P_{SC,Rd} \qquad \text{Eq. 10.41}$$

In the Eurocode 4 (CEN 2004b), the shear connection between the steel beam and the concrete slab is modelled with the behavior represented in Figure 10.29b. The shear deformation produces a reduction of the whole stiffness of the slab in tension.

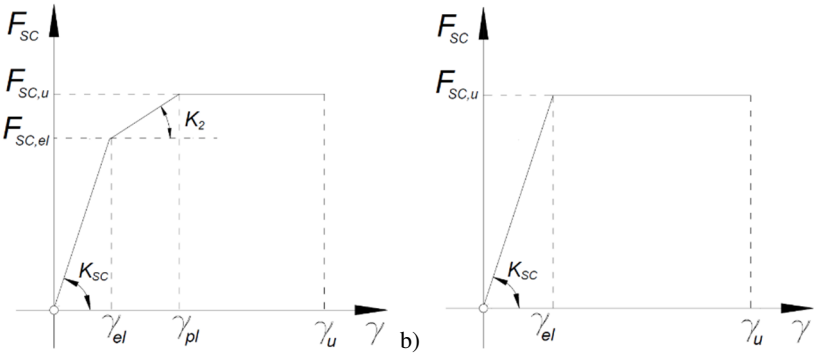

Figure 10.29 Mechanical behavior of the shear connectors: a) modelling of the experimental behavior, and b)schematization proposed by Eurocode 4 (CEN 2004b)

10.2.2.3 Concrete filled column components

In (Li and Han 2011, 2012; Ou et al. 2015) methods for the definition of the strength of the panel zone in case of tubular filled column were proposed. The adopted models consider, as failure mode, the crushing of the concrete in the panel zone. Adopting this model is possible to calculate the panel zone shear strength contribution from concrete. In (Ou et al. 2015) it was shown that if confined concrete strength was used, the panel zone shear strengths calculated with concrete contribution based on the proposed model were, on average, 8% more conservative than the test results. If unconfined concrete strength was used, the calculated panel zone shear strengths were, on average, 63% more conservative than the test results. Therefore, a model that consider the confined model for the concrete in the panel zone.

In the CIDECT design guide for connection with tubular column (Kurobane et al. 2004) the following formula for the definition of the shear strength of the panel zone is provided.

$$V_{c,Rd} = 1.2 \cdot \left(A_{c,p} \cdot \beta \cdot \frac{f_c}{10} + A_{vc} \frac{f_s}{\sqrt{3}} \right) \qquad \text{Eq. 10.42}$$

In the above equation A_{vc} is the shear resistant area of the tube and fs the yielding stress of the steel; $A_{c,p}$ and f_c denotes the cross-sectional area of the concrete panel and the cylinder strength of the concrete, whereas β is a function of the depth to height ratio of the concrete panel, and, for CHS-columns, it can be calculated with the following equation (see Figure 10.30).

$$\beta = 2 \cdot \frac{h_{c,w} - 2 \cdot t_{c,w}}{h_b - 2 \cdot t_d} \leq 4 \qquad \text{Eq. 10.43}$$

The above formula was derived from the yield strength of the panel multiplied by a factor of 1.2 to convert it to the ultimate limit state design strength. The yield strength was evaluated simply as the sum of the yield strengths of the concrete and steel parts, where the concrete part carries the shear load as a diagonal compression strut, whose strength was assumed to be governed only by the compressive strength of concrete.

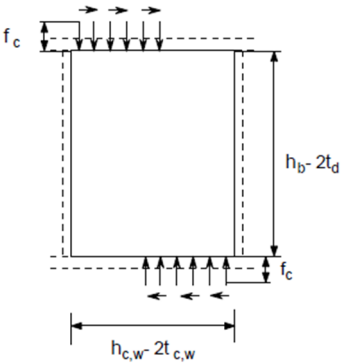

Figure 10.30 Stress distribution in the panel zone in composite node

The column web panel can show a hardening envelope and stable hysteresis loop after reaching the load given by the above equation. This contributes to dissipating energy input during strong earthquake motions. The shear capacity of the column web

panel decreases as the axial load in the columns increases. However, the shear load applied to the panel also decreases because the flexural capacity of the columns decreases with the axial load.

In order to consider the confining effect given by the presence of the steel tube in the composite column, the confined concrete model given in Eurocode 2 (CEN 2004c) can be adopted for concrete in the composite column. Moreover, the presence of the concrete in tension can be neglected. The confined model for concrete is expressed by the following equations.

$$f_{ck,c} = f_{ck} \cdot \left(1 + 5 \cdot \frac{\sigma_2}{f_{ck}}\right) \quad \text{Eq. 10.44}$$

$$f_{ck,c} = f_{ck} \cdot \left(1.125 + 2.5 \cdot \frac{\sigma_2}{f_{ck}}\right) \quad \text{Eq. 10.45}$$

$$\varepsilon_{c2,c} = \varepsilon_{c2} \cdot \left(\frac{f_{ck,c}}{f_{ck}}\right)^2 \quad \text{Eq. 10.46}$$

$$\varepsilon_{cu2,c} = \varepsilon_{cu2} + 0.2 \cdot \frac{\sigma_2}{f_{ck}} \quad \text{Eq. 10.47}$$

where σ_2 is the value of the lateral confining pressure. In absence of experimental evidence, the value of the lateral confining pressure σ_2 can be determined according to (Hu et al. 2003) with the following equation,

$$\frac{\sigma_2}{f_s} = 0.043646 - 0.000832 \cdot \frac{D_{CHS}}{t_{CHS}} \quad \text{Eq. 10.48}$$

which is valid only for:

$$21.7 \leq \frac{D_{CHS}}{t_{CHS}} \leq 47 \quad \text{Eq. 10.49}$$

f_s is the tensile strength of the steel tube, D_{CHS} the external diameter of the tube and t_{CHS} is its thickness. The purpose of these analyses is to obtain an approximation for the expected behavior, not to perform an exhaustive complex analysis.

10.3 Development of preliminary mechanical models

Mechanical models, which can appropriately simulate the real behavior of the proposed joints, are presently defined and developed considering, as an example, the component based model described EN1993-1-8 (CEN 2004a) for open section beam-to-column joints, which is currently the most adopted joint characterization method (Figure 10.31). The definition of the components and the first assembly processes are presented and discussed in this paragraph.

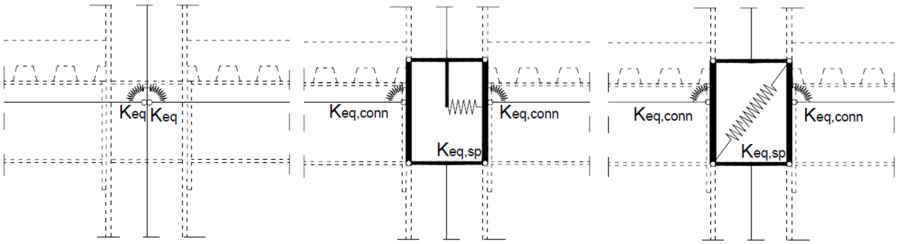

Figure 10.31 Mechanical models proposed by Eurocode 3, part 1-8 (CEN 2004a)

The mechanical performances of the components are previously defined with appropriate classification method, trying to adapt the researches already published on equal or similar components and analyzing the test measurements obtained in the experimental campaign.

10.3.1 Mechanical models for steel connections

A preliminary mechanical-analytical model, based on the component method proposed by Eurocode 3, part 1-8 (CEN 2005a) and on the observation of the results of the experimental tests, is developed for the steel I-beam-to-CHS-column connection with passing-through beam stub. The model, represented in Figure 10.32, is composed by individual springs. For each spring, which represents the singular components of the joint, the stiffness and strength have been defined in the previous paragraphs, adopting force-displacement laws obtained experimentally, i.e. using the evidence of the experimental tests for gravity and horizontal loads.

The comparison between the analytical and experimental results is carried out in this phase at the global level and would allow the calibration of the characteristics of the individual components and the development of methods for the design and characterization of the behavior of the proposed connection. However, a comparison at the local level is also required in order to have reliable models and methods.

The preliminary model developed for the C3 connection (Figure 10.32) does not include the modelling of the connecting welds. In fact, the reliable analytical interpretation of these components requires further studies. In this phase it was preferred to neglect this complex component in order to define simple starting models and to clarify on which aspects the mechanisms linked to the welds are actually influencing the global behavior of the node.

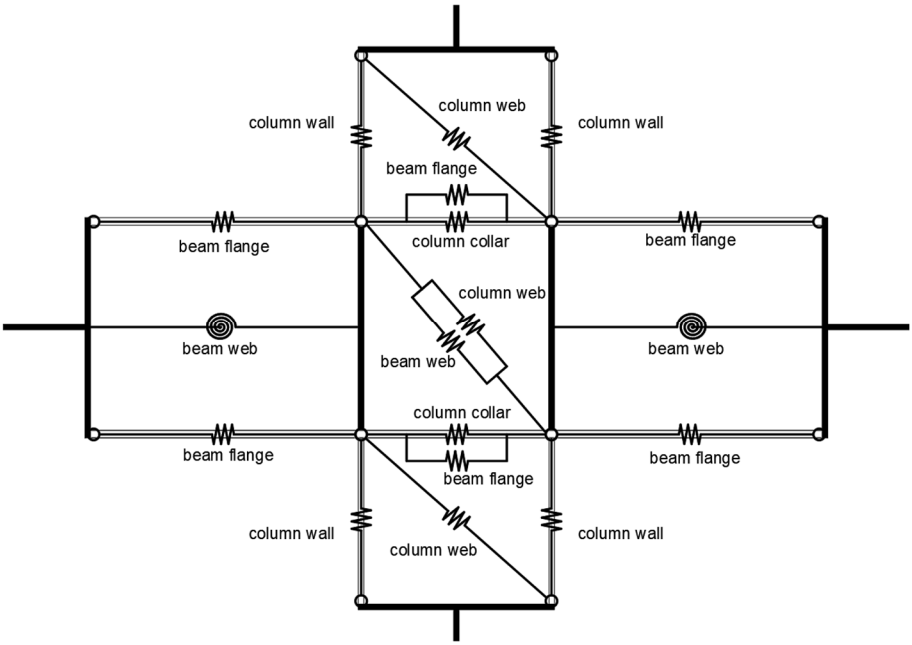

Figure 10.32 Preliminary mechanical model of C3 steel joint

10.3.1.1 Vertical gravity loads on the structure

The comparison of the force-displacement curves experimentally obtained with the ones obtained with the mechanical models, highlights that the numerical diagram agrees with the experimentally behavior as regards the value of the yielding point, as well as regards the initial elastic stiffness (Figure 10.33). The more in-depth observation of the initial behavior (Figure 10.34), shows that the values of the initial stiffness analytically obtained are slightly higher than the experimental evidence.

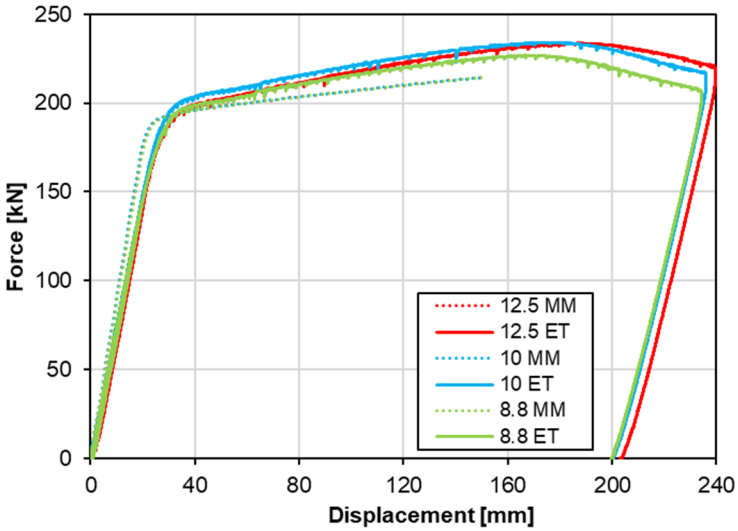

Figure 10.33 Comparison of the mechanical models (MM) and experimental tests (ET) results for the C3 steel joint type under vertical loading

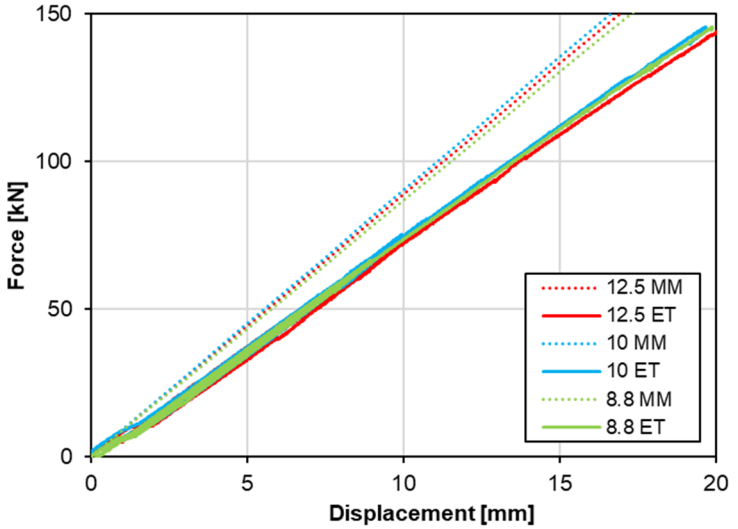

Figure 10.34 Initial stiffness of the mechanical models (MM) and experimental test specimens (ET) for the C3 steel joint type under vertical loading

Such a result may be due to some phenomena related to the test methods, such as for example the sliding phenomena and the deformation of the setups elements herein not modelled, but underlines anyway the need for further studies on the individual components.

10.3.1.2 Horizontal loads on the structure

For horizontal loads on the structure, the comparison of the experimental results the analytical ones (Figure 10.35), highlights that the strength of the joint with stiffer column wall (10 mm and 12.5 mm) can be satisfying modelled neglecting the welds components. In fact, the welds failures in these experimental tests are reach in the end of the test after the complete plasticization of the external girders and of the node panel zone. On the contrary, the specimen with the 8.8 mm stiffer column cannot be model without consider the weld components, since in this way the analytical obtained strength of the joint is the 30 % higher than the real one.

The analysis of the initial behavior (Figure 10.36) shows that the values of the initial stiffness analytically obtained are around the 40 % higher than the experimental evidence. As well as for the vertical gravity loads, such result may be due to the sliding and deformation phenomena in the test setups elements not analytically modelled.

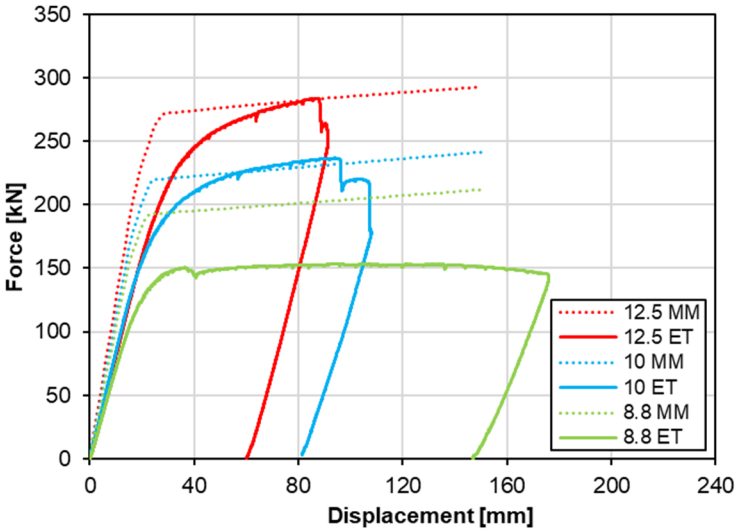

Figure 10.35 Comparison of the mechanical models (MM) and experimental tests (ET) results for the C3 steel joint type under horizontal loading

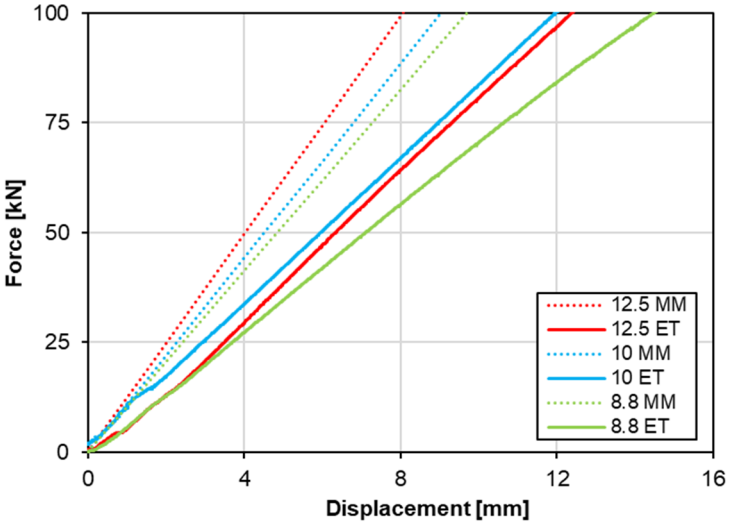

Figure 10.36 Initial stiffness of the mechanical models (MM) and experimental test specimens (ET) for the C3 steel joint type under horizontal loading

10.3.1.3 Further developments

The welded connection between the passing elements and the column wall proved to be the weak element of the connection, causing the loss of resistance of the connection in the experimental tests; this weakness arises not for reasons linked to the quality of the materials used, but rather due to the partial resistance of the connection, its high overall deformability and the high interaction phenomena that occur between the two connected elements. In particular, the simultaneous presence of a tensile stress in the column wall and in the through elements welded to it, limits the strength actually available, since it subjects the weld to a triaxial stress state rather than to a state of tension and shear as expected.

This mechanism requires more accurate studies not only for the description of the phenomenon but above all for the definition of design details and construction solutions to significantly increase the performance of this connection, which, being the fragile element in the beam-to-column analyzed joints, it must be safeguarded by providing greater over-strength. A more in-depth study of the individual components would therefore lead to more refined and correctly calibrated analytical models, thanks to which it would then be possible to define design methods and evaluation of the behavior of the nodes studied. In any case, the result obtained with respect to the

ultimate resistance of the connection is such that the starting model is considered adequate for future interpretations.

10.3.2 Mechanical models for composite connections

To develop complete mechanical models for the composite connections, the mechanical models currently in development for the steel connections, should be upgraded with the described components of the R.C. slab and with the exclusion of the steel mechanism that resulted avoided by the presence of the concrete slab and the concrete column filling.

As well as done for the pure steel joints, the behavior of the composite components is defined by axial springs that act in tension, in compression, or both in tension and compression. A schematic representation of the mechanical model for composite connection is reported in Figure 10.37.

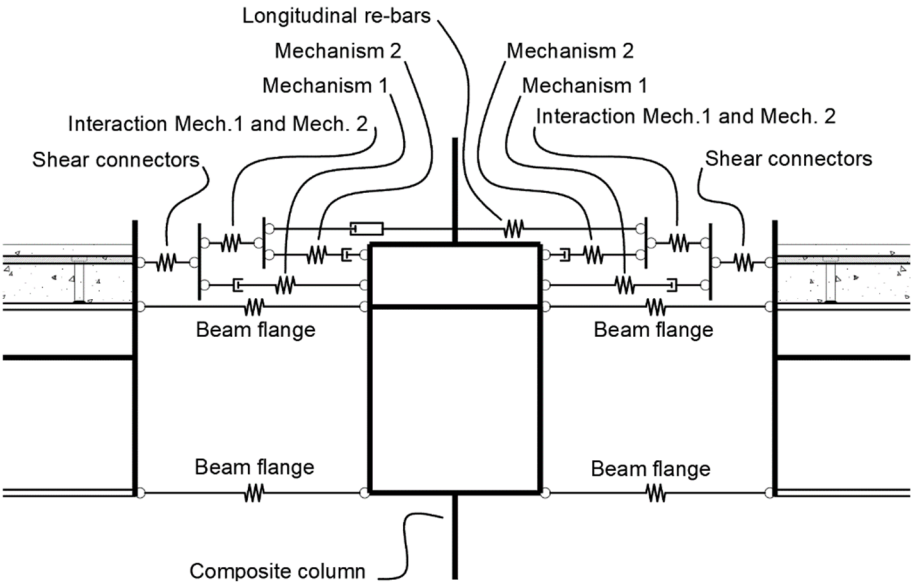

Figure 10.37 Mechanical scheme of the composite beam

The represented mechanical schematization includes all the possible mechanisms that can develop in the composite node except, for simplicity reason, the deformations of the core panel and the column. In the same simplified way, the steel beam elements are schematized through the axial springs representing the two horizontal plates.

Furthermore, the springs that represent the slab mechanisms are disposed, in the schematic view, with different height, whereas in the real model, they are disposed in the geometric center of the concrete slab and reinforcements.

11 Conclusions and further developments

Nowadays, tubular column steel and composite joints are realized with additional interior or exterior diaphragms, which allow the correct transfer of forces from the beam flanges to the column wall, avoiding the tube-wall local distortions that can develop in case of simple direct contact. Therefore, the fabrication of these joints requires extensive additional cutting and welding processes, resulting in the reduction of the production rapidity and in the increment of the overall building; in addition, the presence of plates and diaphragms spoils down the aesthetic of the structures. In conclusion, even though tubular columns should lead to economic and architectural benefits, their use in building construction market is presently limited for the complexity of the beam-to-column connections.

To overcome the main problems previously exposed with the direct and diaphragms connections, innovative solutions with continuous elements inside the column were studied in the recent past. Many researches highlighted that, from a mechanical behavior point of view, the best solution is the one with passing-through flanges and web plates or the whole beam stub. The development of this construction technique has been limited mainly due to the difficulties in implementing high precision cutting processes able to realize fitted slots for the passage of the beam stub or plates, favoring more practice solutions. The objective of the present research is the study of new solutions for I-beam-to-CHS-column connections with passing-through beam stub and/or plates, which may overcome the difficulties that limited the adoption of this technique. To overcome the main problematic, related to the practical aspects, laser cutting machines, commonly used in the industrial field, are proposed to realize the fitted slots with completely automated high precision cutting processes.

Although this opportunity showed good perspectives, several aspects were studied in this thesis, in order to provide more detailed information on the effective quality of the proposed typologies, from a practical and mechanical point of view, and useful

tools for the evaluation of the behavior and the development of practical design methods.

11.1 Conclusions

The application of LCT in cutting operations on steel structural tubes and open profiles was studied analyzing the already performed researches. The analyses of the state of art about LCT highlighted that laser cutting machines are nowadays able to work steel profiles with the typical structural dimensions, obtaining high precision and reduced HAZ on the cutting pieces. However, considering the different tolerances adopted in the laser cutting processes and in the production of structural steel members, the realization of the fitted slot on the basis of the nominal dimensions of beams, can lead to have problems in the passage of the beam stubs through the column. Therefore, possible solutions for the fabrication, assembly and erection processes were presently presented and discussed and, together with the results of the preliminary theoretical and numerical studies herein presented, all the evaluation done were used to propose I-beam-to-CHS-column joint typologies with passing-through elements that are able to accomplish with the necessities that can arise in the steel and composite structures market, for either moment resisting and braced frames. These proposed solutions make possible the realization of beam-to-column connections which have the purpose of behaving either as rigid full-strength joints or nominally pinned connections. Furthermore, some typologies make possible the realization of interior and exterior beam-to-column joints with the beam connected in both the main directions.

An experimental campaign was defined in order to obtain suitable information on the mechanical behavior of the proposed solutions in case of rigid full-strength joints in different load configurations. The whole program included tests on full-scale substructure of steel and composite steel-concrete buildings, characterizing I-beam-to-CHS-column connections, and were designed to assess the global behavior of the connections and to obtain detailed information on the local performance of the singular components. All the tests shown in this thesis were performed within the LASTEICON research project (Castiglioni et al. 2016) in two laboratories at the INSA Rennes University, and University of Pisa. The experimental studies showed that the proposed joints behaved in a significantly different way in case of vertical and horizontal loads on the structure. In fact, in case of vertical loads, the continuity of the beam inside the node allow both the transmission of the load and the stiffener of the column wall, and the rigid full-strength behavior is obtained for the proposed steel and composite connections. In case of horizontal loads on the structure, the

connections behaved as semi-rigid, partial-strength connections, either in the case of steel and composite joints. The failure modes exhibited in the tests involved the area of interaction between through flanges and the column wall. In these regions, the axial load on the beam flanges or plates, and those on the column wall, led to the formation of cracks in the welds in tension, and to the development of local distortions on the column wall in compression. The second aspect is obviously reduced in composite specimens, where the column concrete core avoided the local buckling phenomena. However, although composite specimens exhibited a higher strength, the ductility resulted to be limited by the brittle tearing failures of welds and column wall.

Experimental studies showed that the behavior of the proposed connections differs substantially from those of the most currently adopted beam-to-column connections, where the column is continuous in the node. In fact, in the cases presently studied, the column results to be divided in three parts, the node panel stub and the two external elements, in particular in case of four-way joints, which is the most effective configuration.

Considering the final objective of defining mechanical models for steel and composite joints, which can be useful for the development of linear and non-linear design method, steel and concrete components were defined and studied to propose methods for the definition of their elastic stiffness and strength, trying to adapt the researches already published on similar components and analyzing the obtained test results.

Finally, preliminary mechanical-analytical models, based on the component method proposed by Eurocode 3, part 1-8 (CEN 2005a) and on the observation of the results of the experimental tests, is developed for the steel I-beam-to-CHS-column connection with passing-through beam stub. Models are composed by individual springs, representing the singular components of the joint. For each spring, the stiffness and strength have been defined with the proposed methods. The comparison between the analytical and experimental results showed both good perspectives and model limits, and highlighted the aspects to be further studied to define reliable methods for both the classification and the design of the proposed joints.

11.2 Further developments

Future studies on the proposed connections should aim to clarify some aspects highlighted in the present thesis and to propose new solutions that can improve some characteristics showed in the research carried out. Although the execution of the experimental tests provided suitable information on the mechanical behavior of the proposed joints, the realization of numerical models useful for performing parametric

analyses, would allow to obtain more general information than those available. These numerical models should be calibrated on the basis of the experimental results and, subsequently, some characteristic parameters, such as the geometric dimensions of the elements and the welding methods, should be varied to investigate the influence of the individual parameters on the overall behavior and thus to validate the mechanical models developed in the present thesis.

In parallel with the study of the global behavior of the whole connections, experimental and numerical studies on reduced specimens will be useful to define the behavior of the individual components, validating and calibrating the methods herein reported for their mechanical characterization. For example, it would be useful to carry out studies that aim at better understanding the established mechanisms in the region of connection between the column wall and the passing elements, by means of simplified models. In fact, the preliminary model developed for the proposed connections do not include the modelling of the connecting welds, since the reliable analytical interpretation of these components requires further specific studies. In this phase it was preferred to neglect this complex component in order to define simple starting models and to clarify on which aspects the mechanisms linked to the welds are actually influencing the global behavior of the node. In addition, the penetration weld failures exhibited in the tests showed that the welding processes did not lead to the complete melt of the base material on the surface affected by the laser cutting processes. Considering the lack of studies, it would be useful to appropriate study this phenomenon through experimental and chemical analyses on welds performed on surfaces worked by the laser beam.

Furthermore, future studies will aim at the assessment of the possible application of the proposed connection types to structures sized with the capacity design, in order to obtain a suitable dissipative behavior, as requested in Eurocode 8 (CEN 2004a). In fact, in this case the connections should be designed to develop the plastic hinges at the beam ends and not inside the nodes and in the column. This topic was not addressed in the present thesis, since it was a first study on the behavior of these connections and in this phase a linear design was considered and attention was made in offering tools for defining elastic stiffness and strength of the connection. Moreover, even though the joint ductility has no particular interest in the current regulatory context, which does not involve the development of plastic hinges inside the nodes, the evaluation of the rotational capacity of the proposed connections could have interest in the research on steel and composite structures.

References

AIJ (2001) Architectural Institute of Japan, Standard for Structural Calculation of Steel Reinforced Concrete Structures - 5th Ed. Architectural Institute of Japan

Alderighi E (2007) Performance of Unprotected Composite Frames with Concrete Filled columns under Seismic and Fire loadings, Doctoral Thesis. University of Pisa

Aloke R, Girish V, Scrutton RF, Molian PA (1997) A model for prediction of dimensional tolerances of laser cut holes in mild steel thin plates. Int J Mach Tools Manuf 37:1069–1078. doi: 10.1016/S0890-6955(96)00090-9

Alostaz YM, Schneider SP (1996a) Analytical behavior of connections to concrete-filled steel tubes. J Constr Steel Res 40:95–127. doi: 10.1016/S0143-974X(96)00047-8

Alostaz YM, Schneider SP (1996b) A Report on Research Sponsored by the National Science Foundation - NSF CMS 93-00682 - Connections to Concrete-filled Steel Tubes

Andrés D, García T, Cicero S, et al (2016) Characterization of heat affected zones produced by thermal cutting processes by means of Small Punch tests. Mater Charact 119:55–64. doi: 10.1016/j.matchar.2016.07.017

Ariyoshi M, Makino Y (2000) Load-deformation relationships for Gusset-Plate to CHS tube joints under compression loads. Int J Offshore Polar Eng 10:292–300

Bagheri Sabbagh A, Chan TMM, Mottram JTT (2013) Detailing of I-beam-to-CHS column joints with external diaphragm plates for seismic actions. J Constr Steel Res 88:21–33. doi: 10.1016/j.jcsr.2013.05.006

Barrett-Byrd-Associates (2016) Steel Construction Cost

Bergmann R, Matsui C, Meinsma C, Dutta D (1995) Design Guide for Concrete Filled Hollow Section Columns under Static and Seismic Loading. CIDECT Comité International pour le Développement et l‟Étude de la Construction Tubulaire

BLM Group (2012) Inspired for Tube, 12

Braconi A (2004) Collegamenti trave-colonna a parziale ripristino di resistenza per strutture composte acciaio-calcestruzzo sismo-resistenti ad elevata duttilità, Doctoral Thesis

Braconi A, Elamary A, Salvatore W (2010) Seismic behaviour of beam-to-column partial-strength joints for steelconcrete composite frames. J Constr Steel Res 66:1431–1444. doi: 10.1016/j.jcsr.2010.05.004

Braconi A, Salvatore W, Tremblay R, Bursi OS (2007) Behaviour and modelling of partial-strength beam-to-column composite joints for seismic applications. Earthq Eng Struct Dyn 36:142–161

Bursi OS, D'Incau M, Zanon G, et al (2017) Laser and mechanical cutting effects on the cut-edge properties of steel S355N. J Constr Steel Res 133:181–191. doi: 10.1016/j.jcsr.2017.02.012

Bursi OS, Ferrario F, Haller M, et al (2009) Prefabricated composite beam-to-concrete filled tube or partially reinforced-concrete-encased column connections for severe seismic and fire loadings - Final Report - EU-RFCS Project PRECIOUS - RFSR-CT-2003-00034. Brussels

Campolunghi L (2012) I beams to CHS column connections: An innovative typology, Master Thesis. Politecnico di Milano

Caristan CL (2003) Laser Cutting Guide for Manufacturing. Society of Manufacturing Engineers, United States

Castiglioni CA, Kanyilmaz A, Salvatore W, et al (2016) Laser Technology For Innovative Connections In Steel Construction - EU-RFCS Project LASTEICON 709807(2016) - www.lasteicon.eu

CEN (2004a) European Committee for Standardization, EN 1998-1:2004 Eurocode 8: Design of structures for earthquake resistance - Part 1: General rules, seismic actions and rules for building

CEN (2018) European Committee for Standardization, EN 1090-2:2018 Execution of steel structures and aluminium structures - Part 2: Technical requirements for steel structures

CEN (1993) European Committee for Standardization, EN 10034:1993 Structural steel I and H sections - Tolerances on shape and dimensions

CEN (2005a) European Committee for Standardization, EN 1993-1-8:2005 Eurocode 3: Design of steel structures - Part 1-8: Design of joints

CEN (2005b) European Committee for Standardization, EN 1993-1-1:2005 Eurocode 3: Design of steel structures - Part 1-1: General rules and rules for buildings

CEN (2004b) European Committee for Standardization, EN 1994-1-1:2004 Eurocode 4: Design of composite steel and concrete structures - Part 1-1: General rules and rules for buildings

CEN (2004c) European Committee for Standardization, EN 1992-1-1:2004 Eurocode 2: Design of concrete structures - Part 1-1 : General rules and rules for buildings

CEN (2013) European Committee for Standardization, EN206:2013 Concrete - Specification, performance, production and conformity

CEN (2006) European Committee for Standardization, EN 1993-1-5:2006 Eurocode 3: Design of steel structures - Part 1-5: Plated structural elements

Cheng C, Chung L (2003) Seismic performance of steel beams to concrete-filled steel tubular column connections. J Constr Steel Res 59:405–426. doi: 10.1016/S0143-974X(02)00033-0

de Winkel GD (1998) The Static Strength of I-Beam to Circular Hollow Section Column Connections, Doctoral Thesis. Delft University of Technology

ECCS (1986) Publication n.45: Recommended Testing Procedure for Assessing the Behaviour of Structural Steel Elements under Cyclic Loads. European Convention for Constructional Steelwork - ECCS

ECCS (1999) Publication n.109: Design of Composite Joints for Buildings - Technical Commitee 11 - Composite Structures. ECCS, Brussels

Finetto M, Salvatore W, Hoffmeister B, et al (2007) Optimizing the seismic performance of steel and steel-concrete structures by standardizing material quality control - EU-RFCS Project OPUS RFSR-CT-2007-00039

Han L, Li W (2010) Seismic performance of CFST column to steel beam joint with RC slab : Experiments. J Constr Steel Res 66:1374–1386. doi: 10.1016/j.jcsr.2010.05.003

Harničárová M, Zajac J, Stoić A (2010) Comparison of different material cutting technologies in terms of their impact on the cutting quality of structural steel. Tech Gaz 17:371–376

Hu H-T, Huang C-S, Wu M-H, Wu Y-M (2003) Nonlinear Analysis of Axially Loaded Concrete-Filled Tube Columns with Confinement Effect. J Struct Eng 129:1322–1329. doi: 10.1061/(ASCE)0733-9445(2003)129:10(1322)

Huber G (1999) Non-linear calculations of composite sections and semi-continuous joints, PhD Thesis. University of Insbruck

Jaspart JP, de Ville de Goyet V (1988) Etude experimentale et numerique du comportament des structures composees de poutres a assemblages semi-rigides. Constr Met 2:31–49

Jaspart JP, Weynand K (2015) Design of Hollow Section Joints using the Component Method. In: Batista E, Vellasco P, Lima L (eds) ISTS 2015 - Proceedings of the 15th International Symposium on Tubular Structures. CRC Press/Balkema, Rio de Janeiro, Brazil, pp 405–410

Kanyilmaz A (2019) The problematic nature of steel hollow section joint fabrication, and a remedy using laser cutting technology: A review of research, applications, opportunities. Eng Struct 183:1027–1048. doi: 10.1016/j.engstruct.2018.12.080

Kanyilmaz A, Castiglioni CA (2018) Fabrication of laser cut I-beam-to-CHS-column steel joints with minimized welding. J Constr Steel Res 146:16–32. doi: 10.1016/j.jcsr.2018.02.039

Khador M (2015) Cyclic behaviour of external diaphragm joint between steel I-section beam and circular hollow section column, Doctoral Thesis. University of Warwick

Krawinkler H (1978) Shear in beam-column joints in seismic design of steel frames. Eng Journal, Am Inst Steel Constr

Krawinkler H, Bertero VV, Popov EP (1971) Inelastic behaviour of steel beam-to-column subassemblages. Berkeley

Kurobane Y, Packer JA, Wardenier J, Yeomans N (2004) Design Guide for Structural Hollow Section Column Connections. CIDECT Comité International pour le Développement et l"Étude de la Construction Tubulaire

Li R, Samali B, Tao Z, Hassan K (2017) Cyclic behaviour of composite joints with reduced beam sections. Eng Struct 136:329–344. doi: 10.1016/j.engstruct.2017.01.025

Li W, Han L (2011) Seismic performance of CFST column to steel beam joints with RC slab : Analysis. J Constr Steel Res 67:127–139. doi: 10.1016/j.jcsr.2010.07.002

Li W, Han L (2012) Seismic performance of CFST column to steel beam joint with RC slab : Joint model. J Constr Steel Res 73:66–79. doi: 10.1016/j.jcsr.2012.01.011

Li WQ, Chen YY, Wang W, et al (2010) Experimental Study of External Diaphragm Joint Connecting CHS Column AND H-shaped Beam. Adv Steel Constr 6:578–588

Meurling F, Melander A, Linder J, Larsson M (2001) The influence of mechanical and laser cutting on the fatigue strengths of carbon and stainless sheet steels. Scand J Metall 30:309–319. doi: 10.1034/j.1600-0692.2001.300506.x

Minouei YB, Mirghaderi R (2009) Effect of Through Plate Connection on Transferring Loads in CFT Columns. In: TCLEE2009 - Proceedings of the Technical Council on Lifeline Earthquake Engineering Conference: Lifeline Earthquake Engineering in a Multihazard Environment. p 12

Moazed R, Fotouhi R (2012) The Influence of Mechanical and Laser Cutting on the Fatigue Strengths of Square Hollow-Section Welded T-Joints. J Offshore Mech Arct Eng 134:1–12. doi: 10.1115/1.4005186

Nishiyama I, Fujimoto T, Fukumoto T, Yoshioka K (2004) Inelastic Force-Deformation Response of Joint Shear Panels in Beam-Column Moment Connections to Concrete-Filled Tubes. J Struct Eng 130:244–252. doi: 10.1061/(ASCE)0733-9445(2004)130:2(244)

Ou Y, Tran N, Chen C, Lee H (2015) Panel Zone Shear Behavior of Through-Flange Connections for Steel Beams to Circular Concrete-Filled Steel Tubular Columns. J Struct Eng 141:1–12. doi: 10.1061/(ASCE)ST.1943-541X.0001187

Schneider SP, Alostaz YM (1998) Experimental Behavior of Connections to Concrete- Filled Steel Tubes. J Constr Steel Res 45:321–352

Stark JWB, Bijlaard FSK (1988) Design rules for beam-to-column connections in Europe. J Constr Steel Res 10:415–462

Tschemmernegg F, Humer C (1988) The design of structural steel frames under consideration of the non linear behaviour of joints. J Constr Steel Res 11:73–103

Voth AP (2010) Branch Plate-to-Circular Hollow Structural Section Connections, Doctoral Thesis. University of Toronto

Voth AP, Packer JA (2016) Circular hollow through plate connections. Steel Constr 9:16–23. doi: 10.1002/stco.201610004

Voth AP, Packer JA (2012) Branch Plate-to-Circular Hollow Structural Section Connections. I: Experimental Investigation and Finite-Element Modeling. J Struct Eng 138:995–1006. doi: 10.1061/(asce)st.1943-541x.0000505

Wang W, Chen Y, Li W, Leon RT (2011) Bidirectional seismic performance of steel beam to circular tubular column connections with outer diaphragm. Earthq Eng Struct Dyn 40:1063–1081. doi: 10.1002/eqe1070

Wardenier J (1995) Properties and service performance: Semi-rigid connections between I-beams and tubular columns, Final Report EUR 16066. Luxembourg: Office for Official Publications of the European Communities

Wardenier J (1982) Hollow Section Joints. Delft University Press, Delft

Wardenier J, Kurobane Y, Packer JA, et al (2008) Design Guide for Circular Hollow Section (CHS) Joints under Predominantly Static Loading. CIDECT

Weynand K, Jaspart JP, Ly L (2003) Application of the Component Method To Joints between Hollow and Open Sections - Cidect Final Report: 5BM

Witteveen J, Stark JWB, Bijlaard FSK, Zoetemijer P (1982) Welded and bolted beam-to-column connections. J Struct Div 108:

Zhang D, Gao S, Gong J (2012) Seismic behaviour of steel beam to circular CFST column assemblies with external diaphragms. J Constr Steel Res 76:155–166. doi: 10.1016/j.jcsr.2012.03.024